Carbene-Metal Complexes as Anticancer and Antibacterial Drug Candidates

by

Frauke Marie Hackenberg, MSc.

The thesis is submitted to University College Dublin in fulfilment of the requirements for the degree of Doctor of Philosophy.

Based on the research conducted in the
School of Chemistry and Chemical Biology

Head of School:
Prof. Patrick J. Guiry

Principal Supervisor:
Dr. Matthias Tacke

Doctoral Studies Panel:
Dr. Andrew Phillips, Dr. Francesca Paradisi

September 2013

Jedes Ende ist ein neuer Anfang,
und hinter jedem Anfang wartet ein neues Abenteuer

Table of Contents

List of Figures

List of Schemes

List of Tables

Abbreviations

δ	chemical shift (NMR)
η	hapticity
µM	micromolar
Å	angstrom
Caki-1	human Caucasian kidney carcinoma
$CDCl_3$	deuterated chloroform (NMR)
cm^{-1}	reciprocal centimetre, unit of wavelength for IR)
d	doublet (NMR)
dd	doublet of doublets (NMR)
ddd	doublet of doublet of doublets (NMR)
dt	doublet of triplets (NMR)
DMSO	dimethylsulfoxide
DNA	Deoxyribonucleic acid
E. coli	Escherichia coli
g	gram
h	hour
Hz	Hertz (NMR)
IC_{50}	concentration at which a drug may inhibit the growth of 50% of the test population exposed to it (Inhibitory Concentration)
IR	Infra-Red
J	coupling constant (NMR)
K	Kelvin
KBr	potassium bromide
M	molar
m	multiplet (NMR)
MCF-7	human breast adenocarcinoma cell line
mg	milligram
MHz	Mega Hertz
min	minute
mL	millilitre
mmol	millimole
mol	mole
MRSA	Methicillin resistant staphylococcus aureus
MSSA	Methicillin sensitive staphylococcus aureus
MTT	methylthiazolyldiphenyl tetrazolium bromide
NMR	Nuclear Magnetic Resonance
p	pentet (NMR)
ppm	parts per million (unit)

rt / RT	room temperature
s	singlet (NMR)
S. aureus	*Staphylococcus aureus*
t	triplet (NMR)
THF	tetrahydrofuran

Note: Cell lines, bacterial and fungal strains not listed here are described in brackets preceding / following their abbreviated names and all other abbreviations are described within the text.

Abstract

Within this project, novel silver(I)-, ruthenium(II)- and gold(I)-NHC complexes have been synthesised by the formation of appropriately substituted (benz)imidazolium and 4,5-diaryl-imidazolium halides followed by either metallation with silver acetate, or metallation with silver oxide followed by transmetallation with dichloro ruthenium (*p*-cymene) dimer or dimethylsulfido gold chloride. The three obtained NHC-gold(I) chlorides were further functionalised by reacting them with silver acetate or 2,3,4,6-tetra-*O*-benzyl-1-thio-β-D-glucopyranose to give NHC-gold(I) acetates or NHC-gold(I) thioglucopyranoses, respectively.

All complexes were characterised by NMR (^{1}H and ^{13}C), IR, microanalysis and MS. Melting points were determined for all complexes with the exception of (benz)imidazol-2-ylidene silver(I) acetates. The *in vitro* antibacterial activity against bacterial strains of *E. coli* and *MRSA* of all NHC-Ag(I)OAc complexes has been investigated utilizing the Kirby-Bauer disc diffusion method. *In vitro* MTT-based cytotoxicity assays against the human renal cancer cell line Caki-1 were carried out on all complexes and additionally against the human breast cancer cell line MCF-7 on all 4,5-diaryl-NHC silver(I) acetate as well as on all Ru(II)-NHC and Au(I)-NHC complexes. Lowest IC_{50} values down to 0.51 (± 0.07) μM against Caki-1 and 1.4 (± 0.1) μM against MCF-7 have been found for the most promising NHC-silver(I) acetate complex 1,3-di(*p*-methylbenzyl)-4,5-di(*p*-methylphenyl)imidazol-2-ylidene silver(I) acetate, which is currently under further investigation. Moreover, after identifying Ag(I)-NHC lead structures and subsequently transmetallating them to their ruthenium- and gold-derivatives, four promising Ru(II)-NHC and Au(I)-NHC derivatives have been discovered.

Statement of Original Authorship

I hereby certify that the submitted work is my own work, was completed while registered as a candidate for the degree stated on the Title Page, and I have not obtained a degree elsewhere on the basis of the research presented in this submitted work.

Acknowledgements

First and foremost, I want to thank my supervisor, Dr. Matthias Tacke, for giving me the opportunity to work in his lab. His constant encouragement and the many discussions we had, helped me to grow throughout my 3 years of research and kept me interested in my project.

I want to thank my parents without whom I would not have been able to pursue my studies up to this point. Their unconditional love, encouragement and emotional as well as financial support gave me the assurance that I am never alone, in happy and troubled times, no matter where I am.

My "little" brother who always manages it to bring a smile to my face and who taught me, that it doesn't matter how many miles separate you as long as your hearts are in touch.

All my family members for their constant encouragement.

Many thanks to all past and present co-workers (Siddappa, Brendan, Tony, Grainne) for their help and advice, but especially to Wojtek ("Kiddo") for putting up with me on a daily basis during the last two years.

Also a huge thank you to many groups in the chemistry department and the Conway Institute, particularly the Morgan and Paradisi group for letting me use their equipment and the occasional chemical. Special thanks to Michelle, Lara, A.J., Kev and the ChemSoc committee 2012/13 for funny lunchtimes, daily coffee breaks and the occasional night out.

Additionally, I'd like to thank all the technical staff for help with MS, microanalysis and Helge Müller-Bunz for the X-ray structures.

Lastly, I'd like to thank Zoey and Chrissi for being the best friends one can wish for and who made my life so much richer.

Chapter 1 Introduction

The global burden of cancer continues to increase largely due to the growth and aging of the world population alongside an increasing adoption of cancer-causing behaviours, particularly smoking, in economically developing countries. Based on the GLOBOCAN 2008 estimates [1], about 12.7 million cancer cases and 7.6 million cancer deaths are estimated to have occurred in 2008; of these, 56% of the cases and 64% of the deaths occurred in the economically developing world. Breast cancer is the most frequently diagnosed cancer and the leading cause of cancer death among females, accounting for 23% of the total cancer cases and 14% of the cancer deaths. Lung cancer is the leading cancer site in males, comprising 17% of the total new cancer cases and 23% of the total cancer deaths. Breast cancer is now also the leading cause of cancer death among females in economically developing countries, a shift from the previous decade in which the most prevalent cause of cancer death was cervical cancer [2].

Cancer is a generic term for a large group of diseases that can affect any part of the body. Other terms used are malignant tumours and neoplasms. One defining feature of cancer is the rapid creation of abnormal cells that grow beyond their usual boundaries, and which can then invade adjoining parts of the body and spread to other organs. This process is referred to as metastasis. Metastases are the major cause of death (up to 90%) from cancer [3].

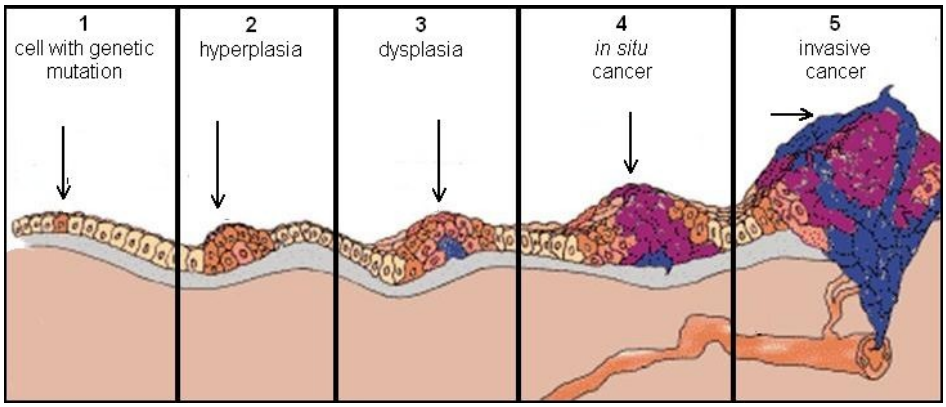

Figure 1.1: Cancer development stages

The development of cancer is shown in Figure 1.1. It results from normal epithelial cells through multiple chromosomal damage (stage 1) and induces stepwise hyper proliferation (stage 2 and 3), adenoma (stage 4) and finally invasive and metastatic carcinoma cells (stage 5). Possible selective external treatment by a drug might occur during stages 2 - 5, but unfortunately until now there are no known tumour therapeutic drugs on the market without any side-effects. Therefore the research on novel target selective anticancer drugs attracts a high level of current interest.

One possible new compound class is coordinated metal ions, based on the knowledge that a wide range of metals play an essential role in biological systems [4]. Metal ions are essential for the function of over one third of all proteins, and are involved in a number of key biological processes including respiration, gene regulation, replication and repair of DNA, antioxidant defence, and neurotransmission, but are in most cases toxic on their own. However, by coordination to organic ligands (mostly by coordinating to C, N, O or S donor ligands) they can become beneficial to the human system. The incorporated organic ligands can contain functionalities capable of influencing the biological activity, lipophilicity and toxicity of the metal compounds. A further tuning factor for the development of novel medical therapeutics exhibiting many different functions is the metal itself with its variable coordination spheres and geometries, kinetic properties, redox activity and potential reactivity with biological ligands. One group of metal coordinating ligands which gained high interest in different fields of research over the past 2 decades are *N*-Heterocyclic carbenes.

1.1 *N*-Heterocyclic carbenes

N-Heterocyclic carbenes (commonly abbreviated as NHCs) are nowadays known for being easy to prepare and to handle, as well as for their versatility and stability, making them an interesting research topic in different fields of chemistry. They mainly find application in catalysis, (e.g. cross coupling reactions [5, 6], lactide polymerization [7], olefin metathesis [8]) and carbene transfer reactions [9, 10] but gained huge interest in the past 20 years as ligands in bioorganometallic and medicinal chemistry [11–16].

1.1.1 Brief history

Interest arose around the topic of NHCs after Wanzlick's report about the α-elimination of chloroform from 1,3-diphenyl-2-trichloromethylimidazolidine [17] in 1960. While obtaining the dimeric entetraamine, Wanzlick was unable to isolate the postulated imidazolidin-2-yildene and cleavage of the entetraamine to yield the free carbene could not be achieved. Moving from the saturated imidazolidine system towards the unsaturated imidazolium compound tetraphenylimidazolium perchlorate, Wanzlick attempted the preparation of the free carbene by deprotonation with KO^{t}Bu. Since it was known that unsaturated heterocyclic azolium cations react in a base-catalyzed H,D-exchange reaction [18, 19], he postulated that the intermediately formed carbene species will be stabilized by the delocalisation of the six π-electrons in this derivative. Wanzlick was not successful in isolating the free carbene, but in 1998 Arduengo *et al.* finally prepared, isolated and characterised crystallographically the desired compound [20] (Figure 1.2).

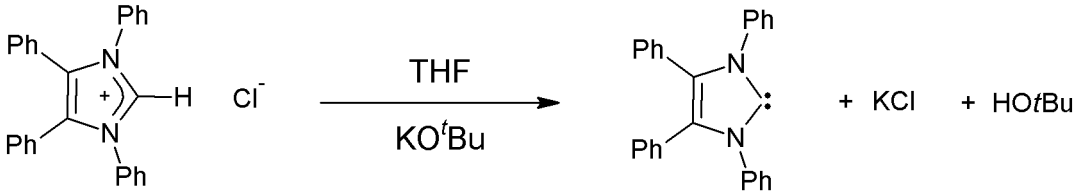

Figure 1.2: Synthesis of the free tetraphenylimidazol-2-ylidene carbene [20]

While as early as 1968 the stabilisation of unsaturated imidazolidin-2-ylidenes in metal complexes was achieved by deprotonating the imidazolium salt in the presence of a suitable coordinatively unsaturated metal complex [21, 22], Arduengo *et al.* were the first to isolate a free *N*-Heterocyclic carbene without forming the olefinic entetraamine. NHCs are strong nucleophiles and bind to both main group and transition metals, often with greater stability than phosphines. Furthermore, for the also very successful phosphine ligand PR_3, a change of R group is the only variable easily controlled by the experimenter, but such a change affects both key ligand properties, steric and electronic. In contrast, these factors are tuneable for NHCs in more ways than just changing the substituents at the heteroatoms N^1 and N^3. Additional R groups can be present at C^4 and C^5, and the

azole can be changed to imidazoline, benzimidazole, triazole or to an oxazole, among many other variants. The steric and electronic tuning is separable to a greater extent in NHCs than in PR_3. Steric effects are predominantly associated with the substituents at the atoms adjacent to the carbene centre and electronic effects are more sensitive to the nature of the azole ring [23, 24]. The stability of the carbene carbon is achieved by the $p\pi$-$p\pi$ electron donation of the two adjacent nitrogen atoms (see Figure 1.3). This accounts for a stabilization energy of approximately 70 kcal/mol, while the aromaticity of unsaturated systems contributes another 25 kcal/mol [25].

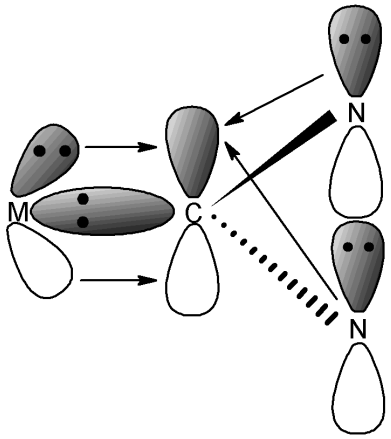

Figure 1.3: NHC to metal centre bonding [26]

Furthermore, inductive stabilisation of the carbene is provided by the lone pair electrons of the nitrogen atoms [27]. Recent structural and theoretical studies suggest the existence of some π-backbonding for certain metal centres, although NHCs are mainly viewed as σ-donors [16]. In 2006 Jacobsen *et al.* carried out a computational study on the π-bonding capability of 36 transition metal NHC complexes for systems in which the formal d-electron count for the transition metal amounts to d^0, d^4, d^6, d^8 and d^{10}. The results of their calculations suggest that the NHC ligand cannot be considered as a pure σ-donor and that even for d^0 systems a considerable amount of π-bonding exists. Additionally, they found that for systems with a low d-electron count both π-donation as well as π-backdonation are of importance while for systems with a high d-electron count backdonation constitutes the major contribution to the π-interaction [28].

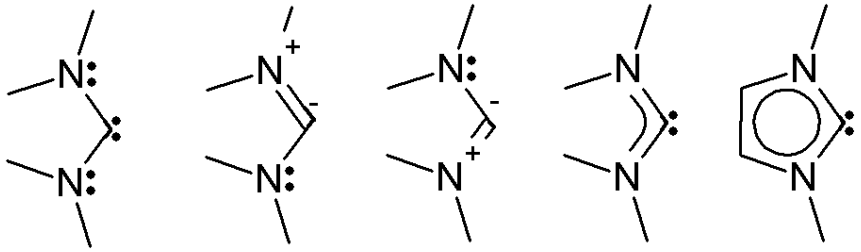

Figure 1.4: Resonance structures on the diamino part of NHCs and aromaticity

Today the most commonly known NHCs are normal *N*-Heterocyclic carbenes (nNHCs) (see Figure 1.4), such as imidazol-2-ylidene, and the next chapters will exclusively deal with this type of NHCs. But there are two other types of NHCs known in literature, namely abnormal (aNHCs) and remote (rNHCs) which were described in detail in a recent review by Crabtree [24].

1.2 Silver complexes in medicinal chemistry

Records of silver being used for its antimicrobial effects date back more than 2100 years where it was first utilized by the ancient Phoenicians, Greeks, Romans and Egyptians to preserve food and water [29]. Silver nitrate was mentioned by Gabor in 702 as a medical agent and Paracelsus applied it as a caustic for the treatment of wounds. During the early pioneer days on the North American continent, when there was no refrigeration and water needed to be transported long distances, it was common practice to drop silver coins into the transport vessel to preserve water. This practice also was used to preserve milk and prevent spoilage, without knowledge that it was the prevention of bacterial growth that caused the effect. Privileged families used silver eating utensils and often developed a bluish-gray discolouration of the skin, thus becoming known as "blue bloods" [30]. Silver nitrate was also used successfully to treat skin ulcers, compound fractures, and suppurating wounds. An important contribution was made in the 1880s by Doctor Carl Siegmund Franz Crede, a German obstetrician, who pioneered the use of silver nitrate eye drops to prevent ophthalmia neonatorum (gonorrheal ophthalmia) in newborn infants [31]. He first used a 2% solution, but this was reduced subsequently to a 1% solution due to irritation caused by higher concentrations. This was a highly effective therapy, reducing the incidence of ophthalmia neonatorum from 7.8% to 0.13% in 13 years. Because of the success of this method, the employment of silver nitrate eye drops in newborn infants was widely accepted throughout the world, and in numerous countries, this therapy was mandated by law and persisted until after the introduction of effective antibiotics. B.C. Crede, a surgeon, is credited with being the first to employ colloidal silver for wound antisepsis in 1891, after observing Halsted applying silver foil to wounds to treat infections [29, 30]. Topical application of silver salts became a common therapy. Crusius used silver nitrate for the treatment of burn injuries in the 1890s, well before its recent rediscovery. Von Naegele realised that the antibacterial effects of silver were attributable primarily to the silver ion, and did systematic studies that led to the finding that silver was an effective antimicrobial agent for almost all unicellular organisms (at least 650 species), but frequently not against mould or parasites [5]. Silver also had another use in medicine during the 19th century, in that Konrad Röntgen discovered in 1895 that

X-rays activated silver halide crystals, making it possible to record radiographic images [32]. Up to now, silver preparations have been used in medicine for treatments of burns, in wound bandage, as silver-coated catheters, and in medical devices. However, silver is not recognized as having any nutritional value. The human body contains minute amounts (< 2.3 µg/l) of silver, with the value higher in persons exposed to silver for long periods [33]. On the one hand it is toxic to pathogen cells because it interferes with metabolic enzymes and DNA replication, but on the other hand it shows low toxicity to humans.

Silver *N*-Heterocyclic carbenes have drawn a lot of attention in the past 20 years due to their successful applications in bioorganometallic chemistry and effectiveness as carbene transfer agents. The extensive investigation of these compounds has led to the discovery of some remarkable biological activity.

1.2.1 Synthesis and Characteristics

The two most widely used routes to synthesise Ag(I)-NHCs are a) the silver base technique or b) the free carbene approach, while the latter is only sparingly used. This might be attributed to the fact that the silver base route, especially by using Ag_2O as the base and simultaneously as Ag source, is very simple. Other silver bases used include Ag_2CO_3 and AgOAc.

The Ag_2O route has many advantages, for example Ag_2O is relatively stable and readily accessible, reactions can be carried out under aerobic conditions at RT, strong bases are not required and solvents do not have to be pre-treated. These factors make this reaction very efficient, although steric hindrance [34–38] of the azolium salt, acidity of the C^2 [39–42] and nucleophilicity of the NHCs [28, 39, 43, 44] have great influence on the feasibility of this reaction.

Figure 1.5 shows the general synthesis scheme for NHC-Ag-halide complexes as well as the different ionic and neutral types of Ag(I)-NHCs which can be produced by the use of mono-azolium halides in the solid state. In addition to mono-azolium salts, various bis-azolium and tris-azolium salts with different linkers in pincer, cyclophane and tripodal architectures react readily with silver oxide but will not be discussed herein.

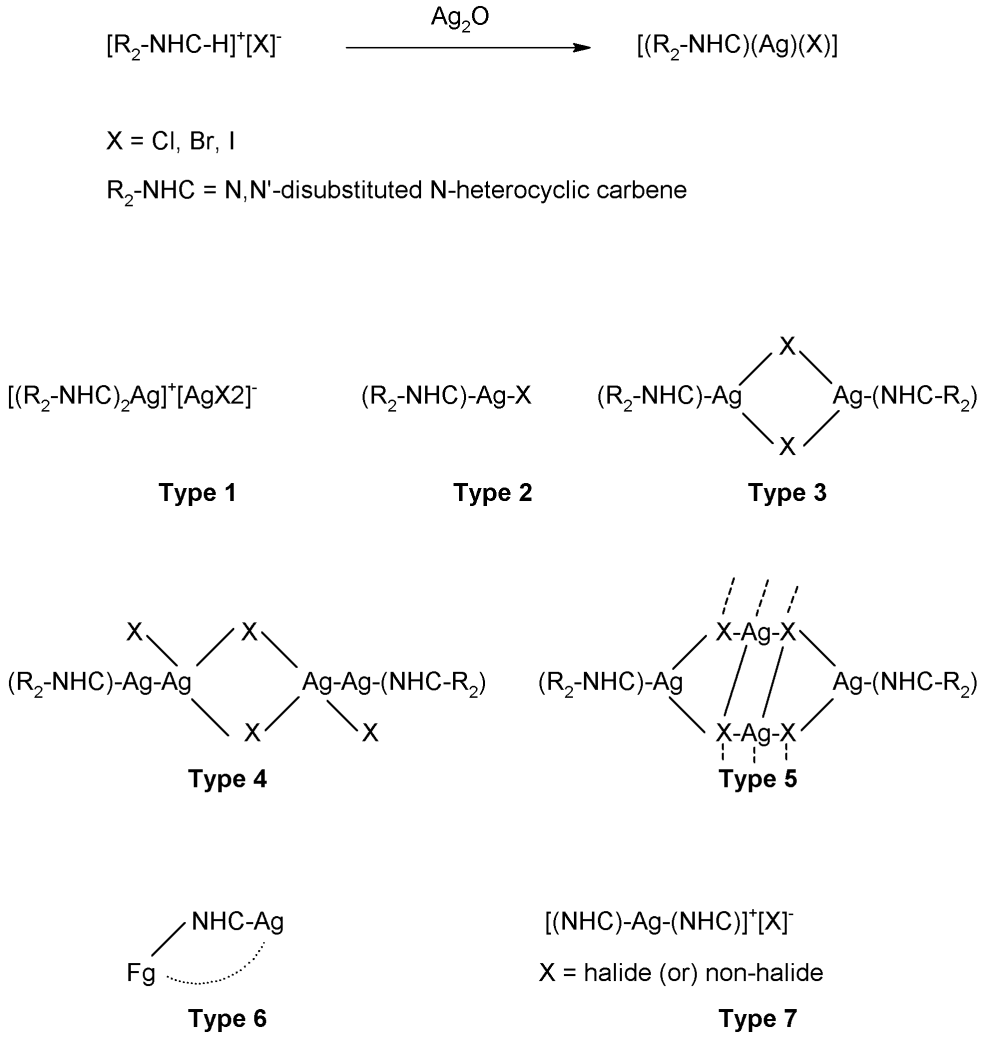

Figure 1.5: General synthesis scheme for NHC-Ag-halide complexes

For *N*,*N*′-dialkyl, *N*,*N*′-diaryl and hetero-disubstituted *N*-alkyl, *N*'-aryl imidazolium chloride and bromide salts the most commonly afforded types of Ag(I)-NHCs are the ionic type 1 or neutral type 2 complexes. The chain length of the azolium halides has direct influence on the geometry of the formed crystals. While short chained azolium halides i.e. (*N*,*N*′-Me_2 or *N*,*N*′-Et_2) imidazolium, benzimidazolium and triazolium chlorides and bromides produce with Ag_2O in CH_2Cl_2 either type 1, 2 or 3 complexes [45, 46], for long chained (C_nH_{2n+1}) azolium chloride and bromide salts (n = 10, 12, 14, 16 and 18) mostly type 3 and type 4 complexes were found [47]. Interestingly, the stoichiometric reactions of long chained azolium [NO_3], [BF_4] and [PF_6] salts produce simple bis-carbene complexes of type 7 [47]. When mono-azolium salts (both halide and non-halide)

with functional groups at one or two N-side arms were employed to react with Ag_2O, the Ag(I)-NHCs were also isolated as type 1 ion-pair, type 2 mononuclear neutral complexes, type 3 halide bridged complexes, type 4 $Ag_2X_4^{2-}$ bridged tetranuclear complexes, and type 7 bis-carbene complexes [42, 48–50]. A type 5 Ag(I)-NHC was only observed when using *N*-Me-*N'*-anthracenyl substituted imidazolium iodide in CH_2Cl_2 [51] and evidence for type 6 halide free Ag(I)-NHC-alkoxyl complexes obtained by the reaction of alcohol functionalized imidazolium halides with Ag_2O leading to the deprotonation of both C^2-H and -OH protons were described based on the observations of EA and NMR data only [50].

It was observed by several groups that if the synthesis is conducted in the presence of excess Ag_2O and / or for longer reaction times, sometimes the solution turned yellow and a silver mirror in addition to a brown powdery solid formed in the reaction vessel. UV/Vis spectra of the yellow solution showed intense surface plasmon resonance (SPR) bands at ~ 426 nm, suggesting the formation of silver nanoparticles which can be removed by the addition of activated carbon [52].

In general, the formation of the Ag-C bond is clearly indicated by a shift in the ^{13}C NMR spectrum with δ values ranging from 170.0 ppm up to 234.0 ppm for the carbene as well as the disappearance of the C^2 proton in the ^1H NMR. The same behaviour is observed when obtaining NHC-silver acetate complexes by reacting azolium halides with silver acetate. This reaction route is very successful and efficient and has been used by several groups, e.g. Tacke [53–57], Youngs [58, 59] and Cowley [60].

Apart from these techniques, reactions of azolium salts with Ag_2CO_3 [61] or with Ag(I) salts under phase transfer conditions (PTC) [45, 62] or by transmetallation from other metal-NHCs were also reported [63].

1.2.2 Biological evaluation and possible applications

The discovery and use of penicillin and sulfonamide antibiotics lead to near abandonment of silver and its related compounds in most parts of the world for 40 years after World War II [64]. The emergence of resistant strain organisms such as methicillin-resistant *Staphylococcus aureus* (MRSA) and multidrug-resistant

Pseudomonas aeruginosa to penicillin and sulfonamide drugs led to the need for new antibiotics. The renaissance of silver has been credited to Moyer *et al.*, for reviving the use of silver nitrate in the 1960s. This led to the introduction of silver sulfadiazine (Figure 1.6) in 1968, which has been found to be efficacious for topical application. It is used for the treatment of burn wounds and was designed to combine the antibiotic sulfadiazine, with silver in order to obtain a wide spectrum antibiotic. It is a water insoluble complex and is polymeric in the solid state [65].

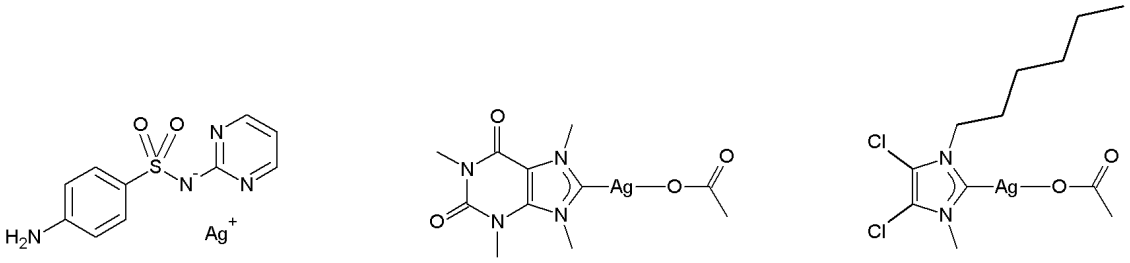

Figure 1.6: Silver sulfadiazine, SCC1 (Silvamist) and SCC10

Silver sulfadiazine has been shown to be effective against a number of gram-positive and gram-negative bacteria, and is marketed as a water soluble cream, Silvadene® Cream 1%. It remains one of the most widely used antimicrobials for infections associated with burns. Silver has been introduced into wound dressings in the form of organic and inorganic silver compounds and as silver metal, usually in the nanocrystalline form. The aim of the silver containing dressings is not only the sustained release of silver to the wound site creating a barrier for infection, but also ease of use, management of wound exudates and provision of moisture required for optimal wound healing. Silver has been impregnated in several different kinds of dressing materials including nylon fabrics, meshes, biodegradable collagens, low adherent materials, carbon fibres, and hydrofiber alginates. Such silver containing dressings have been used in the treatment of acute and chronic wounds, leg ulcers and several degrees of burn wounds [66, 67].

Two other successful silver containing antibacterial drugs are the small-molecule silver(I) carbene complexes, SCC1 (or Silvamist) [58] and SCC10 [68] (see Figure 1.6), which show promising activity for the treatment of pulmonary

infections via inhalation. To achieve clinical utility, a nebulised silver compound must demonstrate efficacy against respiratory pathogens without toxicity to the host. The toxicity of silver compounds can often be linked to the carrier molecules and therefore Cannon *et al.* designed these new silver-based antimicrobials by coordinating the bioactive metal to a nontoxic carrier. SCC1 and SCC10 were tested extensively *in vitro* for their antibacterial activity against a panel of highly resistant opportunistic pathogens recovered from the respiratory tract of patients with cystic fibrosis. SCC1 was as well tested against *E. coli* J53 strains with and without the silver resistance plasmid pMG101 and it showed MIC values between 1 and 8 µg / mL against all pathogens, but did not show any activity against the silver resistant strain of *E. coli*. Furthermore, *in vivo* studies on mice bearing a *P. aeruginosa* infection were carried out with SCC1 to find a 100% survival rate [69]. Since Silvamist and SCC10 are easily nebulised or aerolised, therapeutic outcomes with higher local drug concentration due to high doses delivered to the lung, a proportionally lower systemic drug concentration, and therefore decreased systemic toxicity can be achieved. However, the small size of SCC10 and its quick diffusion across lung epithelium results in rapid clearance from the lungs following administration. Resulting from these findings the efficacy of inhaled nanoparticles loaded with SCC10 is currently under investigation. First results showed that core-loaded and dual-loaded shell cross-linked nanoparticles (SCK NPs) are effective against the cystic fibrosis relevant bacteria *P. aeruginosa* due to the ability of these nanoparticle formulations to provide a sustained release of the encapsulated silver carbene complex [70]. This approach seems to be a promising step towards an efficient antibacterial treatment for patients with cystic fibrosis.

A further approach to overcome side-effects like skin discolouration or too quick release of silver exhibited by commercially available silver containing antimicrobials was made by Youngs *et al.* by synthesising pyridine linked pincer NHC-silver complexes [71, 72].

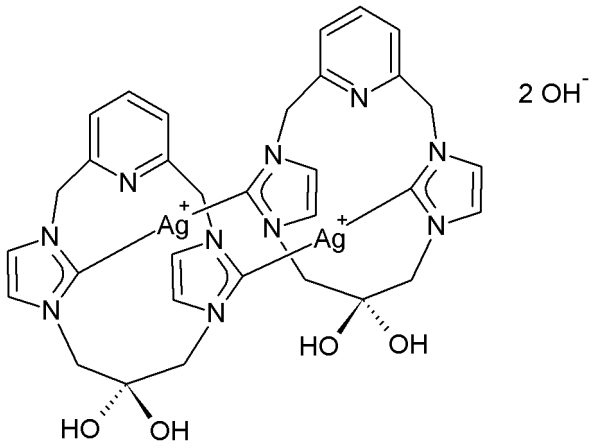

Figure 1.7: Pyridine linked pincer NHC-silver complex (Py-NHC-Ag)

Their lead compound Py-NHC-Ag (Figure 1.7) was encapsulated into an electrospun polymer mat (Tecophilic®) and the antimicrobial activity of this mat was investigated against the bacteria *E. coli*, *P. aeruginosa*, *S. aureus* and the fungi *Candida albicans* (*C. albicans*), *Aspergillus niger* (*A. niger*) and *Saccharomyces cerevisiae* (*S. cerevisiae*). The encapsulated Py-NHC-Ag complex showed promising activity against the bacteria with complete killing of bacteria for days with the addition of a constant volume of freshly grown organisms on a daily basis at a concentration of 140 µg / mL ($[Ag^+]$ = 140 µg / mL, 25 wt. % Py-NHC-Ag - 75 wt. % Tecophilic®). Encapsulation of the silver-NHC complex increased the antimicrobial activity compared to 0.5% silver nitrate and 1% silver sulfadiazine by enabling a slower release of active silver species, which may consist of silver cations, nano-sized silver particles, clusters of silver cations, anionic silver chloride complexes and silver chloride. The fibres of the polymeric mat also provided a greater surface area for the efficiency of the silver [73].

Besides the antimicrobial activity of silver, a lot of interest arose around the possible anticancer properties of silver complexes during the last years. Some of them exhibited antitumor activity *in vitro* and *in vivo*, for example silver complexes derived from coumarin [74] exhibited antitumor activity against certain types of cancer and silver carboxylate dimers [75] possessed antitumor potency. Moreover, some silver complexes with phosphine ligands could even inhibit cisplatin-resistant cell lines and a novel hydrogen bonded bimetallic supramolecular coordination

polymer $[SnMe_3(bpe)][Ag(CN)_2] \cdot 2H_2O$ showed specific *in vivo* and *in vitro* antitumor effects [76]. What all silver complexes seem to have in common is the mode of action which involves the slow release of Ag^+ ions that enter cell membranes and disrupt their function. However, the big problem with the existing silver drugs (such as silver sulfadiazine) is that they lose their effects quickly due to rapid release of the Ag^+ ions. Thus, it is important for silver to form complexes with strongly coordinating ligands which can prevent the quick release of silver and NHCs seem to be a good choice.

Nevertheless, the first reports on the evaluation of anticancer activity of NHC-Ag(I) complexes only occurred in 2008 and are still relatively rare. The group of W. Youngs reported the anticancer activities of several monomeric and dimeric imidazol-2-ylidene and 4,5-dichloroimidazol-2-ylidene silver acetate complexes (**Ag1-5**, Figure 1.8) [77, 78]. Complex **Ag-1** proved to be not stable enough to be evaluated but the IC_{50} values of **Ag-2** and **Ag-3** were found to be in the same range like cisplatin against OVCAR-3 (ovarian) and MB157 (breast) cancer cells and only little activity against HeLa (cervical) cells was observed. On the other hand the dimeric complexes **Ag-4** and **Ag-5** are 10 fold less active against cisplatin than against H460 (lung) cancer cells and no significant activity was observed against HeLa cells.

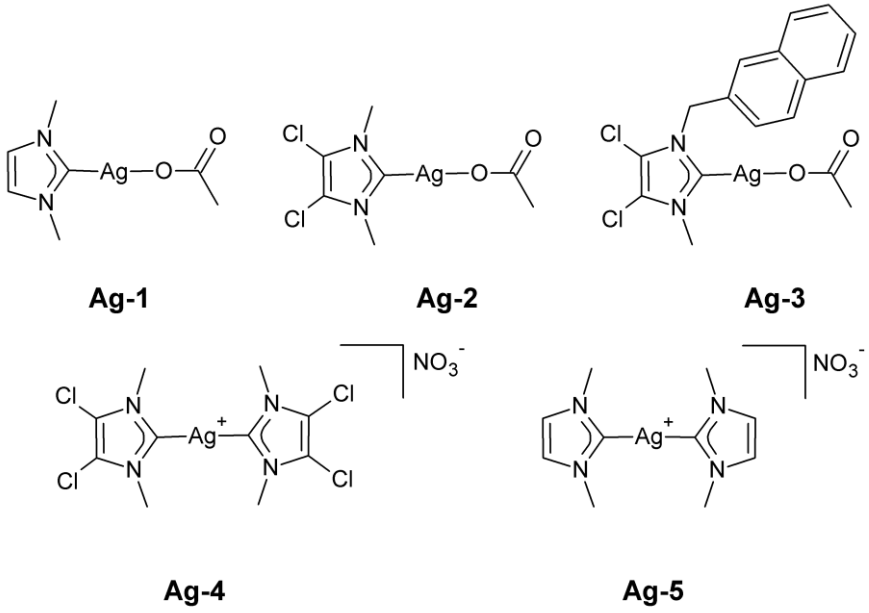

Figure 1.8: Structures of Ag-NHCs **Ag1-5**

Gautier *et al.* and Roland *et al.* reported the IC_{50} values of **Ag-6** to **Ag-9** against MCF-7 (breast) cancer cells and MCR5, a non-cancerous cell line in rapid proliferation and EPC, a quiescent cell line. A 350-fold increase in activity if compared to cisplatin was found against MCF-7 for **Ag-9** and the compound remains until now the most active NHC-Ag(I) complex. However, no discrimination between cancerous and non-cancerous cells in rapid proliferation could be found. The activity seems to be directly correlated with the proliferation rate, since it was shown that the NHC-Ag(I) complexes displayed a 2- to 18-fold lower cytotoxicity for the quiescent EPC cell line [79, 80].

Li *et al.* studied the cytotoxic behaviour of an amino-linked heterocyclic silver (I) bromide complex (**Ag-10**, Figure 1.9) against the human breast cancer cell lines MCF-7 and MDA-MB-231 as well as the glioblastoma cells U-87 MG. In comparison to cisplatin it showed similar activity but the investigated Au and Pd analogues showed much better activity [81].

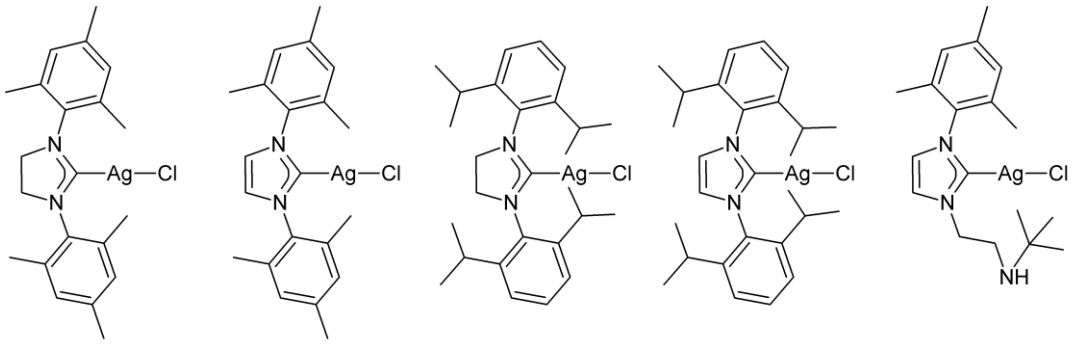

Ag-6 **Ag-7** **Ag-8** **Ag-9** **Ag-10**

Figure 1.9: Structures of Ag(I)-NHCs **Ag-6-10**

Between 2010 and 2011 our group reported the synthesis, characterisation and evaluation of the anticancer activity of over 30 NHC-silver(I) acetate complexes against the human renal cancer cell line Caki-1 (**Ag-11a** to **Ag-18e**, Figure 1.10).

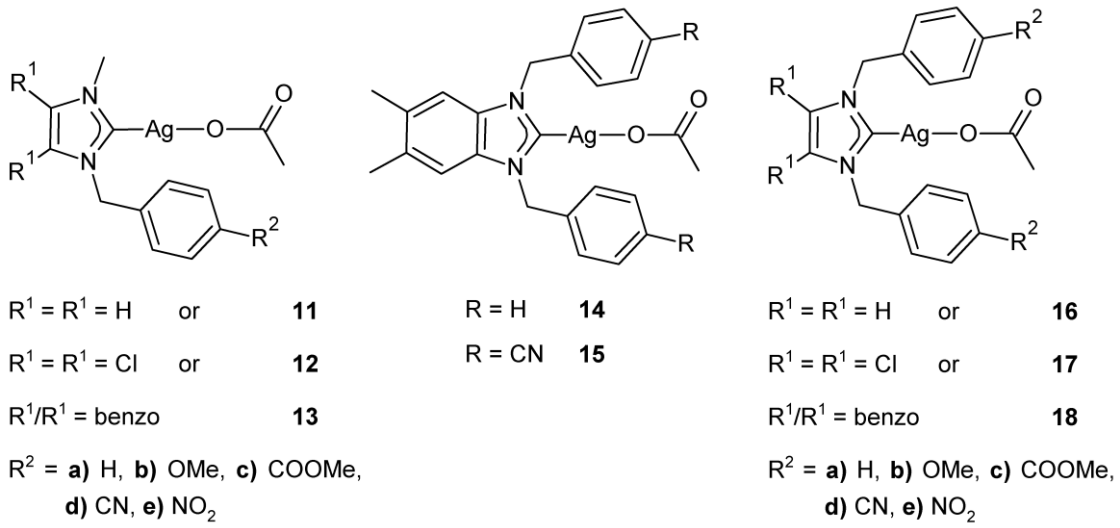

Figure 1.10: Structures of Ag(I)-NHC complexes **Ag-11** to **Ag-18**

In these studies several complexes were found to exhibit activity in the same range or up to 3-fold higher activity than the one of cisplatin (3.3 µM) against Caki-1. **Ag-11a** and **Ag-11c** exhibited values of 3.2 (± 0.6) and 3.3 (± 0.4) µM while **Ag-16a** showed better activity against Caki-1 than cisplatin with an IC_{50} of 2.5 (± 3) µM. However, **Ag-13d**, better known by now as SBC1 showed superior activity with a value of 1.2 (± 0.6) µM against the tested cancer cell line. This led to further investigations into the possible mode of action and *in vivo* testing of the complex which will be discussed later (see chapter 6).

1.3 Gold in medicinal chemistry

Gold has a long known history of being used in medicinal application. Already in 2500 BC the practice of medicine in China was influenced by the "power" of metallic gold. Colloidal red gold, called "Swarma Bhasma", was used in the form of Ayurvedic medicine for rejuvenation and revitalization during old age in India [82, 83]. People who were suffering from nervous disorder were treated for revitalisation for a long time with a gold based drug called "nervin" [84] and in the 16th century, gold was recommended for the treatment of epilepsy [85] for which Paracelsus created a potion called *Aurum Potabile*. Also Arabic and medieval physicians experimented with soluble gold, mainly chlorides which were given orally as part of the "Keeley cure" for alcoholism in the late 1800s. Even the first edition of the Merck Manual in 1899 lists gold chloride for the treatment of tuberculosis and lupus, while gold bromide is mentioned as a treatment for epilepsy and migraine [86]. When Robert Koch discovered the bacteriostatic effect of gold cyanide on *Mycobacterium tuberculosis*, the therapeutic use of gold was established for the first time and the medicinal use of gold for the treatment of tuberculosis was introduced in the 1920s [85]. The main application of gold and gold compounds is its use as drugs for the treatment of rheumatic diseases including psoriasis, palindromic rheumatism, juvenile arthritis and discoid lupus erythematosus [87, 88]. Sodium aurothiomalate and aurothioglucose are just two examples for the treatment of rheumatoid arthritis, but long and extensive exposure of the human body to these gold thiolate drugs can lead to severe side and adverse effects. The gold can accumulate in liver, kidney and spleen while higher concentrations of gold in the kidneys may cause nephrotoxicity. Furthermore skin irritation, liver toxicity, blood disorders and mouth ulcers have been reported [89]. To avoid this toxicity and poor pharmacokinetics, safer and superior second generation drugs like e.g. auranofin (see 1.3.2) or Au-*N*-Heterocyclic carbene complexes had and still have to be developed.

1.3.1 Synthesis and Characteristics

The first report of Au-NHC complexes has been made by Lappert's group in 1974, where they synthesised complexes of the type $[Au(NHC)_2][anion]$ from electron-rich olefins [90] and in the same year Fehlhammer *et al.* described the generation of Au(I)- and Au(III)-NHC complexes through spontaneous cyclisation of isocyanide ligands [91]. In 1989 Au(I)-NHC complexes were isolated through reaction of $[Au(PPh_3)Cl]$ with lithiated benzimidazoles, followed by [92] and later Raubenheimer *et al.* were able to extend this strategy to form *N*-alkyl-substituted Au(I)-NHC complexes [93]. Via oxidative addition of halogens they gained access to Au(III)-NHCs from the corresponding Au(I)-NHCs [94]. The unexpected formation of a Au(I)-NHC complex form the addition of tetrachloroaurate to tris(4,5-dimethylimidazol-2-yl)phosphine was described by Lock *et al.* [95] while Lin and co-workers obtained the first series of liquid crystalline Au(I)-NHC compounds by reacting long chain substituted N,N'-dialkyl-benzimidazolium salts with $[Au(SMe_2)Cl]$ under basic phase transfer conditions in 1997 [96]. A year later they developed a technique to gain access to Au(I)-NHCs by using Ag(I)-NHCs as carbene transfer agents [45]. This technique is nowadays the most used technique to synthesise non-silver metal-NHC complexes.

Au-NHCs are synthesised in general by applying one of the following methods: i) cleavage of electron-rich double bonds, ii) protonation or alkylation of gold carbeniate compounds, iii) transfer of NHCs from group 6, 7 or 11 complexes, and iv) reaction of Au(I) sources with free NHCs. Method i) has been employed in a few cases up to 2004 and method ii) involves two sequential steps where first Au(I)-carbeniate complexes are formed by the reaction of Au(I) sources with lithiated azoles which are subsequently protonated or alkylated to produce Au(I)-NHC complexes. In the most common third method some metal-NHCs, mainly Ag(I)-NHCs, can react with Au(I) sources to form Au(I)-NHCs. Method iv) utilizes free carbenes which can be prepared *in situ* by reacting azolium salts with a strong base or which have been isolated before and reacting these directly with Au(I) sources. As for the Ag(I)-NHC complexes the formation of the Au-C bond is indicated by a shift in the ^{13}C NMR with δ values ranging from 156.3 to 252.2 ppm and the loss of the C^2-H signal in the ^1H NMR spectrum. Similar to the Ag(I)-NHCs the Au(I)-NHCs can be classified as neutral, ionic, multinuclear and other types of

bonding, with neutral and ionic bonding modes being the most common. The most usual types of Au-NHCs are depicted in Figure 1.11.

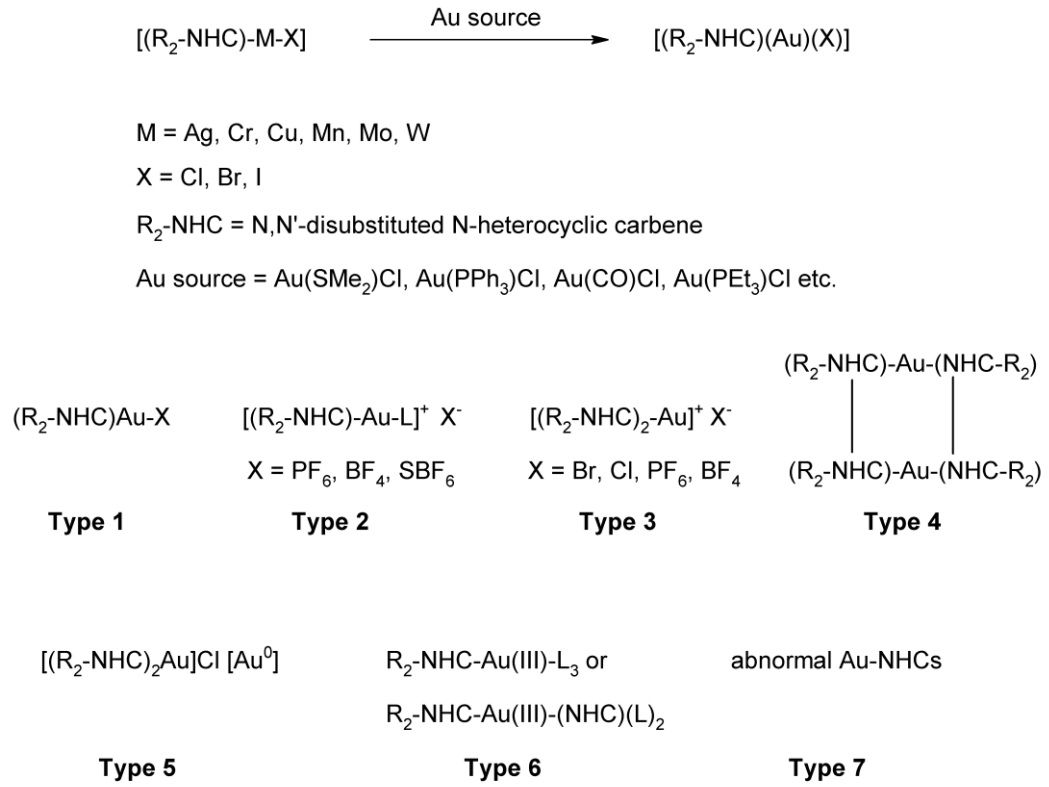

Figure 1.11: General synthesis scheme for NHC-Au-X complexes

Reacting one equivalent Au source directly with one equivalent [NHC-AgX] gives in most cases Au(I)-NHC complexes of type 1, while type 2 complexes can be obtained by further reacting type 1 Au(I)-NHCs with e.g. PPh_3 in the presence of KPF_6 [97] , or with $AgBF_4$ and $AgPF_6$ in acetonitrile [98]. By employing the free carbene route, direct reaction of $Au(SMe_2)X$ [X = Br, Cl] with two equivalents of the appropriate imidazolium salt in the presence of base gave cationic complexes of type 3 [99], but also utilizing the Ag-carbene transfer route, reacting two equivalents of the corresponding [Ag(NHC)Cl] compounds with $[Au(SMe_2)Cl]$ resulted in complexes of this type [100–103]. Multinuclear Au-NHCs of type 4 or higher nuclearity and even heteronuclear (Au(I) and Ag(I)) complexes mostly show Au(I)···Au(I)/Ag(I) interactions and exhibit luminescence properties. Dinuclear complexes are either obtained by directly reacting $Au(SMe_2)Cl$ with the corresponding cyclo-bis-imidazolium salt in the presence of mild base Na(OAc)

[104] or by the Ag-carbene transfer route, in which the Ag(I)-NHCs were generated *in situ* [105] or prior isolated [103, 106]. Examples of Au(III)-NHC complexes (type 6) are relatively rare and until 2008 only the oxidation of [Au(NHC)Br] complexes with Br_2 [107] or $[Au(NHC)_2]^+$ complexes with I_2 [108] were reported, but in 2012 Jiang *et al.* successfully synthesised and characterised a stable Au(III)-NHC from the reaction of an azolium salt with $[NaAuCl_4 \cdot 2H_2O]$ [10]. Fischer *et al.* as well as Bertrand's group have reported the formation of abnormal Au-NHCs (type 7). While Fischer *et al.* attempted the transfer of pyrazolin-3-ylidene and pyrazolidin-3-ylidene carbene ligands from chromium to a Au(I) source [109], Bertrand's group developed a whole new class of unusual metal-NHC complexes. These complexes are obtained by reacting free cyclic (alkyl)(amino)carbenes with $Au(SMe_2)Cl$ and are very useful catalysts in many organic transformations [110].

Interestingly, in 2003 Herrmann *et al.* reported the synthesis of the first Au(I)-NHC complex containing a Au-O bond by reacting (1-diphenylmethyl-3-methylimidazolin-2-ylidene) gold(I) chloride with silver acetate to form the NHC-Au(I) acetate complex [111]. The only other publication which is dealing with gold acetate complexes covers the synthesis of bipyridine- and phenanthroline-Au(III) acetates [112], leaving a lot of room for further synthesis, characterisation and biological evaluation of this novel compound class.

1.3.2 Biological evaluation and possible applications

One of the currently best studied gold based complexes in medicine is the thioredoxin reductase (TrxR) inhibitor auranofin and some of its derivatives (see Figure 1.12). 30 years ago, it was originally developed for the treatment of rheumatoid arthritis as a substitution for the injectable gold compounds aurothiomalate and aurothioglucose, but despite its efficacy in the treatment of both rheumatoid arthritis and psoriasis, auranofin is seldom used since more novel anti-rheumatic medications have become available. Nevertheless, the interest in potential new applications of auranofin never died and during the last years more

and more insight was gained into the possible treatment of other diseases with auranofin.

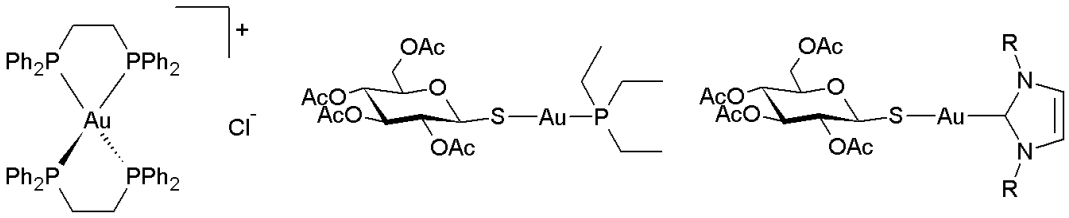

Figure 1.12: [Au(dppe)]Cl, Auranofin and NHC-Auranofin analogues

Klegeris *et al.* [113] recently summarized the vast studies on the biological activity of auranofin. Besides the anti-neoplastic, anti-parasitic, anti-bacterial and anti-viral activity of auranofin also its cytoprotective effects have been studied. It was found that auranofin shows a good balance between anti-inflammatory and protective activities, which makes it a good candidate for the treatment of several diseases associated with inflammation and tissue damage [114, 115]. Many of the currently available anti-inflammatory treatments stop inflammation without inducing protective mechanisms that enhance recovery which makes the potential cytoprotective effects of auranofin particularly exciting. Achieving a balanced inflammatory response by reducing several protective pathways is the aim of a new therapeutic approach in which auranofin may play a role [116]. The reclassification of auranofin as an "orphan drug" to promote its use as a treatment for parasitic infections and the Phase II clinical trial for auranofin in the treatment of chronic lymphocytic leukaemia were pushed by recent studies on the anti-tumour, anti-parasitic and anti-microbial activities of auranofin (clinicaltrials.gov and [117]). Furthermore the drug is now under investigation as a means of reducing the viral reservoir of HIV that lies latent in the body's T-cells. A reintroduction of auranofin in the treatment of inflammatory arthritis might be on its way due to the identification of novel mechanisms of action combined with an acceptable clinical safety profile for this compound [118]. Besides these findings, structure-activity relationship studies on auranofin and Et_3PAuCl have been carried out and indicated that the phosphine ligand is more important for the

biological potency than the halide or the thioglucose and no loss of antitumor activity was observed by exchanging these ligands [119, 120].

During the past 7 years a considerable amount of reports on potential new Au(I/III)-based anticancer drugs with micro- to nanomolar cytotoxic activity has been published. In this work the focus will lay solely on novel monomeric, mononuclear, dinuclear, neutral and cationic Au(I)-NHC and Au(I)-bis(NHC) complexes.

One alternative to the use of phosphines are NHCs and in the last years considerable interest has arose around these ligands for the synthesis of biological active Au(I) complexes. Berners-Price *et al.* reported dinuclear Au(I)-bis(NHC) complexes which induced mitochondrial permeability transition in isolated rat liver mitochondria. In order to adjust the lipophilic character of the complexes, a critical factor for targeting malignant cells, the wingtip groups were adjusted and a further mononuclear, linear, cationic Au-NHC complex series was synthesised leading to Ca^{2+}-sensitive anti-mitochondrial effects. The Ca^{2+}-sensitive mitochondrial swelling is highly influenced by the lipophilicity of the Au(I)-complexes and therefore the fine-tuned bis(1,3-diisopropyl-2H-imidazole-2-ylidene) gold(I) bromide complex (Figure 1.13, **Au-1**), showing intermediate lipophilicity and significant anti-mitochondrial activity was selected for further studies. Apoptosis induction via the activation of Caspase 9 and Caspase 3 in cancer cells as well as selective inhibition of TrxR activity but not GR activity in MDA-MB 231 cells and accumulation in mitochondria was found for the above mentioned compound. Since dinuclear Au(I)-NHCs show luminescence associated to their aurophilic interactions, it was used to visualize (via FCM) the intracellular distribution of two Au(I)-bis(NHC) complexes. The obtained images of mouse macrophage cancer cells showed intracellular localization to lysosomes of one complex while the cell morphology was preserved [97, 99, 104, 121–123].

In 2008 Raubenheimer *et al.* synthesised a bis-ferrocenylcarbene Au(I) complex (Figure 1.13, **Au-2**) with the aim to target mitochondria. While they found enhanced antitumor activity compared to cisplatin against two cancer cell lines, it remained unclear if this was due to the presence of the ferrocenylgroups [102].

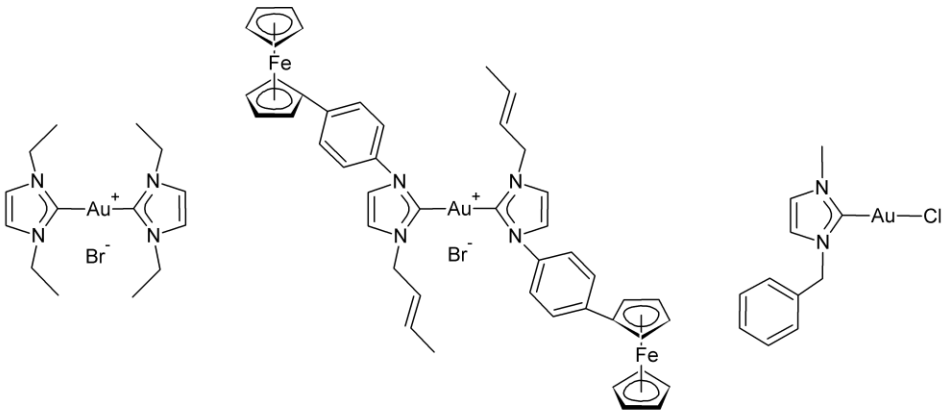

Figure 1.13: Structures of Au-NHC complexes **Au-1, Au-2** and **Au-3**

Barrios *et al.* synthesised a series of Au(I)-NHCs with the aim to find new potential targets for cancer treatment, in this case the inhibition of cysteine-dependent protein tyrosine phosphatases (PTPs). PTPs have shown to be involved in numerous diseases including cancer and therefore this family of enzymes became of interest. In a comparative study with auranofin, the new developed monomeric, neutral Au(I)-NHCs inhibited PTP activity in Jurkat T leukaemia cells and primary mouse thymocytes. (1-methyl-3-benzyl-imidazole-2-ylidene) gold chloride (Figure 1.13, **Au-3**) was an even better inhibitor of PTP than auranofin with an IC_{50} range from 10 to 40 mM on four PTP types [124].

Extensive studies on the structural optimisation and identification of possible targets of Au(I)-NHCs have been carried out by Ott *et al.* A series of benzimidazole-2-ylidene gold(I) complexes have been synthesised based on the gold phosphole complex GoPI (chloro[1-phenyl-2,5-di(2-pyridyl)-phosphole] gold(I)) in the active site of GR and they showed selective TrxR inhibition as well as anti-proliferative effects in cancer cells. Unfortunately, no selectivity towards tumour cells over non-tumour cells (HEK-293 and HFF) was observed as well as no improvement of activity with enhanced lipophilicity and / or surface volume of the side arms in position 1 and 3 of the benzimidazole. Comparison of the corresponding free ligand with the (1,3-diethyl-benzimidazole-2-ylidene) gold(I) chloride complex (Figure 1.14, **Au-4a**) showed that the biological activities, namely i) high increase of ROS formation, ii) apoptosis induction, iii) inhibition of mitochondrial respiration and iv) activity against resistant cell lines, are dependent

on the presence of the Au(I) centre. Moving on from monomeric, neutral Au(I)-NHCs to cationic $[NHC\text{-}Au(I)\text{-}X]^+$ (X = NHC or triphenylphosphine) complexes (Figure 1.14, **Au-4b** and **Au-4c**) led to general improved cytotoxic properties, an increase in cellular uptake, induced mitochondrial accumulation and alternate reactivity towards the target enzyme TrxR [125].

On the search for metal-NHCs with targeted drug delivery routes, Metzler-Nolte *et al.* developed a series of Au(I)- and Au(III)-NHCs bearing cysteine thiolate ligands (Figure 1.14, **Au-5a** and **Au-5b**). These metal-bioconjugates showed similar biological activity if compared to the Au(I)-NHCs without cysteine-derived ligands which shows that the activity as well as pharmacokinetic properties of Au-NHC complexes can be varied and optimized by choosing the appropriate oxidation state of the metal core and ligand system.

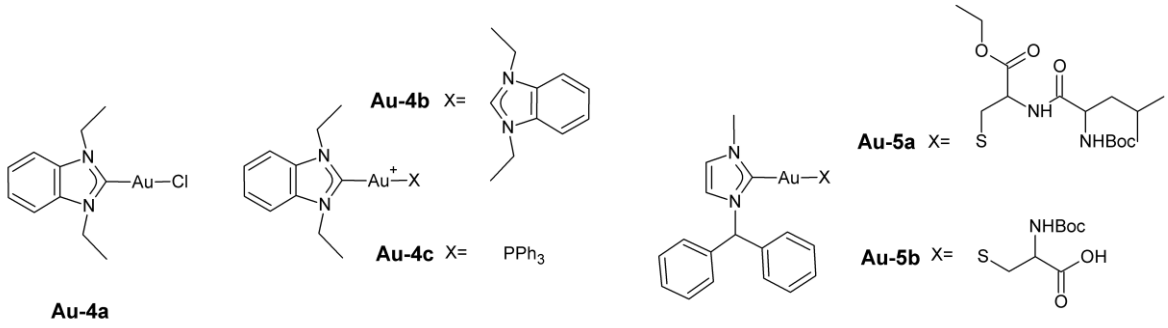

Figure 1.14: Structures of Au-NHC complexes **Au-4a-c** and **Au-5a** and **Au-5b**

Unfortunately, Au(III) complexes are often instable under physiological conditions, but Che *et al.* reported a series of stable Au(III)-NHC-X complexes (X = 2,6-diphenylpyridine or 2,4-diphenyl-6-thiophen-2-yl-pyridine) of which the Au(III) complex containing a 2,6-diphenylpyridine and 1,3-dimethylimidazole-2-ylidene ligand (Figure 1.15, **Au-6**) was selected for several *in vitro* and *in* vivo studies. It showed 18- to 28-fold higher cytotoxic activity than cisplatin against hepatocellular carcinoma (HepG2), cervical epithelioid carcinoma (KB and KB-CPT-100), non-small lung carcinoma (NCI-H460) and nasopharyngeal carcinoma (SUNE1) cell lines and 167-fold higher activity towards non-small lung carcinoma cells (NCI-H460) than against normal lung fibroblast cells (CCD-19Lu). Evaluation of its *in vivo* activity against hepatocellular carcinoma (PLC tumour) in nude mice

displayed significant tumour suppression (47%) compared to the vehicle control at a dose of 10 mg per kg per week for 28 days. Additionally, no apparent toxic side effects including death and weight loss in the mice were observed during the treatment [126].

In 2011 Nolan *et al.* synthesised two series of neutral and cationic Au(I)-NHC complexes and the *in vitro* test against the prostate carcinoma (LNCaP) and breast cancer (MDA-MB-231) cell lines showed higher activity of the cationic species (Figure 1.15, **Au-7**) compared to the neutral complexes [127].

This pattern was also observed by Ott and co-workers [125] and is most likely due to apoptosis induction in the cancer cells via the mitochondrial apoptotic pathway caused by the cationic species. One Au(I)-NHC complex (Figure 1.15, **Au-8**), as well as its Pd and Ag analogues, has been synthesised, characterised and biologically evaluated by Li and co-workers. The compound showed selective activity against the human glioblastoma-astrocytoma, epithelial-like cell line U-87MG, but did not inhibit TrxR indicating that it might trigger apoptosis via a DNA dependent mechanism and it was later found that apoptosis was triggered through a p53-bak pathway. Moreover the complex might mediate S-phase arrest through downregulation of cyclin A and B1 and cdk2 and it has influence on negative regulation of p21, which gives it therapeutic potential in the treatment of glioblastoma in the case of p21-dependent resistance of p53-induced apoptosis [81].

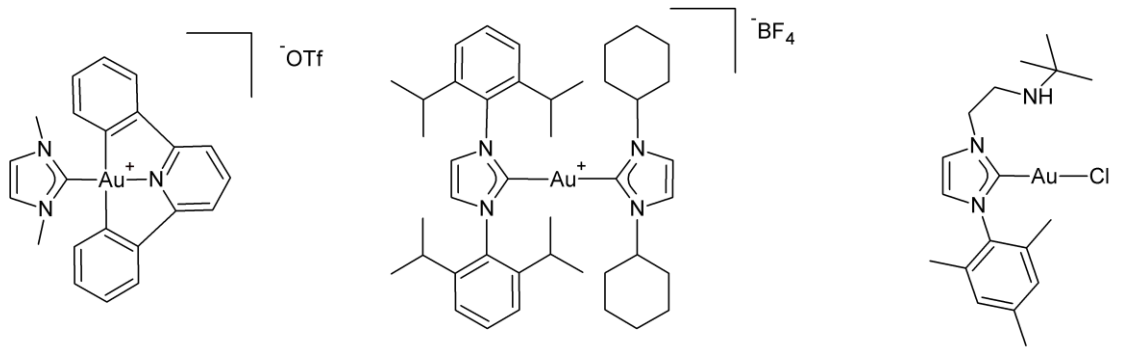

Au-6 **Au-7** **Au-8**

Figure 1.15: Structures of Au-NHC complexes **Au-6**, **Au-7** and **Au-8**

Gust *et al.* synthesised several mononuclear, neutral Au(I)-NHC and neutral as well as cationic Au(I)-bis(NHC) series and evaluated them for their cytotoxic activity against two human breast cancer cell lines (MCF-7 and MDA-MB-231) and the human colon cancer cell line HT-29. Furthermore their potential as TrxR and COX-1 enzyme inhibitors and binding to ER and DNA were investigated. Some Au(I)-NHC complexes were more active than Et_3PAuCl and cisplatin and as active as auranofin against the three cancer cell lines and (1,3-diethyl-4,5-di(*p*-fluorophenyl)-imidazole-2-ylidene) gold(I) bromide exhibited distinctly higher anti-proliferative potency than cisplatin. While all complexes showed TrxR inhibition, no SAR was found and with the missing correlation with cytotoxic properties involvement of further targets was indicated. DNA binding and interference in the hormonal system was excluded based on the investigations on cellular and nuclear uptake and binding to the ER. Nevertheless the most active complex showed selective inhibition of the COX-1 enzyme and might open new perspectives for targeted Au(I)-NHCs. The Au(I)-bis(NHC) complexes displayed increased cytotoxic activity if compared to the Au(I)-NHC complexes against all three cancer cell lines, but was independent of the anionic counter ion or the oxidation state of the metal. If compared to the non-metal containing NHCs it was clearly shown that the gold centre is responsible for the high cytotoxic activity of these complexes. Also the exchange of the bromide ligand for triphenylphosphine or a further NHC ligand showed remarkable influence on the anti-tumour potency of these complexes, leading to low nanomolar IC_{50} values. Despite these findings, preliminary studies on the mode of action indicated only marginal activity at the TrxR and COX-1 inhibition as well as the ER binding [128–130].

Besides classical benzimidazole-derived NHC ligands, Huynh *et al.* also investigated a series of Au(I) and Au(III) mono-, homobis- and heterobis(carbene) complexes with nonclassical pyrazole-derived NHC ligands. Again, the cationic Au-bis(NHC) complexes (Figure 1.16, **Au-10a** and **Au-10b**) showed higher activity against non-small lung cancer cells (NCI-H1666), with IC_{50} values in the nanomolar range, than the neutral Au-NHC complexes and cisplatin [131].

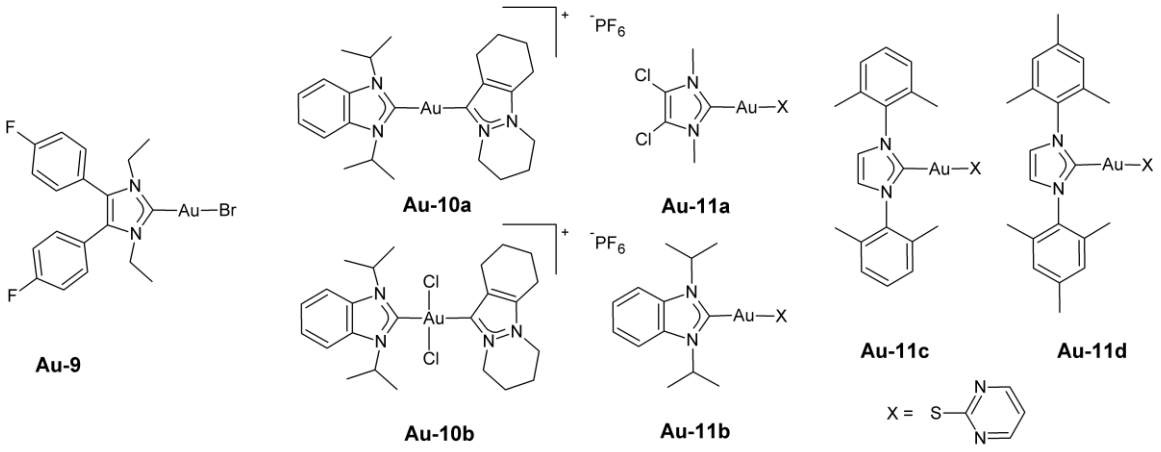

Figure 1.16: Structures of Au-NHC complexes **Au-9**, **Au-10a**, **Au-10b** and **Au-11a-d**

Four cytotoxic imidazole and benzimidazole based Au(I)-NHC complexes (Figure 1.16, **Au-11a-d**) have been selected for screening for their TrxR inhibition properties both on the purified enzyme and on cell extracts *in vitro*, after initial screening for their cytotoxic activity against the cisplatin-sensitive and -resistant human ovarian (A2780S/R) and non-tumourigenic human embryonic kidney (HEK-239T) cell line by Mohr *et al.* Cytosolic TrxR1 was better inhibited by these four complexes than mitochondrial TrxR2 and even to a much lesser extend GR. Interestingly, the inhibition of TrxR by these complexes seems to be relevant in cancerogenic cells, but not in non-tumourigenic cells, which is not the case for auranofin. In the presence of these complexes in tumourigenic cells a correlation between cytotoxicity and thioredoxin oxidation via TrxR inhibition was observed and biochemical assays on glutathione systems and ROS formation displayed great differences compared to auranofin [132].

In 2012, Schobert *et al.* reported their results on the biological evaluation of five *N*-methyl-4,5-diarylimidazole-2-ylidine gold(I) chlorides which showed micromolar cytotoxic activity and selectivity against human colon carcinoma (HT-29), leukaemia (HL-60), melanoma (518A2), cervix carcinoma cells (KB-V1/Vbl) and non-malignant foreskin fibroblasts (HF). The cellular uptake of the complexes occurred mainly via the copper transporter (Ctr1) and the organic cation transporters (OCT-1/2). Furthermore, the complex ((1-*p*-methoxybenzyl-3-(3,4,5-methoxybenzyl)imidazole-2-ylidene) gold(I) chloride (Figure 1.17, **Au-12**) was preferentially accumulated by Na^+/K^+-dependent endocytosis and via the OCT-1/2.

The Au(I)-NHC complexes did not inhibit polymerisation of tubulin to give microtubules, a performance observed for the metal free 1-methyl-4,5-diarylimidazole precursors, therefore their mechanism of action appears to be different from that of their free ligands [133].

Dinda *et al.* synthesised two mononuclear, neutral, benzimidazole based Au(I)-NHC complexes, but the evaluation of the (1-methyl-3-(2-pyridylmethyl)benzimidazole-2-ylidene) gold(I) chloride (Figure 1.17, **Au-13**) showed no improvement of cytotoxic behaviour against mouse melanoma (B16F10), human hepatocarcinoma (HepG2) and human cervical carcinoma (HeLa) cells when compared to cisplatin. When treated with the complex, the cells showed interesting morphological changes (cell rounding and shrinkage, nuclear fragmentation) which indicate an induction of apoptotic cell death. Whereas cisplatin showed 75% cytotoxicity at 10 mM against normal human peripheral blood mononuclear cells, the complex did not show any significant cytotoxic effect at 100 mM [134].

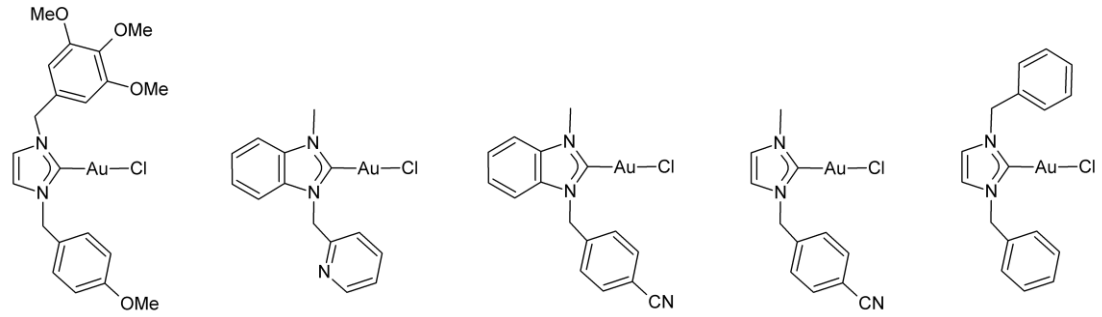

Au-12 **Au-13** **Au-14a** **Au-14b** **Au14c**

Figure 1.17: Structures of Au-NHC complexes **Au-12**, **Au-13** and **Au-14a-c**

Also our group synthesised three novel mononuclear, neutral benzimidazole based Au(I)-NHC complexes (Figure 1.17, **Au-14a-c**) by transmetallation *in situ* from the NHC-Ag(I)Br complexes. The Au(I)-NHC complexes showed good solubility in DMSO and biological medium and were tested against the cancer cell line Caki-1 (renal), but unfortunately no higher activity than cisplatin was observed [135].

Besides the evaluation of Au-NHCs for their cytotoxic properties, some groups started to evaluate the antimicrobial activity of potential active Au(I)-NHC complexes. Özdemir *et al.* tested the activity of six symmetrically substituted, cationic Au(I)-bis(NHC) complexes against the bacterial strains *E. coli*, *Staphylococcus epidermidis* (*S. epidermidis*), *S. aureus*, *Enterococcus faecalis* (*E. faecalis*) , *Enterobacter cloacae* (*E. cloacae*), *P. aeruginosa* and *C. albicans* in 2004. However, only complex **Au-15a** (Figure 1.18) showed low MIC values against most of the strains, with exception of *E. coli* where only **Au-15b** (Figure 1.18) exhibited a MIC value as low as 3.12 µg/ml. Additionally, the free ligand displayed a higher activity than the cationic complexes against *S. epidermidis*, *S. aureus*, *E. faecalis* and *P. aeruginosa*, showing that the activity cannot be attributed to the metal centre. In 2010 three neutral Au(I)-NHC complexes have been evaluated and the methoxy-containing compounds (**Au-16a** and **Au-16b**, Figure 1.18) exhibited good activity against *S. aureus* and *E. faecalis* while the symmetrical methyl-substituted compound **Au-16c** (Figure 1.18) was active against *C. albicans* and *Candida tropicalis* (*C. tropicalis*). However, none of the complexes showed activity against gram-negative bacteria strains. 3 years later the same group reported the antimicrobial activity of another cationic Au(I)-bis(NHC) series, of which two compounds were symmetrically and four unsymmetrically substituted on the nitrogen side arms. The two most active complexes **Au-17a** and **Au-17b** (Figure 1.18) have shown MIC values of 12.5 µg/mL against *S. aureus*, *C. albicans* and *C. tropicalis*, but exhibited no activity against the gram-negative bacterial strain *E. coli* [136–138].

(1-*tert*butyl-3-benzyl-imidazole-2-ylidene) gold(I) chloride (Figure 1.18, **Au-18**) was tested on its antibacterial activity against *Bacillus subtilis* (*B. subtilis*) and *E. coli* by Ghosh *et al*., showing a MIC of 15 µM against *B. subtilis* but no effects were found on *E. coli*. Incubation of *B. subtilis* over 4 h with a concentration of the complex of 4 µM showed that the cell length increased 3.5-fold relative to the control. This finding indicated that the Au(I)-NHC was able to inhibit the bacterial proliferation by blocking cytokinesis. Furthermore the ligand precursor did not show any activity against the two examined bacteria strains [139].

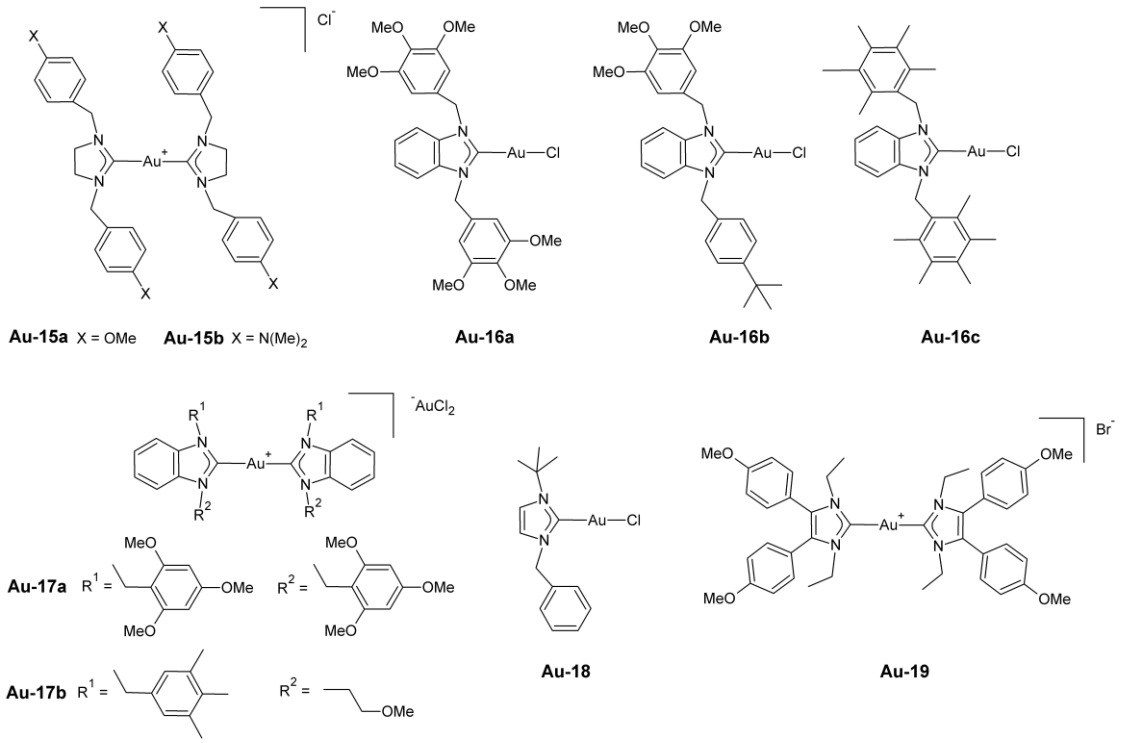

Figure 1.18: Structures of Au-NHC complexes **Au-15a**, **Au-15b**, **Au-16a-c**, **Au-17a**, **Au-17b**, **Au-18** and **Au-19**

In 2012, Gust *et al.* evaluated the cationic Au(I)-bis(NHC) complex **Au-19** (Figure 1.18) for its activity against *Ervinia amylovora* (*E. amylovora*), *E. coli*, *B. subtilis* and *Bacillus megaterium* (*B. megaterium*), where they found no activity for the first two bacteria strains but activity comparable to the one of $AgNO_3$ against the latter two. Interestingly, the methyl-bridged NHC-ligand showed higher activity than the metal-containing complex and even stronger activity against all bacterial strains if compared to $AgNO_3$ [130].

1.4 Ruthenium in medicinal chemistry

Ru(II) and Ru(III) compounds have been widely explored in respect to their potential uses in medicine as chemotherapeutics against different diseases. In particular, they have demonstrated high potentiality for the development of drug candidates for cancer therapy being promising alternatives to platinum complexes. Novel targets like different modes of DNA binding are offered by either classical coordination ruthenium compounds or organoruthenium compounds and they show potential to overcome resistances and side-effects exhibited by cisplatin and platinum-based antitumor drugs. Additionally, the design of ruthenium compounds targeting relevant cellular proteins and cellular signalling pathways overexpressed in tumour cells, mimicking organic enzyme inhibitors or other organic bioactive compounds and those suitable for photodynamic therapy are currently underway [140-142]. The advantages of ruthenium in biological applications are the following: Ru(II) as well as Ru(III) both show preferences for N and S donors, which are found in biomolecules like DNA, serum, cellular proteins and enzymes. Ru(II) and Ru(III) form six coordinated octahedral compounds allowing the *in vivo* interconversion between both oxidation states without extra energy requirements for structural rearrangements. This octahedral geometry offers wider possibilities of coordination to relevant molecular targets than the four coordinated Pt centre. These additional coordination sites could be used to fine-tune the pharmacologically relevant properties of the compounds. Moreover, Ru complexes are kinetically as inert as Pt(II) complexes while ligand exchange determines the activity in biological systems. Furthermore, ruthenium compounds show low toxicity in humans, probably due to metabolic similarities with iron. It can mimic iron in binding biomolecules (e.g. serum albumin and transferrin) and this contributes to a decrease in toxicity and helps the transport of the ruthenium complexes into the cancer cells. Since cancer cells show higher iron requirements than normal cells and therefore exhibit an increased number of transferrin receptors on the cell surface the uptake of ruthenium-compounds is increased in cancer cells [141]. Another advantage is that the redox potential Ru(II)/Ru(III) in many complexes is available in the biological redox potential window. This behaviour can be then exploited to develop ruthenium complexes which can be activated in hypoxic tumour tissues by bioreduction, allowing for achieving

selectivity by reoxidation in healthy normally oxygenated cells. Nevertheless, the kinetic lability of ruthenium ions is highly dependent on the types of bound ligands and substitution rates can vary in many orders of magnitude [143]. These various chemical and biological properties have lead to the discovery of potent Ru-based pro-drugs [144–147].

1.4.1 Synthesis and Characteristics

Ru(II)-NHCs are well known to act as catalysts and they are synthesised in general by applying one of the two following methods: i) transfer of NHCs from Ag(I)-NHCs, or ii) direct metallation of NHCs with Ru(II) sources. As for the Ag(I)-NHC and Au-NHC complexes the formation of the Ru-C bond is indicated by a shift in the ^{13}C NMR with δ values ranging from 156.3 to 252.2 ppm and the loss of the C^2-H signal in the ^1H NMR spectrum [148–156].

1.4.2 Biological evaluation and possible applications

Ruthenium complexes like KP1019, KP1339, NAMI-A and RAPTA-T (Figure 1.19) have been successfully studied for their application as possible anticancer drugs. Of all non-platinum based drugs ruthenium complexes are the most intensively studied for application in cancer chemotherapy. Some unique properties of ruthenium-based drugs can justify the potential expectations posed on these chemical moieties. These properties can be resumed in i) the facility to exchange with O- and N-donor molecules in a way very similar to that of platinum drugs (furthermore their octahedral geometry offers unique possibilities to bind to nucleic acids), ii) the ability to easily access the oxidation states II, III and IV in the biological fluids, iii) the possibility of getting low reactive pro-drugs with the ruthenium ion at +3 oxidation state that can be reduced, then activated, selectively in solid tumour masses where the low oxygen content can create a reducing environment, and iv) the transportation into tumour cells by transferrin, given the presumed higher need of iron of these rapidly dividing cells [157].

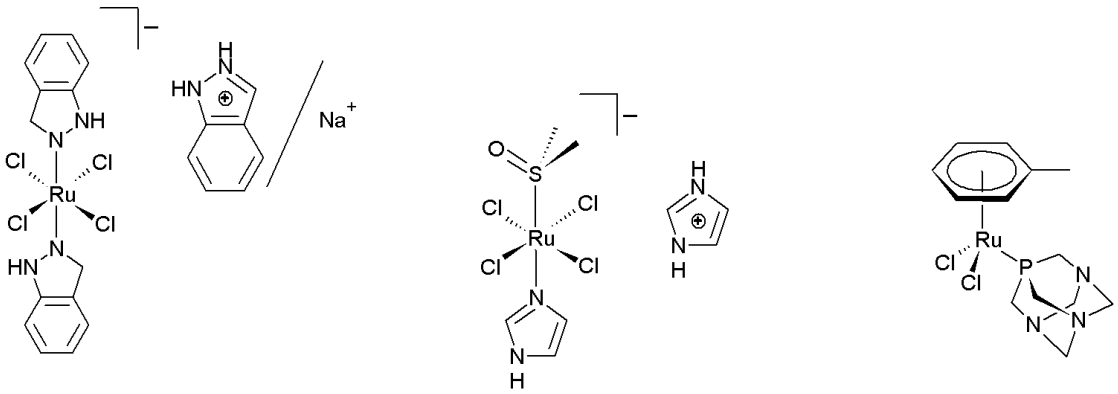

Figure 1.19: KP1019 [144]/ KP1339 [145], NAMI-A [146] and RAPTA-T [147] (from left to right)

Two of the best studied ruthenium complexes, namely KP1019 (imidazolium *trans*-[tetrachloridobis(1H-imidazole)ruthenate(III)) / KP1339 (the much more water soluble [158] Na^+ analogue of KP1019) and NAMI-A (imidazolium *trans*-imidazoledimethylsulfoxidetetrachlororuthenate) have successfully entered clinical trials.

The first ruthenium compound which entered clinical trials was NAMI-A and dose finding was carried out in phase I. PK determination and toxicity evaluation were performed in 24 patients with diverse tumour histotypes and previously treated with surgery and chemotherapy with or without radiotherapy, according to the different tumour type [159, 160]. NAMI-A is characterized by i) no direct cell cytotoxicity on tumour cells *in vitro* up to 0.1 mM concentration ii) a selective effect on lung metastases of solid metastasizing tumours, with no concomitant effect on primary tumour growth, in a number of experimental models, consistent with similar findings obtained with the sodium salt parent compound NAMI, iii) an anti-metastatic effect independent of the stage of growth of lung metastases [active on metastases on advanced stage of growth and/or after surgical removal of primary tumour], iv) a similar activity over a number of treatment schedules, including acute and repeated treatments, v) an activity significantly greater than that of cisplatin on metastases of the human lung cancer H460M2 transplanted into SCID mice, and vi) an activity often synergetic when used in combination with cisplatin and other classical anticancer drugs (taxanes, adriamycin, gemcitabine) *in vitro* and *in vivo*. Today NAMI-A is studied for use as a second line therapy in the metastatic non-small-cell lung carcinoma (NSCLC) in combination with

Gemcitabine. Although the study is still ongoing, preliminary data of dose finding show the possibility to treat these patients with the combination NAMI-A + Gemcitabine. Main toxicities are flebitis at the injection site, for which reason the drug is infused through a central venous catheter (port-a-cath), general malaise and cutaneous blister formation [157].

The biological *in vitro* and *in vivo* effects of KP1019 can be summarised as follows: *in vivo* activity against autochthonous chemically-induced colorectal cancer in mice [161, 162], *in vitro* activity on colorectal colon carcinoma [163–165], *in vivo* activity on the chemo-resistant MAC15A colon carcinoma [166], unable to modify the metastatic cell behaviour [167], transferrin [168] and HSA [158] binding, more cytotoxic after reduction, causes apoptosis via the mitochondrial pathway [168], generation of ROS species [165] and at last solubility problems [168] (which are now overcome by its Na^+ analogue KP1339 [158]).

Another ruthenium based complex which shows some selectivity of anti-tumour activity towards metastases after the discovery of NAMI-A is the RAPTA-T complex by the group of Dyson. RAPTA-T ($Ru(\eta^6\text{-}C_6H_5Me)(PTA)Cl_2$) with PTA = (1,3,5-triaza-7-phosphoadamantane), which is similar to nearly all other derivatives of the RAPTA series [147], shows better cytotoxicity against tumour cells compared to non-tumour cells but is only weakly cytotoxic. Nevertheless it has shown *in vitro* to have significant influence on cell behaviour by modifying invasion and metastasis [169].

Despite this, reports on the tumour growth inhibiting properties of ruthenium NHC complexes are surprisingly rare (see Figure 1.20).

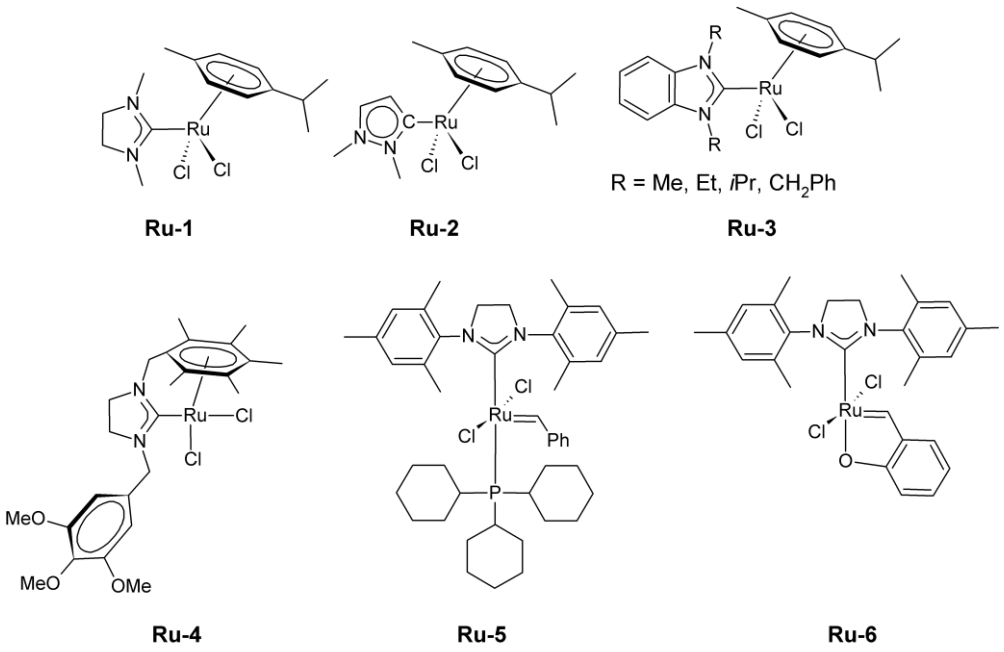

Figure 1.20: Structures of Ru-NHC complexes **Ru-1** to **Ru-6**

In general ruthenium based drugs are much less toxic than platinum-based drugs and are furthermore often capable of overcoming platinum-induced resistances in cancer cells [142, 143, 171–176]. The ability of ruthenium to mimic iron in binding to biological molecules, for example in HSA and transferrin, and the selective activation to more reactive species by the reducing environment of solid tumours seem to be the reasons for these activities [173, 175–179].

Looking at possible DNA targeting some complexes have been especially designed to mimic platinum drugs [178, 179], but unfortunately the ruthenium complexes interact far more weakly with DNA relative to platinum complexes and the mechanisms of action of ruthenium-based antitumor complexes are comparatively unexplored [173, 180].

Recently, Ciftci *et al.* compared the oxidative damage in rat heart tissue induced by Ru(II)–NHC (**Ru-4**, Figure 1.20) and Au(I)–NHC complexes which showed anti-tumour effects *in vitro* [156]. The results indicated that both complexes caused oxidative damage by suppressing the antioxidant defence systems and increasing the lipid peroxidation in heart tissue of rats. This effect was changed in a dose-dependent manner for Au(I)–NHC treatment. Additionally, it was observed that the Au(I)–NHC complex was more cardiotoxic than the Ru(II)–NHC complex which indicated that ruthenium compounds should be

preferred over Au(I)–NHC for cancer treatment when they were used clinically [15].

Metzler-Nolte *et al.* described a way to synthesise ruthenium carbene peptide conjugates to improve the solubility and stability of ruthenium complexes. Using solid phase synthesis they reported the first fully characterised metal-NHC peptide conjugate. A pseudoenkephalin peptide was successfully linked to a functionalised *p*-cymene Ru(II)-NHC ligand [181].

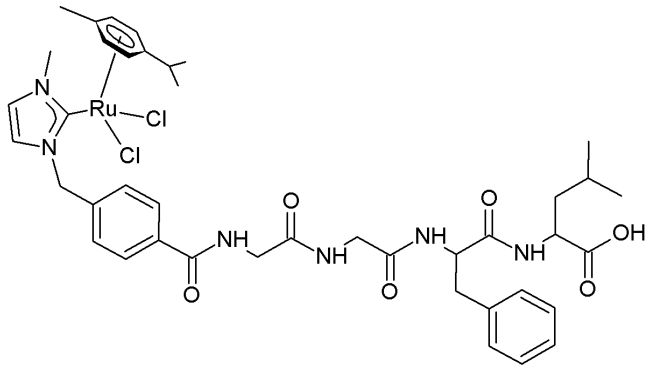

Figure 1.21: ruthenium-NHC pseudoenkephalin [181]

The cytotoxic and potential chemotherapeutic properties of this complex has not been evaluated until now, but the results might be promising when compared to the well studied *p*-cymene containing RAPTA complexes from Dyson *et al.* [142, 143, 174, 176, 182, 183].

However the group around Keppler just recently published their work on the anticancer activity of a ruthenium arene peptide conjugate. The resulting organometallic half-sandwich Ru bioconjugate displayed anti-proliferative activity in the low micromolar range against CH1 ovarian cancer cells, whereas the non-metallated peptide shows no activity. Furthermore they identified a small building block (Figure 1.22) which might open an approach to a wider range of anticancer active Ru bioconjugates [184].

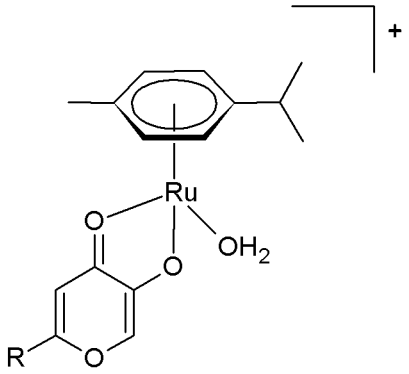

Figure 1.22: Ruthenium-bioconjugate building block [184]

Another series of Ru(II) arene complexes with different NHC ligands (**Ru-1**, Figure 1.20) was studied *in vitro* for antioxidant/pro-oxidant activity by Burgos *et al.* [185]. To investigate and characterise the toxicity of some of these compounds the zebrafish (Danio rerio) has been used additionally as an *in vivo* model. At higher concentrations they showed pro-oxidant capacity while they behaved as antioxidants at low concentrations. Further experiments indicated that zebrafish embryos were not harmed by exposure to Ru(II) complexes. And thus the complexes can be considered as non-toxic. The characteristics as pro-oxidant and/or antioxidant agents together with their biosafety may indicate that this type of complexes have the potential as antitumoural or neuroprotective drugs [15].

Facilitating the promising results of ruthenium arene complexes, Ott *et al.* evaluated archetypical examples of Grubbs catalysts (**Ru-5** and **Ru-6**, Figure 1.20) for their inhibition of enzymatic activities of TrxR, GR, proteases trypsin and cathepsin B and cell growth (MCF-7 and HT-29 cells), as well as on cellular metabolism [186]. The results indicated that **Ru-6** was the most pronounced in terms of enzyme inhibition and anti-proliferative effects in tumour cells, because it interacted with TrxR and albumin considerably stronger and followed a time-dependent process. Similar to other bioactive ruthenium metallodrugs it can be speculated that ligand-exchange processes with thiol- or selenol-containing biomolecules are involved in the biochemistry of the investigated complexes [173, 176]. A reduction of both cell impedance and standard acidification rate, as well as a compensatory increase in glycolysis was found while measuring the effects on cell metabolism. In general, it could be concluded that all results demonstrated that directed cytotoxic effects in cultured tumour cells can be triggered.

Nevertheless, both complexes were less active than their evaluated benzimidazol-2-ylidene gold complexes reported in the same group on inhibition of enzyme TrxR and cell growth [187]. While the potencies of these catalysts are poor to moderate from a drug development prospective, the observed triggering of biological effects might provide a rationale for the use of Ru(II)–NHC fragments in metallo-drug design [15].

1.5 Other metal-NHCs in medicinal chemistry

Besides the evaluation of silver, gold and ruthenium NHCs for their biological applications, also numerous Pd, Pt, Cu and other transition metal NHC complexes have been synthesised and assessed for their suitability as potential novel antimicrobial and anticancer drug candidates.

Unsurprisingly, after the major discovery of cisplatin and its derivatives carboplatin and oxaliplatin as anticancer therapeutics, platinum based NHC complexes were investigated for their possible antitumoural applications. The most promising results were reported in 2011 by Che *et al.* for their cyclometallated Pt(II) complex **Pt-1** (Figure 1.23), showing submicromolar cytotoxicity towards three cancer cell lines and less activity against healthy CCD-19Lu lung fibroblast cells and overall better activity of compared to cisplatin. Furthermore, *in vivo* evaluation of the influence of **Pt-1** on the tumour growth of non-small lung carcinoma NCI-H460 in nude mice at a concentration of 3 mg / kg / d resulted in 55 ± 11% growth inhibition and no observed toxic effects on healthy tissue [188].

Ghosh *et al.* evaluated the anti-proliferative potential of two neutral Pd(II)-NHC complexes (**Pd-1** and **Pd-2**, Figure 1.23) and found 2- to 20-fold increased activity for Pd-2 against HeLa, HCT and MCF-7 cancer cell lines compared to cisplatin. Moreover, they claim that despite the trans configuration of the complex, the same cellular pathway as cisplatin is exhibited by **Pd-2**, with cell cycle arrest in G2/M transition, activation of cyclin B1, activation of a p53-dependent pathway in cell death and phosphorylation of cdc2 [139].

The first Cu(I)-NHC complex has been reported by Arduengo in 1993 [189], but compared to other transition metal NHCs there has been moderate evaluation on the biological properties of Cu(I)- and Cu(II)-NHCs, since their main use is found in catalysis. Nevertheless, the Cu(I)-NHC complexes **Cu-1** to **Cu-3** (Figure 1.23) have shown some interesting results. In 2009 Gautier *et al.* reported the evaluation of the anti-proliferative effects of **Cu-1** against the five cancer cell lines KB (oral carcinoma), HL60 (promyelocytic leukaemia), MCF-7 and MCF-7R (breast) and LNCaP (prostatic) and found overall better and up to 150-fold higher activity than cisplatin. Unlike cisplatin, **Cu-1** arrests the cell cycle progression at the G1 phase and induces apoptosis at a lower concentration. They also assumed

that an aerobic radical process leading to a DNA strand break is responsible for the observed cytotoxicity [190].

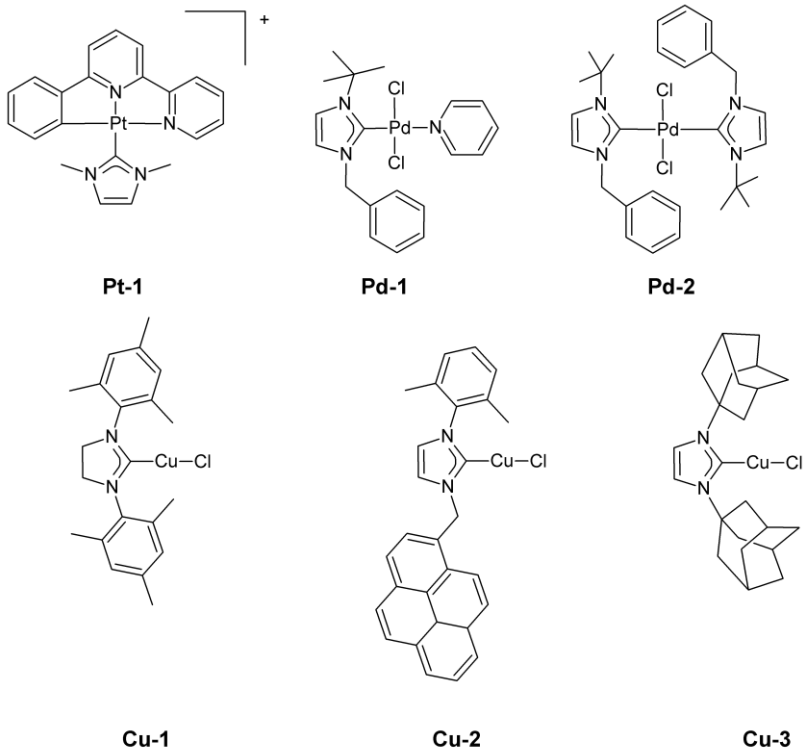

Figure 1.23: Structures of metal-NHC complexes **Pt-1**, **Pd-1**, **Pd-2** and **Cu-1** to **Cu-3b**

During the same year they also evaluated the Cu(I)-NHC complex **Cu-2**, which was designed with the intention of using it for the localisation of intracellular targets by fluorescence microscopy. In fact it presents an intense fluorescence when excited around 360 nm [79]. Santini *et al.* reported the synthesis of a series of metal-NHCs (M = Ag, Au, Cu), among them complex **Cu-3**. Unfortunately, MTT assay data for complex **Cu-3** were not reproducible probably because of the high instability of copper derivatives in physiological media, thus avoiding IC_{50} calculation [191].

1.6 References

[1] http://globocan.iarc.fr/
[2] A. Jemal, F. Bray, M. M. Center, J. Ferlay, E. Ward, D. Forman; *CA Cancer J Clin*, 61, **2011**, 69–90.
[3] http://www.who.int/mediacentre/factsheets/fs297/en/index.html
[4] B. Lakatos, K. Szentmihályi, P. Vinkler, J. Balla, G. Balla; *Orv Hetil*, 145, **2004**, 1315–1319.
[5] K. F. Donnelly, A. Petronilho, M. Albrecht; *Chem. Commun,* 49, **2013**, 1145–1159.
[6] M. Yus and I. M. Pastor; *Chem. Lett,* 42, **2013**, 94–108.
[7] S. Budagumpi and S. Endud; *Organometallics*, 32, **2013**, 1537–1562.
[8] F. B. Hamad, T. Sun, S. Xiao, F. Verpoort; *Coord. Chem. Rev*, 257, **2013**, 2274–2292.
[9] E. A. Baquero, G. F. Silbestri, P. Gómez-Sal, J. C. Flores, E. de Jesús; *Organometallics*, 32, **2013**, 2814–2826.
[10] S. Zhu, R. Liang, H. Jiang; *Tetrahedron*, 68, **2012**, 7949–7955.
[11] A. Gautier and F. Cisnetti; *Metallomics*, 4, **2012**, 23–32.
[12] K. M. Hindi, M. J. Panzner, C. A. Tessier, C. L. Cannon, W. J. Youngs; *Chem. Rev,* 109, **2009**, 3859–3884.
[13] C. N. Banti and S. K. Hadjikakou; *Metallomics*, 5, **2013**, 569–596.
[14] L. Oehninger, R. Rubbiani, I. Ott; *Dalton Trans,* 42, **2013**, 3269–3284.
[15] W. Liu and R. Gust; *Chem. Soc. Rev,* 42, **2013**, 755–773.
[16] A. Kascatan-Nebioglu, M. J. Panzner, C. A. Tessier, C. L. Cannon, W. J. Youngs; *Coord. Chem. Rev*, 251, **2007**, 884–895.
[17] H.-W. Wanzlick and E. Schikora; *Angew. Chem,* 72, **1960**, 494–495.
[18] H. Quast and S. Hünig; *Angew. Chem. Int. Ed. Engl,* 3, **1964**, 800–801.
[19] R. A. Olofson, W. R. Thompson, J. S. Michelman; *J. Am. Chem. Soc,* 86, **1964**, 1865–1866.
[20] A. J. Arduengo III, J. R. Goerlich, R. Krafczyk, W. J. Marshall; *Angew. Chem. Int. Ed,* 37, **1998**, 1963–1965.
[21] K. Öfele; *J. Organomet. Chem,* 12, **1968**, 42–43.
[22] H.-W. Wanzlick and H.-J. Schönherr; *Angew. Chem. Int. Ed. Engl,* 7, **1968**, 141–142.
[23] H. Clavier and S. P. Nolan; *Chem. Commun,* 46, **2010**, 841–861.
[24] R. H. Crabtree; *Coord. Chem. Rev*, 257, **2013**, 755–766.
[25] W. A. Herrmann; *Angew. Chem. Int. Ed,* 41, **2002**, 1290–1309.
[26] J. C. Garrison and W. J. Youngs; *Chem. Rev,* 105, **2005**, 3978–4008.
[27] D. Bourissou, O. Guerret, F. P. Gabbaï, G. Bertrand; *Chem. Rev,* 100, **2000**, 39–92.
[28] H. Jacobsen, A. Correa, C. Costabile, L. Cavallo; *J. Organomet. Chem,* 691, **2006**, 4350–4358.
[29] N. Grier, *Silver and its compounds, In: Disinfection, sterilization, and preservation,* 1st ed. Philadelphia: Lea & Febiger, **1968**, 375-398.
[30] W. R. Hill and D. M. Pillsbury, *Argyria - The Pharmacology of Silver*. Baltimore: Williams & Wilkins, **1939**.
[31] G. Schneider; *Can. Med. Assoc. J,* 131, **1984**, 193–196.
[32] J. W. Alexander; *Surg Infect*, 10, **2009**, 289–292.
[33] A. Melaiye and W. J. Youngs; *Expert Opin. Ther. Patents*, 15, **2005**, 125–130.

[34] O. Kühl, S. Saravanakumar, F. Ullah, M. K. Kindermann, P. G. Jones, M. Köckerling, J. Heinicke; *Polyhedron*, 27, **2008**, 2825–2832.
[35] L. R. Moore, S. M. Cooks, M. S. Anderson, H.-J. Schanz, S. T. Griffin, R. D. Rogers, M. C. Kirk, K. H. Shaughnessy; *Organometallics*, 25, **2006**, 5151–5158.
[36] Q.-X. Liu, L.-N. Yin, X.-M. Wu, J.-C. Feng, J.-H. Guo, H.-B. Song; *Polyhedron*, 27, **2008**, 87–94.
[37] M. Iglesias, D. J. Beetstra, J. C. Knight, L.-L. Ooi, A. Stasch, S. Coles, L. Male, M. B. Hursthouse, K. J. Cavell, A. Dervisi, I. A. Fallis; *Organometallics*, 27, **2008**, 3279–3289.
[38] Q.-X. Liu, L.-N. Yin, J.-C. Feng; *J. Organomet. Chem,* 692, **2007**, 3655–3663.
[39] T. L. Amyes, S. T. Diver, J. P. Richard, F. M. Rivas, K. Toth; *J. Am. Chem. Soc,* 126, **2004**, 4366–4374.
[40] J. C. C. Chen and I. J. B. Lin; *Organometallics*, 19, **2000**, 5113–5121.
[41] J. Dupont; *J. Braz. Chem. Soc,* 15, **2004**, 341–350.
[42] V. J. Catalano, M. A. Malwitz, A. O. Etogo; *Inorg. Chem,* 43, **2004**, 5714–5724.
[43] Y.-J. Kim and A. Streitwieser; *J. Am. Chem. Soc,* 124, **2002**, 5757–5761.
[44] A. M. Magill, K. J. Cavell, B. F. Yates; *J. Am. Chem. Soc,* 126, **2004**, 8717–8724.
[45] H. M. J. Wang and I. J. B. Lin; *Organometallics*, 17, **1998**, 972–975.
[46] P. de Frémont, N. M. Scott, E. D. Stevens, T. Ramnial, O. C. Lightbody, C. L. B. Macdonald, J. A. C. Clyburne, C. D. Abernethy, S. P. Nolan; *Organometallics*, 24, **2005**, 6301–6309.
[47] C. K. Lee, C. S. Vasam, T. W. Huang, H. M. J. Wang, R. Y. Yang, C. S. Lee, I. J. B. Lin; *Organometallics*, 25, **2006**, 3768–3775.
[48] M. K. Samantaray, V. Katiyar, D. Roy, K. Pang, H. Nanavati, R. Stephen, R. B. Sunoj, P. Ghosh; *Eur. J. Inorg. Chem,* 2006, **2006**, 2975–2984.
[49] V. César, S. Bellemin-Laponnaz, L. H. Gade; *Organometallics*, 21, **2002**, 5204–5208.
[50] I. S. Edworthy, M. Rodden, S. A. Mungur, K. M. Davis, A. J. Blake, C. Wilson, M. Schröder, P. L. Arnold; *J. Organomet. Chem,* 690, **2005**, 5710–5719.
[51] Q.-X. Liu, F.-B. Xu, Q.-S. Li, X.-S. Zeng, X.-B. Leng, Y. L. Chou, Z.-Z. Zhang; *Organometallics*, 22, **2003**, 309–314.
[52] J. C. Y. Lin, R. T. W. Huang, C. S. Lee, A. Bhattacharyya, W. S. Hwang, I. J. B. Lin; *Chem. Rev,* 109, **2009**, 3561–3598.
[53] S. Patil, K. Dietrich, A. Deally, B. Gleeson, H. Müller-Bunz, F. Paradisi, M. Tacke; *Helv. Chim. Acta*, 93, **2010**, 2347–2364.
[54] S. Patil, A. Deally, B. Gleeson, F. Hackenberg, H. Müller-Bunz, F. Paradisi, M. Tacke; *Z. Allg. Anorg. Chem,* 637, **2011**, 386–396.
[55] S. Patil, J. Claffey, A. Deally, B. Gleeson, M. Hogan, L. M. Menéndez Méndez, H. Müller-Bunz, F. Paradisi, M. Tacke; *Eur. J. Inorg. Chem,* 2010, **2010**, 1020–1031.
[56] S. Patil, K. Dietrich, A. Deally, B. Gleeson, H. Müller-Bunz, F. Paradisi, M. Tacke; *Appl. Organomet. Chem,* 24, **2010**, 781–793.
[57] S. Patil, A. Deally, B. Gleeson, H. Müller-Bunz, F. Paradisi, M. Tacke; *Metallomics*, 3, **2011**, 74–88.

[58] K. M. Hindi, T. J. Siciliano, S. Durmus, M. J. Panzner, D. A. Medvetz, D. V. Reddy, L. A. Hogue, C. E. Hovis, J. K. Hilliard, R. J. Mallet, C. A. Tessier, C. L. Cannon, W. J. Youngs; *J. Med. Chem,* 51, **2008**, 1577–1583.
[59] A. Kascatan-Nebioglu, A. Melaiye, K. M. Hindi, S. Durmus, M. J. Panzner, L. A. Hogue, R. J. Mallett, C. E. Hovis, M. Coughenour, S. D. Crosby, A. Milsted, D. L. Ely, C. A. Tessier, C. L. Cannon, W. J. Youngs; *J. Med. Chem,* 49, **2006**, 6811–6818.
[60] A. B. Powell, C. W. Bielawski, A. H. Cowley; *J. Am. Chem. Soc,* 132, **2010**, 10184–10194.
[61] A. A. D. Tulloch, A. A. Danopoulos, S. Winston, S. Kleinhenz, G. Eastham; *J. Chem. Soc, Dalton Trans,* **2000**, 4499–4506.
[62] V. J. Catalano and A. L. Moore; *Inorg. Chem,* 44, **2005**, 6558–6566.
[63] R.-Z. Ku, J.-C. Huang, J.-Y. Cho, F.-M. Kiang, K. R. Reddy, Y.-C. Chen, K.-J. Lee, J.-H. Lee, G.-H. Lee, S.-M. Peng, S.-T. Liu; *Organometallics*, 18, **1999**, 2145–2154.
[64] H. Klasen; *Burns*, 26, **2000**, 131–138.
[65] N. C. Baenziger and A. W. Struss; *Inorg. Chem,* 15, **1976**, 1807–1809.
[66] C. Graham; *Br. J. Nurs,* 14, **2005**, 22–28.
[67] A. B. G. Lansdown; *Br. J. Nurs,* 13, **2004**, S6-S19.
[68] M. J. Panzner, A. Deeraksa, A. Smith, B. D. Wright, K. M. Hindi, A. Kascatan-Nebioglu, A. G. Torres, B. M. Judy, C. E. Hovis, J. K. Hillard, R. J. Mallett, E. Cope, D. M. Estes, C. L. Cannon, J. G. Leid, W. J. Youngs; *Eur. J. Inorg. Chem,* 13, **2009**, 1739–1745.
[69] M. J. Panzner, K. M. Hindi, B. D. Wright, J. B. Taylor, D. S. Han, W. J. Youngs, C. L. Cannon; *Dalton Trans,* **2009**, 7308–7313.
[70] P. N. Shah, L. Y. Lin, J. A. Smolen, J. A. Tagaev, S. P. Gunsten, D. S. Han, G. S. Heo, Y. Li, F. Zhang, S. Zhang, B. D. Wright, M. J. Panzner, W. J. Youngs, S. L. Brody, K. L. Wooley, C. L. Cannon; *ACS Nano*, 7, **2013**, 4977–4987.
[71] A. Melaiye, Z. Sun, K. Hindi, A. Milsted, D. Ely, D. H. Reneker, C. A. Tessier, W. J. Youngs; *J. Am. Chem. Soc,* 127, **2005**, 2285–2291.
[72] A. Melaiye, R. S. Simons, A. Milsted, F. Pingitore, C. Wesdemiotis, C. A. Tessier, W. J. Youngs; *J. Med. Chem,* 47, **2004**, 973–977.
[73] A. Kascatan-Nebioglu, M. J. Panzner, C. A. Tessier, C. L. Cannon, W. J. Youngs; *Coord. Chem. Rev,* 251, **2007**, 884–895.
[74] B. Thati, A. Noble, B. S. Creaven, M. Walsh, M. McCann, K. Kavanagh, M. Devereux, D. A. Egan; *Cancer Lett,* 248, **2007**, 321–333.
[75] H.-L. Zhu, X.-M. Zhang, X.-Y. Liu, X.-J. Wang, G.-F. Liu, A. Usman, H.-K. Fun; *Inorg. Chem. Comm,* 6, **2003**, 1113–1116.
[76] S. E.-d. H. Etaiw, A. S. Sultan, A. S. Badr El-din; *Eur. J. Med. Chem,* 46, **2011**, 5370–5378.
[77] D. A. Medvetz, K. M. Hindi, M. J. Panzner, A. J. Ditto, Y. H. Yun, W. J. Youngs; *Met Based Drugs*, **2008**, 384010–384016.
[78] T. J. Siciliano, M. C. Deblock, K. M. Hindi, S. Durmus, M. J. Panzner, C. A. Tessier, W. J. Youngs; *J. Organomet. Chem,* 696, **2011**, 1066–1071.
[79] M.-L. Teyssot, A.-S. Jarrousse, M. Manin, A. Chevry, S. Roche, F. Norre, C. Beaudoin, L. Morel, D. Boyer, R. Mahiou, A. Gautier; *Dalton Trans,* **2009**, 6894–6902.
[80] S. Roland, C. Jolivalt, T. Cresteil, L. Eloy, P. Bouhours, A. Hequet, V. Mansuy, C. Vanucci, J.-M. Paris; *Chem. Eur. J,* 17, **2011**, 1442–1446.

[81] C.-H. Wang, W.-C. Shih, H. C. Chang, Y.-Y. Kuo, W.-C. Hung, T.-G. Ong, W.-S. Li; *J. Med. Chem,* 54, **2011**, 5245–5249.
[82] S. Mahdihassan; *Am. J. Chin. Med,* 09, **1981**, 23–33.
[83] S. Mahdihassan; *Janus*, 58, **1971**, 112–118.
[84] S. P. Fricker and R. G. Buckley; *Anticancer Res,* 16, **1996**, 3755–3760.
[85] M.-C. Daniel and D. Astruc; *Chem. Rev,* 104, **2004**, 293–346.
[86] M. W. Whitehouse; *Inflammopharmacol*, 16, **2008**, 107–109.
[87] C. F. Shaw; *Chem. Rev,* 99, **1999**, 2589–2600.
[88] D. T. Felson, J. J. Anderson, R. F. Meenan; *Arthritis Rheum,* 33, **1990**, 1449–1461.
[89] R. Batthacharya and P. Mukherjee; *Adv. Drug Deliv. Rev*, 60, **2008**, 1289–1306.
[90] B. Cetinkaya, P. Dixneuf, M. F. Lappert; *J. Chem. Soc, Dalton Trans,* **1974**, 1827–1833.
[91] K. Bartel and W. P. Fehlhammer; *Angew. Chem,* 86, **1974**, 588–589.
[92] F. Bonati, A. Burini, B. R. Pietroni, B. Bovio; *J. Organomet. Chem,* 375, **1989**, 147–160.
[93] H. G. Raubenheimer, F. Scott, M. Roos, R. Otte; *J. Chem. Soc, Chem. Commun,* **1990**, 1722–1723.
[94] P. Kühlkamp, H. G. Raubenheimer, J. S. Field, M. Desmet; *J. Organomet. Chem,* 552, **1998**, 69–74.
[95] J. F. Britten, C. J. L. Lock, Z. Wang; *Acta Crystallogr C Cryst Struct Commun*, 48, **1992**, 1600–1603.
[96] K. M. Lee, C. K. Lee, I. J. B. Lin; *Angew. Chem. Int. Ed. Engl,* 36, **1997**, 1850–1852.
[97] M. V. Baker, P. J. Barnard, S. J. Berners-Price, S. K. Brayshaw, J. L. Hickey, B. W. Skelton, A. H. White; *J. Organomet. Chem,* 690, **2005**, 5625–5635.
[98] P. de Frémont, E. D. Stevens, M. R. Fructos, M. Mar Díaz-Requejo, P. J. Pérez, S. P. Nolan; *Chem. Commun,* **2006**, 2045–2047.
[99] M. V. Baker, P. J. Barnard, S. J. Berners-Price, S. K. Brayshaw, J. L. Hickey, B. W. Skelton, A. H. White; *Dalton Trans,* **2006**, 3708–3715.
[100] V. J. Catalano and A. O. Etogo; *Inorg. Chem,* 46, **2007**, 5608–5615.
[101] R. Corberán, J. Ramírez, M. Poyatos, E. Peris, E. Fernández; *Tetrahedron Asymm.*, 17, **2006**, 1759–1762.
[102] U. E. I. Horvath, G. Bentivoglio, M. Hummel, H. Schottenberger, K. Wurst, M. J. Nell, C. E. J. van Rensburg, S. Cronje, H. G. Raubenheimer; *New J. Chem,* 32, **2008**, 533–539.
[103] M. K. Samantaray, K. Pang, M. M. Shaikh, P. Ghosh; *Inorg. Chem,* 47, **2008**, 4153–4165.
[104] P. J. Barnard, L. E. Wedlock, M. V. Baker, S. J. Berners-Price, D. A. Joyce, B. W. Skelton, J. H. Steer; *Angew. Chem. Int. Ed,* 45, **2006**, 5966–5970.
[105] B. Liu, W. Chen, S. Jin; *Organometallics*, 26, **2007**, 3660–3667.
[106] Y. Zhou and W. Chen; *Organometallics*, 26, **2007**, 2742–2746.
[107] A. Corma, E. Gutiérrez-Puebla, M. Iglesias, A. Monge, S. Pérez-Ferreras, F. Sánchez; *Adv. Synth. Catal,* 348, **2006**, 1899–1907.
[108] R. Jothibasu, H. V. Huynh, L. L. Koh; *J. Organomet. Chem,* 693, **2008**, 374–380.
[109] F. Kessler, N. Szesni, C. Maaß, C. Hohberger, B. Weibert, H. Fischer; *J. Organomet. Chem,* 692, **2007**, 3005–3018.

[110] G. D. Frey, R. D. Dewhurst, S. Kousar, B. Donnadieu, G. Bertrand; *J. Organomet. Chem,* 693, **2008**, 1674–1682.
[111] S. K. Schneider, W. A. Herrmann, E. Herdtweck; *Z. anorg. allg. Chem,* 629, **2003**, 2363–2370.
[112] N. S. Akhmadullina, A. V. Churakov, V. M. Retivov, R. A. Sandu, O. N. Shishilov; *Russ J Coord Chem*, 38, **2012**, 589–595.
[113] J. M. Madeira, D. L. Gibson, W. F. Kean, A. Klegeris; *Inflammopharmacol*, 20, **2012**, 297–306.
[114] F. Shabani, J. McNeil, L. Tippett; *Free Radic Res*, 28, **1998**, 115–123.
[115] T. Ashino, J. Sugiuchi, J. Uehara, Y. Naito-Yamamoto, S. Kenmotsu, Y. Iwakura, S. Shioda, S. Numazawa, T. Yoshida; *J. Toxicol. Sci,* 36, **2011**, 635–643.
[116] C. N. Serhan and J. M. Drazen; *J. Clin. Invest,* 99, **1997**, 1147–1148.
[117] A. Debnath, D. Parsonage, R. M. Andrade, C. He, E. R. Cobo, K. Hirata, S. Chen, G. García-Rivera, E. Orozco, M. B. Martínez, S. S. Gunatilleke, A. M. Barrios, M. R. Arkin, L. B. Poole, J. H. McKerrow, S. L. Reed; *Nat Med*, 18, **2012**, 956–960.
[118] S. J. Berners-Price and A. Filipovska; *Metallomics*, 3, **2011**, 863–873.
[119] I. Ott, X. Qian, Y. Xu, D. H. W. Vlecken, I. J. Marques, D. Kubutat, J. Will, W. S. Sheldrick, P. Jesse, A. Prokop, C. P. Bagowski; *J. Med. Chem,* 52, **2009**, 763–770.
[120] C. K. Mirabell, R. K. Johnson, D. T. Hill, L. F. Faucette, G. R. Girard, G. Y. Kuo, C. M. Sung, S. T. Crooke; *J. Med. Chem,* 29, **1986**, 218–223.
[121] J. L. Hickey, R. A. Ruhayel, P. J. Barnard, M. V. Baker, S. J. Berners-Price, A. Filipovska; *J. Am. Chem. Soc,* 130, **2008**, 12570–12571.
[122] P. J. Barnard, M. V. Baker, S. J. Berners-Price, D. A. Day; *J. Inorg. Biochem,* 98, **2004**, 1642–1647.
[123] P. J. Barnard, M. V. Baker, S. J. Berners-Price, B. W. Skelton, A. H. White; *Dalton Trans,* **2004**, 1038–1047.
[124] D. Krishnamurthy, M. R. Karver, E. Fiorillo, V. Orrú, S. M. Stanford, N. Bottini, A. M. Barrios; *J. Med. Chem,* 51, **2008**, 4790–4795.
[125] R. Rubbiani, S. Can, I. Kitanovic, H. Alborzinia, M. Stefanopoulou, M. Kokoschka, S. Mönchgesang, W. S. Sheldrick, S. Wölfl, I. Ott; *J. Med. Chem,* 54, **2011**, 8646–8657.
[126] J. J. Yan, A. L.-F. Chow, C.-H. Leung, R. W.-Y. Sun, D.-L. Ma, C.-M. Che; *Chem. Commun,* 46, **2010**, 3893–3895.
[127] J. Weaver, S. Gaillard, C. Toye, S. Macpherson, S. P. Nolan, A. Riches; *Chem. Eur. J,* 17, **2011**, 6620–6624.
[128] W. Liu, K. Bensdorf, M. Proetto, A. Hagenbach, U. Abram, R. Gust; *J. Med. Chem,* 55, **2012**, 3713–3724.
[129] W. Liu, K. Bensdorf, M. Proetto, U. Abram, A. Hagenbach, R. Gust; *J. Med. Chem,* 54, **2011**, 8605–8615.
[130] W. Liu, X. Chen, R. Gust; *Arch. Pharm.*, 345, **2012**, 557–564.
[131] H. Sivaram, J. Tan, H. V. Huynh; *Organometallics*, 31, **2012**, 5875–5883.
[132] E. Schuh, C. Pflüger, A. Citta, A. Folda, M. P. Rigobello, A. Bindoli, A. Casini, F. Mohr; *J. Med. Chem,* 55, **2012**, 5518–5528.
[133] L. Kaps, B. Biersack, H. Müller-Bunz, K. Mahal, J. Münzner, M. Tacke, T. Mueller, R. Schobert; *J. Inorg. Biochem,* 106, **2012**, 52–58.
[134] S. D. Adhikary, D. Bose, P. Mitra, K. D. Saha, V. Bertolasi, J. Dinda; *New J. Chem,* 36, **2012**, 759–767.

[135] S. Patil, A. Deally, F. Hackenberg, L. Kaps, H. Müller-Bunz, R. Schobert, M. Tacke; *Helv. Chim. Acta*, 94, **2011**, 1551–1562.
[136] Ö. Doğan, N. Kaloğlu, S. Demir, İ. Özdemir, S. Günal, İ. Özdemir; *Monatsh Chem*, 144, **2013**, 313–319.
[137] İ. Özdemir, N. Temelli, S. Günal, S. Demir; *Molecules*, 15, **2010**, 2203–2210.
[138] İ. Özdemir, A. Denizci, H. T. Öztürk, B. Çetinkaya; *Appl. Organometal. Chem,* 18, **2004**, 318–322.
[139] S. Ray, R. Mohan, J. K. Singh, M. K. Samantaray, M. M. Shaikh, D. Panda, P. Ghosh; *J. Am. Chem. Soc,* 129, **2007**, 15042–15053.
[140] S. H. van Rijt, P. J. Sadler; *Drug Discov Today*, 14, **2009**, 1089–1097.
[141] W. H. Ang, P. J. Dyson; *Eur. J. Inorg. Chem*., 2006, **2006**, 3993–4000.
[142] G. Gasser, I. Ott, N. Metzler-Nolte; *J. Med. Chem,* 54, **2011**, 3–25.
[143] Y. K. Yan, M. Melchart, A. Habtemariam, P. J. Sadler; *Chem. Commun,* **2005**, 4764–4776.
[144] L. Kersten, H. Bräunlich, B. K. Keppler, C. Gliesing, M. Wendelin, J. Westphal; *J. Appl. Toxicol,* 18, **1998**, 93–101.
[145] K. Połeć-Pawlak, J. K. Abramski, J. Ferenc, L. S. Foteeva, A. R. Timerbaev, B. K. Keppler, M. Jarosz; *J Chromatogr A*, 1192, **2008**, 323–326.
[146] G. Sava, I. Capozzi, K. Clerici, G. Gagliardi, E. Alessio, G. Mestroni; *Clin. Exp. Metastasis*, 16, **1997**, 371–379.
[147] C. Scolaro, A. Bergamo, L. Brescacin, R. Delfino, M. Cocchietto, G. Laurenczy, T. J. Geldbach, G. Sava, P. J. Dyson; *J. Med. Chem,* 48, **2005**, 4161–4171.
[148] O. Ciftci, A. Beytur, N. Vardi, I. Ozdemir; *Drug Dev Ind Pharm*, 38, **2012**, 40–46.
[149] J. Mormul, M. Steimann, C. Maichle-Mössmer, U. Nagel; *Eur. J. Inorg. Chem,* **2013**, 3421–3428.
[150] V. Leigh, W. Ghattas, R. Lalrempuia, H. Müller-Bunz, M. T. Pryce, M. Albrecht; *Inorg. Chem,* 52, **2013**, 5395–5402.
[151] L. Oehninger, M. Stefanopoulou, H. Alborzinia, J. Schur, S. Ludewig, K. Namikawa, A. Muñoz-Castro, R. W. Köster, K. Baumann, S. Wölfl, W. S. Sheldrick, I. Ott; *Dalton Trans,* 42, **2013**, 1657–1666.
[152] A. Prades, M. Viciano, M. Sanaú, E. Peris; *Organometallics*, 27, **2008**, 4254–4259.
[153] S. Burling, B. M. Paine, D. Nama, V. S. Brown, M. F. Mahon, T. J. Prior, P. S. Pregosin, M. K. Whittlesey, J. M. J. Williams; *J. Am. Chem. Soc,* 129, **2007**, 1987–1995.
[154] S. Demir, I. Özdemir, O. Şahin, B. Çetinkaya, O. Büyükgüngör; *Synlett*, 2010, **2010**, 496–500.
[155] S. Demir, I. Özdemir, B. Çetinkaya; *J. Organomet. Chem,* 694, **2009**, 4025–4031.
[156] O. Ciftci, I. Ozdemir, O. Cakir, S. Demir; *Toxicol Ind Health*, 27, **2011**, 735–741.
[157] A. Bergamo, C. Gaiddon, J. Schellens, J. Beijnen, G. Sava; *J. Inorg. Biochem,* 106, **2012**, 90–99.
[158] O. Dömötör, C. G. Hartinger, A. K. Bytzek, T. Kiss, B. K. Keppler, E. A. Enyedy; *J Biol Inorg Chem*, 18, **2013**, 9–17.
[159] E. E. M. Brouwers, M. M. Tibben, H. Rosing, J. H. M. Schellens, J. H. Beijnen; *Rapid Commun. Mass Spectrom,* 21, **2007**, 1521–1530.
[160] J. M. Rademaker-Lakhai; *Clin. Cancer Res,* 10, **2004**, 3717–3727.

[161] M. H. Seelig, M. R. Berger, B. K. Keppler; *J Cancer Res Clin Oncol*, 118, **1992**, 195–200.
[162] M. R. Berger, F. T. Garzon, B. K. Keppler, D. Schmähl; *Anticancer Res,* 9, **1989**, 761–765.
[163] S. Kapitza, M. Pongratz, M. A. Jakupec, P. Heffeter, W. Berger, L. Lackinger, B. K. Keppler, B. Marian; *J Cancer Res Clin Oncol*, 131, **2005**, 101–110.
[164] S. Frühauf and W. J. Zeller; *Cancer Res,* 51, **1991**, 2943–2948.
[165] S. Kapitza, M. A. Jakupec, M. Uhl, B. K. Keppler, B. Marian; *Cancer Lett,* 226, **2005**, 115–121.
[166] C. G. Hartinger, M. A. Jakupec, S. Zorbas-Seifried, M. Groessl, A. Egger, W. Berger, H. Zorbas, P. J. Dyson, B. K. Keppler; *Chem. Biodivers,* 5, **2008**, 2140–2155.
[167] A. Bergamo, A. Masi, M. A. Jakupec, B. K. Keppler, G. Sava; *Met Based Drugs*, 2009, **2009**, 9 pages.
[168] C. G. Hartinger, S. Zorbas-Seifried, M. A. Jakupec, B. Kynast, H. Zorbas, B. K. Keppler; *J. Inorg. Biochem,* 100, **2006**, 891–904.
[169] A. Bergamo, A. Masi, P. J. Dyson, G. Sava; *Int J Oncol*, 33, **2008**, 1281–1289.
[170] I. Ott and R. Gust; *Arch. Pharm. Chem. Life Sci,* 340, **2007**, 117–126.
[171] N. P. E. Barry and P. J. Sadler; *Chem. Soc. Rev,* 41, **2012**, 3264–3279.
[172] R. G. de Lima, A. Lever, I. Y. Ito, R. Santana da Silva; *Trans. Met. Chem,* 28, **2003**, 272–275.
[173] A. Bergamo and G. Sava; *Dalton Trans,* 40, **2011**, 7817–7823.
[174] A. Casini, C. Gabbiani, F. Sorrentino, M. P. Rigobello, A. Bindoli, T. J. Geldbach, A. Marrone, N. Re, C. G. Hartinger, P. J. Dyson, L. Messori; *J. Med. Chem,* 51, **2008**, 6773–6781.
[175] P. Mura, M. Camalli, A. Bindoli, F. Sorrentino, A. Casini, C. Gabbiani, M. Corsini, P. Zanello, M. Pia Rigobello, L. Messori; *J. Med. Chem,* 50, **2007**, 5871–5874.
[176] W. H. Ang, A. Casini, G. Sava, P. J. Dyson; *J. Organomet. Chem,* 696, **2011**, 989–998.
[177] C. Kunick and I. Ott; *Angew. Chem. Int. Ed,* 49, **2010**, 5226–5227.
[178] A. M. Pizarro and P. J. Sadler; *Biochimie*, 91, **2009**, 1198–1211.
[179] H.-K. Liu and P. J. Sadler; *Acc. Chem. Res,* 44, **2011**, 349–359.
[180] A. Levina, A. Mitra, P. A. Lay; *Metallomics*, 1, **2009**, 458–470.
[181] J. Lemke and N. Metzler-Nolte; *Eur. J. Inorg. Chem,* 2008, **2008**, 3359–3366.
[182] P. Nowak-Sliwinska, J. R. van Beijnum, A. Casini, A. A. Nazarov, G. Wagnières, H. van den Bergh, P. J. Dyson, A. W. Griffioen; *J. Med. Chem,* 54, **2011**, 3895–3902.
[183] A. F. A. Peacock and P. J. Sadler; *Chem. Asian J,* 3, **2008**, 1890–1899.
[184] S. M. Meier, M. Novak, W. Kandioller, M. A. Jakupec, V. B. Arion, N. Metzler-Nolte, B. K. Keppler, C. G. Hartinger; *Chem. Eur. J,* **2013**, in print.
[185] J. M. Alfaro, A. Prades, M. del Carmen Ramos, E. Peris, J. Ripoll-Gómez, M. Poyatos, J. S. Burgos; *Zebrafish*, 7, **2010**, 13–21.
[186] L. Oehninger, H. Alborzinia, S. Ludewig, K. Baumann, S. Wölfl, I. Ott; *ChemMedChem*, 6, **2011**, 2142–2145.
[187] R. Rubbiani, I. Kitanovic, H. Alborzinia, S. Can, A. Kitanovic, L. A. Onambele, M. Stefanopoulou, Y. Geldmacher, W. S. Sheldrick, G. Wolber, A. Prokop, S. Wölfl, I. Ott; *J. Med. Chem,* 53, **2010**, 8608–8618.

[188] R. Wai-Yin Sun, A. Lok-Fung Chow, X.-H. Li, J. J. Yan, S. Sin-Yin Chui, C.-M. Che; *Chem. Sci,* 2, **2011**, 728–736.
[189] A. J. Arduengo, H. V. R. Dias, J. C. Calabrese, F. Davidson; *Organometallics*, 12, **1993**, 3405–3409.
[190] M.-L. Teyssot, A.-S. Jarrousse, A. Chevry, A. De Haze, C. Beaudoin, M. Manin, S. P. Nolan, S. Díez-González, L. Morel, A. Gautier; *Chem. Eur. J,* 15, **2009**, 314–318.
[191] M. Pellei, V. Gandin, M. Marinelli, C. Marzano, M. Yousufuddin, H. V. R. Dias, C. Santini; *Inorg. Chem,* 51, **2012**, 9873–9882.

Chapter 2 Non-symmetrically *p*-benzyl-substituted (benz)imidazole *N*-Heterocyclic carbene-silver(I) acetate complexes

Work published as:

Novel non-symmetrically p-benzyl-substituted (benz)imidazole N-Heterocyclic carbene-silver(I) acetate complexes – synthesis and biological evaluation, F. Hackenberg, A. Deally, G. Lally, S. Malenke, H. Müller-Bunz, F. Paradisi, S. Patil, D. Quaglia and M. Tacke, *International Journal of Inorganic Chemistry*, **2012**, 13 pages, doi:10.1155/2012/121540.

Novel non-symmetrically *p*-benzyl-substituted (benz)imidazole *N*-Heterocyclic carbene-silver(I) acetate complexes – synthesis and biological evaluation

Frauke Hackenberg, Anthony Deally, Grainne Lally, Sina Malenke, Helge Müller-Bunz, Francesca Paradisi, Siddappa Patil, Daniela Quaglia and Matthias Tacke*

Conway Institute of Biomolecular and Biomedical Research, Centre for Synthesis and Chemical Biology (CSCB), UCD School of Chemistry and Chemical Biology, University College Dublin, Belfield, Dublin 4, Ireland

2.1 Key Words

Anticancer drugs, antibacterial drugs, silver(I) acetate, NHC, Caki-1, *Staphylococcus aureus, Escherichia coli.*

2.2 Abstract

Non-symmetrically substituted *N*-Heterocyclic carbene (NHC) precursors **1a-d** and **3a-d** were synthesised by first reacting 1H-(benz)imidazole with *p*-cyanobenzyl bromide to give 4-(1H-imidazole-1-ylmethyl)benzonitrile (**1**) and 4-(1H-benzimidazole-1-ylmethyl)benzonitrile (**3**) and afterwards introducing benzyl bromide, 1-(bromomethyl)-4-methylbenzene, 1-(bromomethyl)-4-methoxybenzene and methyl 4-(bromomethyl)benzoate. The NHC-silver(I) acetate complexes (1-benzyl-3-(4-cyanobenzyl)-2,3-dihydro-1H-imidazole-2-ylidene) silver(I) acetate (**2a**), (1-(4-cyanobenzyl)-3-(4-methylbenzyl)-2,3-dihydro-1H-imidazole-2-ylidene) silver(I) acetate (**2b**), (1-(4-cyanobenzyl)-3-[4-(methoxycarbonyl)benzyl]-2,3-dihydro-1H-imidazole-2-ylidene) silver(I) acetate (**2c**), (1-benzyl-3-(4-cyanobenzyl)-2,3-dihydro-1H-benzimidazole-2-ylidene) silver(I) acetate (**4a**), (1-(4-cyanobenzyl)-3-(4-methylbenzyl)-2,3-dihydro-1H-benzimidazole-2-ylidene) silver(I) acetate (**4b**), (1-(4-cyanobenzyl)-3-(4-methoxybenzyl)-2,3-dihydro-1H-benzimidazole-2-ylidene) silver(I) acetate (**4c**) and (1-(4-cyanobenzyl)-3-[4-

(methoxycarbonyl)benzyl]-2,3-dihydro-1H-benzimidazole-2-ylidene) silver(I) acetate (**4d**) were yielded by reacting these NHC precursors with silver(I) acetate. The silver(I) acetate complex **4b** was characterised by single crystal X-ray diffraction. Preliminary *in vitro* antibacterial studies against the Gram-positive bacteria *Staphylococcus aureus* and the Gram-negative bacteria *Escherichia coli*, using the Kirby-Bauer disc diffusion method were carried out on the seven NHC-silver(I) acetate complexes **2a-c** and **4a-d**. Also the IC_{50} values of these seven complexes were determined by an MTT-based assay against the human renal cancer cell line Caki-1. The complexes **2a-c** and **4a-c** revealed the following IC_{50} values respectively: 25 (± 1), 15 (± 2), 5.4 (± 0.8), 16 (± 2), 7.1 (± 1), 20 (± 4) and 14 (± 1) μM.

2.3 Introduction

N-Heterocyclic carbenes (NHCs) are versatile ligands in silver complexes exhibiting antimicrobial activity, in particular for the possible treatment of pulmonary infections accompanying cystic fibrosis (CF) and chronic lung infections [1-3] and maybe in the treatment of cancer [4]. Youngs' research group have reported antimicrobial activity of NHC-silver complexes derived from 1H-imidazole, 4,5-dichloro-1H-imidazole and xanthines against a panel of highly resistant pathogens recovered from the respiratory tract of cystic fibrosis (CF) patients [1,3,5]. Another important contribution by the Ghosh research group led to the synthesis and antimicrobial evaluation of NHC-silver complexes derived from 1-benzyl-3-tert-butylimidazole [6]. In addition, *in vitro* and murine *in vivo* efficacy and toxicity studies of nebulised methylated caffeine-silver(I) complex (SCC1), for treatment of pulmonary infections [7]. Recently, a larger number of known compounds were evaluated as potential antibiotics by Roland and Jolivalt [8].

In addition, silver complexes have been reported to have anticancer activity *in vitro*. Egan has reported that silver complexes of coumarin derivatives possess anticancer activity against certain types of cancer [9]. Zhu has reported that silver carboxylate dimers possess anticancer activity against human carcinoma cells [10]. McKeage has shown phosphine complexes of silver to be active anticancer agents, even against cisplatin-resistant cell lines [11]. Youngs and co-workers have reported anticancer activity of NHC-silver complexes derived from 4,5-dichloro-1H-imidazole against the human cancer cell lines OVCAR-3 (ovarian), MB157 (breast), and HeLa (cervical) [4]. We have reported the anticancer (CAKI-1, renal) and antibacterial (E. coli, S. aureus) activity of benzyl-substituted *N*-Heterocyclic carbene-silver [12-17] and carbene-gold complexes [18, 19].

Within this paper we present a new series of non-symmetrically *p*-benzyl-substituted *N*-Heterocyclic carbene-silver acetate complexes derived from imidazole and benzimidazole, their synthesis, cytotoxicity and antibacterial studies.

2.4 Experimental

2.4.1 General:

All reactions were carried out under aerobic conditions. All silver(I) acetate reactions were carried out under exclusion of light. 1H-Imidazole, 1H-benzimidazole, benzyl bromide, 4-methylbenzyl bromide, methyl 4-(bromomethyl)benzoate, 4-cyanobenzyl bromide, silver(I)acetate and K_2CO_3 were procured commercially from Sigma-Aldrich Chemical Company and were used without further purification. IR Spectra were recorded on a Perkin-Elmer Paragon 1000 FT-IR spectrometer employing a KBr disc. NMR Spectra were measured either on a Varian 300 MHz or 400 MHz spectrometer. All chemical shifts are reported in ppm and referenced to TMS. ESI MS was performed on a quadrupole tandem mass spectrometer (Quattro Micro, Micromass/Water's Corp., USA), using solutions in 100% MeOH. MS spectra were obtained in the ES+ (electron spray positive ionisation) mode for all compounds. CHN Analysis was carried out in an Exeter Analytical CE-440 elemental analyzer. Crystal Data was collected using an Agilent Technologies (former Oxford Diffraction) SuperNova diffractometer fitted with an Atlas detector. **4b** was measured with Mo-Kα (0.71073 Å) at 100 K. A four times redundant dataset was collected, assuming that the Friedel pairs are not equivalent. An analytical absorption correction based on the shape of the crystal was performed [20]. The structure was solved by direct methods using SHELXS-97 [21] and refined by full matrix least-squares on F^2 for all data using SHELXL-97 [21]. Hydrogen atoms were added at calculated positions and refined using a riding model. Their isotropic thermal displacement parameters were fixed to 1.2 (1.5 for methyl groups) times the equivalent ones of the parent atom. Anisotropic thermal displacement parameters were used for all non-hydrogen atoms. A suitable crystal of **4b** was grown in a saturated solution of chloroform with slow infusion of pentane. Further details about the data collection are listed in Table 1.
CCDC 853680 (for **4b**) contains the supplementary crystallographic data for this paper. These data can be obtained free of charge from the Cambridge Crystallographic Data Centre via www.ccdc.cam.ac.uk/data_request/cif.

2.4.2 Synthesis:

4-(1H-Imidazole-1-ylmethyl)benzonitrile (1):

1H-Imidazole (1.478 g, 22.03 mmol), 4-(bromomethyl)benzonitrile (4.319 g, 22.03 mmol) and K_2CO_3 (4.560 g, 33.00 mmol) were stirred in CH_3CN at room temperature for 2 d. After the solvent was removed under reduced pressure, water (30 mL) was added. The aqueous phase was extracted with CH_2Cl_2 (3x 20 mL) and the combined organic phases were dried with magnesium sulfate. After removing the solvent under reduced pressure the product (**1**) was yielded (3.511 g, 19.14 mmol, 87% yield) as a white powder.

^{1}H NMR (δ ppm, $CDCl_3$, 300 MHz): 7.65 (d, *J*= 7.7, 2H, $CH_{cyanobenzyl}$), 7.56 (s, 1H, $CH_{imidazole}$), 7.21(d, *J*= 7.2, 2H, $CH_{cyanobenzyl}$), 7.12 (d, 1H, $CH_{imidazole}$), 6.89 (s, 1H, NCHN), 5.20 (s, 2H, CH_2).

^{13}C NMR (δ ppm, $CDCl_3$, 100 MHz, proton decoupled): 139.6, 134.4, 132.9, 128.4, 128.2, 118.7, 113.9, 111.9 (NCHN, CN, $C_{imidazole}$), 50.2 (CH_2).

IR absorptions (KBr, cm^{-1}): 3427 (m), 3132 (s), 3063 (m), 2981 (s), 2852 (s), 2226 (s), 1608 (m), 1567 (s), 1411 (s), 1355 (m), 1209 (s), 1161 (s), 769 (m), 634 (m), 550 (m).

MS (m/z, QMS-MS/MS): 182.07 [M^+-H].

Micro Analysis Calculated for $C_{11}H_9N_3$ (183.21): Calcd.: C, 72.11%; H, 4.95%; N, 22.94%; Found: C, 72.03%; H, 5.05%; N, 22.92%.

1-Benzyl-3-(4-cyanobenzyl)-2,3-dihydro-1H-imidazole-2-ylium bromide (1a):

4-(1H-Imidazole-1-ylmethyl)benzonitrile (**1**) (0.500 g, 2.73 mmol) and 1.5 equivalents of benzyl bromide (0.701 g, 4.10 mmol) were dissolved in toluene (30 mL) and heated under reflux for 6 h. After removing the solvent under reduced pressure the obtained sticky white product was washed with pentane (2x 10 ml), diethylether (3x 5 mL) and THF (2x 10 mL) to yield a white powder (0.512 g, 1.44 mmol, 53% yield).

^{1}H NMR (δ ppm, $CDCl_3$, 300 MHz): 11.36 (s, 1H, NCHN), 7.71 (bs, 4H, $CH_{cyanobenzyl}$), 7.44 (s, 5H, CH_{benzyl}), 7.08 (s, 1H, $CH_{imidazole}$), 7.04 (s, 1H, $CH_{imidazole}$), 5.78 (s, 2H, CH_2), 5.48 (s, 2H, CH_2).

^{13}C NMR (δ ppm, $CDCl_3$, 100 MHz, proton decoupled): 137.9 (NCHN), 137.8, 133.2, 132.1, 129.9, 129.8, 129.7, 129.0, 121.8, 121.7, 117.9, 113.6 (CN + $C_{imidazole}$ + $C_{cyanobenzyl}$ + C_{benzyl}), 53.9, 52.6 (CH_2).

IR absorptions (KBr, cm^{-1}): 3461 (m), 3130 (s), 3058 (s), 2980 (s), 2920 (s), 2226 (s), 1608 (m), 1567 (s), 1411 (m), 1355 (m), 1209 (s), 1160 (s), 770 (s), 634 (m), 549 (m).

MS (m/z, QMS-MS/MS): 274.12 [M^+-Br].

Micro Analysis Calculated for $C_{18}H_{16}BrN_3$ (354.24): Calcd.: C, 61.03%; H, 4.55%; N, 11.86%; Found: C, 60.96%; H, 4.52%, N, 11.68%.

1-(4-Cyanobenzyl)-3-(4-methylbenzyl)-2,3-dihydro-1H-imidazole-2-ylium bromide (1b):

4-(1H-Imidazole-1-ylmethyl)benzonitrile (**1**) (0.500 g, 2.73 mmol) and 1.5 equivalents of 1-(bromomethyl)-4-methylbenzene (0.759 g, 4.10 mmol) were dissolved in toluene (30 mL) and heated under reflux for 6 h. After removing the solvent under reduced pressure the obtained sticky white product was washed with pentane (2x 10 mL), diethylether (3x 5 mL) and THF (2x 10 mL) to yield a white powder (0.784 g, 2.13 mmol, 78% yield).

^{1}H NMR (δ ppm, $CDCl_3$, 300 MHz): 10.74 (s, 1H, NCHN), 7.76 (d, *J* = 8.2 Hz, 2H, $CH_{cyanobenzyl}$), 7.64 (d, *J* = 8.2 Hz, 2H, $CH_{cyanobenzyl}$), 7.52 (s, 1H, $CH_{imidazole}$), 7.35 – 7.26 (m, 2H, $CH_{imidazole}$, $CH_{methylbenzyl}$), 7.18 (d, *J* = 7.6 Hz, 3H, $CH_{imidazole}$, $CH_{methylbenzyl}$), 5.82 (s, 2H, CH_2), 5.45 (s, 2H, CH_2), 2.33 (s, 3H, CH_3).

^{13}C NMR (δ ppm, $CDCl_3$, 100 MHz, proton decoupled): 139.8(NCHN), 138.3, 136.9, 133.0, 130.2, 129.9, 129.4, 128.9, 122.5, 121.9, 118.1, 113.2 (CN + $C_{imidazole}$ + $C_{cyanobenzyl}$ + $C_{methylbenzyl}$), 53.4, 52.3 (CH_2), 21.2 (CH_3).

IR absorptions (KBr, cm^{-1}): 3455 (m), 3130 (s), 3052 (s), 2981 (s), 2852 (s), 2227 (s), 1609 (m), 1566 (s), 1411 (m), 1209 (m), 1160 (s), 769 (s), 635 (m), 551 (s).

MS (m/z, QMS-MS/MS): 288.11 [M^+-Br].

Micro Analysis Calculated for $C_{19}H_{18}BrN_3$ (368.27): Calcd.: C, 61.97%; H, 4.93%; N, 11.41%; Found: C, 62.34%; H, 5.01%; N, 11.21%.

1-(4-Cyanobenzyl)-3-(4-methoxybenzyl)-2,3-dihydro-1H-imidazole-2-ylium bromide (1c):

4-(1H-Imidazole-1-ylmethyl)benzonitrile (1) (0.500 g, 2.73 mmol) and 1.5 equivalents of 1-(bromomethyl)-4-methoxybenzene (0.59 mL, 4.1 mmol) were dissolved in toluene (30 mL) and heated under reflux for 6 h. After removing the solvent under reduced pressure the obtained sticky white product was washed with pentane (2x 10 mL), diethylether (3x 5 mL) and THF (2x 10 mL) to yield a white powder (1.038 g, 2.70 mmol, 99% yield).

^{1}H NMR (δ ppm, $CDCl_3$, 300 MHz): 11.24 (s, 1H, NCHN), 7.69 (d, *J* = 9.2 Hz, 4H, $CH_{cyanobenzyl}$), 7.50 – 7.17 (m, 4H, $CH_{methoxybenzyl}$), 6.92 (s, 2H, $CH_{imidazole}$), 5.81 (s, 2H, CH_2), 5.42 (s, 2H, CH_2), 3.80 (s, 3H, CH_3).

^{13}C NMR (δ ppm, $CDCl_3$, 100 MHz, proton decoupled): 138.3(NCHN), 137.0, 133.0, 130.7, 129.8, 129.3, 124.3, 122.2, 121.8, 121.5, 118.1, 114.9, 113.2 (CN + $C_{imidazole}$ + $C_{cyanobenzyl}$ + $C_{methylbenzyl}$), 55.4 (OCH_3), 53.3, 52.4 (CH_2).

IR absorptions (KBr, cm^{-1}): 3414 (m), 3059 (s), 2986 (s), 2964 (s), 2223 (s), 1610 (m), 1553 (s), 1516 (s), 1257 (m), 1146 (s), 1032 (m), 846 (m), 629 (s), 562 (m).

MS (m/z, QMS-MS/MS): 304.06 [M^+-Br].

Micro Analysis Calculated for $C_{19}H_{18}BrN_3O$ (384.27): Calcd.: C, 59.39%; H, 4.72%; N, 10.94%; Found: C, 59.01%; H, 4.80%; N, 10.47%.

1-(4-Cyanobenzyl)-3-[4-(methoxycarbonyl)benzyl]-2,3-dihydro-1H-imidazole-2-ylium bromide (1d):

4-(1H-Imidazole-1-ylmethyl)benzonitrile (1) (0.500 g, 2.73 mmol) and 1.5 equivalents of methyl 4-(bromomethyl)benzoate (0.939 g, 4.10 mmol) were dissolved in toluene (30 mL) and heated under reflux for 6 h. After removing the solvent under reduced pressure the obtained sticky white product was washed with pentane (2x 10 mL), diethylether (3x 5 mL) and THF (2x 10 mL) to yield a white powder (0.461 g, 1.12 mmol, 41% yield).

^{1}H NMR (δ ppm, $CDCl_3$, 300 MHz): 10.99 (s, 1H, NCHN), 8.02 (d, 2H, J = 8.4 Hz, $CH_{cyanobenzyl}$), 7.67 (m, 4H, $CH_{methoxycarbonylbenzyl}$), 7.54 (d, 2H, J = 8.4 Hz, $CH_{cyanobenzyl}$), 7.40 (s, 1H, $CH_{imidazole}$), 7.28 (s, 1H, $CH_{imidazole}$), 5.77 (s, 2H, $CH_{2cyanobenzyl}$), 5.65 (s, 2H, $CH_{2methoxycarbonylbenzyl}$), 3.92 (s, 3H, CH_3).

^{13}C NMR (δ ppm, $CDCl_3$, 100 MHz, proton decoupled): 160.1 (C=O), 142.6 (NCHN), 137.9, 137.2, 133.1, 131.3, 130.6, 130.0, 129.9, 129.0, 122.4, 122.2, 117.9, 113.4 ($C_{imidazole}$ + $C_{cyanobenzyl}$ + $C_{methoxycarbonylbenzyl}$), 55.1, 52.2 ($CH_2$) ,32.2 ($CH_3$).

IR absorptions (KBr, cm^{-1}): 3403 (m), 3132 (s), 3062 (s), 2983 (s), 2851 (s), 2226 (s), 1718 (m), 1609 (m), 1566 (s), 1412 (s), 1286 (s), 1161 (s), 769 (s), 635 (m), 556 (s).

MS (m/z, QMS-MS/MS): 332.09 [M^+-Br].

Micro Analysis Calculated for $C_{20}H_{18}BrN_3O_2$ (412.28): Calcd.: C, 58.26%; H, 4.40%; N, 10.19%; Found: C, 59.01%; H, 4.68%; N, 10.89%.

(1-Benzyl-3-(4-cyanobenzyl)-2,3-dihydro-1H-imidazole-2-ylidene) silver(I) acetate (2a):

1-Benzyl-3-(4-cyanobenzyl)-2,3-dihydro-1H-imidazole-2-ylium bromide (1a) (0.499 g, 1.41 mmol) and 2 equivalents of silver(I) acetate (0.471 g, 2.82 mmol) were dissolved in 30 mL of methanol/dichloromethane (1:1) and stirred in darkness at room temperature for 4 d. After filtering off the AgBr by-product, the solvent was reduced to 3 mL and by adding dropwise 10 mL of pentane a white powder

precipitated. The solvent was decanted and the white precipitate was washed with pentane (2x, 10 mL) and diethylether (3x, 10 mL) to yield a white powder (0.422 g, 0.96 mmol, 68% yield).

^{1}H NMR (δ ppm, $CDCl_3$, 300 MHz): 7.70 (m, 5H, $CH_{cyanobenzyl}$, CH_{benzyl}), 7.39 (m, 4H, $CH_{cyanobenzyl}$, CH_{benzyl}), 7.01 (d, 2H, $CH_{imidazole}$), 5.40 (s, 4H, CH_2), 2.05 (s, 3H, $CH_{3acetate}$).

^{13}C NMR (δ ppm, $CDCl_3$, 100 MHz, proton decoupled): 188.1 (NCN), 166.1 (C=O), 144.1, 137.5, 136.9, 133.1, 131.2, 130.6, 129.1, 128.2, 127.5, 117.9 ($C_{cyanobenzyl}$ + $C_{imidazole}$ + C_{benzyl}), 52.4, 51.2 (CH_2), 21.7 ($CH_{3acetate}$).

IR absorptions (KBr, cm^{-1}): 3410 (s), 3154 (s), 2230 (s), 1564 (s), 1411 (s), 1237 (m), 777 (m), 672 (w), 557 (m).

MS (m/z, QMS-MS/MS): 382.23 [M^+-$OCOCH_3$].

Micro Analysis Calculated for $C_{20}H_{18}AgN_3O_2$ (440.24): Calcd.: C, 54.56%; H, 4.12%; N, 9.54%; Found: C, 55.01%; H, 4.24%; N, 9.07%.

(1-(4-Cyanobenzyl)-3-(4-methylbenzyl)-2,3-dihydro-1H-imidazole-2-ylidene) silver(I) acetate (2b):

1-(4-Cyanobenzyl)-3-(4-methylbenzyl)-2,3-dihydro-1H-imidazole-2-ylium bromide (1b) (0.501 g, 1.36 mmol) and 2 equivalents of silver(I) acetate (0.451 g, 2.72 mmol) were dissolved in 30 mL of methanol/dichloromethane (1:1) and stirred in darkness at room temperature for 4 d. After filtering off the AgBr by-product, the solvent was reduced to 3 mL and by adding dropwise 10 ml of pentane a white powder precipitated. The solvent was decanted and the white precipitate was washed with pentane (2x, 10 mL) and diethylether (3x, 10 mL) to yield a white powder (0.296 g, 0.650 mmol, 48% yield).

^{1}H NMR (δ ppm, $CDCl_3$, 300 MHz): 7.70 (m, 4H, $CH_{cyanobenzyl}$, $CH_{methylbenzyl}$), 7.40 (m, 4H, $CH_{cyanobenzyl}$, $CH_{methylbenzyl}$), 7.01 (d, 2H, $CH_{imidazole}$), 5.40 (d, 4H, CH_2), 1.91 (d, 6H, $CH_{3acetate}$, $CH_{3methylbenzyl}$).

^{13}C NMR (δ ppm, $CDCl_3$, 100 MHz, proton decoupled): 178.4 (NCN), 176.5 (C=O), 140.4, 138.0, 133.2, 132.9, 129.5, 128.4, 121.9, 121.3, 118.0, 112.8, 110.0 (CN + $C_{imidazole}$ + $C_{cyanobenzyl}$ + $C_{methylbenzyl}$), 55.2, 52.7 (CH_2), 30.9 ($CH_{3methylbenzyl}$), 23.3 ($CH_{3actetate}$).

IR absorptions (KBr, cm^{-1}): 3391 (s), 3053 (m), 2227 (s), 1567 (s), 1410 (s), 1238 (m), 1158 (m), 771 (s), 690 (s), 624 (m).

MS (m/z, QMS-MS/MS): 392.23 [M^+-$OCOCH_3$].

Micro Analysis Calculated for $C_{21}H_{20}AgN_3O_2$ (454.27): Calcd.: C, 55.52%; H, 4.44%; N, 9.25%; Found: C, 55.48%; H, 4.62%; N, 9.09%.

(1-(4-Cyanobenzyl)-3-[4-(methoxycarbonyl)benzyl]-2,3-dihydro-1H-imidazole-2-ylidene) silver(I) acetate (2c):

1-(4-Cyanobenzyl)-3-[4-(methoxycarbonyl)benzyl]-2,3-dihydro-1H-imidazole-2-ylium bromide (**1d**) (0.449 g, 1.09 mmol) and 2 equivalents of silver(I) acetate (0.363 g, 2.18 mmol) were dissolved in 30 mL of methanol/dichloromethane (1:1) and stirred in darkness at room temperature for 3 d. After filtering off the AgBr by-product, the solvent was reduced to 3 mL and by adding dropwise 10 mL of pentane a white powder precipitated. The solvent was decanted and the white precipitate was washed with pentane (2x, 10 mL) and diethylether (3x, 10 mL) to yield a white powder (0.309 g, 0.620 mmol, 57% yield).

^1H NMR (δ ppm, $CDCl_3$, 300 MHz): 7.68 (d, 4H, $CH_{cyanobenzyl}$, $CH_{methoxycarbonylbenzyl}$), 7.40 (d, 4H, $CH_{cyanobenzyl}$, $CH_{methoxycarbonylbenzyl}$), 7.01 (s, 2H, $CH_{imidazole}$), 5.75 (d, 2H, CH_2), 5.72 (d, 2H, CH_2), 3.91 (s, 3H, $CH_{3\ methoxycarbonylbenzyl}$), 2.07 (s, 3H, $CH_{3acetate}$).

^{13}C NMR (δ ppm, $CDCl_3$, 100 MHz, proton decoupled): 178.3 (NCN), 156.2 (C=O), 140.2, 133.0, 130.5, 128.5, 122.0, 118.0, 112.9, 110.0 ($C_{imidazole}$ + $C_{methoxycarbonylbenzyl}$ + $C_{cyanobenzyl}$), 55.4, 55.3 (CH_2), 30.9 ($OCH_{3methoxycarbonylbenzyl}$), 22.4 ($OCH_{3acetate}$).

IR absorptions (KBr, cm^{-1}): 3417 (s), 3080 (s), 2229 (s), 1720 (m), 1566 (s), 1412 (s), 1281 (w), 656 (s).

MS (m/z, QMS-MS/MS): 440.23 [M^+-$OCOCH_3$].

Micro Analysis Calculated for $C_{22}H_{20}AgN_3O_4$ (498.28): Calcd.: C, 53.03%; H, 4.05%; N, 8.43%; Found: C, 52.66%; H, 4.12%, N, 8.01%.

4-(1H-Benzimidazole-1-ylmethyl)benzonitrile (3):

1H-Benzimidazole (1.488 g, 12.70 mmol), 4-(bromomethyl)benzonitrile (2.489 g, 12.70 mmol) and K_2CO_3 (2.633 g, 19.05 mmol) were stirred in CH_3CN at room temperature for 2 d. After the solvent was removed under reduced pressure, water (30 mL) was added. The aqueous phase was extracted with CH_2Cl_2 (3x 20 mL) and the combined organic phases were dried with magnesium sulfate. After removing the solvent under reduced pressure the product (**3**) was yielded as a white powder (2.637 g, 11.81 mmol, 93% yield).

^{1}H NMR (δ ppm, $CDCl_3$, 300 MHz): 7.98 (s, 1H, NCHN), 7.86 (d, 1H, $CH_{benzimidazole}$), 7.64 (d, 2H, $CH_{cyanobenzyl}$), 7.24 (m, 5H, $CH_{cyanobenzyl}$, $CH_{benzimidazole}$), 5.45 (s, 2H, CH_2).

^{13}C NMR (δ ppm, $CDCl_3$, 100 MHz, proton decoupled): 138.2, 137.9, 134.6, 134.2, 128.9, 128.1, 120.3, 119.1, 118.4, 113.7 (NCHN, CN, $C_{benzimidazole}$), 47.3 (CH_2).

IR absorptions (KBr, cm^{-1}): 3427 (m), 3060 (m), 2222 (s), 1615 (m), 1490 (s), 1457 (s), 1364 (m), 1284 (s), 1259 (s), 1167 (s), 761 (m), 745 (m), 556 (s).

MS (m/z, QMS-MS/MS): 232.09 [M^+-H].

Micro Analysis Calculated for $C_{15}H_{11}N_3$ (223.27): Calcd.: C, 77.23%, H, 4.75%; N, 18.01%; Found: C, 76.47%; H, 4.73%; N, 17.77%.

1-Benzyl-3-(4-cyanobenzyl)-2,3-dihydro-1H-benzimidazole-2-ylium bromide (3a):

4-(1H-Benzimidazole-1-ylmethyl)benzonitrile (**3**) (0.500 g, 2.24 mmol) and 1.5 equivalents of benzyl bromide (0.575 g, 3.36 mmol) were dissolved in toluene (30 mL) and heated under reflux for 6 h. After removing the solvent under reduced

pressure the obtained sticky white product was washed with pentane (2x 10 mL), diethylether (3x 5 mL) and THF (2x 10 mL) to yield a white powder (0.624 g, 1.54 mmol, 69% yield).

^{1}H NMR (δ ppm, $CDCl_3$, 300 MHz): 12.02 (s, 1H, NCHN), 7.73 (d, *J* = 8.0 Hz, 2H, $CH_{cyanobenzyl}$), 7.65 (d, *J* = 8.0 Hz, 2H, $CH_{cyanobenzyl}$), 7.53 (d, *J* = 10.9 Hz, 6H, $CH_{benzimidazole}$, CH_{benzyl}), 7.39 (d, *J* = 5.1 Hz, 3H, $CH_{benzimidazole}$, CH_{benzyl}), 6.10 (s, 2H), 5.83 (s, 2H).

^{13}C NMR (δ ppm, $CDCl_3$, 100 MHz, proton decoupled): 143.7 (NCHN), 137.7, 133.1, 132.1, 131.2, 129.5, 129.1, 128.3, 127.4, 117.9, 113.9, 113.3 (CN + $C_{benzimidazole}$ + $C_{cyanobenzyl}$ + C_{benzyl}), 51.9, 50.7 (CH_2).

IR absorptions (KBr, cm^{-1}): 3451 (s), 3384 (s), 3121 (s), 3035 (s), 2877 (s), 2228 (s), 1607 (m), 1554 (s), 1454 (s), 1184 (s), 1020 (m), 770 (s), 622 (m).

MS (m/z, QMS-MS/MS): 324.14 [M^+-Br].

Micro Analysis Calculated for $C_{22}H_{18}BrN_3$ (404.30): Calcd.: C, 65.36%; H, 4.49%; N, 10.39%; Found: C, 65.40%; H, 4.40%, N, 10.21%.

1-(4-Cyanobenzyl)-3-(4-methylbenzyl)-2,3-dihydro-1H-benzimidazole-2-ylium bromide (3b):

4-(1H-Benzimidazole-1-ylmethyl)benzonitrile (**3**) (0.500 g, 2.24 mmol) and 1.5 equivalents of 1-(bromomethyl)-4-methylbenzene (0.622 g, 3.36 mmol) were dissolved in toluene (30 mL) and heated under reflux for 6 h. After removing the solvent under reduced pressure the obtained sticky white product was washed with pentane (2x 10 mL), diethylether (3x 5 mL) and THF (2x 10 mL) to yield a white powder (0.787 g, 1.88 mmol, 84% yield).

^{1}H NMR (δ ppm, $CDCl_3$, 300 MHz): 11.94 (s, 1H, NCHN), 7.72 (d, *J* = 8.2 Hz, 2H, $CH_{cyanobenzyl}$), 7.64 (d, *J* = 8.2 Hz, 2H, $CH_{cyanobenzyl}$), 7.53 (d, *J* = 16.2 Hz, 4H, $CH_{benzimidazole}$), 7.39 (d, *J* = 8.0 Hz, 2H, $CH_{methylbenzyl}$), 7.18 (d, *J* = 8.0 Hz, 2H, $CH_{methylbenzyl}$), 6.10 (s, 2H, CH_2), 5.77 (s, 2H, CH_2), 2.33 (s, 3H, CH_3).

^{13}C NMR (δ ppm, $CDCl_3$, 100 MHz, proton decoupled): 143.5 (NCHN), 139.5, 137.8, 133.0, 131.2, 130.1, 129.1, 128.3, 127.3, 118.0, 114.0, 113.4, 113.1 143.7, 137.7, 133.1, 132.1, 131.2, 129.5, 129.1, 128.3, 127.4, 117.9, 113.9, 113.3 (CN + $C_{benzimidazole}$ + $C_{cyanobenzyl}$ + $C_{methylbenzyl}$), 51.8, 50.7 (CH_2), 21.2 (CH_3).

IR absorptions (KBr, cm^{-1}): 3465 (s), 3397 (s), 3127 (s), 3032 (s), 2968 (s), 2885 (s), 2230 (s), 1608 (m), 1561 (s), 1416 (m), 1372 (s), 1191 (s), 1019 (m), 761 (s), 613 (m), 554 (m).

MS (m/z, QMS-MS/MS): 338.13 [M^+-Br].

Micro Analysis Calculated for $C_{23}H_{20}BrN_3$ (418.33): Calcd.: C, 66.04%; H, 4.82%; N, 10.04%; Found: C, 65.99%; H, 4.79%, N, 10.04%.

1-(4-Cyanobenzyl)-3-(4-methoxybenzyl)-2,3-dihydro-1H-benzimidazole-2-ylium bromide (3c):

4-(1H-Benzimidazole-1-ylmethyl)benzonitrile (**3**) (0.500 g, 2.24 mmol) and 1.5 equivalents of 1-(bromomethyl)-4-methoxybenzene (0.484 ml, 3.36 mmol) were dissolved in toluene (30 mL) and heated under reflux for 6 h. After removing the solvent under reduced pressure the obtained sticky white product was washed with pentane (2x 10 mL), diethylether (3x 5 mL) and THF (2x 10 mL) to yield a white powder (0.651 g, 1.50 mmol, 67% yield).

^1H NMR (δ ppm, $CDCl_3$, 300 MHz): 11.91 (s, 1H, NCHN), 7.72 (d, *J* = 8.2 Hz, 2H, $CH_{cyanobenzyl}$), 7.63 (d, *J* = 8.2 Hz, 2H, $CH_{cyanobenzyl}$), 7.60 – 7.41 (m, 6H, $CH_{benzimidazole}$, $CH_{methoxybenzyl}$), 6.89 (d, *J* = 8.6 Hz, 2H, $CH_{methoxybenzyl}$), 6.09 (s, 2H, CH_2), 5.75 (s, 2H, CH_2), 3.77 (s, 3H, CH_3).

^{13}C NMR (δ ppm, $CDCl_3$, 100 MHz, proton decoupled): 144.3 (NCHN), 137.9, 133.1, 131.2, 129.9, 129.1, 127.3, 124.2, 117.9, 114.8, 113.9, 113.2 (CN + $C_{benzimidazole}$ + $C_{cyanobenzyl}$ + $C_{methoxybenzyl}$), 55.34 (OCH_3), 51.5, 50.6 (CH_2).

IR absorptions (KBr, cm^{-1}): 3420 (s), 3122 (s), 3035 (s), 2968 (s), 2840 (s), 2229 (s), 1792 (w), 1609 (s), 1555 (s), 1514 (s), 1459 (s), 1370 (s), 1254 (s), 1178 (s), 1112 (s), 1013 (s), 763 (s), 613 (s).

MS (m/z, QMS-MS/MS): 355.08 [M^+-Br].

Micro Analysis Calculated for $C_{23}H_{20}BrN_3O$ (434.33): Calcd.: C, 63.60%; H: 4.64%; N, 9.67%; Found: C, 63.41%; H, 4.70%; N, 9.69%.

1-(4-Cyanobenzyl)-3-[4-(methoxycarbonyl)benzyl]-2,3-dihydro-1H-benzimidazole-2-ylium bromide (3d):

4-(1H-Benzimidazole-1-ylmethyl)benzonitrile (**3**) (0.500 g, 2.24 mmol) and 1.5 equivalents of methyl 4-(bromomethyl)benzoate (0.770 g, 3.36 mmol) were dissolved in toluene (30 mL) and heated under reflux for 6 h. After removing the solvent under reduced pressure the obtained sticky white product was washed with pentane (2x 10 mL), diethylether (3x 5 mL) and THF (2x 10 mL) to yield a white powder (0.735 g, 1.59 mmol, 71% yield).

^{1}H NMR (δ ppm, $CDCl_3$, 300 MHz): 12.09 (s, 1H, NCHN), 8.03 (d, *J* = 8.2 Hz, 2H, $CH_{cyanobenzyl}$), 7.72 (d, *J* = 8.2 Hz, 2H, $CH_{cyanobenzyl}$), 7.66 (d, *J* = 8.2 Hz, 2H, $CH_{benzimidazole}$), 7.58 (d, *J* = 8.2 Hz, 2H, $CH_{benzimidazole}$), 7.51 (d, *J* = 5.5 Hz, 4H, $CH_{methoxycarbonylbenzyl}$), 6.07 (s, 2H, CH_2), 5.96 (s, 2H, CH_2), 3.91 (s, 3H, CH_3).

^{13}C NMR (δ ppm, $CDCl_3$, 100 MHz, proton decoupled): 166.20 (C=O), 143.88 (NCHN), 139.76, 139.48, 133.32, 131.50, 130.17, 129.56, 129.03, 127.42, 118.86, 114.45, 114.39, 111.93 (CN + $C_{benzimidazole}$ + $C_{cyanobenzyl}$ + $C_{methoxycarbonylbenzyl}$), 52.75 (OCH3), 50.14, 49.96 ($CH_{2cyanobenzyl}$ + $CH_{2methoxycarbonylbenzyl}$).

IR absorptions (KBr, cm^{-1}): 3433 (s), 2963 (s), 2228 (s), 1717 (s), 1560 (m), 1435 (m), 1416 (m), 1283 (s), 1189 (m), 1107 (m), 748 (m), 601 (m).

MS (m/z, QMS-MS/MS): 382.05 [M^+-Br].

Micro Analysis Calculated for $C_{24}H_{20}BrN_3O_2$ (462.34): Calcd.: C, 62.35%; H, 4.36%; N, 9.09%; Found: C, 61.90%; H, 4.14%; N, 9.10%.

(1-Benzyl-3-(4-cyanobenzyl)-2,3-dihydro-1H-benzimidazole-2-ylidene) silver(I) acetate (4a):

1-Benzyl-3-(4-cyanobenzyl)-2,3-dihydro-1H-benzimidazole-2-ylium bromide (**3a**) (0.150 g, 0.370 mmol) and 2 equivalents of silver(I) acetate (0.124 g, 0.740 mmol) were dissolved in 30 ml of dichloromethane and stirred in darkness at room temperature for 3 d. After filtering off the AgBr by-product, the solvent was reduced to 3 mL and by adding dropwise 10 mL of pentane a white powder precipitated. The solvent was decanted and the white precipitate was washed with pentane (2x, 10 mL) and diethylether (3x, 10 mL) to yield a white powder (0.094 g, 0.192 mmol, 52% yield).

^{1}H NMR (δ ppm, $CDCl_3$, 300 MHz): 7.64 (d, 2H, $CH_{cyanobenzyl}$), 7.30 (m, 11H, $CH_{cyanobenzyl}$, $CH_{benzimidazole}$, CH_{benzyl}), 5.74 (s, 2H, CH_2), 5.66 (s, 2H, CH_2), 2.09 (s, 3H, $CH_{3acetate}$).

^{13}C NMR (δ ppm, $CDCl_3$, 100 MHz, proton decoupled): 189.21 (NCN), 165.20 (C=O), 142.29, 136.61, 133.19, 129.23, 128.74, 128.50, 128.00, 124.63, 118.95, 113.02, 112.72, 111.28, 109.99 ($C_{cyanobenzyl}$, $C_{benzimidazole}$, C_{benzyl}), 52.56, 51.85 (CH_2), 23.82 ($CH_{3acetate}$).

IR absorptions (KBr, cm^{-1}): 3476 - 3364 (m), 3037-2922 (s), 2229 (m), 1607 (s), 1562 (s), 1390 (s), 1335 (m), 740 (s), 657 (s), 614 (s), 552 (m), 454 (m).

MS (m/z, QMS-MS/MS): 430.05 [M^+-$OCOCH_3$].

Micro Analysis Calculated for $C_{24}H_{20}AgN_3O_2$ (490.30): Calcd.: C, 58.79%; H, 4.11%; N, 8.57%; Found: C, 58.71%; H, 4.03%; N, 8.69%.

(1-(4-Cyanobenzyl)-3-(4-methylbenzyl)-2,3-dihydro-1H-benzimidazole-2-ylidene) silver(I) acetate (4b):

1-(4-Cyanobenzyl)-3-(4-methylbenzyl)-2,3-dihydro-1H-benzimidazole-2-ylium bromide (**3b**) (0.498 g, 1.19 mmol) and 2 equivalents of silver(I) acetate (0.399 g, 2.39 mmol) were dissolved in 30 mL of dichloromethane and stirred in darkness at room temperature for 3 d. After filtering off the AgBr by-product, the solvent was reduced to 3 mL and by adding dropwise 10 mL of pentane a white powder

precipitated. The solvent was decanted and the white precipitate was washed with pentane (2x, 10 mL) and diethylether (3x, 10 mL) to yield a white powder (0.462 g, 0.916 mmol, 77% yield).

^{1}H NMR (δ ppm, $CDCl_3$, 300 MHz): 7.25 (m, 12 H, $CH_{cyanobenzyl}$, $CH_{methylbenzyl}$, $CH_{benzimidazole}$), 5.73 (d, 2H, CH_2), 5.61 (d, 2H, CH_2), 2.32 (s, 3H, $CH_{3\ methylbenzyl}$), 2.08 (s, 3H, $CH_{3acetate}$).

^{13}C NMR (δ ppm, $CDCl_3$, 100 MHz, proton decoupled): 179.1 (NCN), 138.5, 133.9, 133.7, 132.9, 131.7, 131.7, 129.8, 127.9, 127.3, 124.5, 118.2, 112.4, 111.6 ($C_{cyanobenzyl}$, $C_{benzimidazole}$, $C_{methylbenzyl}$), 55.5, 52.8 (CH_2), 22.8, 21.1 ($CH_{3methylbenzyl}$, $CH_{3actetate}$).

IR absorptions (KBr, cm^{-1}): 3417 (m), 3030 (s), 2229 (m), 1571 (s), 1391 (s), 796 (m), 743 (m), 668 (m), 612 (m).

MS (m/z, QMS-MS/MS): 445.95 [M^{+}-$OCOCH_3$].

Micro Analysis Calculated for $C_{25}H_{22}AgN_3O_2$ (504.33): Calcd.: C, 59.54%; H, 4.40%; N, 8.33%; Found: C, 60.04%; H, 4.38%, N, 8.37%.

(1-(4-Cyanobenzyl)-3-(4-methoxybenzyl)-2,3-dihydro-1H-benzimidazole-2-ylidene) silver(I) acetate (4c):

1-(4-Cyanobenzyl)-3-(4-methoxybenzyl)-2,3-dihydro-1H-benzimidazole-2-ylium bromide (**3c**) (0.499 g, 1.15 mmol) and 2 equivalents of silver(I) acetate (0.383 g, 2.30 mmol) were dissolved in 30 mL of dichloromethane and stirred in darkness at room temperature for 2 d. After filtering off the AgBr by-product, the solvent was reduced to 3 mL and by adding dropwise 10 mL of pentane a white powder precipitated. The solvent was decanted and the white precipitate was washed with pentane (2x, 10 mL) and diethylether (3x, 10 mL) to yield a white powder (0.418 g, 0.805 mmol, 70% yield).

^{1}H NMR (δ ppm, $CDCl_3$, 300 MHz): 7.25 (m, 12H, $CH_{cyanobenzyl}$, $CH_{methoxybenzyl}$, $CH_{benzimidazole}$), 5.74 (d, 2H, CH_2), 5.58 (d, 2H, CH_2), 3.78 (s, 3H, CH_3), 2.07 (s, 3H, $OCH_{3acetate}$).

^{13}C NMR (δ ppm, $CDCl_3$, 100 MHz, proton decoupled): 178.8 (NCN), 159.8 (C=O), 133.9, 133.7, 132.9, 128.8, 127.9, 124.4, 118.1, 114.5, 112.4, 111.5 ($C_{cyanobenzyl}$, $C_{benzimidazole}$, $C_{methoxybenzyl}$), 55.3, 53.2 (CH_2), 30.9 ($CH_{3methoxybenzyl}$), 22.9 ($CH_{3acetate}$).

IR absorptions (KBr, cm-1): 3390 (m), 2929 (s) [C-H], 2228 (s), 1608 (s), 1571 (s), 1513 (s), 1393 (s), 1249 (s), 1176 (s), 1116 (w), 1024 (s), 799 (s), 745 (s), 538 (s).

MS (m/z, QMS-MS/MS): 461.97 [M^+-$OCOCH_3$].

Micro Analysis Calculated for $C_{25}H_{22}AgN_3O_3$ (520.33): Calcd.: C, 57.71%; H, 4.26%; N, 8.08%; Found: C, 57.72%; H, 4.18%; N, 8.27%.

(1-(4-Cyanobenzyl)-3-[4-(methoxycarbonyl)benzyl]-2,3-dihydro-1H-benzimidazole-2-ylidene) silver(I) acetate (4d):

1-(4-Cyanobenzyl)-3-[4-(methoxycarbonyl)benzyl]-2,3-dihydro-1H-benzimidazole-2-ylium bromide (**3d**) (0.499 g, 1.08 mmol) and 2 equivalents of silver(I) acetate (0.360 g, 2.16 mmol) were dissolved in 30 mL of dichloromethane and stirred in darkness at room temperature for 2 d. After filtering off the AgBr by-product, the solvent was reduced to 3 mL and by adding dropwise 10 mL of pentane a white powder precipitated. The solvent was decanted and the white precipitate was washed with pentane (2x, 10 mL) and diethylether (3x, 10 mL) to yield a white powder (0.361 g, 0.658 mmol, 61% yield).

^1H NMR (δ ppm, $CDCl_3$, 300 MHz): 7.39 (m, 12H, $CH_{cyanobenzyl}$, $CH_{methoxycarbonylbenzyl}$, $CH_{benzimidazole}$), 5.74 (d, 2H, CH_2), 5.72 (d, 2H, CH_2), 3.90 (s, 3H, CH_3), 2.08 (s, 3H, $OCH_{3acetate}$).

^{13}C NMR (δ ppm, $CDCl_3$, 100 MHz, proton decoupled): 179.3 (NCN), 166.3 (C=O), 140.0, 139.4, 133.8, 133.7, 133.0, 130.4, 127.9, 127.2, 124.8, 118.1, 112.7, 112.2, 111.8 ($C_{cyanobenzyl}$, $C_{benzimidazole}$, $C_{methoxycarbonylbenzyl}$), 53.4, 53.0 ($CH_2$), 52.3 ($CH_{3methoxycarbonylbenzyl}$), 22.6 ($CH_{3actetate}$).

IR absorptions (KBr, cm-1): 3422 (m), 2952 (s), 2229 (m), 1715 (s), 1573 (s), 1394 (s), 1283 (s), 1106 (m), 1018 (w), 739 (m).

MS (m/z, QMS-MS/MS): 490.07 [M^+-$OCOCH_3$].

Micro Analysis Calculated for C26H22AgN3O4 (548.34): Calcd.: C, 56.95%; H, 4.04%; N, 7.66%; Found: C, 56.77%; H, 4.03%; N, 7.48%.

2.4.3 Antibacterial studies

The silver(I) acetate complexes were screened in preliminary *in vitro* antibacterial tests against two bacterial strains. The test organisms included *Staphylococcus aureus* (SA) (NCTC 7447) as a Gram-positive bacteria and *Escherichia coli* (E. coli) as Gram-negative bacteria.

To assess the biological activity of compounds **2a-c** and **4a-d**, the qualitative Kirby–Bauer disk-diffusion method was applied [22]. All bacteria were individually cultured from a single colony in sterile LB medium [23] overnight at 37°C in an orbital shaker incubator. All the work carried out was performed under sterile conditions.

For each strain, 70 µL of culture were spread evenly on agar-LB medium. Four 5 mm diameter Whatman paper discs were placed evenly separated on each plate. Two stock solutions (9:1 DMSO:H_2O) of every compound were prepared at 2.2 µM and 4.4 µM to be able to test the effect of different concentrations. Each plate was then tested with 5 µL and 7 µL of 2.2 µM solution and 5 µL and 10 µL for the 4.4 µM solution. The plates were covered and placed in an incubator at 37°C for 24 h. The plates were then removed and the area of clearance, which is defined as the distance between the edge of the filter paper disc and the beginning of the bacterial growth, was measured for each sample in mm.

2.4.4 Cytotoxicity studies

Preliminary *in vitro* cell tests were performed on the human cancerous renal cell line Caki-1 in order to compare the cytotoxicity of the compounds presented in this paper. This cell line was chosen based on its regular and long-lasting growth behaviour, which is similar to the one shown in kidney carcinoma cells. The cells

were obtained from the ATCC (American Tissue Cell Culture Collection) and maintained in Dulbecco's Modified Eagle Medium containing 10% (v/v) FCS (fetal calf serum), 1% (v/v) penicillin streptomycin and 1% (v/v) L-glutamine. Cells were seeded in 96-well plates containing 200 µL microtitre wells at a density of 3000 cells/200 µL of medium and were incubated at 37^{o}C for 24 h to allow for exponential growth. Then the compounds used for the testing were dissolved in the minimal amount of DMSO (dimethylsulfoxide) possible and diluted with medium to obtain stock solutions of 5 x 10^{-4} M in concentration and less than 0.7% of DMSO. The cells were then treated with varying concentrations of the compounds and incubated for 48 h at 37°C. Then, the solutions were removed from the wells and the cells were washed with PBS (phosphate buffer solution) and fresh medium was added to the wells. Following a recovery period of 24 h incubation at 37°C, individual wells were treated with 200 µL of a solution of MTT (3-(4,5-Dimethylthiazol-2-yl)-2,5-diphenyltetrazolium bromide) in medium. The solution consisted of 22 mg of MTT in 40 mL of medium. The cells were incubated for 3 h at 37°C. The medium was then removed and the purple formazan crystals were dissolved in 200 µL DMSO per well. For all tests cells with low passage numbers were used. A Wallac Victor (Multilabel HTS Counter) Plate Reader was used to measure absorbance at 540 nm. Cell viability was expressed as a percentage of the absorbance recorded for control wells. The values used for the dose response curves represent the values obtained from four consistent MTT-based assays for each compound tested.

2.5 Results and Discussion

In Scheme 2.1 and Scheme 2.2 the synthetic routes for the asymmetric substituted *N*-Heterocyclic carbene ligand precursors as well as their corresponding silver(I) acetate complexes are given. The initial precursors 4-(1H-imidazole-1-ylmethyl)benzonitrile (**1**) and 4-(1H-benzimidazole-1-ylmethyl)benzonitrile (**3**) were prepared by stirring 1H-imidazole and 1H-benzimidazole with 4-(bromomethyl)benzonitrile in acetonitrile and K_2CO_3 at room temperature for 2 d with 69 and 93% yields respectively. 1-benzyl-3-(4-cyanobenzyl)-2,3-dihydro-1H-imidazole-2-ylium bromide (**1a**), 1-(4-cyanobenzyl)-3-(4-methylbenzyl)-2,3-dihydro-1H-imidazole-2-ylium bromide (**1b**), 1-(4-cyanobenzyl)-3-(4-methoxybenzyl)-2,3-dihydro-1H-imidazole-2-ylium bromide (**1c**) and 1-(4-cyanobenzyl)-3-[4-(methoxycarbonyl)benzyl]-2,3-dihydro-1H-imidazole-2-ylium bromide (**1d**) were synthesised by stirring (**1**) with benzyl bromide, 1-(bromomethyl)-4-methylbenzene, 1-(bromomethyl)-4-methoxybenzene and 4-(bromomethyl)benzoate in toluene under reflux for 6 h to yield the *N*-Heterocyclic carbene ligand precursors in 53, 78, 99 and 41%, respectively. The benzimidazole containing precursors 1-benzyl-3-(4-cyanobenzyl)-2,3-dihydro-1H-benzimidazole-2-ylium bromide (**3a**), 1-(4-cyanobenzyl)-3-(4-methylbenzyl)-2,3-dihydro-1H-benzimidazole-2-ylium bromide (**3b**), 1-(4-cyanobenzyl)-3-(4-methoxybenzyl)-2,3-dihydro-1H-benzimidazole-2-ylium bromide (**3c**) and 1-(4-cyanobenzyl)-3-[4-(methoxycarbonyl)benzyl]-2,3-dihydro-1H-benzimidazole-2-ylium bromide (**3d**) followed the same reaction route to give the respective yields of 69, 84, 67 and 71%.

In the absence of light, the silver(I) acetate complexes (1-benzyl-3-(4-cyanobenzyl)-2,3-dihydro-1H-imidazole-2-ylidene) silver(I) acetate (**2a**), (1-(4-cyanobenzyl)-3-(4-methylbenzyl)-2,3-dihydro-1H-imidazole-2-ylidene) silver(I) acetate (**2b**) and (1-(4-cyanobenzyl)-3-[4-(methoxycarbonyl)benzyl]-2,3-dihydro-1H-imidazole-2-ylidene) silver(I) acetate (**2c**) were prepared by stirring the respective precursor with 2 equivalents of silver(I) acetate in a mixture of dichloromethane and methanol (1:1) at room temperature for 3-4 d. The silver complexes were obtained in 68, 48 and 57% yield respectively.

The synthesis of the asymmetric benzimidazole silver(I) acetate complexes were carried out under the same conditions but in dichloromethane and with shorter

reaction times of 2-3 d to give the silver(I) acetate complexes (1-benzyl-3-(4-cyanobenzyl)-2,3-dihydro-1H-benzimidazole-2-ylidene) silver(I) acetate (**4a**), (1-(4-cyanobenzyl)-3-(4-methylbenzyl)-2,3-dihydro-1H-benzimidazole-2-ylidene) silver(I) acetate (**4b**), (1-(4-cyanobenzyl)-3-(4-methoxybenzyl)-2,3-dihydro-1H-benzimidazole-2-ylidene) silver(I) acetate (**4c**) and (1-(4-cyanobenzyl)-3-[4-(methoxycarbonyl)benzyl]-2,3-dihydro-1H-benzimidazole-2-ylidene) silver(I) acetate (**4d**) in 52, 77, 70 and 61% yields.

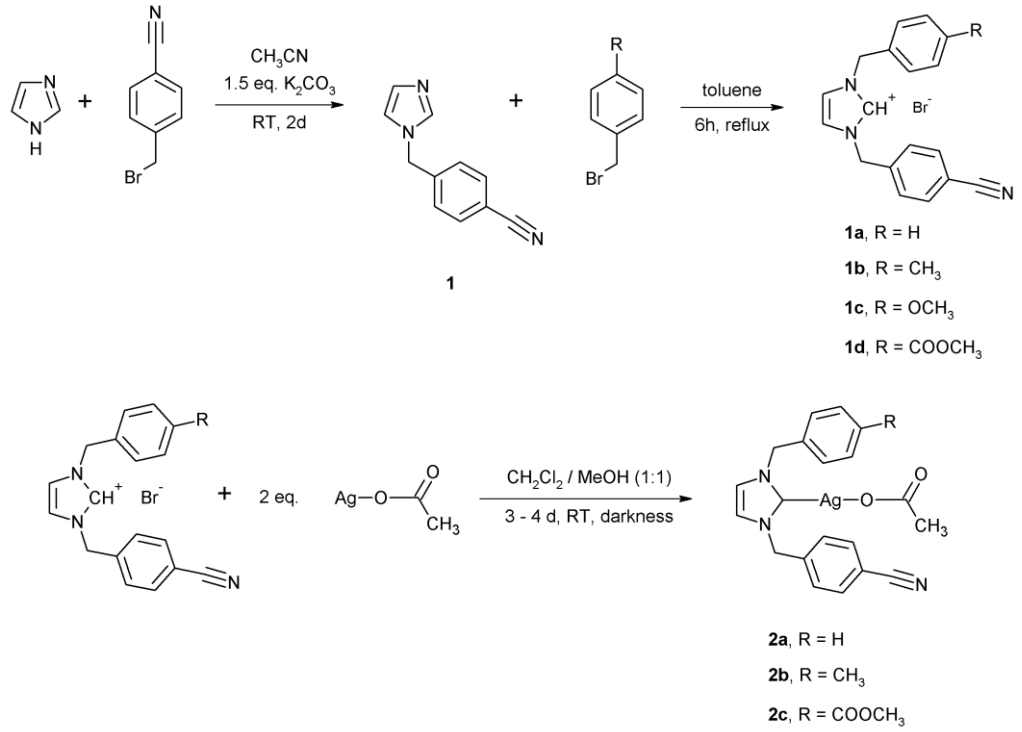

Scheme 2.1: General reaction scheme for the synthesis of imidazole containing asymmetric substituted NHC precursors **1a-d** and their corresponding NHC-silver(I) acetate complexes **2a-c**.

The asymmetric substituted *N*-Heterocyclic carbene ligand precursors as well as the silver(I) acetate complexes were fully characterized by spectral (^{1}H NMR, ^{13}C NMR, IR, mass) and elemental analysis studies.

Furthermore the solid state structure of the silver(I) acetate complex **4b** was determined by single crystal X-ray diffraction.

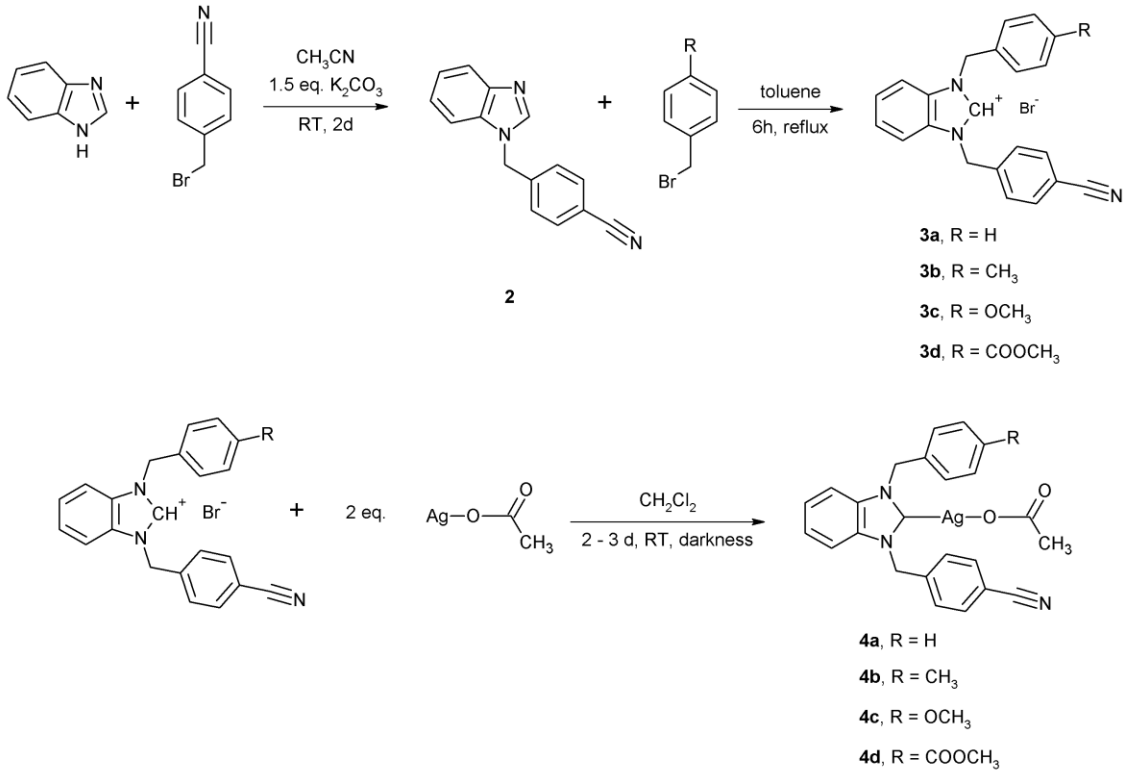

Scheme 2.2: General reaction scheme for the synthesis of benzimidazole containing asymmetric substituted NHC precursors **3a-d** and their corresponding NHC-silver(I) acetate complexes **4a-d**.

Due to the positive charge of the molecule, the ^{1}H NMR spectra of all NHC precursors **1a-d** and **3a-d** show a characteristic downfield shift in the range δ = 10.74-12.09 ppm for the NCHN proton [23-25]. In addition, their identities have also been confirmed by a base peak for the [M^{+}- Br] fragments in their positive mode ESI mass spectra. A successful formation of the complexes **2a-c** and **4a-d** is indicated by the absence of a downfield NCHN signal and presence of new signals at 2.09-1.91 ppm for the acetate protons in all the ^{1}H NMR spectra. The ^{13}C NMR resonances of the carbene carbon atoms in complexes **2a-c** and **4a-d** occur in the range δ 188.1-178.3 ppm respectively. These signals are shifted downfield compared to the corresponding precursors of **1a-d** and **3a-d** carbene carbons resonance at the range 144.3-137.9 ppm respectively which further demonstrates the formation of expected NHC-silver(I) acetate complexes. Also the appearance of the ^{13}C NMR resonances for the carbonyl and methyl carbons of the acetate group of complexes **2a-c** and **4a-d** in the range 176.5-156.2 and 23.3-21.1 ppm respectively showed the formation of the NHC-silver(I) acetate

complexes [1,3]. Furthermore, positive mode ESI mass spectra of all six NHC-silver(I) acetate complexes (**2a-c, 4a-d**) are dominated by [M^+-O_2CCH_3] fragment peaks arising from the loss of one acetate ligand.

2.5.1 Structural discussion

The crystal of **4b** was formed in a saturated solution of chloroform with slow infusion of pentane. It crystallized in the monoclinic space group $P2_1/n$ (#14) in absence of any solvent molecules. The crystal data and refinements are found in Table 1, whereas selected bond lengths and bond angles are compiled in Table 2. The X-ray structure shows that the benzimidazole ring is planar and the bond lengths and angles in the five membered imidazole ring (NCNCC) are in good agreement with those in similar compounds reported earlier by our group [13-16]. Complex **4b** crystallises in two different species, which are shown in Figure 2.1 and Figure 2.2.

The major species (95%, Figure 2.1) shows a nearly linear bond angle of 170.76(7)º at the two-coordinated silver atom. The bond distance Ag(1)-C(9) of 2.060(2) Å agrees very well with previously reported examples of this compound class [13-17] and shows that the silver is strongly bonded to the carbene.

The Ag(1)-O(1) bond length of 2.1088(14) Å is quite short compared to the ones our group previously reported, but is still within range of the corresponding ones in similar molecules (see for example [26, 27]). This short distance suggests a predominantly covalent character of the Ag(1)-O(1) bond.

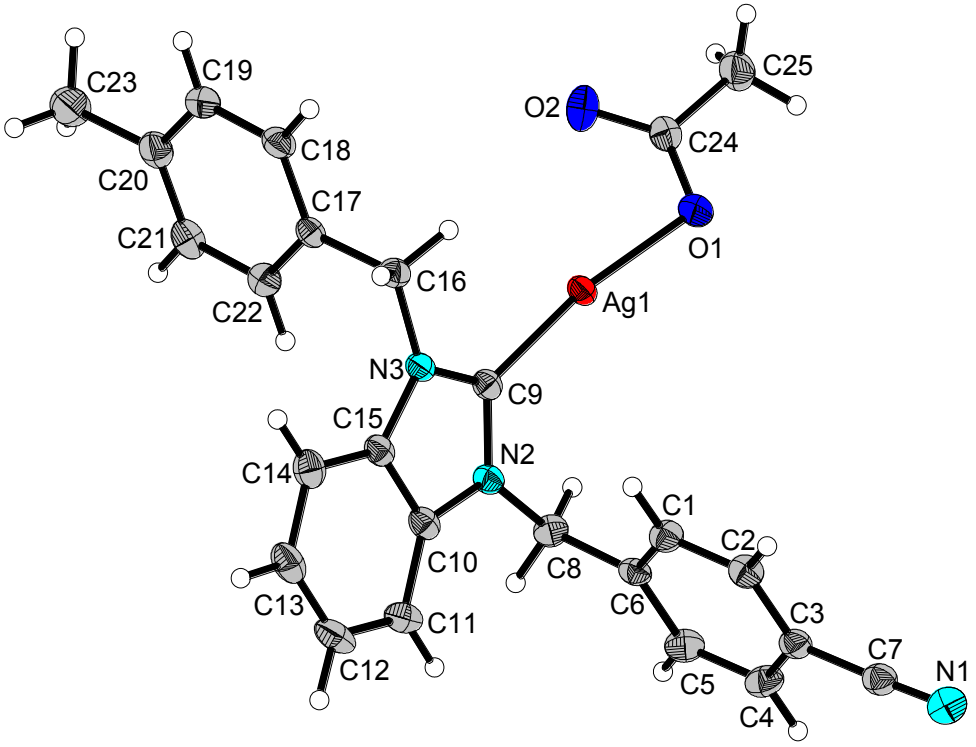

Figure 2.1: X-ray diffraction structure of **4b** showing the major occupied Ag position; thermal ellipsoids are drawn on the 50% probability level.

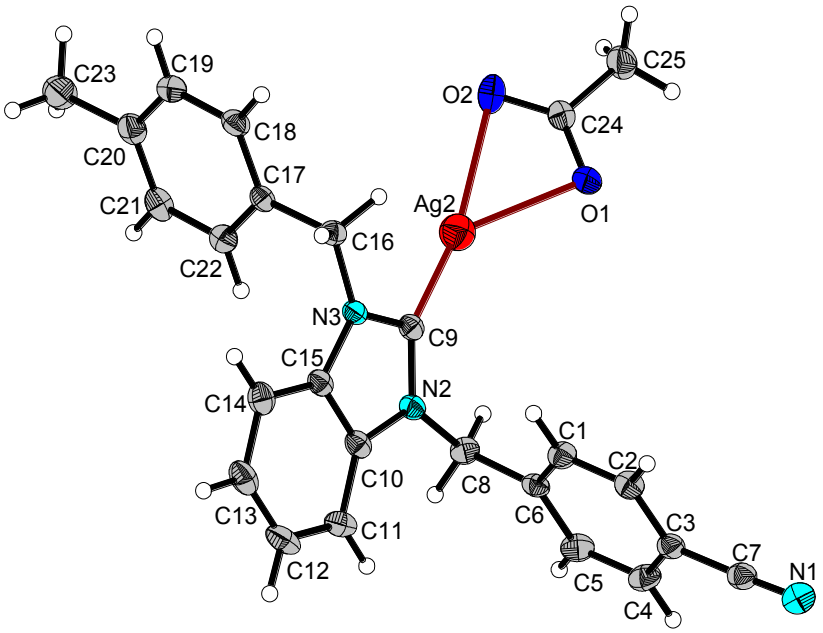

Figure 2.2: X-ray diffraction structure of **4b** showing the minor occupied Ag position; thermal ellipsoids are drawn on the 50% probability level, Ag2 with fixed radius

In comparison to this, the minor species (5%, Figure 2.2), where the silver atom is bonded to both oxygen atoms of the acetate group, the bond lengths to the oxygen atoms are much longer (Ag(2)-O(1): 2.408(6) Å and Ag(2)-O(2): 2.554(5) Å). Furthermore the bond angle C(9)-Ag(2)-O(1) is no longer linear with 135.9(4)º and the C(9)-Ag(2)-O(2) angle is found to be 164.9(3)º. This bonding pattern is characteristic for a predominantly ionic coordination of the acetate to the silver. Both these modes have been observed earlier (see for example [17]). Having both of them in the same structure suggests a rather small energy difference between the two forms.

Table 2.1: Crystal Data and Structure Refinement for **4b**.

		4b
Empirical formula		$C_{25}H_{22}N_3O_2Ag$
Formula weight [g/mol]		504.33
Crystal system		Monoclinic
Space Group		$P2_1/n$ (#14)
Unit cell dimensions [Å]	a	7.6287(2)
	b	12.4073(3)
	c	23.0001(6)
	β	94.496(3)°
Volume [$Å^3$]		2170.30(10)
Z		4
Density [mg/m^3] (calc.)		1.543
Absorption coefficient [mm^{-1}]		0.956
F(000)		1024
Crystal size [mm^3]		0.2663 x 0.1227 x 0.1080
Theta range for data collection		3.32 to 26.42°.
Index ranges		–9<=h<=9
		–15<=k<=15
		–28<=l<=28
Reflections collected		35074
Independent reflections		4454 [R(int) = 0.0421]
Completeness to θ_{max}		99.6 %
Max. and min transmission		0.913 and 0.808
Data/restraints/parameters		4454 / 0 / 287
Goodness-of-fit in F^2		1.086
Final R indices (I>2σ(I))		R1 = 0.0238
		wR2 = 0.0512
R Indices (all data)		R1 = 0.0301
		wR2 = 0.0543
Largest diff. peak and hole		0.871 and –0.323 $e.Å^{-3}$

Table 2.2: Selected bond lengths [Å] and angles [º] for **4b**.

Bond length [Å]			**Bond angle [º]**		
	4b (95% species)	**4b (5% species)**		**4b (95% species)**	**4b (5% species)**
Ag(1)-C(9)	2.060(2)		C(9)-Ag(1)-O(1)	170.76(7)	
Ag(1)-O(1)	2.1088(14)		C(9)-Ag(2)-O(1)		135.9(4)
Ag(2)-C(9)		2.074(5)	C(9)-Ag(2)-O(2)		164.9(3)
Ag(2)-O(1)		2.408(6)	O(1)-Ag(2)-O(2)		53.05(11)
Ag(2)-O(2)		2.554(5)	N(3)–C(9)–N(2)	105.98(17)	
N(2)-C(9)	1.350(3)		N(3)–C(9)–Ag(1)	127.63(14)	
N(2)-C(10)	1.395(2)		N(2)–C(9)–Ag(1)	125.82(14)	
C(9)-N(3)	1.348(2)		N(3)–C(9)–Ag(2)		118.7(2)
C(10)-C(15)	1.388(3)		N(2)–C(9)–Ag(2)		133.79(19)
C(15)-N(3)	1.391(3)		C(15)–C(10)–N(2)	105.82(17)	
O(1)-C(24)	1.276(3)		C(10)–C(15)–N(3)	106.11(17)	
O(2)-C(24)	1.237(2)		C(9)–N(3)–C(15)	111.09(16)	
C(24)-C(25)	1.511(3)		C(9)–N(2)–C(10)	110.96(16)	
			C(24)–O(1)–Ag(1)	109.21(12)	
			C(24)–O(1)–Ag(2)		93.9(2)
			C(24)–O(2)–Ag(2)		88.1(2)
			O(2)–C(24)–O(1)		124.18(19)
			O(2)–C(24)–C(25)		119.62(19)
			O(1)–C(24)–C(25)		116.19(18)

2.5.2 Biological evaluation

2.5.2.1 Antibacterial Testing

Using the Kirby-Bauer disk diffusion method the *in vitro* antibacterial activity of the NHC-silver(I) acetate complexes was tested and are summarised in Figure 2.3 and Figure 2.4. The metal salt (silver(I) acetate) used to prepare the complexes and the solvent (DMSO) used to prepare the stock solutions played no role in growth inhibition on the same bacteria as previously reported [17,28].

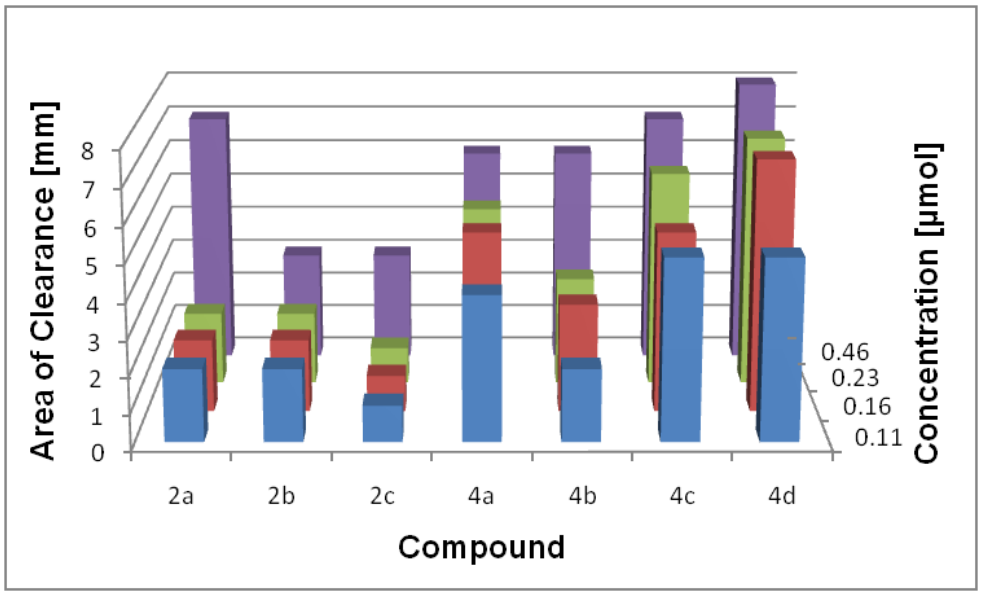

Figure 2.3: Area of clearance on *Staphylococcus aureus* (Gram +ve) by **2a-c** and **4a-d**.

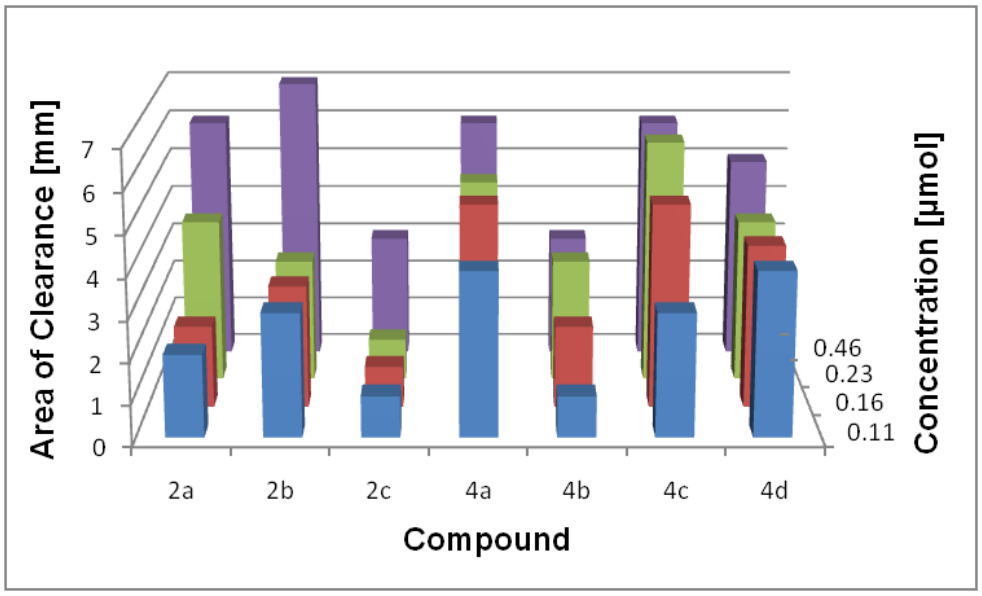

Figure 2.4: Area of clearance on *Escherichia coli* (Gram -ve) by **2a-c** and **4a-d**.

Compounds **2b** and **2c** showed almost no antibacterial activity against the Gram positive bacteria *Staphylococcus aureus* and compound **4d** showed the best activity against this bacterial strain, but in comparison to previous reported NHC-silver(I) acetate complexes the activity is more in a medium range. Hereby, an area of clearance of 0 mm is considered as no activity, areas of 1-4 mm as low, 5-9 as medium and areas of clearance ≥ 10 mm as high activity. Low antibacterial

activity was observed for complexes **2c** and **4b** against the Gram negative bacteria *Escherichia coli* and all other complexes (**2a**, **2b**, **4a**, **4c** and **4d**) exhibited only medium activity against this bacteria strain.

2.5.2.2 Cytotoxicity Studies

Our interest focuses on the probable difference in activity due to the influence of different lipophilicity in the two compound classes. The *in vitro* anticancer activity of the asymmetric substituted NHC-silver(I) acetate complexes was tested in an MTT based assay against the human renal cancer cell line Caki-1. In this test a 48 h drug exposure period was followed by a 24 h recovery period and the log dose response curve for complexes **2a-c** and **4a-d** are shown in Figure 2.5 and Figure 2.6 respectively.

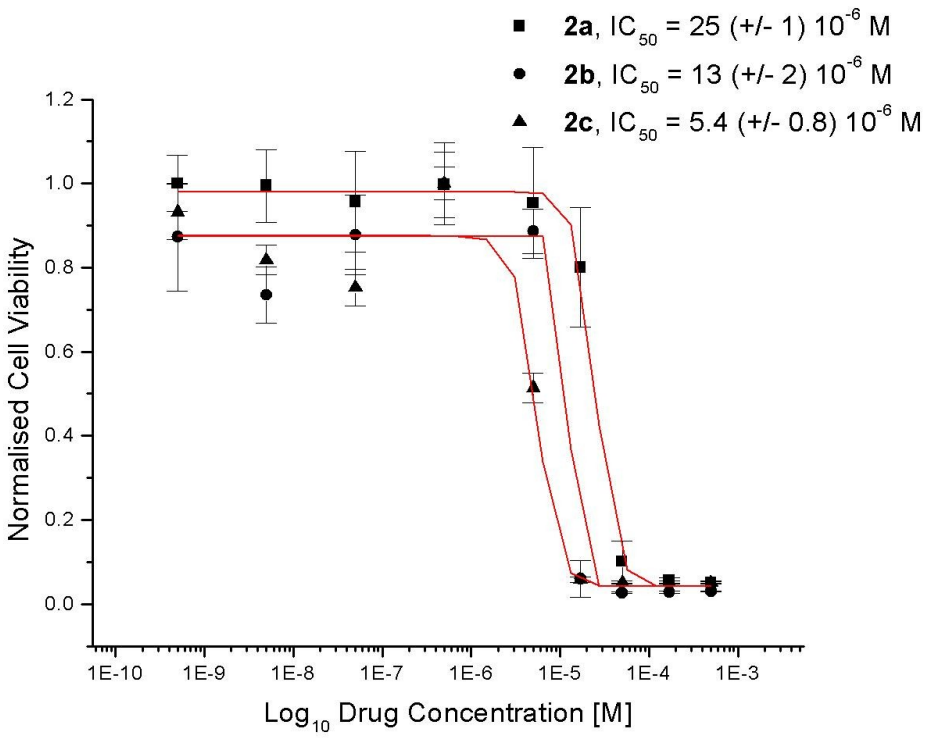

Figure 2.5: Cytotoxicity curves from typical MTT assays showing the effect of compounds **2a-c** on the viability of Caki-1 cells.

The IC_{50} values of the imidazole containing complexes are **2a**: 25 (± 1), **2b**: 15 (± 2), **2c**: 5.4 (± 0.8) µM. Slightly less activity was observed for the more lipophilic NHC-silver(I) acetate complexes **4a-d**, which gave IC_{50} values of 16 (± 2), 7.1 (± 1), 20 (± 4), 14 (± 1) µM respectively. Compounds **2c** and **4b** show the highest cytotoxic activities with single digit micromolar IC_{50} values.

It has been shown that there is no difference between the cytotoxic activities of the two compound classes, since all compounds show a good level of activity. The solubility of all compounds in DMSO was good and they are stable in saline solution with respect to silver chloride precipitation.

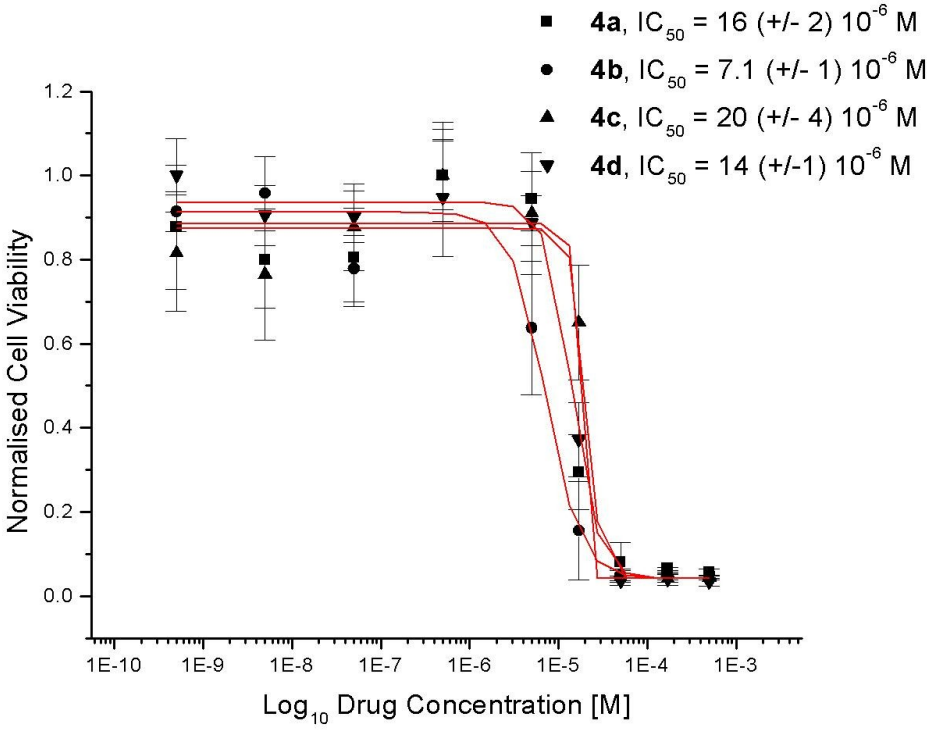

Figure 2.6: Cytotoxicity curves from typical MTT assays showing the effect of compounds **4a-d** on the viability of Caki-1 cells.

2.6 Conclusion and Outlook

In summary, a series of seven non-symmetrically *p*-cyanobenzyl-substituted NHC-silver(I) acetate complexes **2a-c** and **4a-d** were synthesised by reacting appropriate non-symmetrically *p*-cyanobenzyl-substituted *N*-Heterocyclic carbenes

with silver(I) acetate. The preliminary antibacterial activity of the NHC-silver(I) acetate complexes were tested *in vitro* against two bacteria strains, where complex **4d** showed superior activity against *Staphylococcus aureus* and complex **2b** against *Escherichia coli*. Against the renal cancer cell line Caki-1 the NHC-silver(I) acetate complexes **2a-c** and **4a-d** yielded IC_{50} values of 25 (± 1), 15 (± 2), 5.4 (± 0.8), 16 (± 2), 7.1 (± 1.0), 20 (± 4) and 14 (± 1) μM, respectively. The complex **2c** however gave a superior IC_{50} value of 5.4 (± 0.8) μM. Further work is currently underway to improve these results by varying the substituents on the imidazole ring in order to enhance stability and on the benzimidazole nitrogen atoms in order to improve biological activity. Overall, this should lead to enhanced solubility, stability and activity in biological media and enable *in vivo* testing of a NHC-silver(I) acetate in the nearby future.

Acknowledgement

This project was funded by the UCD School of Chemistry and Chemical Biology.

2.7 References

[1] K. M. Hindi, T. J. Siciliano, S. Durmus, M. J. Panzner, D. A. Medvetz, D. V. Reddy, L. A. Hogue, C. E. Hovis, J. K. Hilliard, R. J. Mallet, C. A. Tessier, C. L. Cannon and W. J. Youngs, "Synthesis, stability, and antimicrobial studies of electronically tuned silver acetate *N*-Heterocyclic carbenes," *J. Med. Chem.*, vol. 51, no. 6, pp. 1577 – 1583, 2008.

[2] A. Kascatan-Nebioglu, M. J. Panzner, C. A. Tessier, C. L. Cannon and W. J. Youngs, "*N*-Heterocyclic carbene–silver complexes: A new class of antibiotics," *Coord. Chem. Rev.,* vol. 251, no. 5 - 6, pp. 884 – 895, 2007.

[3] A. Kascatan-Nebioglu, A. Melaiye, K. M. Hindi, S. Durmus, M. J. Panzner, L. A. Hogue, R. J. Mallett, C. E. Hovis, M. Coughenour, S. D. Crosby, A. Milsted, D. L. Ely, C. A. Tessier, C. L. Cannon and W. J. Youngs, "Synthesis from caffeine of a mixed *N*-Heterocyclic carbene-silver acetate complex active against resistant respiratory pathogens," *J. Med. Chem.,* vol. 49, no. 23, pp. 6811 - 6818, 2006.

[4] D. A. Medvetz, K. M. Hindi, M. J. Panzner, A. J. Ditto, Y. H. Yun and W. J. Youngs, "Anticancer Activity of Ag(I) *N*-Heterocyclic Carbene Complexes Derived from 4,5-Dichloro-1H-Imidazole," *Metal-Based Drugs* 2008, Article ID 384010, 7 pages, http://dx.doi.org/10.1155/2008/384010.

[5] A. Melaiye, R. S. Simons, A. Milsted, F. Pingitore, C. Wesdemiotis, C. A. Tessier and W. J. Youngs, "Formation of water-soluble pincer silver(I)-carbene complexes: a novel antimicrobial agent," *J. Med. Chem.,* vol. 47, no. 4, pp. 973 – 977, 2004.

[6] S. Ray, R. Mohan, J. K. Singh, M. K. Samantaray, M. M. Shaikh, D. Panda and P. Ghosh, "Anticancer and antimicrobial metallopharmaceutical agents based on palladium, gold, and silver *N*-Heterocyclic carbene complexes," *J. Am. Chem. Soc.,* vol. 129, no. 48, pp. 15042 – 15053, 2007.

[7] C. L. Cannon, L. A. Hogue, R. K. Vajravelu, G. H. Capps, A. Ibricevic, K. M. Hindi, A. Kascatan-Nebioglu, M. J. Walter, S. L. Brody and W. J. Youngs, "*In vitro* and murine efficacy and toxicity studies of nebulized SCC1, a methylated caffeine-silver(I) complex, for treatment of

pulmonary infections," *Antimicrobial Agents and Chemotherapy,* vol. 53, no. 8, pp. 3285 – 3293, 2009.

[8] S. Roland, C. Jolivalt, T. Cresteil, L. Eloy, P. Bouhours, A. Hequet, V. Mansuy, C. Vanucci and J.-M. Paris, "Investigation of a Series of Silver–*N*-Heterocyclic Carbenes as Antibacterial Agents: Activity, Synergistic Effects, and Cytotoxicity," *Chem. Eur. J.*, vol. 17, no. 5, pp. 1442 – 1446, 2011.

[9] B. Thati, A. Noble, B. S. Creaven, M. Walsh, M. McCann, K. Kavanagh, M. Devereux, D. A. Egan, "*In vitro* anti-tumour effect of coumarin-3-carboxylic acid and three of its hydroxylated derivatives, along with their silver-based complexes, using human epithelial carcinoma cell lines," *Cancer Letters*, vol. 248, no. 2, pp. 321-333, 2007.

[10] H.-L. Zhu, X.-M. Zhang, X.-Y. Liu, *et al.*, "Clear Ag-Ag bonds in three silver(I) carboxylate complexes with high cytotoxicity properties," *Inorganic Chemistry Communications*, vol. 6, no. 8, pp. 1113–1116, 2003.

[11] J. J. Liu, P. Galettis, A. Farr, *et al.*, "*In vitro* antitumor and hepatotoxicity profiles of Au(I) and Ag(I) bidentate pyridyl phosphine complexes and relationships to cellular uptake," *Journal of Inorganic Biochemistry*, vol. 102, no. 2, pp. 303–310, 2008.

[12] S. Patil and M. Tacke, "NHC-Silver(I) Acetates as Bioorganometallic Anticancer and Antibacterial Drugs," *Insights into Coordination, Bioinorganic and Applied Inorganic Chemistry*, Edited by M. Melník, P. Segľa, M. Tatarko, Press of Slovak University of Technology, Bratislava, pp. 555 – 566, 2011.

[13] S. Patil, A. Deally, B. Gleeson, F. Hackenberg, H. Müller-Bunz, F. Paradisi and M. Tacke, "Synthesis, Cytotoxicity and Antibacterial Studies of Novel Symmetrically and Non-Symmetrically p-Nitrobenzyl-Substituted *N*-Heterocyclic Carbene-Silver(I) Acetate Complexes," *Z. Allg. Anorg. Chem.*, vol. 637, no. 3 – 4, pp. 386 – 396, 2011.

[14] S. Patil, A. Deally, B. Gleeson, H. Müller-Bunz, F. Paradisi and M. Tacke, "Novel Benzyl-Substituted N-Heterocyclic Carbene–Silver Acetate Complexes: Synthesis, Cytotoxicity and Antibacterial Studies," *Metallomics*, vol. 3, no. 1, pp. 74 – 88, 2011.

[15] S. Patil, K. Dietrich, A. Deally, B. Gleeson, H. Müller-Bunz, F. Paradisi and M. Tacke, ”Synthesis, Cytotoxicity and Antibacterial Studies of Novel Symmetrically and Nonsymmetrically 4-(Methoxycarbonyl)benzyl-Substituted *N*-Heterocyclic Carbene – Silver Acetate Complexes,” *Helv. Chim. Acta*, vol. 93, no. 12, pp. 2347 – 2364, 2010.

[16] S. Patil, A. Deally, B. Gleeson, H. Müller-Bunz, F. Paradisi and M. Tacke, “Synthesis, Cytotoxicity and Antibacterial Studies of Symmetrically and Non-Symmetrically Benzyl- or p-Cyanobenzyl-Substituted *N*-Heterocyclic Carbene-Silver Complexes,” *Appl. Organomet. Chem.*, vol. 24, no. 11, pp. 781 – 793, 2010.

[17] S. Patil, J. Claffey, A. Deally, B. Gleeson, M. Hogan, L. M. Menéndez Méndez, H. Müller-Bunz, F. Paradisi and M. Tacke, “Synthesis, Cytotoxicity and Antibacterial Studies of p-Methoxybenzyl-Substituted and Benzyl-Substituted *N*-Heterocyclic Carbene-Silver Complexes,” *Eur. J. Inorg. Chem.*, no. 7, pp. 1020 – 1031, 2010.

[18] L. Kaps, B. Biersack, H. Müller-Bunz, K. Mahal, J. Münzner, M. Tacke, T. Mueller and R. Schobert, „Gold(I)-NHC complexes of antitumoral diarylimidazoles: structures, cellular uptake routes and anticancer activities,” *J. Inorg. Biochem.*, vol. 106, no. 1, pp. 52 – 58, 2012

[19] S. Patil, A. Deally, F. Hackenberg, L. Kaps, H. Müller-Bunz, R. Schobert and M. Tacke, “Novel Benzyl- or 4-Cyanobenzyl-Substituted *N*-Heterocyclic (Bromo)(carbene)silver(I) and (Carbene)(chloro)gold(I) Complexes: Synthesis and Preliminary Cytotoxicity Studies,” *Helv. Chim. Acta*, vol. 94, no. 9, pp. 1551 – 1562, 2011.

[20] Program CrysalisPro Version 1.171.34.49, Agilent Technologies, 2011.

[21] G. M. Sheldrick, “A short history of *SHELX*”, *Acta Crystallogr.* vol. A64, no. 1, pp. 112 – 122, 2008.

[22] A. Bondi, H. E. Spaulding, E. D. Smith and C. C. Dietz, "A routine method for the rapid determination of susceptibility to penicillin and other antibiotics", *Am. J. Med. Sci*., vol. 213, no. 2, pp. 221 - 225, 1947.

[23] S. E. Luria, "Recent Advances in Bacterial Genetics", *Bacteriol Rev*., vol. 11, no. 1, pp. 1 - 40, 1947.

[24] W. A. Herrmann and C. Kocher, "*N*-Heterocyclic Carbenes", *Angew. Chem., Int. Ed*., vol. 36, no. 20, pp. 2162 - 2187, 1997.

[25] A.J. Arduengo, H.V. Rasika-Dias, J. C. Calabrese and F. Davidson, "Homoleptic carbene-silver(I) and carbene-copper(I) complexes", *Organometallics*, vol. 12, no. 9, pp. 3405 - 3409, 1993.

[26] C. C. Scarborough, B. V. Popp, I. A. Guzei and S. S. Stahl, "Development of 7-membered *N*-Heterocyclic carbene ligands for transition metals", *J. Organomet. Chem*, vol. 690, no. 25, pp. 6143 - 6155, 2005.

[27] M. J. Panzner, A. Deeraksa, A. Smith, B. D. Wright, K. M. Hindi, A. Kascatan-Nebioglu, A. G. Torres, B. M. Judy, C. E. Hovis, J. K. Hilliard, R. J. Mallett, E. Cope, D. M. Estes, C. L. Cannon, J. G. Leid and W. J. Youngs, "Synthesis and *in vitro* Efficacy Studies of Silver Carbene Complexes on Biosafety Level 3 Bacteria", *Eur. J. Inorg. Chem*, no. 13, pp. 1739 - 1745, 2009.

[28] B. Gleeson, J. Claffey, D. Ertler, M. Hogan, H. Müller-Bunz, F. Paradisi, D. Wallis and M. Tacke, "Novel Organotin Antibacterial and Anticancer Drugs" *Polyhedron,* vol. 27, no. 18, pp. 3619 - 3614, 2008.

Chapter 3 4,5-Diaryl-imidazole *N*-Heterocyclic carbene-silver(I) acetate complexes - Part 1

Work published as:

Novel symmetrically p-benzyl-substituted 4,5-diaryl-imidazole N-Heterocyclic carbene-silver(I) acetate complexes – synthesis and biological evaluation, F. Hackenberg, G. Lally, H. Müller-Bunz, F. Paradisi, D. Quaglia, W. Streciwilk and M. Tacke, *Journal of Organometallic Chemistry*, **2012**, *717*, 123-134.

Novel symmetrically *p*-benzyl-substituted 4,5-diaryl-imidazole *N*-Heterocyclic carbene-silver(I) acetate complexes – synthesis and biological evaluation

Frauke Hackenberg, Grainne Lally, Helge Müller-Bunz, Francesca Paradisi, Daniela Quaglia, Wojciech Streciwilk and Matthias Tacke*

Conway Institute of Biomolecular and Biomedical Research, Centre for Synthesis and Chemical Biology (CSCB), UCD School of Chemistry and Chemical Biology, University College Dublin, Belfield, Dublin 4, Ireland

3.1 Key Words

Anticancer drugs; antibacterial drugs; silver(I) acetate; NHC; Caki-1; MCF-7; *Escherichia coli*; *Staphylococcus aureus.*

3.2 Abstract

Symmetrically substituted *N*-Heterocyclic carbene (NHC) precursors **1a-e** and **3a-e** were synthesised by reacting 4,5-bisaryl-1H-imidazole with 2 equivalents of 4-benzyl bromide, 4-methylbenzyl bromide, 4-methoxybenzyl chloride, 4-methoxycarbonylbenzyl bromide or 4-cyanobenzyl bromide to give the 1,3-bis(*p*-benzyl substituted)-4,5-bisaryl-imidazolium halides. The NHC-silver(I) acetate complexes (1,3-bisbenzyl-4,5-bisphenyl-imidazole-2-ylidene) silver(I) acetate (**2a**), (1,3-bis(4-methylbenzyl)-4,5-bisphenyl-imidazole-2-ylidene) silver(I) acetate (**2b**), (1,3-bis(4-methoxybenzyl)-4,5-bisphenyl-imidazole-2-ylidene) silver(I) acetate (**2c**), (1,3-bis(4-methoxycarbonylbenzyl)-4,5-bisphenyl-imidazole-2-ylidene) silver(I) acetate (**2d**), (1,3-bis(4-cyanobenzyl)-4,5-bisphenyl-imidazole-2-ylidene) silver(I) acetate (**2e**), (1,3-bisbenzyl-4,5-bis(4-methoxyphenyl)-imidazole-2-ylidene) silver(I) acetate (**4a**), (1,3-bis(4-methylbenzyl)-4,5-bis(4-methoxyphenyl)-imidazole-2-ylidene) silver(I) acetate (**4b**), (1,3-bis(4-methoxybenzyl)-4,5-bis(4-

methoxyphenyl)-imidazole-2-ylidene) silver(I) acetate (**4c**), (1,3-bis(4-methoxycarbonylbenzyl)-4,5-bis(4-methoxyphenyl)-imidazole-2-ylidene) silver(I) acetate (**4d**) and (1,3-bis(4-cyanobenzyl)-4,5-bis(4-methoxyphenyl)-imidazole-2-ylidene) silver(I) acetate (**4e**) were yielded by reacting these NHC precursors with silver(I) acetate. The silver(I) acetate complexes **2d**, **2e** and **4c** were characterised by single crystal X-ray diffraction. Qualitative antibacterial studies against the Gram-negative bacteria *Escherichia coli* and the Gram-positive bacteria *Staphylococcus aureus*, using the Kirby-Bauer disc diffusion method were carried out on the ten NHC-silver(I) acetate complexes **2a-e** and **4a-e**. Also the IC_{50} values of these ten complexes were determined by an MTT-based assay against the human renal cancer cell line Caki-1 and the human breast cancer cell line MCF-7. The complexes **2a-e** and **4a-e** revealed the following IC_{50} values in μM against Caki-1: 14 (± 1), 3.6 (± 1.0), 4.2 (± 0.5), 33 (± 2), 59 (± 4), 21 (± 1), 21 (± 2), 21 (± 1), 34 (± 2), 46 (± 2) and against MCF-7: 5.8 (± 0.6), 3.5 (± 0.4), 5.4 (± 0.3), 28 (± 1), 25 (± 2), 11 (± 2), 5.0 (± 0.3), 6.5 (± 0.4), 17 (± 1), 13 (± 1); respectively.

3.3 Introduction

For many years silver complexes have been reported to exhibit antibacterial as well as anticancer activity *in vitro*. Silver complexes of coumarin derivatives and silver carboxylate dimers possess anticancer activity against human carcinoma cells as reported by Egan [1] and Zhu [2], respectively. McKeage has shown phosphine complexes of silver to be active anticancer agents, even against cisplatin-resistant cell lines [3]. By combining the bioactive properties of silver with *N*-Heterocyclic carbene ligands, new antibiotic complexes for the possible treatment of pulmonary infections accompanying cystic fibrosis (CF) and chronic lung infections were developed [4–7]. Youngs *et al.* have reported NHC-silver complexes derived from 4,5-dichloro-1H-imidazole, which show anticancer activity against the human cancer cell lines OVCAR-3 (ovarian), MB157 (breast), and HeLa (cervical) [5]. Furthermore led the synthesis and antimicrobial evaluation of NHC silver complexes derived from 1-benzyl-3-tert-butylimidazole by Ghosh *et al.* to another important contribution [8]. Additionally, a larger number of known compounds were evaluated as potential antibiotics by Roland and Jolivalt [9]. Recently, Gust *et al.* reported the anticancer activity of 4,5-diaryl-imidazole derived NHC silver complexes against MCF-7, MDA-MB-231 (breast) and HT-29 (colon) cancer cell lines [10].

As previously reported by us, novel benzyl-substituted *N*-Heterocyclic carbene-silver [11–17] and carbene-gold complexes [18, 19] exhibited good activity against the cancer cell line Caki-1 (renal) and antibacterial activity against the strains *Escherichia coli* and *Staphylococcus aureus*.

Within this paper we present a new series of symmetrically *p*-benzyl-substituted *N*-Heterocyclic carbene-silver acetate complexes derived from 4,5-bisphenyl-imidazole and 4,5-bisanisyl-imidazole, their synthesis, cytotoxicity and antibacterial studies.

3.4 Experimental part

3.4.1 General conditions

All reactions were carried out under aerobic conditions. All reactions involving silver(I) acetate were carried out under exclusion of light. 4,5-Bisphenyl-1H-imidazole, benzyl bromide, 4-methylbenzyl bromide, 4-methoxybenzyl chloride, methyl 4-(bromomethyl)benzoate, 4-cyanobenzyl bromide, formamide, 4,4-*p*-methoxy-benzoin, silver(I)acetate and K_2CO_3 were procured commercially from Sigma-Aldrich Chemical Company and were used without further purification. IR Spectra were recorded on a Perkin-Elmer Paragon 1000 FT-IR spectrometer employing a KBr disc. NMR Spectra were measured either on a Varian 300 MHz or 400 MHz spectrometer. All chemical shifts are reported in ppm and referenced to TMS. ESI MS was performed on a quadrupole tandem mass spectrometer (Quattro Micro, Micromass/Water's Corp., USA), using solutions in 100% MeOH. MS spectra were obtained in the ES+ (electron spray positive ionisation) mode for all compounds. CHN Analysis was carried out in an Exeter Analytical CE-440 elemental analyzer. Crystal Data was collected using an Agilent Technologies (former Oxford Diffraction) SuperNova diffractometer fitted with an Atlas detector. **2d**, and **2e** were measured with Mo-Kα (0.71073 Å), **4c** with Cu-Kα (1.54184 Å) at 100 K. A three-fold redundant (**2d**), complete assuming inequivalent Friedel pairs (**2e**) and complete assuming equivalent Friedel pairs (**4c**) dataset was collected. An analytical absorption correction based on the shape of the crystal was performed [20]. The structures were solved by direct methods using SHELXS-97 [21] and refined by full matrix least-squares on F^2 for all data using SHELXL-97 [21]. Hydrogen atoms were added at calculated positions and refined using a riding model. Their isotropic thermal displacement parameters were fixed to 1.2 (1.5 for methyl groups) times the equivalent ones of the parent atom. Anisotropic thermal displacement parameters were used for all non-hydrogen atoms. A suitable crystal of **2d** and **2e** was grown in a saturated solution of chloroform with slow infusion of pentane, while **4c** was grown in a saturated solution of dichloromethane with slow infusion of pentane. Further details about the data collection are listed in Table 3.1.

CCDC 881255 (for **2d**), CCDC 881256 (for **2e**) and CCDC 881257 (for **4c**) contain the supplementary crystallographic data for this paper. These data can be obtained free of charge from the Cambridge Crystallographic Data Centre via www.ccdc.cam.ac.uk/data_request/cif.

3.4.2 Synthesis

1,3-Bis-benzyl-4,5-bisphenyl-imidazolium bromide (1a)

1,3-Bisbenzyl-4,5-bisphenyl-imidazolium bromide was synthesised according to literature [13] to give a yield of 66.2%. The formation of the product was confirmed by NMR.

1,3-Bis-(4-methylbenzyl)-4,5-bisphenyl-imidazolium bromide (1b)

4,5-Bisphenyl-1H-imidazole (1g, 4.54 mmol), equivalents of 4-methylbenzyl bromide (1.680 g, 9.08 mmol) and 1.5 equivalents of K_2CO_3 (942 mg, 6.82 mmol) were dissolved in acetonitrile and stirred for 2 d at room temperature. After filtering off the precipitate and removing the solvent under reduced pressure the obtained sticky white solid was washed with pentane (2 x 20 mL) and diethyl ether (2 x 20 mL) to yield a white powder (2.051 g, 4.03 mmol, 88.7% yield).

^{1}H NMR (δ ppm, $CDCl_3$, 300 MHz): 11.17 (s, 1H, NCHN), 7.48 – 7.30 (m, 6H, CH_{phenyl} + $CH_{methylbenzyl}$), 7.14 – 6.87 (m, 12H, CH_{phenyl} + $CH_{methylbenzyl}$), 5.44 (s, 4H, CH_2), 2.29 (s, 6H, CH_3).

^{13}C NMR (δ ppm, $CDCl_3$, 100 MHz): 138.91 (NCHN), 132.01, 130.77, 130.39, 130.29, 129.70, 129.04, 128.50, 124.78 (C_{benzyl} + C_{phenyl} + $C_{imidazole}$), 51.13 (CH_2), 21.14 (CH_3).

IR absorptions (KBr, cm^{-1}): 3416 (m), 2992 (m), 1560 (s), 1516 (s), 1448 (s), 1212 (s), 1023 (s), 802 (s).

MS (m/z, QMS-MS/MS): 429.55 [M^+-Br].

Micro Analysis Calculated for $C_{31}H_{29}BrN_2$ (509.50): Calcd.: C, 73.08%; H, 5.74%; N, 5.50%; Found: C, 72.98%; H, 5.72%; N, 5.19%.

Melting point: 220-226°C.

1,3-Bis-(4-methoxybenzyl)-4,5-bisphenyl-imidazolium chloride (1c)

4,5-Bisphenyl-1H-imidazole (1 g, 4.54 mmol), equivalents of 4-methoxybenzyl chloride (1.23 mL, 9.08 mmol) and 1.5 equivalents of K_2CO_3 (942 mg, 6.82 mmol) were dissolved in acetonitrile and refluxed for 5 d. After filtering off the precipitate and removing the solvent under reduced pressure the obtained sticky white solid was washed with pentane (2 x 20 mL) and diethyl ether (2 x 20 mL) to yield a white powder (0.977 g, 1.97 mmol, 43.3% yield).

^{1}H NMR(δ ppm, d_6-DMSO, 400 MHz): 9.63 (s, 1H, NCHN), 7.87 (d, J = 8.4 Hz, 4H, CH_{phenyl} + $CH_{methoxybenzyl}$), 7.37 (d, J = 7.2 Hz, 2H, CH_{phenyl} + $CH_{methoxybenzyl}$), 7.32 (t, J = 7.6 Hz, 4H, CH_{phenyl} + $CH_{methoxybenzyl}$), 7.28 - 7.21 (m, 8 H, CH_{phenyl} + $CH_{methoxybenzyl}$), 5.53 (s, 4H, CH_2), 3.83 (s, 6H, CH_3).

^{13}C NMR (δ ppm, $CDCl_3$, 100 MHz): 159.93 (NCHN), 138.06, 131.79, 130.76, 130.38, 130.26, 129.07, 125.51, 124.94, 114.31 (C_{benzyl} + C_{phenyl} + $C_{imidazole}$), 55.25 (CH_2), 50.90 (OCH_3).

IR absorptions (KBr, cm^{-1}): 3438 (m), 2930 (m), 1613 (s), 1514 (s), 1453 (s), 1251 (s), 1179 (s), 1030 (s), 817 (s).

MS (m/z, QMS-MS/MS): 461.52 [M^+-Cl].

Micro Analysis Calculated for $C_{31}H_{29}ClN_2O_2$ (497.03): Calcd.: C, 74.91%; H, 5.88%; N, 5.64%; Found: C, 74.63%; H, 5.82%; N, 5.45%.

Melting point: 194-196°C.

1,3-Bis-(4-methoxycarbonylbenzyl)-4,5-bisphenyl-imidazolium bromide (1d)

4,5-Bisphenyl-1H-imidazole (1.000 g, 4.54 mmol), equivalents of 4-methoxycarbonyl-benzyl bromide (2.080 g, 9.08 mmol) and 1.5 equivalents of K_2CO_3 (942 mg, 6.82 mmol) were dissolved in acetonitrile and stirred for 2 d at room temperature. After filtering off the precipitate and removing the solvent under reduced pressure the obtained sticky white solid was washed with pentane (2 x 20 mL) and diethyl ether (2 x 20 mL) to yield a white powder (1.958 g, 3.28 mmol, 72.2% yield).

^{1}H NMR (δ ppm, DMSO, 400 MHz): 9.63 (s, 1H, NCHN), 7.87 (d, *J* = 8.0 Hz, 4H, CH_{phenyl} + $CH_{methoxycarbonylbenzyl}$), 7.37 (d, *J* = 7.0 Hz, 2H, CH_{phenyl} + $CH_{methoxycarbonylbenzyl}$), 7.32 (t, *J* = 7.2 Hz, 4H, CH_{phenyl} + $CH_{methoxycarbonylbenzyl}$), 7.28 – 7.21 (m, 4H, CH_{phenyl} + $CH_{methoxycarbonylbenzyl}$), 5.53 (s, 4H, CH_2), 3.83 (s, 6H, CH_3).

^{13}C NMR (δ ppm, DMSO, 101 MHz): 166.17 (C=O), 139.65 (NCHN), 137.58, 132.38, 131.17, 130.63, 129.90, 129.22, 128.50, 125.20 ($C_{methoxycarbonylbenzyl}$ + C_{phenyl} + $C_{imidazole}$), 52.73 (OCH_3), 50.71 (CH_2).

IR absorptions (KBr, cm^{-1}): 3398 (m), 2998 (m), 1720 (s), 1561 (s), 1431 (s), 1286 (s), 1187 (s), 1108 (s), 754 (s).

MS (m/z, QMS-MS/MS): 517.48 [M^+-Br].

Micro Analysis Calculated for $C_{33}H_{29}BrN_2O_4$ (597.50): Calcd.: C, 66.34%; H, 4.89%; N, 4.69%; Found: C, 66.21%; H, 4.83%; N, 4.49%.

Melting point: 238-240°C.

1,3-Bis-(4-cyanobenzyl)-4,5-bisphenyl-imidazolium bromide (1e)

4,5-Bisphenyl-1H-imidazole (1.000 g, 4.54 mmol), equivalents of 4-cyanobenzyl bromide (1.78 g, 9.08 mmol) and 1.5 equivalents of K_2CO_3 (942 mg, 6.82 mmol) were dissolved in acetonitrile and stirred for 3 d at room temperature. After filtering off the precipitate and removing the solvent under reduced pressure the obtained sticky white solid was washed with pentane (2 x 20 mL) and diethyl ether (2 x 20 mL) to yield a white powder (1.956 g, 3.68 mmol, 81.0% yield).

^{1}H NMR (δ ppm, $CDCl_3$, 400 MHz): 11.65 (s, 1H, NCHN), 7.52 (d, *J* = 8.0 Hz, 4H, CH_{phenyl} + $CH_{cyanobenzyl}$), 7.44 (d, *J* = 7.5 Hz, 2H, CH_{phenyl} + $CH_{cyanobenzyl}$), 7.35 (t, *J* = 7.6 Hz, 4H, CH_{phenyl} + $CH_{cyanobenzyl}$), 7.30 (d, *J* = 8.0 Hz, 4H, CH_{phenyl} + $CH_{cyanobenzyl}$), 7.07 (d, *J* = 7.4 Hz, 3H, CH_{phenyl} + $CH_{cyanobenzyl}$), 5.64 (s, 4H, CH_2).

^{13}C NMR (δ ppm, 101 MHz): 138.26 (NCHN), 137.75, 132.79, 132.27, 130.94, 130.52, 129.43, 129.38, 124.03, 117.86, 113.17 ($C_{cyanobenzyl}$ + C_{phenyl} + $C_{imidazole}$), 50.93 (CH_2).

IR absorptions (KBr, cm^{-1}): 3408 (m), 2960 (s), 2226 (s), 1557 (s), 1446 (s), 1216 (s), 1022 (s), 840 (s), 817 (s).

MS (m/z, QMS-MS/MS): 451.50 [M^+-Br].

Micro Analysis Calculated for $C_{31}H_{23}BrN_4$ (531.45): Calcd.: C, 70.06%; H, 4.36%; N, 10.54%; Found: C, 69.57%; H, 4.05%; N, 10.33%.

Melting point: 290-293°C.

(1,3-Bisbenzyl-4,5-bisphenyl-imidazole-2-ylidene) silver(I) acetate (2a)

1,3-Bisbenzyl-4,5-bisphenyl-imidazolium silver(I) acetate was synthesised according to literature [13] to give a yield of 70.7%. The formation of the product was confirmed by NMR.

(1,3-Bis-(4-methylbenzyl)-4,5-bisphenyl-imidazole-2-ylidene) silver(I) acetate (2b)

1,3-Bis-(4-methylbenzyl)-4,5-bisphenyl-imidazolium bromide (**1b**) (500 mg, 0.98 mmol) and 2.2 equivalents of silver(I) acetate (360 mg, 2.16 mmol) were dissolved in 30 mL of dichloromethane and stirred in darkness at room temperature for 3 d. After filtering off the AgBr by-product, the solvent was reduced to 3 mL and by adding drop wise 10 mL of pentane a white powder precipitated. The solvent was decanted and the white precipitate was washed with pentane (2 x 10 mL) and diethyl ether (3 x 10 mL) to yield a white powder (370.6 mg, 0.62 mmol, 63.4% yield).

^{1}H NMR (δ ppm, $CDCl_3$, 400 MHz): 7.26 (dt, *J* = 19.0, 7.1 Hz, 8H, CH_{phenyl} + $CH_{methylbenzyl}$), 7.01 (dd, *J* = 7.2, 4.6 Hz, 8H, CH_{phenyl} + $CH_{methylbenzyl}$), 6.87 (d, *J* = 7.7 Hz, 2H, CH_{phenyl} + $CH_{methylbenzyl}$), 5.27 (s, 4H, CH_2), 2.28 (s, 6H, CH_3), 2.08 (s, 3H, $CH_{3actetate}$).

^{13}C NMR (δ ppm, $CDCl_3$, 101 MHz): 178.64 (NCN), 156.23 (C=O), 137.69, 133.21, 132.49, 130.65, 129.29, 129.05, 128.52, 127.85, 127.39 ($C_{methylbenzyl}$ + C_{phenyl} + $C_{imidazole}$), 53.38 (CH_2), 22.82 ($CH_{3actetate}$), 21.08 (CH_3).

IR absorptions (KBr, cm^{-1}): 3440 (m), 3050 (s), 2922 (m), 1568 (s), 1515 (s), 1442 (s), 1402 (s), 801 (s).

MS (m/z, QMS-MS/MS): 491.48 [M^+-C_8H_9(methylbenzyl)].

Micro Analysis Calculated for $C_{33}H_{32}AgN_2O_2$ (596.49): Calcd.: C, 66.45%; H, 5.41%; N, 4.70%; Found: C, 66.17%; H, 5.21%; N, 4.38%.

Melting point: 180-182°C.

(1,3-Bis-(4-methoxybenzyl)-4,5-bisphenyl-imidazole-2-ylidene) silver(I) acetate (2c)

1,3-Bis-(4-methoxybenzyl)-4,5-bisphenyl-imidazolium chloride (**1c**) (150 mg, 0.30 mmol) and 2 equivalents of silver(I) acetate (315 mg, 0.60 mmol) were dissolved in 30 mL of dichloromethane and stirred in darkness at room temperature for 7 d. After filtering off the AgBr by-product, the solvent was reduced to 3 mL and by adding drop wise 10 mL of pentane a white powder precipitated. The solvent was decanted and the white precipitate was washed with pentane (2 x 10 mL) and diethyl ether (3 x 10 mL) to yield a white powder (154.0 mg, 0.25 mmol, 81.7% yield).

^{1}H NMR (δ ppm, $CDCl_3$, 400 MHz): 7.36 – 7.18 (m, 6H), 7.01 (d, *J* = 8.3 Hz, 4H, CH_{phenyl} + $CH_{methoxybenzyl}$), 6.91 (d, *J* = 8.3 Hz, 4H, CH_{phenyl} + $CH_{methoxybenzyl}$), 6.73 (d, *J* = 8.3 Hz, 4H, CH_{phenyl} + $CH_{methoxybenzyl}$), 5.25 (s, 4H, CH_2), 3.76 (s, 6H, OCH_3), 2.10 (s, 3H, $CH_{3acetate}$).

^{13}C NMR (δ ppm, $CDCl_3$, 101 MHz): 178.61 (NCN), 159.26 (C=O), 132.43, 130.67, 129.08, 128.97, 128.54, 128.24, 127.89, 113.97, 113.45 ($C_{methoxycarbonylbenzyl}$ + C_{phenyl} + $C_{imidazole}$), 55.22 (CH_2), 53.16 (OCH_3), 22.91 ($CH_{3acetate}$).

IR absorptions (KBr, cm^{-1}): 3414 (m), 2992-2929 (w), 1611 (s), 1579 (s), 1514 (s), 1445 (s), 1251 (s), 1177 (s), 1023 (s), 701 (s).

MS (m/z, QMS-MS/MS): 569.45 [M^+-$COOCH_3$].

Micro Analysis Calculated for $C_{33}H_{32}AgN_2O_4$ (628.49): Calcd.: C, 63.06%; H, 5.13%; N, 4.46%; Found: C, 62.99%; H, 4.92%; N, 4.37%.

Melting point: 144-146°C.

(1,3-Bis-(4-methoxycarbonylbenzyl)-4,5-bisphenyl-imidazole-2-ylidene) silver(I) acetate (2d)

1,3-Bis-(4-methoxycarbonylbenzyl)-4,5-bisphenyl-imidazolium bromide (**1d**) (500 mg, 0.84 mmol) and 2 equivalents of silver(I) acetate (279 mg, 1.68 mmol) were dissolved in 30 mL of dichloromethane and stirred in darkness at room temperature for 2 d. After filtering off the AgBr by-product, the solvent was reduced to 3 mL and by adding drop wise 10 mL of pentane a white powder precipitated. The solvent was decanted and the white precipitate was washed with pentane (2 x 10 mL) and diethyl ether (3 x 10 mL) to yield a white powder (400 mg, 0.58 mmol, 69.1% yield).

^{1}H NMR (δ ppm, $CDCl_3$, 400 MHz): 7.83 (d, J = 8.2 Hz, 4H, CH_{phenyl} + $CH_{methoxycarbonylbenzyl}$), 7.09 (d, J = 8.1 Hz, 4H, CH_{phenyl} + $CH_{methoxycarbonylbenzyl}$), 7.01-6.89 (m, 6H, CH_{phenyl} + $CH_{methoxycarbonylbenzyl}$), 6.82 (d, J = 8.2 Hz, 4H, CH_{phenyl} + $CH_{methoxycarbonylbenzyl}$), 6.72 (d, J = 8.2 Hz, 4H, CH_{phenyl} + $CH_{methoxycarbonylbenzyl}$), 5.34 (s, 4H, CH_2), 3.87 (s, 6H, OCH_3), 2.09 (s, 3H, $CH_{3actetate}$).

^{13}C NMR (δ ppm, $CDCl_3$, 101 MHz): 178.90 (NCN), 166.56 ($C=O_{methoxycarbonylbenzyl)}$), 160.18 (C=O), 141.16, 132.54, 131.82, 130.00, 129.89, 129.86, 127.20, 119.38, 114.14 (C_{phenyl} + $C_{methoxycarbonylbenzyl}$ + $C_{imidazole}$), 55.23 (CH_2), 52.17 ($OCH_{3methoxycarbonylbenzyl}$), 22.70 ($CH_{3acetate}$).

IR absorptions (KBr, cm^{-1}): 3421 (m), 3054 (m), 1724 (s), 1611 (s), 1565 (s), 1435 (s), 1281 (s), 1108 (s), 1018 (s), 751 (s), 701 (s).

MS (m/z, QMS-MS/MS): 517.50 [M^+-AgOAc].

Micro Analysis Calculated for $C_{35}H_{32}AgN_2O_6$ (684.51): Calcd.: C, 61.41%; H, 4.71%; N, 4.09%; Found: C, 61.56%; H, 4.60%; N, 3.94%.

Melting point: 204-206°C.

(1,3-Bis-(4-cyanobenzyl)-4,5-bisphenyl-imidazole-2-ylidene) silver(I) acetate (2e)

1,3-Bis-(4-cyanobenzyl)-4,5-bisphenyl-imidazolium bromide (**1e**) (100 mg, 0.19 mmol) and 2 equivalents of silver(I) acetate (66 mg, 0.40 mmol) were dissolved in 30 mL of dichloromethane and stirred in darkness at room temperature for 2 d. After filtering off the AgBr by-product, the solvent was reduced to 3 mL and by adding drop wise 10 mL of pentane a white powder precipitated. The solvent was decanted and the white precipitate was washed with pentane (2 x 10 mL) and diethyl ether (3 x 10 mL) to yield a white powder (95.5 mg, 0.15 mmol, 81.3% yield).

^{1}H NMR (δ ppm, $CDCl_3$, 400 MHz): 7.53 (d, *J* = 8.0 Hz, 4H, CH_{phenyl} + $CH_{cyanobenzyl}$), 7.39 – 7.30 (m, 2H, CH_{phenyl} + $CH_{cyanobenzyl}$), 7.30 – 7.23 (m, 4H, CH_{phenyl} + $CH_{cyanobenzyl}$), 7.09 (d, *J* = 7.9 Hz, 4H, CH_{phenyl} + $CH_{cyanobenzyl}$), 7.03 – 6.94 (m, 4H, CH_{phenyl} + $CH_{cyanobenzyl}$), 5.41 (s, 4H, CH_2), 2.07 (s, 3H, $CH_{3acetate}$).

^{13}C NMR (δ ppm, $CDCl_3$, 100 MHz): 206.90 (NCN), 156.54 (C=O), 140.76 (CN), 132.88, 132.55, 130.38, 129.75, 128.93, 128.16, 126.89, 118.18, 112.31 (C_{phenyl} + $C_{imidazole}$ + $C_{cyanobenzyl}$), 53.32 (CH_2), 22.91 ($CH_{3acetate}$).

IR absorptions (KBr, cm^{-1}): 3427 (s), 3057 (s), 2228 (s), 1608 (s), 1580 (s), 1504 (s), 1445 (s), 1403 (s), 815 (s), 701 (s).

MS (m/z, QMS-MS/MS): 559.36 [M^+-$COOCH_3$].

Micro Analysis Calculated for $C_{33}H_{26}AgN_4O_2$ (618.45): Calcd.: C, 64.09%; H, 4.24%; N, 9.06%; Found: C, 64.28%; H, 4.11%; N, 9.05%.

Melting point: 206-209°C

4,5-Bis-(4-methoxyphenyl)-1H-imidazole (3)

4,5-Bis(4-methoxyphenyl)-1H-imidazole was synthesised according to literature [22] to give a yield of 38.5%. The formation of the product was confirmed by NMR.

1,3-Bis-benzyl-4,5-bis-(4-methoxyphenyl)-imidazolium bromide (3a)

4,5-Bis-(4-methoxyphenyl)-1H-imidazole (280 mg, 1.00 mmol), equivalents of benzyl bromide (0.24 mL, 2.00 mmol) and 1.50 equivalents of K_2CO_3 (207 mg, 1.5 mmol) were dissolved in acetonitrile and stirred for 2 d at room temperature. After filtering off the precipitate and removing the solvent under reduced pressure the obtained sticky white solid was washed with pentane (2 x 20 mL) and diethyl ether (2 x 20 mL) to yield a white powder (396 mg, 0.731 mmol, 73.1% yield).

^{1}H NMR (δ ppm, DMSO, 400 MHz): 11.11 (s, 1H, NCHN), 7.29 (m, 6H, CH_{anisyl} + CH_{benzyl}), 7.15 (dd, *J* = 6.6, 2.9 Hz, 4H, CH_{anisyl} + CH_{benzyl}), 6.99 (m, 4H, CH_{anisyl} + CH_{benzyl}), 6.84 (m, 4H, CH_{anisyl} + CH_{benzyl}), 5.47 (s, 4H, CH_2), 3.80 (s, 6H, OCH_3).

^{13}C NMR (δ ppm, DMSO, 101 MHz): 160.96 (NCN), 137.02, 133.51, 132.16, 131.97, 129.08, 128.92, 128.46, 116.64, 114.52 (C_{anisyl} + C_{benzyl}), 55.34 (CH_2), 51.21 (CH_3).

IR absorptions (KBr, cm^{-1}): 3425 (m), 2949 (s), 2835 (w), 1611 (s), 1506 (s), 1450 (s), 1296 (m), 1254 (s), 1160 (s), 1024 (s), 840 (m), 704 (s).

MS (m/z, QMS-MS/MS): 461.46 [M^+-Br^-].

Micro Analysis Calculated for $C_{31}H_{29}BrN_2O_2$ (541.48): Calcd.: C, 68.76%; H, 5.40%; N, 5.17%; Found: C 67.35%; H, 5.39%; N, 5.00%.

Melting point: 192-194°C.

1,3-Bis-(4-methylbenzyl)-4,5-bis-(4-methoxyphenyl)-imidazolium bromide (3b)

4,5-Bis-(4-methoxyphenyl)-1H-imidazole (280 mg, 1.00 mmol), equivalents of 4-methylbenzyl bromide (371 mg, 2.00 mmol) and 1.5 equivalents of K_2CO_3 (207 mg, 1.50 mmol) were dissolved in acetonitrile and stirred for 2 d at room temperature. After filtering off the precipitate and removing the solvent under reduced pressure the obtained sticky white solid was washed with pentane (2 x 20 mL) and diethyl ether (2 x 20 mL) to yield a white powder (175 mg, 0.31 mmol, 30.7% yield).

^{1}H NMR (δ ppm, $CDCl_3$, 300 MHz): 11.43 (s, 1H, NCHN), 7.92 (dd, *J* = 8.3 Hz, 4H, CH_{anisyl} + $CH_{methylbenzyl}$), 7.20 (d, *J* = 7.6 Hz, 4H, CH_{anisyl} + $CH_{methylbenzyl}$), 7.12 (d, *J* = 7.6 Hz, 4H, CH_{anisyl} + $CH_{methylbenzyl}$), 6.93 (dd, *J* = 8.2 Hz, 4H, CH_{anisyl} + $CH_{methylbenzyl}$), 5.58 (s, 4H, CH_2), 3.90 (s, 6H, OCH_3), 2.33 (s, 6H, $CH_{3acetate}$).

^{13}C NMR (δ ppm, $CDCl_3$, 101 MHz): 166.30 (NCHN), 141.02, 137.99, 137.66, 132.29, 130.73, 130.47, 130.29, 129.90, 128.40, 121.32 (C_{anisyl} + $C_{methylbenzyl}$), 52.27 (CH_2), 50.87 (OCH_3), 21.39 ($CH_{3methylbenzyl}$).

IR absorptions (KBr, cm^{-1}): 3431 (m), 2956 (w), 2835 (w), 1580 (w), 1575 (s), 1505 (s), 1440 (m), 1253 (s), 1178 (s), 1025 (s), 831 (m), 706 (m).

MS (m/z, QMS-MS/MS): 489.55 [M^+-Br^-].

Micro Analysis Calculated for $C_{33}H_{33}BrN_2O_2$ (569.53): Calcd.: C, 69.59%; H, 5.84%; N, 4.92%; Found: C, 69.90%; H, 5.30%; N, 4.62%.

Melting point: 238-240°C.

1,3-Bis-(4-methoxybenzyl)-4,5-bis-(4-methoxyphenyl)-imidazolium chloride (3c)

4,5-Bis-(4-methoxyphenyl)-1H-imidazole (280 mg, 1.00 mmol), equivalents of 4-methoxybenzyl chloride (0.24 mL, 2.00 mmol) and 1.5 equivalents of K_2CO_3 (207 mg, 1.50 mmol) were dissolved in acetonitrile and refluxed for 5 d. After filtering off the precipitate and removing the solvent under reduced pressure the obtained

sticky white solid was washed with pentane (2 x 20 mL) and diethyl ether (2 x 20 mL) to yield a white powder (245 mg, 0.44 mmol, 43.9% yield).

^{1}H NMR (δ ppm, $CDCl_3$, 300 MHz): 11.48 (s, 1H, NCHN), 7.11 (m, 4H, CH_{anisyl} + $CH_{methoxybenzyl}$), 6.99 (m, 4H, CH_{anisyl} + $CH_{methoxybenzyl}$), 6.85 (m, 4H, CH_{anisyl} + $CH_{methoxybenzyl}$), 6.78 (m, 4H, CH_{anisyl} + $CH_{methoxybenzyl}$), 5.38 (s, 4H, CH_2), 3.81 (s, 6H, OCH_3), 3.76 (s, 6H, OCH_3).

^{13}C NMR (δ ppm, $CDCl_3$, 101 MHz): 160.88 (NCHN), 159.89, 137.52, 132.16, 131.58, 130.22, 125.79, 116.95, 114.50, 114.31 (C_{anisyl} + $C_{methoxybenzyl}$), 55.34 ($CH_{3anisyl}$), 55.26 ($CH_{3methoxybenzyl}$), 50.69 (CH_2).

IR absorptions (KBr, cm^{-1}): 3422 (w), 2930 (m), 2838 (w), 1612 (s), 1515 (s), 1457 (m), 1294 (m), 1252 (s), 1178 (s), 1026 (m), 839 (m).

MS (m/z, QMS-MS/MS): 521.52 [M^+-Br^-].

Micro Analysis Calculated for $C_{33}H_{33}ClN_2O_4$ (557.08): Calcd.: C, 71.15%; H, 5.97%; N, 5.03%; Found: C, 70.74%; H, 5.89%; N, 5.12%.

Melting point: 106-108°C.

1,3-Bis-(4-methoxycarbonylbenzyl)-4,5-bis-(4-methoxyphenyl)-imidazolium bromide (3d)

4,5-Bis-(4-methoxyphenyl)-1H-imidazole (280 mg, 1.00 mmol), equivalents of 4-methoxycarbonylbenzyl bromide (458 mg, 2.00 mmol) and 1.5 equivalents of K_2CO_3 (207 mg, 1.50 mmol) were dissolved in acetonitrile and stirred for 3 d at room temperature. After filtering off the precipitate and removing the solvent under reduced pressure the obtained sticky white solid was washed with pentane (2 x 20 mL) and diethyl ether (2 x 20 mL) to yield a white powder (250 mg, 0.38 mmol, 38.0% yield).

^{1}H NMR (δ ppm, DMSO, 400 MHz): 11.37 (s, 1H, NCHN), 7.94 (d, *J* = 8.1 Hz, 4H, CH_{anisyl} + $CH_{methoxycarbonylbenzyl}$), 7.22 (d, *J* = 8.1 Hz, 4H, CH_{anisyl} + $CH_{methoxycarbonylbenzyl}$), 6.96 (d, J = 8.6 Hz, 4H, CH_{anisyl} + $CH_{methoxycarbonylbenzyl}$), 6.82

(d, *J* = 8.6 Hz, 4H, CH_{anisyl} + $CH_{methoxycarbonylbenzyl}$), 5.57 (s, 4H, CH_2), 3.90 (s, 6H, OCH_3), 3.79 (s, 6H, OCH_3).

^{13}C NMR (δ ppm, DMSO, 101 MHz): 166.29 (C=O), 161.08 (NCHN), 138.12, 137.47, 132.13, 132.05, 130.64, 130.27, 128.33, 116.23, 114.61 (C_{anisyl} + $C_{methoxycarbonylbenzyl}$ + $C_{imidazole}$), 55.34 (CH_2), 52.25 ($CH_{3methoxycarbonylbenzyl}$), 50.91 ($CH_{3anisyl}$).

IR absorptions (KBr, cm^{-1}): 3427 (w), 2953 (w), 1721 (s), 1612 (m), 1556 (m), 1507 (m), 1434 (s), 1284 (s), 1180 (s), 1108 (s), 1022 (m), 838 (m), 757 (m), 672 (m).

MS (m/z, QMS-MS/MS): 577.51 [M^+-Br^-].

Micro Analysis Calculated for $C_{35}H_{33}BrN_2O_6$ (657.55): Calcd.: C, 63.93%; H, 5.06%; N, 4.26%; Found: C, 63.52%; H, 4.86%; N, 4.18%.

Melting point: 202-203°C.

1,3-Bis-(4-cyanobenzyl)-4,5-bis-(4-methoxyphenyl)-imidazolium bromide (3e)

4,5-Bis-(4-methoxyphenyl)-1H-imidazole (280 mg, 1.00 mmol), 2 equivalents of 4-cyanobenzyl bromide (391 mg, 2.00 mmol) and 1.50 equivalents of K_2CO_3 (207 mg, 1.5 mmol) were dissolved in acetonitrile and stirred for 2 d at room temperature. After filtering off the precipitate and removing the solvent under reduced pressure the obtained sticky white solid was washed with pentane (2 x 20 mL) and diethyl ether (2 x 20 mL) to yield a white powder (286 mg, 0.48 mmol, 48.3% yield).

^1H NMR (δ ppm, DMSO, 400 MHz): 11.54 (s, 1H, NCHN), 7.55 (d, *J* = 7.9 Hz, 4H, CH_{anisyl} + $CH_{cyanobenzyl}$), 7.33 (d, *J* = 7.9 Hz, 4H, CH_{anisyl} + $CH_{cyanobenzyl}$), 6.97 (d, *J* = 8.8 Hz, 4H, CH_{anisyl} + $CH_{cyanobenzyl}$), 6.84 (d, *J* = 8.8 Hz, 4H, CH_{anisyl} + $CH_{cyanobenzyl}$), 5.60 (s, 4H, CH_2), 3.80 (s, 6H, OCH_3).

^{13}C NMR (δ ppm, DMSO, 101 MHz): 161.20 (NCHN), 138.22, 137.82, 132.72, 132.07, 131.98, 129.30, 117.97, 115.96, 114.71, 112.90 (C_{anisyl} + $C_{cyanobenzyl}$ + $C_{imidazole}$), 55.38 (CH_2), 50.81 ($CH_{3anisyl}$).

IR absorptions (KBr, cm^{-1}): 3420 (m), 3006 (m), 2838 (w), 2229 (s), 1638 (w), 1609 (s), 1558 (m), 1508 (s), 1455 (m), 1416 (m), 1296 (m), 1254 (s), 1178 (s), 1022 (s), 826 (s), 665 (m).

MS (m/z, QMS-MS/MS): 511.48 [M^+-Br^-].

Micro Analysis Calculated for $C_{33}H_{27}BrN_4O_2$ (591.50): Calcd.: C, 67.01%; H, 4.60%; N, 9.47%; Found: C, 66.89%; H, 4.55%; N, 9.42%.

Melting point: 238-240°C.

(1,3-Bis-benzyl-4,5-bis-(4-methoxyphenyl)-imidazole-2-ylidene) silver(I) acetate (4a)

1,3-Bis-benzyl-4,5-bis-(4-methoxyphenyl)-imidazolium bromide (**3a**) (100 mg, 0.18 mmol) and 2.1 equivalents of silver(I) acetate (63 mg, 0.38 mmol) were dissolved in 30 mL of dichloromethane and stirred in darkness at room temperature for 2 d. After filtering off the AgBr by-product, the solvent was reduced to 3 mL and by adding drop wise 10 mL of pentane a white powder precipitated. The solvent was decanted and the white precipitate was washed with pentane (2 x 10 mL) and diethyl ether (3 x 10 mL) to yield a white powder (60 mg, 0.52 mmol, 51.7 % yield).

^{1}H NMR (δ ppm, $CDCl_3$, 300 MHz): 7.23 (m, 6H, CH_{anisyl} + CH_{benzyl}), 7.01(m, 4H, CH_{anisyl} + CH_{benzyl}), 6.90 (m,4H, CH_{anisyl} + CH_{benzyl}), 6.74 (m, 4H, CH_{anisyl} + CH_{benzyl}), 5.29 (s, 4H, CH_2), 3.76 (s, 3H, $CH_{3acetate}$).

^{13}C NMR (δ ppm, $CDCl_3$, 101 MHz): 170.34 (NCN), 159.99 (C=O), 136.40, 132.33, 131.94, 128.90, 128.64, 127.93, 127.33, 119.92, 114.37, 113.98, 55.20 (CH_2), 53.55 (OCH_3), 22.92 ($CH_{3acetate}$).

IR absorptions (KBr, cm^{-1}): 3445 (w), 3004 (m), 2953 (w), 1722 (s), 1613 (m), 1559 (m), 1508 (m), 1434 (m), 1281 (s), 1183 (s), 1108 (s), 1018 (m), 821 (m), 754 (m).

MS (m/z, QMS-MS/MS): 461.46 [M^+-$AgOCOCH_3$].

Micro Analysis Calculated for $C_{33}H_{32}AgN_2O_4$ (628.49): Calcd.: C, 63.06%; H, 5.13%; N, 4.46%; Found: C, 63.06%; H, 4.92%; N, 4.36%.

Melting point: 118-122°C.

(1,3-Bis-(4-methylbenzyl)-4,5-bis-(4-methoxyphenyl)-imidazole-2-ylidene) silver(I) acetate (4b)

1,3-Bis-(4-methylbenzyl)-4,5-bis-(4-methoxyphenyl)-imidazolium bromide (**3b**) (100 mg, 0.18 mmol) and 2 equivalents of silver(I) acetate (63 mg, 0.38 mmol) were dissolved in 30 mL of dichloromethane and stirred in darkness at room temperature for 2 d. After filtering off the AgBr by-product, the solvent was reduced to 3 mL and by adding drop wise 10 mL of pentane a white powder precipitated. The solvent was decanted and the white precipitate was washed with pentane (2 x 10 mL) and diethyl ether (3 x 10 mL) to yield a white powder (78 mg, 0.11 mmol, 67.8 % yield).

^{1}H NMR (δ ppm $CDCl_3$, 400 MHz): 7.91 (d, *J* = 8.0 Hz, 4H, CH_{anisyl} + $CH_{methylbenzyl}$), 7.17 – 6.94 (m, 8H, CH_{anisyl} + $CH_{methylbenzyl}$), 6.85 (d, *J* = 7.9 Hz, 4H, CH_{anisyl} + $CH_{methylbenzyl}$), 5.37 (s, 4H, CH_2), 3.91 (s, 6H, $OCH_{3anisyl}$), 2.29 (s, 6H, $CH_{3methylbenzyl}$), 2.06 (s, 3H, $CH_{3acetate}$).

^{13}C NMR (δ ppm, $CDCl_3$, 101 MHz): 178.94 (NCN), 166.56 (C=O), 141.14, 139.45, 132.75, 130.35, 129.99, 129.87, 129.40, 127.21, 124.32 (C_{anisyl} + $C_{methylbenzyl}$ + $C_{imidazole}$), 53.30 (CH_2), 52.16 (OCH_3), 22.73 ($CH_{3acetate}$), 21.27 ($CH_{3methylbenzyl}$).

IR absorptions (KBr, cm^{-1}): 3416 (m), 2950 (m), 1724 (s), 1612 (m), 1574 (s), 1435 (m), 1404 (w), 1280 (s), 1182 (m), 1110 (s), 1018 (m), 822 (w), 753 (m), 669 (m).

MS (m/z, QMS-MS/MS): 489.55 [M^+-$AgOCOCH_3$].

Micro Analysis Calculated for $C_{35}H_{36}AgN_2O_4$ (656.54): Calcd.: C, 64.03%; H, 5.53%; N, 4.27%; Found: C, 63.65%; H, 5.03%; N, 3.90%.

Melting point: 155-156°C.

(1,3-Bis-(4-methoxybenzyl)-4,5-bis-(4-methoxyphenyl)-imidazole-2-ylidene) silver(I) acetate (4c)

1,3-Bis-(4-methoxybenzyl)-4,5-bis-(4-methoxyphenyl)-imidazolium chloride (**3c**) (100 mg, 0.18 mmol) and 2.1 equivalents of silver(I) acetate (63 mg, 0.38 mmol) were dissolved in 30 mL of dichloromethane and stirred in darkness at room temperature for 7 d. After filtering off the AgBr by-product, the solvent was reduced to 3 mL and by adding drop wise 10 mL of pentane a white powder precipitated. The solvent was decanted and the white precipitate was washed with pentane (2 x 10 mL) and diethyl ether (3 x 10 mL) to yield a white powder (70 mg, 0.10 mmol, 56.7% yield).

^{1}H NMR (δ ppm, $CDCl_3$, 300 MHz): 6.93 (t, *J* = 8.5 Hz, 8H, CH_{anisyl} + $CH_{methoxybenzyl}$), 6.86 – 6.62 (m, 8H, CH_{anisyl} + $CH_{methoxybenzyl}$), 5.21 (s, 4H, CH_2), 3.77 (d, *J* = 1.5 Hz, 12H, $CH_{3anisyl}$ + $CH_{3methoxybenzyl}$), 2.10 (s, 3H, $CH_{3acetate}$).

^{13}C NMR (δ ppm, $CDCl_3$, 101 MHz): 178.85 (NCN), 159.95 (C=O), 133.51, 133.02, 132.00, 128.93, 128.50, 128.38, 127.76, 127.24, 120.11, 113.97 (C_{anisyl} + $C_{methoxybenzyl}$ + $C_{imidazole}$), 55.24 (CH_2), 55.21 ($OCH_{3anisyl}$), 53.04 ($OCH_{3methoxybenzyl}$), 22.95 ($CH_{3acetate}$).

IR absorptions (KBr, cm^{-1}): 3417 (w), 2954 (w), 2929 (w), 1611 (m), 1580 (m), 1513 (s), 1439 (m), 1403 (w), 1291 (m), 1252 (s), 1176 (s), 1027 (s), 835 (m).

MS (m/z, QMS-MS/MS): 521.52 [M^+-$AgOCOCH_3$].

Micro Analysis Calculated for $C_{35}H_{36}AgN_2O_6$ (688.54): Calcd.: C, 61.05%; H, 5.27%; N, 4.07%; Found: C, 62.00%; H, 5.26%; N, 4.01%.

Melting point: 119-122°C.

(1,3-Bis-(4-methoxycarbonylbenzyl)-4,5-bis-(4-methoxyphenyl)-imidazole-2-ylidene) silver(I) acetate (4d)

1,3-Bis-(4-methoxycarbonylbenzyl)-4,5-bis-(4-methoxyphenyl)-imidazolium bromide (**3d**) (100 mg, 0.15 mmol) and 2 equivalents of silver(I) acetate (53 mg, 0.32 mmol) were dissolved in 30 mL of dichloromethane and stirred in darkness at

room temperature for 2 d. After filtering off the AgBr by-product, the solvent was reduced to 3 mL and by adding drop wise 10 mL of pentane a white powder precipitated. The solvent was decanted and the white precipitate was washed with pentane (2 x 10 mL) and diethyl ether (3 x 10 mL) to yield a white powder (60 mg, 0.08 mmol, 53.0% yield).

^{1}H NMR (δ ppm, $CDCl_3$, 300 MHz): 7.92 (d, *J* = 8.2 Hz, 4H, CH_{anisyl} + $CH_{methoxycarbonylbenzyl}$), 7.06 (d, *J* = 8.3 Hz, 4H, CH_{anisyl} + $CH_{methoxycarbonylbenzyl}$), 6.87 (d, *J* = 8.7 Hz, 4H, CH_{anisyl} + $CH_{methoxycarbonylbenzyl}$), 6.73 (d, *J* = 8.7 Hz, 4H, CH_{anisyl} + $CH_{methoxycarbonylbenzyl}$), 5.36 (s, 4H, CH_2), 3.91 (s, 6H, OCH_3), 3.75 (s, 6H, OCH_3), 2.06 (s, 3H, $CH_{3acetate}$).

^{13}C NMR (δ ppm, $CDCl_3$, 101 MHz): 178.90 (NCN), 166.56 ($C{=}O_{methoxycarbonylbenzyl)}$), 160.18 (C=O), 141.16, 132.54, 131.82, 130.00, 129.89, 129.86, 127.20, 119.38, 114.14 (C_{anisyl} + $C_{methoxycarbonylbenzyl}$ + $C_{imidazole}$), 55.23 (CH_2), 53.34 ($OCH_{3anisyl}$), 52.17 ($OCH_{3methoxycarbonylbenzyl}$), 22.70 ($CH_{3acetate}$).

IR absorptions (KBr, cm^{-1}): 3434 (w), 2951 (m), 1723 (s), 1587 (m), 1506 (m), 1434 (s), 1280 (s), 1253 (s), 1179 (s), 1109 (s), 1024 (s), 837 (s).

MS (m/z, QMS-MS/MS): 577.51 [M^+-$AgOCOCH_3$].

Micro Analysis Calculated for $C_{37}H_{36}AgN_2O_8$ (744.56): Calcd.: C, 59.69%; H, 4.87%; N, 3.76%; Found: C, 58.95%; H, 4.53%; N, 3.53%.

Melting point: 145-146°C.

(1,3-Bis-(4-cyanobenzyl)-4,5-bis-(4-methoxyphenyl)-imidazole-2-ylidene) silver(I) acetate (4e)

1,3-Bis-(4-cyanobenzyl)-4,5-bis-(4-methoxyphenyl)-imidazolium bromide (**3e**) (100 mg, 0.17 mmol) and 2.1 equivalents of silver(I) acetate (61 mg, 0.36 mmol) were dissolved in 30 mL of dichloromethane and stirred in darkness at room temperature for 2 d. After filtering off the AgBr by-product, the solvent was reduced to 3 mL and by adding drop wise 10 mL of pentane a white powder precipitated. The solvent was decanted and the white precipitate was washed with

pentane (2 x 10 mL) and diethyl ether (3 x 10 mL) to yield a white powder (104 mg, 0.16 mmol, 90.4% yield).

^{1}H NMR (δ ppm, $CDCl_3$, 300 MHz): 7.54 (d, *J* = 8.2 Hz, 4H, CH_{anisyl} + $CH_{cyanobenzyl}$), 7.11 (d, *J* = 8.2 Hz, 4H, CH_{anisyl} + $CH_{cyanobenzyl}$), 6.89 (d, *J* = 8.2 Hz, 4H, CH_{anisyl} + $CH_{cyanobenzyl}$), 6.77 (d, *J* = 8.2 Hz, 4H, CH_{anisyl} + $CH_{cyanobenzyl}$), 5.37 (s, 4H, CH_2), 3.77 (s, 3H, OCH_3), 2.07 (s, 3H, $CH_{3acetate}$).

^{13}C NMR (δ ppm, $CDCl_3$, 101 MHz): 179.16 (NCN), 160.40 (C=O), 141.05 (CN), 132.60, 132.55, 131.74, 130.78, 128.12, 118.95, 118.24, 114.33, 112.23 (C_{anisyl} + $C_{cyanobenzyl}$ + $C_{imidazole}$), 55.28 (CH_2), 53.19 ($CH_{3anisyl}$), 22.75 ($CH_{3acetate}$).

IR absorptions (KBr, cm^{-1}): 3415 (w), 2964 (w), 2927 (w), 2228 (s), 1662 (w), 1609 (m), 1574 (m), 1506 (s), 1402 (m), 1253 (s), 1177 (s), 1025 (m), 834 (m).

MS (m/z, QMS-MS/MS): 511.45 [M^+-$AgOCOCH_3$].

Micro Analysis Calculated for $C_{35}H_{30}AgN_4O_4$ (678.51): Calcd.: C, 61.96%; H, 4.46%; N, 8.26%; Found: C, 62.23%; H, 4.19%; N, 8.16%.

Melting point: 149-152°C.

3.4.3 Antibacterial studies

The silver(I) acetate complexes were screened in preliminary *in vitro* antibacterial tests against two bacterial strains. The test organisms included *Staphylococcus aureus* (*S. aureus*) (NCTC 7447) as a Gram-positive bacteria and *Escherichia coli* (*E. coli*) as Gram-negative bacteria.

To assess the biological activity of compounds **2a-e** and **4a-e**, the qualitative Kirby–Bauer disk-diffusion method was applied [23]. All bacteria were individually cultured from a single colony in sterile LB medium [24] overnight at 37°C in an orbital shaker incubator. All the work carried out was performed under sterile conditions.

For each strain, 70 µL of culture were spread evenly on agar-LB medium. Four 5 mm diameter Whatman paper discs were placed evenly separated on each plate.

Two stock solutions (9:1 DMSO/H_2O) of every compound were prepared at 2.2 µM and 4.4 µM to be able to test the effect of different concentrations. Each plate was then tested with 5 µL and 7 µL of 2.2 µM solution and 5 µL and 10 µL for the 4.4 µM solution. The plates were covered and placed in an incubator at 37°C for 24 h. The plates were then removed and the area of clearance, which is defined as the distance between the edge of the filter paper disc and the beginning of the bacterial growth, was measured for each sample in mm.

3.4.4 Cytotoxicity studies

Preliminary *in vitro* cell tests were performed on the human cancerous renal cell line Caki-1 and the human cancerous breast cell line MCF-7 in order to compare the cytotoxicity of the compounds presented in this paper. These cell lines were chosen based on their regular and long-lasting growth behaviour. The cells were obtained from the ATCC (American Tissue Cell Culture Collection) and maintained in Dulbecco's Modified Eagle Medium containing 10% (v/v) FCS (fetal calf serum), 1% (v/v) penicillin streptomycin and 1% (v/v) L-glutamine. Cells were seeded in 96-well plates containing 200 µL microtitre wells at a density of 5,000-cells/200 µL of medium and were incubated at 37°C for 24 h to allow for exponential growth. Then the compounds used for the testing were dissolved in the minimal amount of DMSO (dimethylsulfoxide) possible and diluted with medium to obtain stock solutions of 5 x 10^{-4} M in concentration and less than 0.7% of DMSO. The cells were then treated with varying concentrations of the compounds and incubated for 48 h at 37°C. Then, the solutions were removed from the wells and the cells were washed with PBS (phosphate buffer solution) and fresh medium was added to the wells. Following a recovery period of 24 h incubation at 37°C, individual wells were treated with 200 µL of a solution of MTT (3-(4,5-Dimethylthiazol-2-yl)-2,5-diphenyltetrazolium bromide) in medium. The solution consisted of 22 mg of MTT in 40 mL of medium. The cells were incubated for 3 h at 37°C. The medium was then removed and the purple formazan crystals were dissolved in 200 µL DMSO per well. For all tests cells with low passage numbers were used. A Wallac Victor (Multilabel HTS Counter) Plate Reader was used to measure absorbance at 540 nm. Cell viability was expressed as a percentage of the absorbance recorded for

control wells. The values used for the dose response curves represent the values obtained from four consistent MTT-based assays for each compound tested.

3.5 Results and Discussion

In Scheme 3.1 the synthetic routes for the symmetric substituted *N*-Heterocyclic carbene ligand precursors as well as their corresponding silver(I) acetate complexes are given. The initial precursor 4,5-bisphenyl-1h-imidazole (**1**) was purchased from Sigma Aldrich and used without further purification, whereas the precursor 4,5-bis-(methoxyphenyl)-1H-imidazole (**3**) was prepared by stirring 2-bis-(4-methoxyphenyl)ethane-1,2-dione with formamide according to literature [22]. 1,3-Bis-benzyl-4,5-bisphenyl-1H-imidazolium bromide (**1a**) was prepared according to literature [13] with a yield of 66.2% while 1,3-bis-(4-methylbenzyl)-4,5-bisphenyl-1H-imidazolium bromide (**1b**), 1,3-bis-(4-methoxybenzyl)-4,5-bisphenyl-1H-imidazolium chloride (**1c**), 1,3-bis-(4-methoxycarbonyl-benzyl)-4,5-bisphenyl-1H-imidazolium bromide (**1d**) and 1,3-bis-(4-cyanobenzyl)-4,5-bisphenyl-1H-imidazolium bromide (**1e**) were synthesised by stirring (**1**) with 2 equivalents of 4-methylbenzyl bromide, 4-methoxybenzyl chloride, 4-methoxycarbonylbenzyl bromide and 4-cyanobenzyl bromide with 1.5 equivalents of K_2CO_3 in acetonitrile for 2-5 d at room temperature to yield the *N*-Heterocyclic carbene ligand precursors in 88.7, 43.3, 72.2 and 81.0%, respectively.

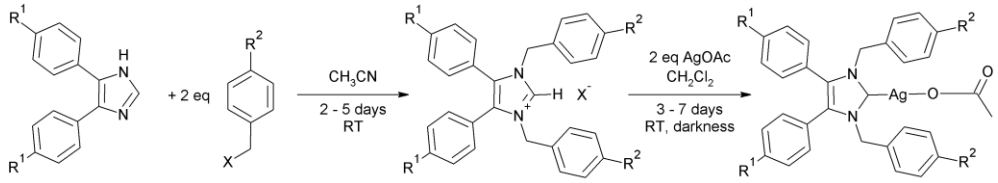

1: R^1 = H,	R^2 = H,	X = Br	**1a**: R^1 = H,	R^2 = H,	X = Br	**2a**: R^1 = H,	R^2 = H
2: R^1 = OCH_3	CH_3,	X = Br	**1b**: R^1 = H,	R^2 = CH_3,	X = Br	**2b**: R^1 = H,	R^2 = CH_3
	OCH_3,	X = Cl	**1c**: R^1 = H,	R^2 = OCH_3,	X = Cl	**2c**: R^1 = H,	R^2 = OCH_3
	$COOCH_3$,	X = Br	**1d**: R^1 = H,	R^2 = $COOCH_3$,	X = Br	**2d**: R^1 = H,	R^2 = $COOCH_3$
	CN,	X = Br	**1e**: R^1 = H,	R^2 = CN,	X = Br	**2e**: R^1 = H,	R^2 = CN
			3a: R1 = OCH_3,	R^2 = H,	X = Br	**4a**: R1 = OCH_3,	R^2 = H
			3b: R^1 = OCH_3,	R^2 = CH_3,	X = Br	**4b**: R^1 = OCH_3,	R^2 = CH_3
			3c: R^1 = OCH_3,	R^2 = OCH_3,	X = Cl	**4c**: R^1 = OCH_3,	R^2 = OCH_3
			3d: R^1 = OCH_3,	R^2 = $COOCH_3$,	X = Br	**4d**: R^1 = OCH_3,	R^2 = $COOCH_3$
			3e: R^1 = OCH_3,	R^2 = CN,	X = Br	**4e**: R^1 = OCH_3,	R^2 = CN

Scheme 3.1: General reaction scheme for the synthesis of symmetric substituted NHC precursors **1a-e**, **3a-e** and their corresponding NHC-silver(I) acetate complexes **2a-e** and **4a-e**.

The 4,5-bis-(4-methoxyphenyl)-imidazole containing precursors 1,3-bis-benzyl-4,5-bis(4-methoxyphenyl)-1H-imidazolium bromide (**3a**), 1,3-bis-(4-methylbenzyl)-4,5-bis(4-methoxyphenyl)-1H-imidazolium bromide (**3b**), 1,3-bis-(4-methoxybenzyl)-4,5-bis(4-methoxyphenyl)-1H-imidazolium chloride (**3c**), 1,3-bis-(4-methoxycarbonyl-benzyl)-4,5-bis(4-methoxyphenyl)-1H-imidazolium bromide (**3d**) and 1,3-bis-(4-cyanobenzyl)-4,5-bis(4-methoxyphenyl)-1H-imidazolium bromide (**3e**) followed the same reaction route to give the respective yields of 35.3, 98.6, 38.0, 38.0 and 50.1%.

The silver(I) acetate complex **2a** was synthesised according to [13] to give a yield of 70.7%. In the absence of light, the silver(I) acetate complexes (1,3-bis(4-methylbenzyl)-4,5-bisphenyl-imidazole-2-ylidene) silver(I) acetate (**2b**), (1,3-bis(4-methoxybenzyl)-4,5-bisphenyl-imidazole-2-ylidene) silver(I) acetate (**2c**), (1,3-bis(4-methoxycarbonylbenzyl)-4,5-bisphenyl-imidazole-2-ylidene) silver(I) acetate (**2d**) and (1,3-bis(4-cyanobenzyl)-4,5-bisphenyl-imidazole-2-ylidene) silver(I) acetate (**2e**) were prepared by stirring the respective precursor with 2 equivalents of silver(I) acetate in dichloromethane at room temperature for 3-7 d. The silver complexes were obtained in 81.0, 63.4, 81.7, 69.1 and 81.3% yield respectively.

The synthesis of the symmetric 4,5-bis(4-methoxyphenyl)-imidazole silver(I) acetate complexes were carried out under the same conditions to give the silver(I) acetate complexes (1,3-bisbenzyl-4,5-bis(4-methoxyphenyl)-imidazole-2-ylidene) silver(I) acetate (**4a**), (1,3-bis(4-methylbenzyl)-4,5-bis(4-methoxyphenyl)-imidazole-2-ylidene) silver(I) acetate (**4b**), (1,3-bis(methoxybenzyl)-4,5-bis(4-methoxyphenyl)-imidazole-2-ylidene) silver(I) acetate (**4c**), (1,3-bis(methoxycarbonylbenzyl)-4,5-bis(4-methoxyphenyl)-imidazole-2-ylidene) silver(I) acetate (**4d**) and (1,3-bis(4-cyanobenzyl)-4,5-bis(4-methoxyphenyl)-imidazole-2-ylidene) silver(I) acetate (**4e**) in 51.7, 67.8, 56.7, 53.0 and 90.4% yields.

The symmetric substituted *N*-Heterocyclic carbene ligand precursors as well as the silver(I) acetate complexes were fully characterized by spectral (^{1}H NMR, ^{13}C NMR, IR, mass), elemental analysis studies and melting point determination.

Furthermore the solid state structure of the silver(I) acetate complexes **2d**, **2e** and **4c** was determined by single crystal X-ray diffraction.

Due to the positive charge of the molecule, the ^{1}H NMR spectra of all NHC precursors **1a-e** and **3a-e** show a characteristic downfield shift in the range δ =

9.63-11.65 ppm for the NCHN proton [25–27]. In addition, their identities have also been confirmed by a base peak for the [M^+- Br] fragments in their positive mode ESI mass spectra. A successful formation of the complexes **2a-e** and **4a-e** is indicated by the absence of a downfield NCHN signal and presence of new signals at 3.76-2.06 ppm for the acetate protons in all the ^{1}H NMR spectra. The ^{13}C NMR resonances of the carbene carbon atoms in complexes **2a-e** and **4a-e** occur in the range δ = 206.90-170.34 ppm respectively. These signals are shifted downfield compared to the corresponding precursors of **1a-e** and **3a-e** carbene carbons resonance at the range δ = 166.30-138.26 ppm, respectively which further demonstrates the formation of expected NHC-silver(I) acetate complexes. Also the appearance of the ^{13}C NMR resonances for the carbonyl and methyl carbons of the acetate group of complexes **2a-e** and **4a-e** in the range 166.56-156.23 and 22.95-22.70 ppm respectively show the formation of the NHC-silver(I) acetate complexes [4, 6]]. Furthermore, positive mode ESI mass spectra of all ten NHC-silver(I) acetate complexes (**2a-e, 4a-e**) are dominated by [M^+-O_2CCH_3] fragment peaks arising from the loss of one acetate ligand. The melting points of the NHC precursors **1a-e** range between 220 and 293°C with the only exception for the chloride containing precursor **1c**, which melting point occurs at a lower temperature (192-194°C). The same pattern is observed in the melting points of **3a-e** where the bromide containing precursors exhibit much higher melting points (192-240°C) than the correspondent chloride containing precursor **3c** (106-108°C). The formation of the silver acetate complexes has a significant influence on the thermal stability of the compounds and leads to lower melting points of 144-209°C for **2a-e** and 118-156°C for **4a-e**. Overall the thermal stability of the 4,5-bisphenyl-imidazole compounds is higher than their correspondent 4,5-bis(4-methoxyphenyl) substituted imidazole analogues.

3.5.1 Structural discussion:

The crystals of **2b** and **2e** were formed in a saturated solution of chloroform with slow infusion of pentane, while the crystal of **4c** was grown in a saturated solution of dichloromethane with slow infusion of pentane. **2b** crystallized in the triclinic space group P-1, **2e** in the monoclinic space group C2/c (#15) and 4c in the

triclinic space group P–1 (#2); all in absence of any solvent molecules. The crystal data and refinements are found in Table 1, whereas selected bond lengths and bond angles are compiled in Table 2. The X-ray structures show that the imidazole ring is planar and the bond lengths and angles in the five membered imidazole ring (NCNCC) are in good agreement with those in similar compounds reported earlier by our group [12–17].

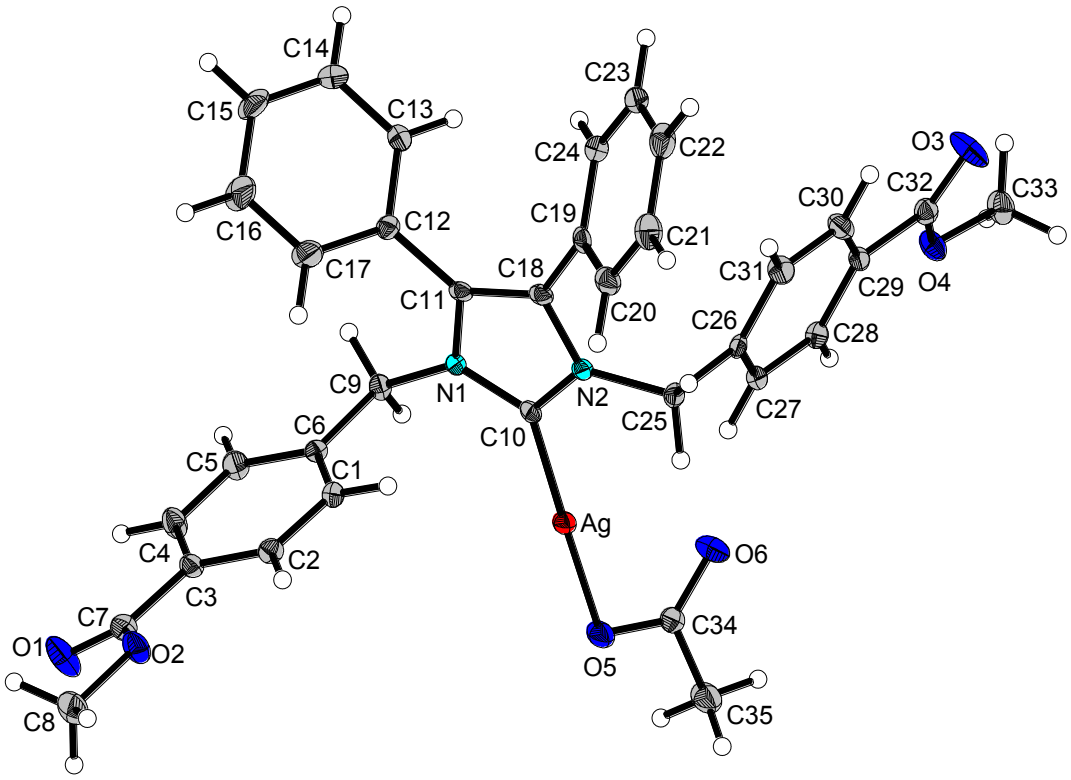

Figure 3.1: X-ray diffraction structure of **2d**; thermal ellipsoids are drawn on the 50% probability level.

The crystal structure of **2d** and **2e** show a nearly linear bond angle of 178.76(7)° and 174.69(5)° respectively at the two-coordinated silver atom. The bond distances of the silver atom to the carbene of Ag–C(10) = 2.060(2) Å (**2d**) and Ag-C(9) = 2.0588(17) Å (**2e**) agree very well with previously reported examples of this compound class [12–17] and show that the silver is strongly bonded to the carbene. The bond length of the silver(I) atom to the acetate oxygen is in all three structures relatively short with Ag–O(5) = 2.1013(16) Å (**2d**) and Ag-O(1) = 2.1164(13) Å (**2e**) compared to the ones our group previously reported, but still within range of the corresponding ones in similar molecules (see for example [26,

27]). This short distance suggests a predominantly covalent character of the Ag-O bond.

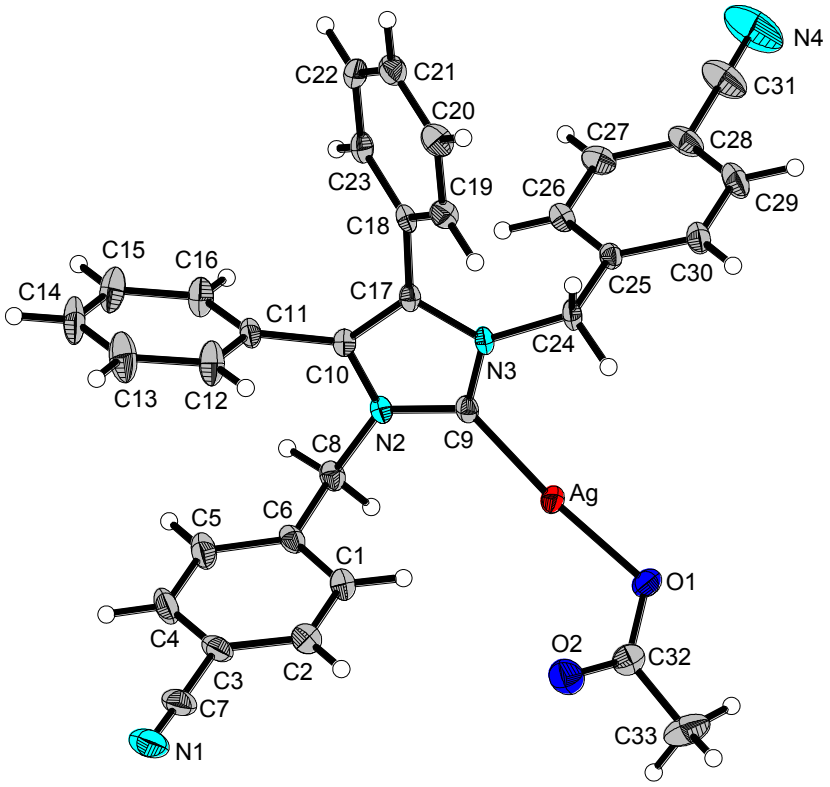

Figure 3.2: X-ray diffraction structure of **2e**; thermal ellipsoids are drawn on the 50% probability level.

In the NHC silver(I) acetate complex **4c** (Fig. 3, 4), one of the two silver atoms (Ag(2)) coordinates to two acetate groups. One can see an almost linear bond angle of 173.89(7)° at the two coordinate silver atom C(9)–Ag(1)–O(5). The C(44)-Ag(2)-O(11) bond angle is with 167.77(7) bent a bit more, and the displacement of Ag(2) from the line C(44)-O(11) is towards O(6) (Fig. 4). This, together with the Ag(I)-O(6) distance of 2.6279(16) Å, suggests a weak bond between the two atoms.

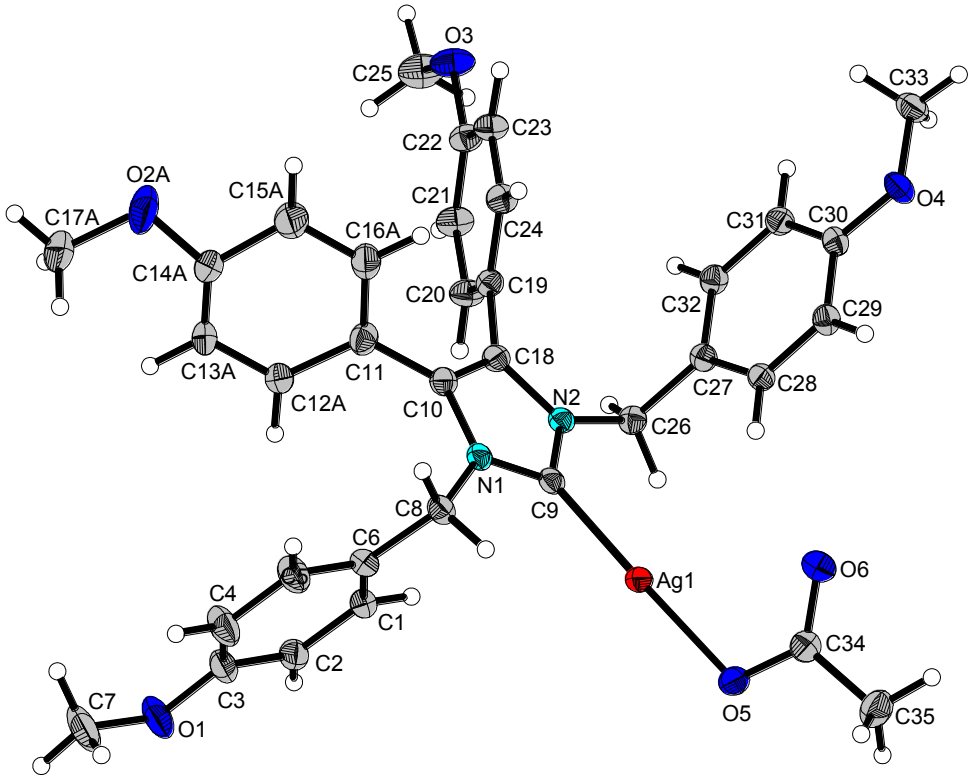

Figure 3.3: X-ray diffraction structure of **4c**; thermal ellipsoids are drawn on the 50% probability level, disorder neglected.

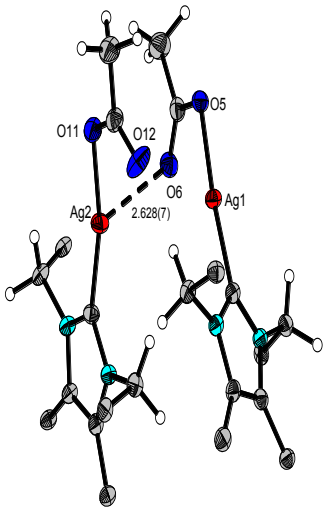

Figure 3.4: interaction between two adjacent molecules via a short Ag···O contact; thermal ellipsoids are drawn on the 50% probability level, aryl groups are represented by their ipso carbons only.

Table 3.1: Crystal Data and Structure Refinement for **2d**, **2e** and **4c**.

		2d	**2e**	**4c**
Empirical formula		$C_{35}H_{32}AgN_2O_6$	$C_{33}H_{26}AgN_4O_2$	$C_{70.75}H_{71.5}N_4O_{12}Cl_{1.5}Ag_2$
Formula weight [g/mol]		802.86	617.44	1438.74
Crystal system		Triclinic	Monoclinic	Triclinic
Space Group		P -1	C2/c (#15)	P-1 (#2)
Unit cell dimensions [Å]	a	8.8250(3)	29.4955(9)	13.4580(4)
	b	14.9450(4)	8.2592(2)	16.9528(5)
	c	15.2246(4)	24.1508(7)	17.1298(5)
	α	116.877(3)°.		107.092(3)°.
	β	101.163(2)°	104.100(3)°.	112.693(3)°.
	γ	97.006(2)°		96.891(2)°.
Volume [$Å^3$]		1706.08(9)	5706.1(3)	3323.5(2)
Z		2	8	2
Density [mg/m^3] (calc.)		1.563	1.437	1.438
Absorption coefficient [mm^{-1}]		0.875	0.743	5.808
F(000)		816	2512	1479
Crystal size [mm^3]		0.3211 x 0.2116 x 0.1567	0.2206 x 0.1980 x 0.1272	0.2785 x 0.1791 x 0.1199
Theta range for data collection		3.30 to 26.42°.	3.42 to 29.71°.	3.01 to 76.47°.
Index ranges		-10<=h<=11	–37<=h<=37	-16<=h<=16
		-18<=k<=18	–11<=k<=11	-21<=k<=21
		-19<=l<=19	–33<=l<=32	-21<=l<=21
Reflections collected		48384	31477	35819
Independent reflections		6973 [R(int) = 0.0586]	7085 [R(int) = 0.0279]	13796 [R(int) = 0.0286]
Completeness to θ_{max}		99.5 %	99.2 %	98.8%
Max. and min transmission		0.904 and 0.830	0.896 and 0.849	0.630 and 0.440
Data/restraints/parameters		6973 / 0 / 436	7085 / 0 / 362	13796 / 34 / 868
Goodness-of-fit in F^2		1.047	1.053	1.028
Final R indices (I>2σ(I))		R1 = 0.0285	R1 = 0.0266	R1 = 0.0291

	wR2 = 0.0647	wR2 = 0.0643	wR2 = 0.0730
R Indices (all data)	R1 = 0.0346	R1 = 0.0325	R1 = 0.0319
	wR2 = 0.0685	wR2 = 0.0681	wR2 = 0.0749
Largest diff. peak and hole	0.623 and -0.764 e $Å^{-3}$	0.418 and –0.554 e. $Å^{-3}$	0.602 and –0.863 e.$Å^{-3}$

Table 3.2: Selected bond lengths [Å] and angles [º] for **2d**, **2e** and **4c**.

2d	**Bond length [Å]**	**2e**	**Bond length [Å]**	**4c**	**Bond length [Å]**
Ag–C(10)	2.060(2)	Ag–C(9)	2.0588(17)	Ag(I)-C(9)	2.087(2)
Ag–O(5)	2.1013(16)	Ag-O(1)	2.1164(13)	Ag(I)-O(5)	2.1582(14)
N(1)–C(10)	1.350(3)	N(2)-C(9)	1.350(2)	N(1)-C(9)	1.350(3)
N(1)–C(11)	1.398(3)	N(2)–C(10)	1.392(2)	C(9)-N(2)	1.348(3)
C(10)–N(2)	1.348(3)	C(9)–N(3)	1.351(2)	N(1)-C(10)	1.399(3)
C(18)-N(2)	1.396(3)	C(17)–N(3)	1.397(2)	C(10)-C(18)	1.360(3)
C(11)–C(18)	1.359(3)	C(10)–C(17)	1.361(2)	C(18)-N(2)	1.393(3)
				Ag(2)-O(11)	2.1197(16)
				Ag(2)–C(44)	2.073(2)
				O(6)–Ag(2)	2.6279(16)
2d	**Bond angle [º]**	**2e**	**Bond angle [º]**	**4c**	**Bond angle [°]**
C(10)–Ag–O(5)	178.76(7)	C(9)–Ag–O(1)	174.69(5)	C(9)–Ag(1)–O(5)	173.89(7)
N(2)–C(10)–N(1)	104.73(17)	N(2)–C(9)–N(3)	104.39(14)	N(2)–C(9)–N(1)	104.90(17)
N(2)–C(10)–Ag	125.82(15)	N(2)–C(9)–Ag	128.09(12)	N(2)–C(9)–Ag(1)	126.78(14)
N(1)–C(10)–Ag	129.43(15)	N(3)–C(9)–Ag	127.21(12)	N(1)–C(9)–Ag(1)	127.84(14)
C(18)–C(11)–N(1)	106.31(18)	C(17)–C(10)–N(2)	106.44(14)	C(18)–C(10)–N(1)	105.95(18)
C(11)–C(18)–N(2)	105.99(18)	C(10)–C(17)–N(3)	105.76(14)	C(10)–C(18)–N(2)	106.49(18)

C(10)–N(2)–C(18)	111.67(17)	C(9)–N(3)–C(17)	111.75(13)	C(9)–N(2)–C(18)	111.34(17)
				C(44)–Ag(2)–O(6)	104.32(6)
				O(11)–Ag(2)–O(6)	84.95(6)
C(34)–O(5)–Ag	111.11(13)	C(32)–O(1)–Ag	107.66(12)	C(34)–O(5)–Ag(1)	108.72(13)
				C(34)–O(6)–Ag(2)	109.57(13)
O(6)–C(34)–O(5)	124.3(2)	O(2)–C(32)–O(1)	123.60(18)	O(6)–C(34)–O(5)	124.3(2)
O(6)–C(34)–C(35)	120.5(2)	O(2)–C(32)–C(33)	119.80(17)	O(6)–C(34)–C(35)	119.7(2)
O(5)–C(34)–C(35)	115.27(19)	O(1)–C(32)–C(33)	116.61(17)	O(5)–C(34)–C(35)	116.0(2)
				C(69)–O(11)–Ag(2)	119.64(14)
				O(12)–C(69)–O(11)	125.7(2)
				O(12)–C(69)–C(70)	119.3(2)
				O(11)–C(69)–C(70)	115.01(19)

3.5.2 Biological evaluation

3.5.2.1 Antibacterial Testing

Using the Kirby-Bauer disk diffusion method, the antibacterial activity of the NHC-silver acetate complexes was tested and summarised in Figure 3.5-3.8. The metal salt (silver(I) acetate) used to prepare the complexes and the solvent (DMSO) used to prepare the stock solutions played no role in growth inhibition on the same bacteria as previously reported [28, 29]]. An area of clearance of 0 mm was considered as no activity, areas of 1–3 mm as low, 4–7 mm as medium, and areas of clearance ≥8 mm as high activity. The primary aim was to synthesise a derivative of the target molecule (1,3-bisbenzyl-4,5-bisphenyl imidazole-2-ylidene) silver(I) acetate **2a**, that would exhibit greater antimicrobial properties than this leading compound against *E. coli* and *S. aureus* bacteria strains.

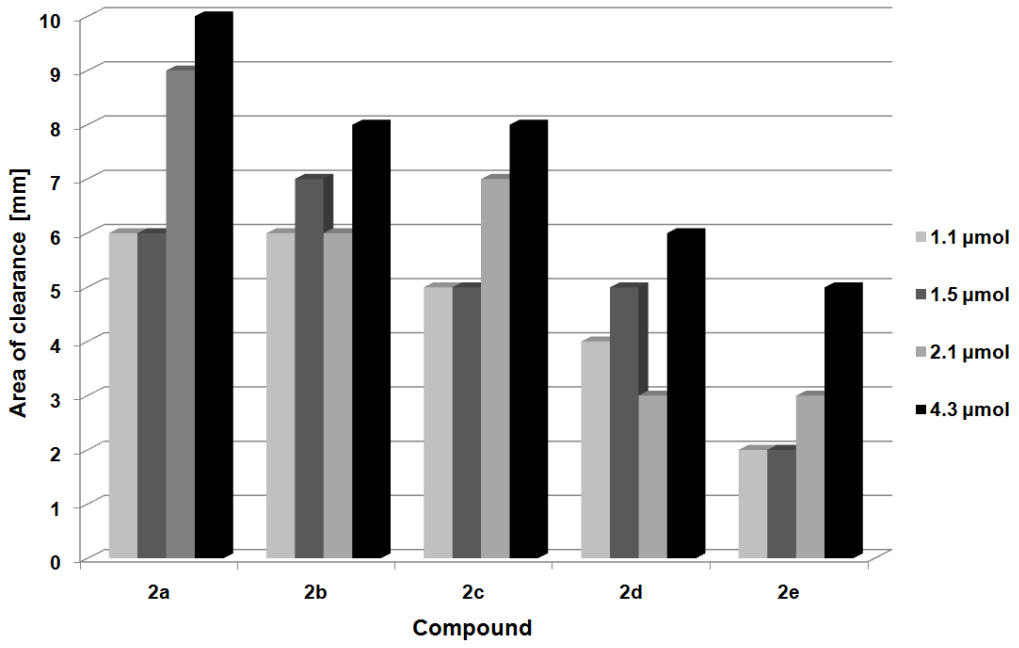

Figure 3.5: Area of clearance on *Escherichia coli* (Gram -ve) by **2a-e**.

Almost no antibacterial activity against *E. coli* was found for the compounds **4b-4d**, and against *S. aureus* nearly no activity was found for **2e** and **4d**. Medium

activity against *E. coli* was found only for two bisphenyl-imidazole silver complexes (**2d**, 6 mm; **2e**, 7 mm), whereas more complexes were active in this range against *S. aureus* (**2a**, 7 mm; **2b**, 5 mm, **2d**, 4 mm and **4c**, 5 mm).

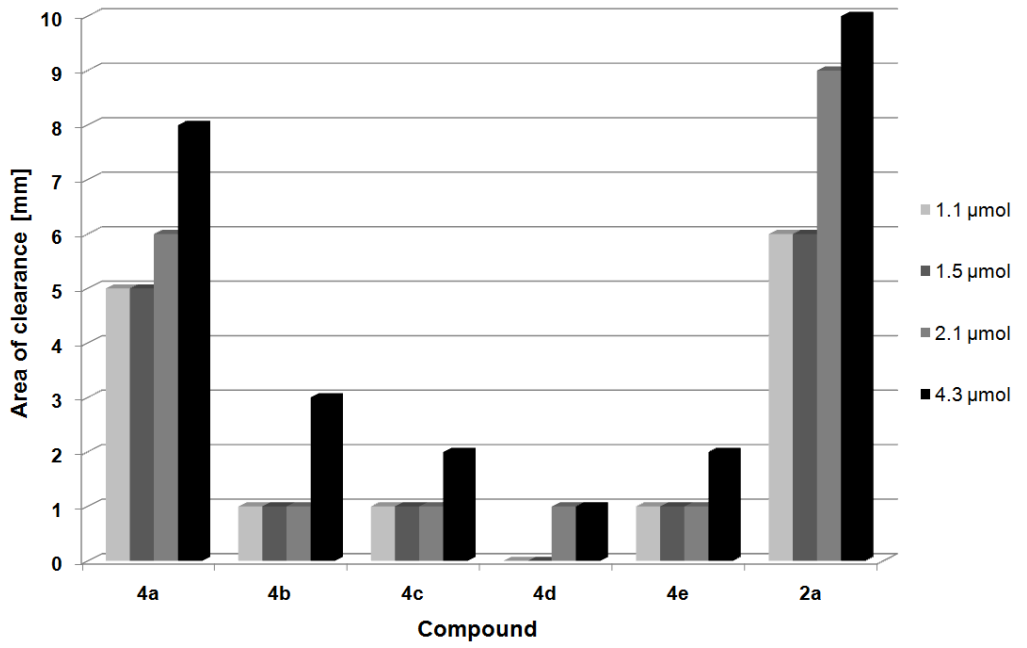

Figure 3.6: Area of clearance on *Escherichia coli* (Gram -ve) by **4a-e**.

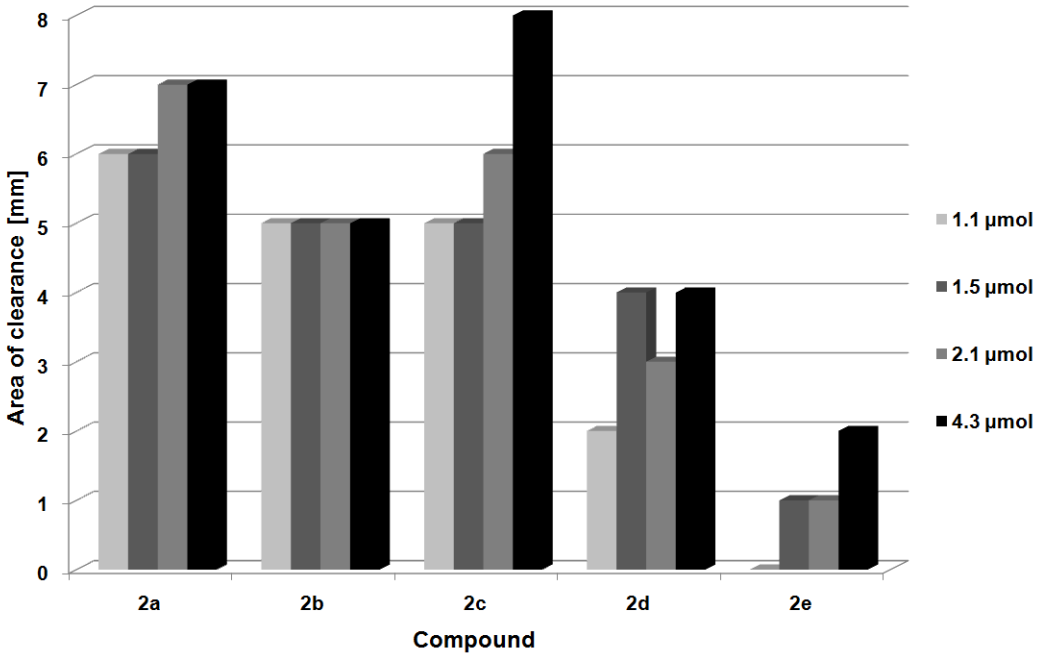

Figure 3.7: Area of clearance on *Staphylococcus aureus* (Gram +ve) by **2a-e**.

Only compounds **2c** and **4a**, showed slightly higher activity against *S. aureus* compared to **2a**.

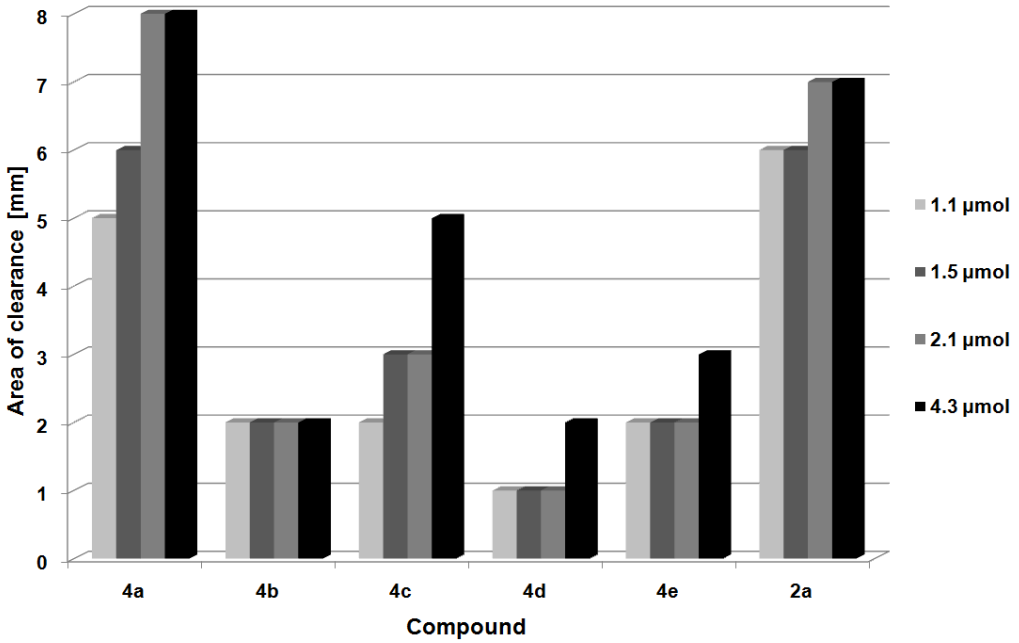

Figure 3.8: Area of clearance on *Staphylococcus aureus* (Gram +ve) by **4a-e**.

3.5.2.2 Cytotoxicity Studies

The log dose response curves for complexes **2a-e** and **4a-e** against the cancer cell line Caki-1 are shown in Figure 3.9 and Figure 3.10, respectively. All compounds were well soluble in DMSO and stable in the biological medium over the period of the testing time.

As well as for the antibacterial studies (see above), all IC_{50} cell test results were compared to our previously reported complex **2a** , which has shown to have an IC_{50} value against the human renal cancer cell line Caki-1 of 14 (± 1) µM [13]. Unfortunately all 4,5-bis-(methoxyphenyl)-imidazole silver acetates **4a-e** exhibited lower cytotoxic activity against this cell line with 21 (± 1), 21 (± 2), 21 (± 1), 34 (± 2) and 46 (± 2) µM, respectively.

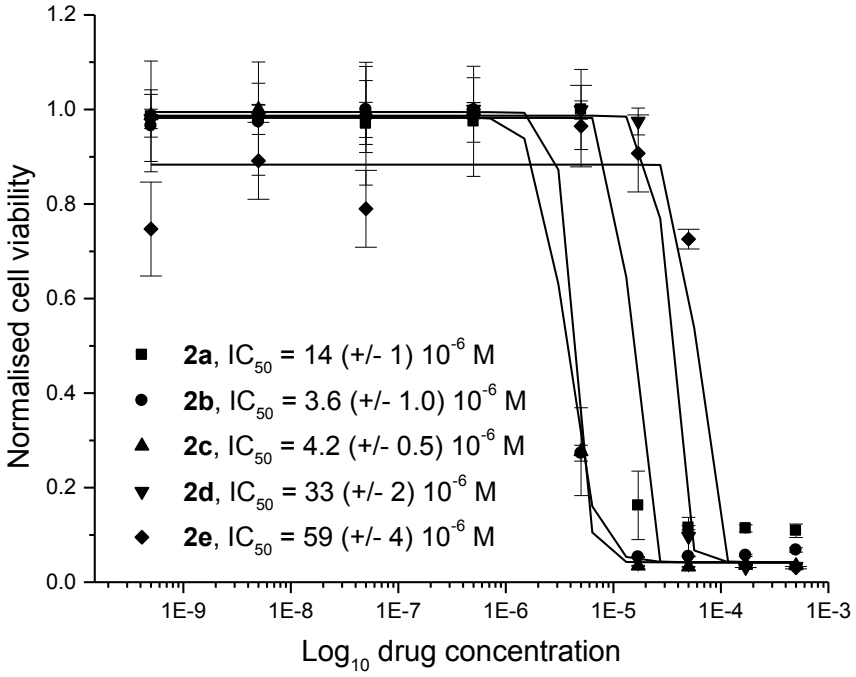

Figure 3.9: Cytotoxicity curves from typical MTT assays showing the effect of compounds **2a-e** on the viability of Caki-1 cells.

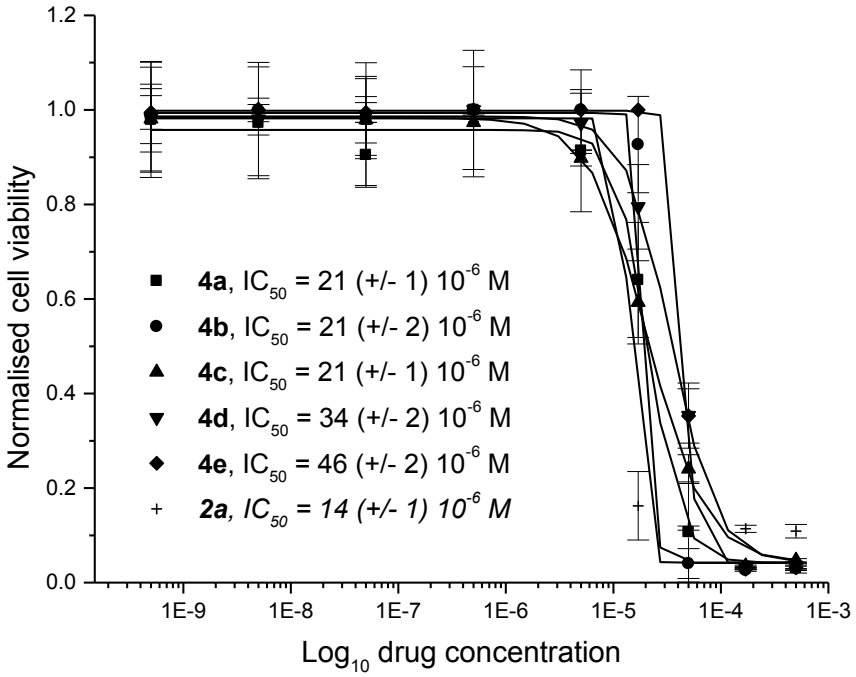

Figure 3.10: Cytotoxicity curves from typical MTT assays showing the effect of compounds **4a-e** on the viability of Caki-1 cells.

In contrast to this the 4,5-bisphenyl-imidazole silver acetates **2b-e** have shown partial improvement in cytotoxic activity against Caki-1. Compounds **2b** and **2c** both show a 3-4 fold increase in biological activity and exhibit therefore IC_{50} values of 3.6 (± 1) and 4.2 (± 0.5) µM. **2d** and **2e** show like their analogues **4d** and **4e** a significant lower activity with IC_{50} values of 33 (± 2) and 59(± 4) µM. The strong decrease in activity in these complexes might be due to the introduction of the more hydrophilic 4-cyanobenzyl (**2d** and **4d**) and 4-methoxycarbonylbenzyl (**2e** and **4e**) groups in position 1 and 3 of the imidazole. The overall tendency seems to be that the 4,5-bisphenyl substitution is superior to its 4,5-bisanisyl counterpart with respect to cytotoxicity.

The log dose response curves for complexes **2a-e** and **4a-e** against the cancer cell line MCF-7 are shown in Figure 3.11 and Figure 3.12, respectively.

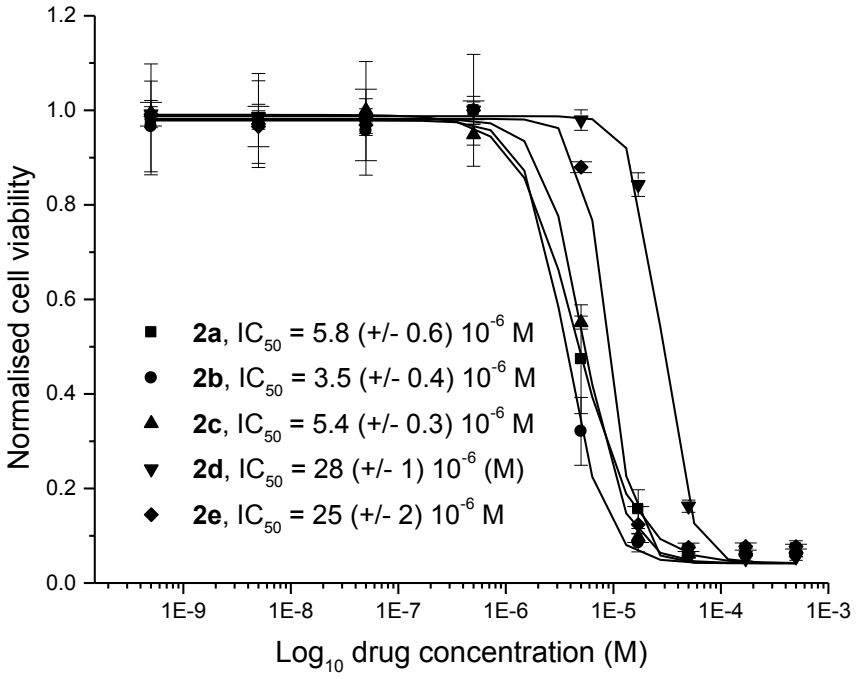

Figure 3.11: Cytotoxicity curves from typical MTT assays showing the effect of compounds **2a-e** on the viability of MCF-7 cells.

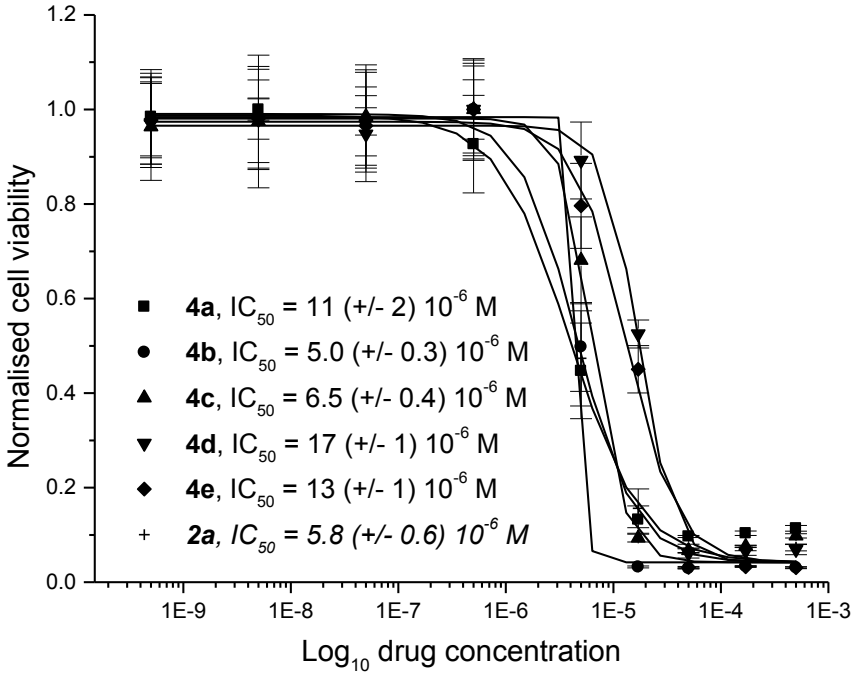

Figure 3.12: Cytotoxicity curves from typical MTT assays showing the effect of compounds **4a-e** on the viability of MCF-7 cells.

In comparison to the cell test results against the human renal cancer cell line Caki-1 (see above), not only 4,5-bisphenyl-imidazole silver acetates **2b** and **2c** exhibited comparable or better IC_{50} values (3.5 (± 0.4) and 5.4 (± 0.3) µM) against this cell line, but also the two 4,5-bis(methoxyphenyl)-imidazole silver acetates **4b** and **4c** have shown a good level of activity with values of 5.0 (± 0.3) and 6.5 (± 0.4) µM.

Interestingly, the substitution pattern in position 1 and 3 of the imidazole ring seems to play an overall big role in the cytotoxic activity of these ten new symmetrical substituted NHC silver acetate complexes. While all four more hydrophilic substituted complexes **2d**, **2e**, **4d** and **4e** show moderate biological activity against both human cancer cell lines, good activity is found for **2b** and **2c** against Caki-1 and MCF-7 and for **4b** and **4c** against MCF-7 alone. The difference in activity against Caki-1 comparing complexes **2b** and **2c** versus **4b** and **4c** must be directly related to the change from a proton in position 4 on the phenyl rings to a methoxy group instead. The therefore more hydrophilic substitution pattern

seems to have a direct impact on either the cellular uptake or the interaction in the cell itself.

3.6 Conclusion and Outlook

These newly synthesised *N*-Heterocyclic carbene silver acetate complexes derived from 4,5-diaryl-imidazole have shown some promising cytotoxic results against the human cancer cell lines Caki-1 and MCF-7; the cytotoxicity is already comparable to platinum-based drugs on these specific cell lines. In addition, significant antibacterial activity against *E. coli* and *S. aureus* were observed but the level of conventional antibiotics was not reached yet for the derivatives described. Most promising results were obtained for complexes **2b** and **2c** against both cancer cell lines as well as against both bacterial strains.
Further studies on the influence of more hydrophilic and hydrophobic substitution patterns of the imidazole ring on the cytotoxicity and antibacterial properties of such complexes are in progress; in future experiments the mode of action of the NHC-silver acetate complexes and their toxicity *in vivo* will be investigated.

Acknowledgement

This project was funded by the UCD School of Chemistry and Chemical Biology.

3.7 References

[1] B. Thati, A. Noble, B. S. Creaven, M. Walsh, M. McCann, K. Kavanagh, M. Devereux, and D. A. Egan, ""*In vitro* anti-tumour effect of coumarin-3-carboxylic acid and three of its hydroxylated derivatives, along with their silver-based complexes, using human epithelial carcinoma cell lines," *Cancer Letters*, vol. 248, no. 2, pp. 321–333, 2007.

[2] H.-L. Zhu, X.-M. Zhang, X.-Y. Liu, X.-J. Wang, G.-F. Liu, A. Usman, and H.-K. Fun, "Clear Ag-Ag bonds in three silver(I) carboxylate complexes with high cytotoxicity properties," *Inorg. Chem. Comm,* vol. 6, no. 8, pp. 1113–1116, 2003.

[3] J. J. Liu, P. Galettis, A. Farr, L. Maharaj, H. Samarasinha, A. C. McGechan, B. C. Baguley, R. J. Bowen, S. J. Berners-Price, and M. J. McKeage, "*In vitro* antitumour and hepatotoxicity profiles of Au(I) and Ag(I) bidentate pyridyl phosphine complexes and relationships to cellular uptake," *J. Inorg. Biochem,* vol. 102, no. 2, pp. 303–310, 2008.

[4] K. M. Hindi, T. J. Siliciano, S. Dumus, M. J. Panzner, D. A. Medvetz, D. V. Reddy, L. A. Hogue, C. E. Hovis, J. K. Hillard, R. J. Mallet, C. A. Tessier, C. L. Cannon, and W. J. Youngs, "Synthesis, stability and antimicrobial studies of electronically tuned silver acetate *N*-Heterocyclic carbenes," *J. Med. Chem,* vol. 51, no. 6, pp. 1577–1583, 2008.

[5] D. A. Medvetz, K. M. Hindi, M. J. Panzner, A. J. Ditto, Y. H. Yun, and W. J. Youngs, "Anticancer Activity of Ag(I) *N*-Heterocyclic Carbene Complexes Derived from 4,5-Dichloro-1H-Imidazole," *Metal-Based Drugs*, 2008.

[6] A. Kascatan-Nebioglu, A. Melaiye, K. M. Hindi, S. Durmus, M. J. Panzner, L. A. Hogue, R. J. Mallett, C. E. Hovis, M. Coughenour, S. D. Crosby, A. Milsted, D. L. Ely, C. A. Tessier, C. L. Cannon, and W. J. Youngs, "Synthesis from caffeine of a mixed N-Heterocyclic carbene-silver acetate complex active against resistant respiratory pathogens," *J. Med. Chem,* vol. 49, no. 23, pp. 6811–6818, 2006.

[7] A. Melaiye, R. S. Simons, A. Milsted, F. Pingitore, C. Wesdemiotis, C. A. Tessier, and W. J. Youngs, "Formation of water-soluble pincer silver(I)-carbene complexes: a novel antimicrobial agent," *J. Med. Chem,* vol. 47, no. 4, pp. 973–977, 2004.

[8] C. L. Cannon, L. A. Hogue, R. K. Vajravelu, G. H. Capps, A. Ibricevic, K. M. Hindi, A. Kascatan-Nebioglu, M. J. Walter, S. L. Brody, and W. J. Youngs, "*In vitro* and murine efficacy and toxicity studies of nebulized SCC1, a methylated caffeine-silver(I) complex, for treatment of pulmonary infections," *Antimicrobial Agents and Chemotherapy*, vol. 53, no. 8, pp. 3285–3293, 2009.

[9] S. Roland, C. Jolivalt, T. Cresteil, L. Eloy, P. Bouhours, A. Hequet, V. Mansuy, C. Vanucci, and J.-M. Paris, "Investigation of a Series of Silver–*N*-Heterocyclic Carbenes as Antibacterial Agents: Activity, Synergistic Effects, and Cytotoxicity," *Chem. Eur. J,* vol. 17, no. 5, pp. 1442–1446, 2011.

[10] W. Liu, K. Bensdorf, A. Hagenbach, U. Abram, B. Niu, A. Mariappan, and R. Gust, "Synthesis and biological studies of silver *N*-Heterocyclic carbene complexes derived from 4,5-diarylimidazole," *Eur. J. Med. Chem,* vol. 46, pp. 5927–5934, 2011.

[11] S. Patil and M. Tacke, “NHC-Silver(I) Acetates as Bioorganometallic Anticancer and Antibacterial Drugs,” *Insights into Coordination, Bioinorganic and Applied Inorganic Chemistry*, pp. 555–566, 2011.
[12] S. Patil, A. Deally, B. Gleeson, F. Hackenberg, H. Müller-Bunz, F. Paradisi, and M. Tacke, “Synthesis, Cytotoxicity and Antibacterial Studies of Novel Symmetrically and Non-Symmetrically p-Nitrobenzyl-Substituted *N*-Heterocyclic Carbene-Silver(I) Acetate Complexes,” *Z. Allg. Anorg. Chem,* vol. 637, no. 3-4, pp. 386–396, 2011.
[13] S. Patil, A. Deally, B. Gleeson, H. Müller-Bunz, F. Paradisi, and M. Tacke, “Novel Benzyl-Substituted N-Heterocyclic Carbene–Silver Acetate Complexes: Synthesis, Cytotoxicity and Antibacterial Studies,” *Metallomics*, vol. 3, no. 1, pp. 74–88, 2011.
[14] S. Patil, K. Dietrich, A. Deally, B. Gleeson, H. Müller-Bunz, F. Paradisi, and M. Tacke, “Synthesis, Cytotoxicity and Antibacterial Studies of Novel symmetrically and Nonsymmetrically 4-(Methoxycarbonyl)benzyl-Substituted *N*-Heterocyclic Carbene-Silver Acetate Complexes,” *Helv. Chim. Acta*, vol. 93, no. 12, pp. 2347–2364, 2010.
[15] S. Patil, A. Deally, B. Gleeson, H. Müller-Bunz, F. Paradisi and M. Tacke, “Synthesis, Cytotoxicity and Antibacterial Studies of Symmetrically and Non-Symmetrically Benzyl- or p-Cyanobenzyl-Substituted *N*-Heterocyclic Carbene-Silver Complexes,” *Appl. Organomet. Chem,* vol. 24, no. 11, pp. 781–793, 2010.
[16] S. Patil, J. Claffey, A. Deally, B. Gleeson, M. Hogan, L. M. Menéndez Méndez, H. Müller-Bunz, F. Paradisi, and M. Tacke, “Synthesis, Cytotoxicity and Antibacterial Studies of p-Methoxybenzyl-Substituted and Benzyl-Substituted *N*-Heterocyclic Carbene-Silver Complexes,” *Eur. J. Inorg. Chem,* vol. 2010, no. 7, pp. 1020–1031, 2010.
[17] F. Hackenberg, A. Deally, G. Lally, S. Malenke, H. Müller-Bunz, F. Paradisi, S. Patil, D. Quaglia, and M. Tacke, “Novel Nonsymmetrically p-Benzyl-Substituted (Benz)imidazole *N*-Heterocyclic Carbene-Silver(I) Acetate Complexes : Synthesis and Biological Evaluation,” *Int. J. Inorg. Chem,* vol. 2012, 2012.
[18] L. Kaps, B. Biersack, H. Müller-Bunz, K. Mahal, J. Münzner, M. Tacke, T. Mueller, and R. Schobert, “Gold(I)-NHC complexes of antitumoral diarylimidazoles: structures, cellular uptake routes and anticancer activities,” *J. Inorg. Biochem,* vol. 106, no. 1, pp. 52–58, 2012.
[19] S. Patil, A. Deally, F. Hackenberg, L. Kaps, H. Müller-Bunz, R. Schobert, and M. Tacke, “Novel Benzyl- or 4-Cyanobenzyl-Substituted *N*-Heterocyclic (Bromo)(carbene)silver(I) and (Carbene)(chloro)gold(I) Complexes: Synthesis and Preliminary Cytotoxicity Studies,” *Helv. Chim. Acta*, vol. 94, no. 9, pp. 1551–1562, 2011.
[20] *CrysalisPro*: Agilent Technologies, 2011.
[21] G. M. Sheldrick, “A short history of SHELX,” *Acta Crystallogr,* vol. A64, no. 1, pp. 112–122, 2008.
[22] H. Bredereck and G. Theilig, “Imidazolsynthesen mit Formamid,” *Chem. Ber,* vol. 86, no. 1, pp. 88–96, 1952.
[23] A. Bondi, H. E. Spaulding, E. D. Smith, and C. C. Dietz, “A routine method for the rapid determination of susceptibility to penicillin and other antibiotics,” *Am. J. Med. Sci,* vol. 213, no. 2, pp. 221–225, 1947.

[24] S. E. Luria, “Recent Advances in Bacterial Genetics,” *Bacteriol. Rev,* vol. 11, no. 1, pp. 1–40, 1947.
[25] W. A. Herrmann and C. Kocher, “*N*-Heterocyclic Carbenes,” *Angew. Chem. Int. Ed,* vol. 36, no. 20, pp. 2162–2187, 1997.
[26] A. J. Arduengo, H. V. Rasika-Dias, J. C. Calabrese, and F. Davidson, “Homoleptic carbene-silver(I) and carbene-copper(I) complexes,” *Organometallics*, vol. 12, no. 9, pp. 3405–3409, 1993.
[27] C. C. Scarborough, B. V. Popp, I. A. Guzei, and S. S. Stahl, “Development of 7-membered *N*-Heterocyclic carbene ligands for transition metals,” *J. Organomet. Chem,* vol. 690, no. 25, pp. 6143–6155, 2005.
[28] M. J. Panzner, A. Deeraksa, A. Smith, B. D. Wright, K. M. Hindi, A. Kascatan-Nebioglu, A. G. Torres, B. M. Judy, C. E. Hovis, J. K. Hillard, R. J. Mallett, E. Cope, D. M. Estes, C. L. Cannon, J. G. Leid, and W. J. Youngs, “Synthesis and *in vitro* Efficacy Studies of Silver Carbene Complexes on Biosafety Level 3 Bacteria,” *Eur. J. Inorg. Chem,* vol. 13, pp. 1739–1745, 2009.
[29] B. Gleeson, J. Claffey, D. Ertler, M. Hogan, H. Müller-Bunz, F. Paradisi, D. Wallis, and M. Tacke, “Novel Organotin Antibacterial and Anticancer Drugs,” *Polyhedron*, vol. 27, no. 18, pp. 3619–3624, 2008.

Chapter 4 4,5-Diaryl-imidazole *N*-Heterocyclic carbene-silver(I) acetate complexes - Part 2

Work published as:

Synthesis and biological evaluation of N-Heterocyclic carbene-silver(I) acetate complexes derived from 4,5-ditolyl-imidazole, F. Hackenberg, G. Lally, H. Müller-Bunz, F. Paradisi, D. Quaglia, W. Streciwilk and M. Tacke, *Inorganica Chimica Acta*, **2013**, *395*, 135-144.

Synthesis and biological evaluation of *N*-Heterocyclic carbene-silver(I) acetate complexes derived from 4,5-ditolyl-imidazole

Frauke Hackenberg, Grainne Lally, Helge Müller-Bunz, Francesca Paradisi, Daniela Quaglia, Wojciech Streciwilk and Matthias Tacke

Centre for Synthesis and Chemical Biology (CSCB), UCD School of Chemistry and Chemical Biology, University College Dublin, Belfield, Dublin 4, Ireland

4.1 Keywords

NHC-silver complexes; Caki-1; MCF-7; *E. coli*; *S. aureus.*

4.2 Abstract

From the reaction of 1,2-bis-(4-methylphenyl)ethane-1,2-dione with formamide, symmetrically substituted 4,5-bis-(4-methylphenyl)-1H-imidazole (**1**) was synthesised ad further reacted with *p*-benzyl substituted halides to give the symmetrically substituted *N*-Heterocyclic carbene (NHC) precursors **1a-e**.

The NHC precursors were then reacted with silver(I) acetate to yield NHC-silver(I) acetate complexes 1,3-bis-(benzyl)-4,5-bis-(4-methylphenyl)-imidazole-2-ylidene silver(I) acetate (**2a**), 1,3-bis-(4-methylbenzyl)-4,5-bis-(4-methylphenyl)-imidazole-2-ylidene silver(I) acetate (**2b**), 1,3-bis-(4-methoxylbenzyl)-4,5-bis-(4-methylphenyl)-imidazole-2-ylidene silver(I) acetate (**2c**), 1,3-bis-(4-methoxycarbonylbenzyl)-4,5-bis-(4-methylphenyl)-imidazole-2-ylidene silver(I) acetate (**2d**) and 1,3-bis-(4-cyanobenzyl)-4,5-bis-(4-methylphenyl)-imidazole-2-ylidene silver(I) acetate (**2e**).

Two NHC-silver acetate complexes **2a** and **2e** were characterised by single crystal X-ray diffraction. The preliminary *in vitro* antibacterial activity of the NHC–silver complexes **2a-e** was investigated against Gram-positive bacteria *Staphylococcus*

aureus and Gram-negative bacteria *Escherichia coli* using the qualitative Kirby–Bauer disk-diffusion method. The areas of clearance determined for the maximum dose (4.3 μM) range between 1 mm and 7 mm for MSSA and 0 mm and 7 mm for *E. coli*. All of the newly synthesised silver(I) acetate complexes were tested for their cytotoxicity by MTT based *in vitro* tests on the human renal cancer cell line Caki-1 and human breast cancer cell line MCF-7 in order to determine their IC_{50} values.

The NHC-silver complexes **2a-e** were found to have IC_{50} values of 3.0 (± 0.6), 0.51 (± 0.07), 4.2 (± 1.2), 9.0 (± 0.6), 26 (± 2) μM, against the renal cancer cell-line Caki-1 and IC_{50} values of 2.3 (± 0.4), 1.4 (± 0.2), 3.0 (± 0.5), 3.4 (± 1.2) and 14 (± 2) μM against the breast cancer cell line MCF-7, respectively. Compared to our lead compound **SBC3** (1,3-bisbenzyl-4,5-bisphenyl-imidazole-2-ylium silver(I) acetate) (IC_{50} value = 14 (± 1) μM against Caki-1 and 5.8 (± 0.6) μM against MCF-7) these values represent improved cytotoxicity against both cell lines, especially for the silver complexes **2a** and **2b**. These two compounds are not only more active than **SBC3** but also exhibit in the case of **2b** a 7 times higher biological activity than cisplatin (IC_{50} value = 3.3 μM) against Caki-1.

4.3 Introduction

In the treatment of cancer, platinum-based drugs such as cisplatin, oxaliplatin and carboplatin are widely used, but due to several factors resistance against these drugs may develop during treatment. To overcome resistance many groups focus on the design of novel platinum based complexes [1] by using specific carriers, or a change from platinum to other transition metals. Novel carrier ligands must initially meet certain criteria, such as being easily accessible in few steps, substituents can be widely varied and their reactivity in biological medium can be easily fine-tuned. All these criteria are met by *N*-Heterocyclic carbenes (NHCs), which are nowadays not only used in organometallic chemistry and catalysis, but more and more also in the design and synthesis of cytotoxic and antibacterial transition metal complexes. Most commonly used transition metals in the development of new anticancer and antibacterial drugs are platinum, palladium, rhodium, ruthenium, copper, silver and gold [2–15].

Silver salts such as silver nitrate are used for many years as antimicrobial agents and have exhibited low toxicity for humans, but recently an increased number of research groups focuses on the activity of new silver therapeutics as anticancer agents [4, 11]. Youngs and co-workers have reported anticancer activity of NHC-silver complexes derived from 4,5-dichloro-1H-imidazole against the human cancer cell lines OVCAR-3 (ovarian), MB157 (breast), and HeLa (cervical). Activity was even demonstrated *in vivo* for [4,5-dichloro-1,3-dimethylimidazol-2-ylidene] silver(I) acetate against an ovarian cancer xenograft model [10]. The groups of Gautier and Morel reported an *N,N'*-diaryl-substituted carbene of high lipophilicity as suitable ligand for metal complexes. The cytotoxicity of the resulting silver complex was 40-fold (MCF-7 and HL60) to 7-fold (MCF-7R) higher than that of cisplatin [6]. Also Gust *et al.* have recently reported that symmetrically and unsymmetrically substituted NHC-silver(I) halides show promising activity against different cancer cell lines as well as bacteria strains [16], which correlates well with the findings in our group [17–26].

Within this paper we present a new series of symmetrically *p*-benzyl-substituted *N*-Heterocyclic carbene silver acetate complexes derived from 4,5-ditolyl-imidazole, their synthesis, cytotoxicity, and antibacterial studies.

4.4 Experimental Part

4.4.1 General conditions

All silver(I) acetate reactions were carried out under exclusion of light. All solvents used were of analytical grade and were used without further purification. 4,4-Dimethylbenzoin, formamide, benzyl bromide, 4-methylbenzyl bromide, 4-methoxybenzyl chloride, methyl 4-(bromomethyl)benzoate, 4-(bromomethyl) benzonitrile, silver(I) acetate and K_2CO_3 were purchased from Sigma-Aldrich Chemical Company and were used without further purification.

^{1}H NMR spectra were measured on a Varian 300 MHz spectrometer while ^{13}C spectra were measured on a Varian 400 MHz spectrometer. All chemical shifts are reported in ppm and referenced to TMS. IR spectra were recorded on a Perkin-Elmer Paragon 1000 FT-IR spectrometer employing a KBr disc. ESI MS was performed on a quadrupole tandem mass spectrometer (Quattro Micro, Micromass/Water's Corp., USA), using solutions in 100% methanol. MS spectra were obtained in the ES+ (electron spray positive ionisation) mode for all compounds. CHN Analysis was carried out in an Exeter Analytical CE-440 elemental analyzer. Crystal Data was collected using an Agilent Technologies (former Oxford Diffraction) SuperNova diffractometer fitted with an Atlas detector. A suitable crystal of **2a** was grown from a saturated solution of diethyl ether and slow evaporation of the solvent while crystals of **2e** were grown in a saturated dichloromethane solution with slow infusion of pentane. **2a** and **2e** were measured with Mo-K*α* (0.71073 A°) at 100 K. A five-time redundant (**2a**) or a complete (**2e**) dataset was collected, assuming that the Friedel pairs are not equivalent. An analytical absorption correction based on the shape of the crystal was performed [27]. The structure was solved by direct methods using SHELXS-97 [28] and refined by full matrix least-squares on F2 for all data using SHELXL-97 [28]. Hydrogen atoms were added at calculated positions and refined using a riding model. Their isotropic thermal displacement parameters were fixed to 1.2 (1.5 for methyl groups) times the equivalent ones of the parent atom. Anisotropic thermal displacement parameters were used for all non hydrogen atoms. CCDC 897777 (for **2a**) and CCDC 897778 (for **2e**) contain the supplementary crystallographic

data for this paper. These data can be obtained free of charge from the Cambridge Crystallographic Data Centre via http://www.ccdc.cam.ac.uk/cgi-bin/catreq.cgi/.

4.4.2 Synthesis

Synthesis of 4,5-Bis(4-methylphenyl)-1H-imidazole (1)

4,5-Bis(4-methylphenyl)-1H-imidazole was synthesised according to literature [29] to give a yield of 66%. The formation of the product was confirmed by NMR.

Synthesis of 1,3-Bis-benzyl-4,5-bis-(4-methylphenyl)-imidazolium bromide (1a)

4,5-Bis-(4-methylphenyl)-1H-imidazole (248 mg, 1.00 mmol), 2 equivalents of benzyl bromide (0.24 mL, 2.00 mmol) and 1.5 equivalents of K_2CO_3 (207 mg, 1.50 mmol) were dissolved in acetonitrile and stirred for 2 d at room temperature. After filtering off the precipitate and removing the solvent under reduced pressure the obtained sticky white solid was washed with pentane (2 x 20 mL) and diethyl ether (2 x 20 mL) to yield a white powder (280 mg, 0.55 mmol, 55% yield).

^{1}H NMR (δ ppm, DMSO, 400 MHz): 9.57 (s, 1H, NCHN), 7.35 – 7.28 (m, 6H), 7.16 (s, 10H), 7.12 – 7.06 (m, 5H), 5.37 (s, 4H, CH_2), 2.26 (s, 6H, CH_3).

^{13}C NMR (δ ppm, DMSO, 101 MHz): 140.28 (NCHN), 136.82, 134.63, 132.25, 131.10, 129.83, 129.27, 128.93, 128.17, 122.47 (C_{benzyl} + C_{tolyl} + $C_{imidazole}$), 50.82 (CH_2), 21.30 (CH_3).

IR absorptions (KBr, cm^{-1}): 3421 (m), 3031 (s), 2942 (s), 1619 (s), 1558 (s), 1502 (s), 1452 (s), 817 (s).

MS (m/z, QMS-MS/MS): 509.00 [M^+-H].

Micro Analysis Calculated for $C_{31}H_{29}BrN_2$ (509.48): Calcd.: C, 73.08%; H, 5.74%; N, 5.50%; Found: C, 72.37%, H 5.52%, N 5.41%.

Melting point: 203-206°C.

Synthesis of 1,3-Bis-(4-methylbenzyl)-4,5-bis-(4-methylphenyl)-imidazolium bromide (1b)

4,5-Bis-(4-methylphenyl)-1H-imidazole (248 mg, 1.00 mmol), 2 equivalents of 4-methylbenzyl bromide (371 mg, 2.00 mmol) and 1.5 equivalents of K_2CO_3 (207 mg, 1.50 mmol) were dissolved in acetonitrile and stirred for 2 d at room temperature. After filtering off the precipitate and removing the solvent under reduced pressure the obtained sticky white solid was washed with pentane (2 x 20 mL) and diethyl ether (2 x 20 mL) to yield a white powder (200 mg, 0.37 mmol, 37% yield).

^{1}H NMR (δ ppm, $CDCl_3$, 300 MHz): 11.07 (s, 1H, NCHN), 7.14 (d, *J* = 7.7 Hz, 4H), 7.10 – 7.00 (m, 8H), 6.97 (d, *J* = 7.8 Hz, 4H), 5.41 (s, 4H, CH_2), 2.35 (s, 6H, CH_{3tolyl}), 2.30 (s, 6H, $CH_{3benzyl}$).

^{13}C NMR (δ ppm, $CDCl_3$, 101 MHz): 140.60 (NCHN), 138.86, 136.96, 132.01, 130.64, 130.54, 129.73, 129.70, 128.48, 121.86 ($C_{methylbenzyl}$ + C_{tolyl} + $C_{imidazole}$), 50.96 (CH_2), 21.39 (CH_{3tolyl}), 21.16 ($CH_{3benzyl}$).

IR absorptions (KBr, cm^{-1}): 3423 (m), 3010 (s), 2865 (s), 1558 (s), 1515 (s), 1450 (s), 817 (s).

MS (m/z, QMS-MS/MS): 457.64 [M^+-Br].

Micro Analysis Calculated for $C_{33}H_{33}BrN_2$ (537.53): Calcd.: C, 73.74%; H, 6.19%; N, 5.21%; Found: C, 73.44%; H, 6.12%; N, 5.01%.

Melting point: 212-214°C.

Synthesis of 1,3-Bis-(4-methoxybenzyl)-4,5-bis-(4-methylphenyl)-imidazolium chloride (1c)

4,5-Bis-(4-methylphenyl)-1H-imidazole (248 mg, 1.00 mmol), 2 equivalents of 4-methoxybenzyl chloride (0.24 mL, 2.00 mmol) and 1.5 equivalents of K_2CO_3 (207

mg, 1.50 mmol) were dissolved in acetonitrile and refluxed for 3 d. After filtering off the precipitate and removing the solvent under reduced pressure the obtained sticky white solid was washed with pentane (2 x 20 mL) and diethyl ether (2 x 20 mL) to yield a white powder (200 mg, 0.38 mmol, 38% yield).

^{1}H NMR (δ ppm, $CDCl_3$, 300 MHz): 11.57 (s, 1H, NCHN), 7.12 (dd, *J* = 15.7, 8.2 Hz, 8H), 6.95 (d, *J* = 8.1 Hz, 4H), 6.77 (d, *J* = 8.7 Hz, 4H), 5.39 (s, 4H, CH_2), 3.76 (s, 6H, OCH_3), 2.36 (s, 6H, CH_3).

^{13}C NMR (δ ppm, $CDCl_3$, 101 MHz): 159.90 (NCHN), 140.56, 131.69, 130.62, 130.27, 129.74, 128.45, 125.75, 122.00, 114.29, ($C_{methoxybenzyl}$ + C_{tolyl} + $C_{imidazole}$) 55.25 (CH_2), 50.67 (OCH_3), 21.39 (CH_3).

IR absorptions (KBr, cm^{-1}): 3421 (m), 3088-2956 (m), 1613 (s), 1514 (s), 1452 (s), 1250 (s), 1178 (s), 821 (s).

MS (m/z, QMS-MS/MS): 489.49 [M^+-HCl].

Micro Analysis Calculated for $C_{33}H_{33}ClN_2O_2$ (525.08): Calcd.: C, 75.48%; H, 6.33%; N, 5.34%; Found: C, 75.28%; H, 6.22%; N, 5.13%.

Melting point: 196-198°C.

Synthesis of 1,3-Bis-(4-methoxycarbonylbenzyl)-4,5-bis-(4-methylphenyl)-imidazolium bromide (1d)

4,5-Bis-(4-methylphenyl)-1H-imidazole (248 mg, 1.00 mmol), 2 equivalents of 4-methoxycarbonylbenzyl bromide (458 mg, 2.00 mmol) and 1.5 equivalents of K_2CO_3 (207 mg, 1.50 mmol) were dissolved in acetonitrile and stirred for 3 d at room temperature. After filtering off the precipitate and removing the solvent under reduced pressure the obtained sticky white solid was washed with pentane (2 x 20 mL) and diethyl ether (2 x 20 mL) to yield a white powder (100 mg, 0.16 mmol, 16% yield).

^{1}H NMR (δ ppm, DMSO, 400 MHz): 9.57 (s, 1H, NCHN), 7.89 (d, *J* = 8.4 Hz, 4H), 7.25 (d, *J* = 8.1 Hz, 4H), 7.14 (s, 8H), 5.49 (s, 4H, CH_2), 3.83 (s, 6H, CH_3), 2.24 (s, 6H, CH_{3tolyl}).

^{13}C NMR (δ ppm, DMSO, 101 MHz): 166.19 (C=O), 140.37 (NCHN), 139.83, 132.39, 131.04, 129.96, 129.82, 128.92, 128.38, 124.98, 122.26 ($C_{methoxycarbonylbenzyl}$ + C_{phenyl} + $C_{imidazole}$), 52.74 (CH_2), 50.55 (OCH_3), 21.28 (CH_{3tolyl}).

IR absorptions (KBr, cm^{-1}): 3423 (m), 2950 (s), 1722 (s), 1614 (s), 1434 (s), 1280 (s), 821 (s).

MS (m/z, QMS-MS/MS): 545.54 [M^{+}-Br].

Micro Analysis Calculated for $C_{35}H_{33}BrN_2O_4$ (625.55): Calcd.: C, 67.20%; H, 5.32%; N, 4.48%; Found: C, 67.10%; H, 5.20%; N, 4.80%.

Melting point: 207-211°C.

Synthesis of 1,3-Bis-(4-cyanobenzyl)-4,5-bis-(4-methylphenyl)-imidazolium bromide (1e)

4,5-Bis-(4-methylphenyl)-1H-imidazole (248 mg, 1.00 mmol), 2 equivalents of 4-cyanobenzyl bromide (391 mg, 2.00 mmol) and 1.5 equivalents of K_2CO_3 (207 mg, 1.50 mmol) were dissolved in acetonitrile and stirred for 2 d at room temperature. After filtering off the precipitate and removing the solvent under reduced pressure the obtained sticky white solid was washed with pentane (2 x 20 mL) and diethyl ether (2 x 20 mL) to yield a white powder (327 mg, 0.58 mmol, 58% yield).

^{1}H NMR (δ ppm, DMSO, 400 MHz): 9.57 (s, 1H, NCHN), 7.81 (d, *J* = 8.3 Hz, 4H), 7.32 (d, *J* = 8.4 Hz, 4H), 7.13 (s, 8H), 5.50 (s, 4H, CH_2), 2.24 (s, 6H, CH_3).

^{13}C NMR (δ ppm, DMSO, 101 MHz): 140.39 (NCHN), 140.02 (CN), 137.51, 133.06, 132.32, 131.02, 129.82, 129.06, 122.21, 118.86, 111.57 ($C_{cyanobenzyl}$ + C_{tolyl} + $C_{imidazole}$), 50.47 (CH_2), 21.29 (CH_3).

IR absorptions (KBr, cm^{-1}): 3461 (m), 2966 (m), 2227 (s), 1614 (s), 1560 (s), 1448 (s), 821 (s).

MS (m/z, QMS-MS/MS): 479.57 [M^+-HBr].

Micro Analysis Calculated for $C_{33}H_{27}BrN_4$ (559.50): Calcd.: C, 70.84%; H, 4.86%; N, 10.01%; Found: C, 70.56%; H, 4.62%; N, 9.85%.

Melting point: 279-281°C.

Synthesis of 1,3-Bis-benzyl-4,5-bis-(4-methylphenyl)-imidazole-2-ylidene silver(I) acetate (2a)

1,3-Bis-benzyl-4,5-bis-(4-methylphenyl)-imidazolium bromide (1a) (100 mg, 0.19 mmol) and 2.1 equivalents of silver(I) acetate (69 mg, 0.41 mmol) were dissolved in 30 mL of dichloromethane and stirred in darkness at room temperature for 2 d. After filtering off the AgBr by-product, the solvent was reduced to 3 mL and by adding dropwise 10 mL of pentane a white powder precipitated. The solvent was decanted and the white precipitate was washed with pentane (2 x 10 mL) and diethyl ether (3 x 10 mL) to yield a white powder (90 mg, 0.15 mmol, 77% yield).

^{1}H NMR (δ ppm, $CDCl_3$, 300 MHz): 7.25 – 7.20 (m, 6H), 7.02 (d, *J* = 7.9 Hz, 8H), 6.87 (d, *J* = 7.9 Hz, 4H), 5.30 (s, 4H, CH_2), 2.29 (s, 6H, CH_{3tolyl}), 2.07 (s, 3H, $CH_{3acetate}$).

^{13}C NMR (δ ppm, $CDCl_3$, 101 MHz): 198.98 (NCN), 164.32 (C=O), 138.07, 135.40, 129.48, 128.93, 128.23, 127.62, 126.91, 126.34, 124.76, 123.81 (C_{tolyl} + $C_{imidazole}$ + C_{benzyl}), 52.51 (CH_2), 20.27 (CH_{3tolyl}).

IR absorptions (KBr, cm^{-1}): 3480-3416 (m), 2360 (s), 1598 (s), 1440 (s), 1375 (s), 1020 (s), 817 (s).

MS (m/z, QMS-MS/MS): 429.61 [M^+-AgOAc].

Micro Analysis Calculated for $C_{33}H_{32}AgN_2O_2$ (596.49): Calcd.: C, 66.45%; H, 5.41%; N, 4.70%; Found: C, 66.44%; H, 5.39%; N, 4.54%.

Melting point: 143-147°C.

Synthesis of 1,3-Bis-(4-methylbenzyl)-4,5-bis-(4-methylphenyl)-imidazole-2-ylidene silver(I) acetate (2b)

1,3-Bis-(4-methylbenzyl)-4,5-bis-(4-methylphenyl)-imidazolium bromide (1b) (100 mg, 0.19 mmol) and 2 equivalents of silver(I) acetate (65 mg, 0.39 mmol) were dissolved in 30 mL of dichloromethane and stirred in darkness at room temperature for 2 d. After filtering off the AgBr by-product, the solvent was reduced to 3 mL and by adding dropwise 10 mL of pentane a white powder precipitated. The solvent was decanted and the white precipitate was washed with pentane (2 x 10 mL) and diethyl ether (3 x 10 mL) to yield a white powder (90 mg, 0.14 mmol, 78% yield).

^{1}H NMR (δ ppm, $CDCl_3$, 300 MHz): 7.91 (d, *J* = 8.0 Hz, 4H, CH_{benzyl} + CH_{tolyl}), 7.04 (t, *J* = 8.0 Hz, 8H, CH_{benzyl} + CH_{tolyl}), 6.85 (d, *J* = 8.0 Hz, 4H, CH_{benzyl} + CH_{tolyl}), 5.37 (s, 4H, CH_2), 3.90 (s, 6H, $CH_{3benzyl}$), 2.29 (s, 6H,CH_{3tolyl}), 2.06 (s, 1H, $CH_{3actetate}$).

^{13}C NMR (δ ppm, $CDCl_3$, 101 MHz): 177.16 (NCN), 138.97 (C=O), 137.60, 133.47, 132.38, 130.52, 129.53, 129.27, 129.22, 128.26, 127.37, 124.95 (CH_{tolyl} + CH_{benzyl} + $CH_{imidazole}$), 53.19 (CH_2), 21.27 (CH_3), 21.09 (CH_3).

IR absorptions (KBr, cm^{-1}): 3437 (m), 3028 (s), 2921 (s), 1708 (s), 1517 (s), 819 (s).

MS (m/z, QMS-MS/MS): 451.53 [M^+-AgOAc].

Micro Analysis Calculated for $C_{35}H_{36}AgN_2O_2$ (624.54): Calcd.: C, 67.31%; H, 5.81%; N, 4.49%; Found: C, 66.98%; H, 5.53%; N, 4.09%.

Melting point: 126-128ºC.

Synthesis of 1,3-Bis-(4-methoxybenzyl)-4,5-bis-(4-methylphenyl)-imidazole-2-ylidene silver(I) acetate (2c)

1,3-Bis-(4-methoxybenzyl)-4,5-bis-(4-methylphenyl)-imidazolium chloride (1c) (100 mg, 0.18 mmol) and 2.1 equivalents of silver(I) acetate (62 mg, 0.38 mmol) were dissolved in 30 mL of dichloromethane and stirred in darkness at room temperature for 2 d. After filtering off the AgBr by-product, the solvent was reduced to 3 mL and by adding dropwise 10 mL of pentane a white powder precipitated. The solvent was decanted and the white precipitate was washed with pentane (2 x 10 mL) and diethyl ether (3 x 10 mL) to yield a white powder (70 mg, 0.10 mmol, 56% yield).

^{1}H NMR (δ ppm, $CDCl_3$, 300 MHz): 7.05 (d, *J* = 8.0 Hz, 4H), 6.91 (m, 8H), 6.74 (d, *J* = 8.0 Hz, 4H), 5.22 (s, 4H, CH_2), 3.76 (s, 6H, $CH_{3methoxybenzyl}$), 2.31 (s, 6H, CH_{3tolyl}), 2.09 (s, 3H, $CH_{3acetate}$).

^{13}C NMR (δ ppm, $CDCl_3$, 101 MHz): 178.62 (NCN), 159.21 (C=O), 138.99, 132.31, 130.54, 129.23, 128.95, 128.51, 124.98, 123.56, 113.95 ($C_{methoxybenzyl}$ + C_{tolyl} + $C_{imidazole}$), 55.23 (CH_2), 52.98 (OCH_3), 22.81 (CH_{3tolyl}), 21.28 ($CH_{3acetate}$).

IR absorptions (KBr, cm^{-1}): 3398 (m), 3003 (s), 2920 (s), 1576 (s), 1513 (s), 1384 (s), 1252 (s), 820 (s).

MS (m/z, QMS-MS/MS): 489.52 [M^+-AgOAc].

Micro Analysis Calculated for $C_{35}H_{36}AgN_2O_4$ (656.54): Calcd.: C, 64.03%; H, 5.53%; N, 4.27%; Found: C, 63.41%; H, 5.28%; N, 4.03%.

Melting point: 166-168°C.

Synthesis of 1,3-Bis-(4-methoxycarbonylbenzyl)-4,5-bis-(4-methyl-phenyl)-imidazole-2-ylidene silver(I) acetate (2d)

1,3-Bis-(4-methoxycarbonylbenzyl)-4,5-bis-(4-methylphenyl)-imidazolium bromide (1d) (100 mg, 0.16 mmol) and 2 equivalents of silver(I) acetate (56 mg, 0.33 mmol) were dissolved in 30 mL of dichloromethane and stirred in darkness at room temperature for 2 d. After filtering off the AgBr by-product, the solvent was

reduced to 3 mL and by adding dropwise 10 mL of pentane a white powder precipitated. The solvent was decanted and the white precipitate was washed with pentane (2 x 10 mL) and diethyl ether (3 x 10 mL) to yield a white powder (60 mg, 0.08 mmol, 53% yield).

^{1}H NMR (δ ppm, $CDCl_3$, 300 MHz): 7.91 (d, *J* = 8.0 Hz, 4H), 7.04 (t, *J* = 8.3 Hz, 8H), 6.85 (d, *J* = 8.0 Hz, 4H), 5.37 (s, 4H, CH_2), 3.91 (s, 6H, $CH_{3methoxycarbonylbenzyl}$), 2.29 (s, 6H, CH_{3tolyl}), 2.06 (s, 3H, $CH_{3acetate}$).

^{13}C NMR (δ ppm, $CDCl_3$, 101 MHz): 179.13 (NCN), 169.67 (C=O), 166.56 (C=O), 141.15, 139.45, 132.75, 130.34, 129.99, 129.87, 129.40, 127.20, 124.31, 53.29 (CH_2), 52.16 (OCH_3), 22.79 ($CH_{3acetate}$), 21.27 (CH_{3tolyl}).

IR absorptions (KBr, cm^{-1}): 3434 (m), 2950 (w), 1724 (s), 1579 (m), 1434 (m), 819 (s).

MS (m/z, QMS-MS/MS): 547.45 [M^+-AgOAc].

Micro Analysis Calculated for $C_{37}H_{36}AgN_2O_6$ (712.56): Calcd.: C, 62.37%; H, 5.09%; N, 3.93%; Found: C, 61.66%; H, 4.78%; N, 3.72%.

Melting point: 196-198°C.

Synthesis of 1,3-Bis-(4-cyanobenzyl)-4,5-bis-(4-methylphenyl)-imidazole -2-ylidene silver(I) acetate (2e)

1,3-Bis-(4-cyanobenzyl)-4,5-bis-(4-methylphenyl)-imidazolium bromide (1e) (100 mg, 0.18 mmol) and 2.1 equivalents of silver(I) acetate (63 mg, 0.37 mmol) were dissolved in 30 mL of dichloromethane and stirred in darkness at room temperature for 2 d. After filtering off the AgBr by-product, the solvent was reduced to 3 mL and by adding dropwise 10 mL of pentane a white powder precipitated. The solvent was decanted and the white precipitate was washed with pentane (2 x 10 mL) and diethyl ether (3 x 10 mL) to yield a white powder (104 mg, 0.16 mmol, 90% yield).

^{1}H NMR (δ ppm, $CDCl_3$, 300 MHz): 7.53 (d, *J* = 7.9 Hz, 4H), 7.08 (dd, *J* = 11.0, 8.0 Hz, 8H), 6.86 (d, *J* = 7.9 Hz, 4H), 5.37 (s, 4H, CH_2), 2.31 (s, 6H, CH_{3tolyl}), 2.06 (s, 3H, $CH_{3acetate}$).

^{13}C NMR (δ ppm, $CDCl_3$, 101 MHz): 179.13 (NCN), 165.98 (C=O), 141.04 (CN), 139.84, 132.80, 132.53, 130.24, 129.59, 128.12, 123.96, 118.24, 112.20 ($C_{cyanobenzyl}$ + C_{tolyl} + $C_{imidazole}$), 53.15 (CH_2), 22.70 (CH_{3tolyl}), 21.29 ($CH_{3acetate}$).

IR absorptions (KBr, cm^{-1}): 3430 (s), 2925 (w), 2227 (m), 1581 (s), 1506 (m), 1405 (s), 819 (m).

MS (m/z, QMS-MS/MS): 479.44 [M^+-AgOAc].

Micro Analysis Calculated for $C_{35}H_{30}AgN_4O_2$ (646.51): Calcd.: C, 65.02%; H, 4.68%; N, 8.67%; Found: C, 64.82%; H, 4.37%; N, 8.28%.

Melting point: 161-163°C.

4.4.3 Antibacterial studies

The silver(I) acetate complexes were screened in preliminary *in vitro* antibacterial tests against two bacterial strains. The test organisms included *Staphylococcus aureus* (SA) (NCTC 7447) as a Gram-positive bacteria and *Escherichia coli* (*E. coli*) as Gram-negative bacteria.

To assess the biological activity of compounds **2a-e** the qualitative Kirby–Bauer disk-diffusion method was applied [30]. All bacteria were individually cultured from a single colony in sterile LB medium [31] overnight at 37°C in an orbital shaker incubator. All the work carried out was performed under sterile conditions.

For each strain, 70 µL of culture were spread evenly on agar-LB medium. Four 5 mm diameter Whatman paper discs were placed evenly separated on each plate. Two stock solutions (9:1 DMSO:H_2O) of every compound were prepared at 2.2 µM and 4.4 µM to be able to test the effect of different concentrations. Each plate was then tested with 5 µL and 7 µL of 2.2 µM solution and 5 µL and 10 µL for the 4.4 µM solution. The plates were covered and placed in an incubator at 37°C for 24 h. The plates were then removed and the area of clearance, which is defined as the

distance between the edge of the filter paper disc and the beginning of the bacterial growth, was measured for each sample in mm.

4.4.4 Cytotoxicity studies

Preliminary *in vitro* cell tests were performed on the human cancerous renal cell line Caki-1 and human cancerous breast cell line MCF-7 in order to compare the cytotoxicity of the compounds presented in this paper. This cell lines were chosen based on their regular and long-lasting growth behaviour. The cells were obtained from the ATCC (American Tissue Cell Culture Collection) and maintained in Dulbecco's Modified Eagle Medium containing 10% (v/v) FCS (fetal calf serum), 1% (v/v) penicillin streptomycin and 1% (v/v) L-glutamine. Cells were seeded in 96-well plates containing 200 µL microtitre wells at a density of 5,000-cells/200 µL of medium and were incubated at 37°C for 24 h to allow for exponential growth. Then the compounds used for the testing were dissolved in the minimal amount of DMSO (dimethylsulfoxide) possible and diluted with medium to obtain stock solutions of 5 x 10^{-4} M in concentration and less than 0.7% of DMSO. The cells were then treated with varying concentrations of the compounds and incubated for 48 h at 37°C. Then, the solutions were removed from the wells and the cells were washed with PBS (phosphate buffer solution) and fresh medium was added to the wells. Following a recovery period of 24 h incubation at 37°C, individual wells were treated with 200 µL of a solution of MTT (3-(4,5-dimethylthiazol-2-yl)-2,5-diphenyltetrazolium bromide) in medium. The solution consisted of 22 mg of MTT in 40 mL of medium. The cells were incubated for 3 h at 37°C. The medium was then removed and the purple formazan crystals were dissolved in 200 µL DMSO per well. For all tests cells with low passage numbers were used. A Wallac Victor (Multilabel HTS Counter) Plate Reader was used to measure absorbance at 540 nm. Cell viability was expressed as a percentage of the absorbance recorded for control wells. The values used for the dose response curves represent the values obtained from four consistent MTT-based assays for each compound tested.

4.5 Results and Discussion

The synthetic route for symmetrically substituted imidazole starting materials, *N*-Heterocyclic carbenes as ligand precursors and their corresponding silver complexes described in here is given in Scheme 4.1. The initial symmetrically 4,5-diaryl-substituted imidazole starting material was prepared by reacting 2-bis(4-methylphenyl)ethane-1,2-dione with formamide to form 4,5-bis(4-methylphenyl)-1H-imidazole (**1**) according to literature [29], with 60% yield.

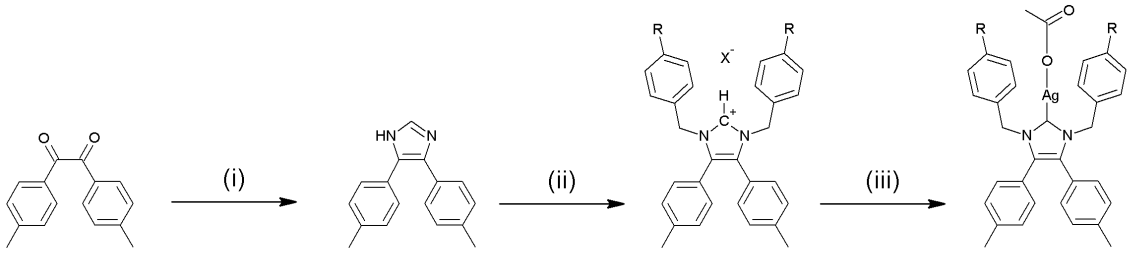

R/X = H / Br	(**1a**)	R =	H	(**2a**)
CH_3 / Br	(**1b**)		CH_3	(**2b**)
OCH_3 / Cl	(**1c**)		OCH_3	(**2c**)
$COOCH_3$ / Br	(**1d**)		$COOCH_3$	(**2d**)
CN / Br	(**1e**)		CN	(**2e**)

Scheme 4.1: General reaction scheme for the synthesis of (i) 4,5-bistolyl-imidazole (1), (ii) 1,3-bis-(*p*-substituted benzyl)-4,5-bistolyl imidazolium halides (**1a-e**) and (iii) 1,3-bis-(*p*-substituted benzyl)-4,5-bistolyl imidazole-2-ylium silver acetates (**2a-e**).

The symmetrically substituted NHC precursors 1,3-bis-benzyl-4,5-bis-(4-methylphenyl)-imidazolium bromide (**1a**), 1,3-bis-(4-methylbenzyl)-4,5-bis-(4-methylphenyl)-imidazolium bromide (**1b**), 1,3-bis-(4-methoxycarbonylbenzyl)-4,5-bis-(4-methylphenyl)-imidazolium bromide (**1d**) and 1,3-bis-(4-cyanobenzyl)-4,5-bis-(4-methylphenyl)-imidazolium bromide (**1e**) were prepared by stirring 4,5-bis(4-methoxylphenyl)-1H-imidazole (**1**) with 2 equivalents of appropriately *p*-substituted benzyl bromide in the presence of K_2CO_3 in acetonitrile at room temperature for 1-5 d with 35, 99, 38 and 50% yields, respectively. The symmetrically substituted NHC precursor 1,3-bis-(4-methoxybenzyl)-4,5-bis-(4-methylphenyl)-imidazolium chloride (**1c**) was synthesised by stirring 4,5-bis(4-methoxylphenyl)-1H-imidazole

(**1**) with 2 equivalents of 4-methoxybenzyl chloride in the presence of K_2CO_3 in acetonitrile at 80ºC temperature for 9 d with 38% yield (ii).

The NHC precursors were characterized by spectral (^1H, ^{13}C NMR, IR and MS) and elemental analysis studies. The ^1H NMR spectra of all NHC precursors **1a**-**e** show a characteristic downfield shift in the range δ = 9.27–11.05 ppm for the NCHN proton attributable to the positive charge of the molecule [32, 33] .In addition, their identities have also been confirmed by a base peak for the [M^+-Br] or [M^+-Cl] fragments in their positive mode ESI mass spectra.

The NHC–silver complexes 1,3-bis-benzyl-4,5-bis-(4-methylphenyl)-imidazole-2-ylidene silver(I) acetate (**2a**), 1,3-bis-(4-methylbenzyl)-4,5-bis-(4-methylphenyl)-imidazole-2-ylidene silver(I) acetate (**2b**), 1,3-bis-(4-methoxybenzyl)-4,5-bis-(4-methylphenyl)-imidazole-2-ylidene silver(I) acetate (**2c**), 1,3-bis-(4-methoxycarbonylbenzyl)-4,5-bis-(4-methylphenyl)-imidazole-2-ylidene silver(I) acetate (**2d**) and 1,3-bis-(4-cyanobenzyl)-4,5-bis-(4-methylphenyl)-imidazole-2-ylidene silver(I) acetate (**2e**) were synthesised by the reaction of **1a**-**e** with 2.1 equivalents of silver acetate in dichloromethane. The reaction mixture was stirred for 1–3 d at room temperature to afford the NHC-silver acetate complexes as off white solid in 77, 78, 56, 53 and 90% yields, respectively.

The complexes were characterised by spectral (^1H, ^{13}C NMR, IR, UV-visible and MS) and elemental analysis studies. Furthermore, the solid state structures of **2a** and **2e** were analysed by single crystal X-ray diffraction. Absence of a downfield NCHN signal in the range between 11.57-9.57 ppm and presence of new signals at 2.09–2.06 ppm for the acetate protons in all ^1H NMR spectra for **2a**-**e** however, indicates a successful complex formation. The ^{13}C NMR resonances of the carbene carbon atoms in complexes **2a**-**e** occur in the range δ = 198.98–178.16 ppm respectively. These signals are shifted downfield compared to the corresponding precursors of **1a**-**e** carbene carbons resonance in the range of 159.90-140.28 ppm respectively, which further demonstrates the formation of the expected NHC-silver acetate complexes. Finally, positive mode ESI mass spectra of all five NHC-silver complexes (**2a**-**e**) are dominated by [M^+–O_2CCH_3] fragment peaks arising from the loss of the acetate ligand.

4.5.1 Structural discussion

Suitable crystals for X-ray crystallography to determine the molecular structure of **2a** were formed from a saturated solution of diethyl ether and slow evaporation of the solvent. **2e** was grown from a saturated solution of chloroform with slow infusion of pentane.

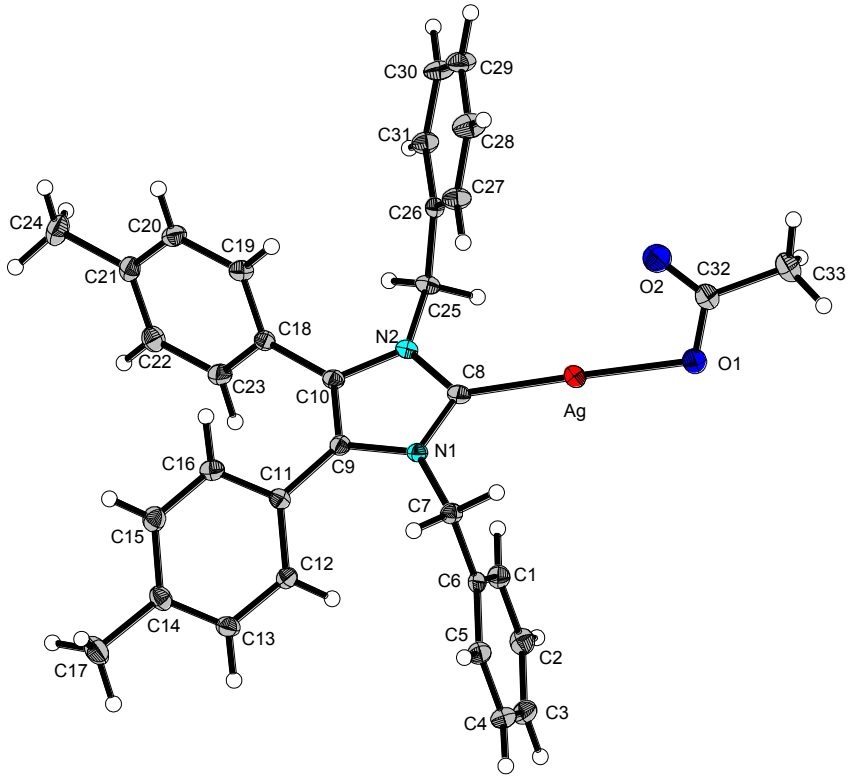

Figure 4.1: X-Ray diffraction structure of **2a**; thermal ellipsoids are drawn on the 50% probability level.

Compound **2a** crystallises in the monoclinic space group P21/c (#14) while **2e** crystallised in the triclinic space group P–1 (#2). Both compounds **2a** and **2e** crystallise with 4 molecules in the unit cell. The molecular structures of the compounds **2a** and **2e** are shown in Figures 4.1-4.3. The crystal data and refinement details for the compounds mentioned above are tabulated in Table 4.1, while selected bond lengths and bond angles are compiled in Tables 4.2 (**2a**) and 4.3 (**2e**). The NHC–silver complexes **2a** and **2e** are mononuclear complexes. In the NHC–silver complex **2a** (Figure 4.1) the bond lengths and bond angles within

the ligand agree with literature data for complexes of related ligands [34–38]. Complex **2e** shows two independent molecules in the unit cell, which are shown in Figures 4.2 and 4.3. Selected bond lengths (Å) and bond angles (°) for both types of species for complex **2e** are shown in Table 4.3.

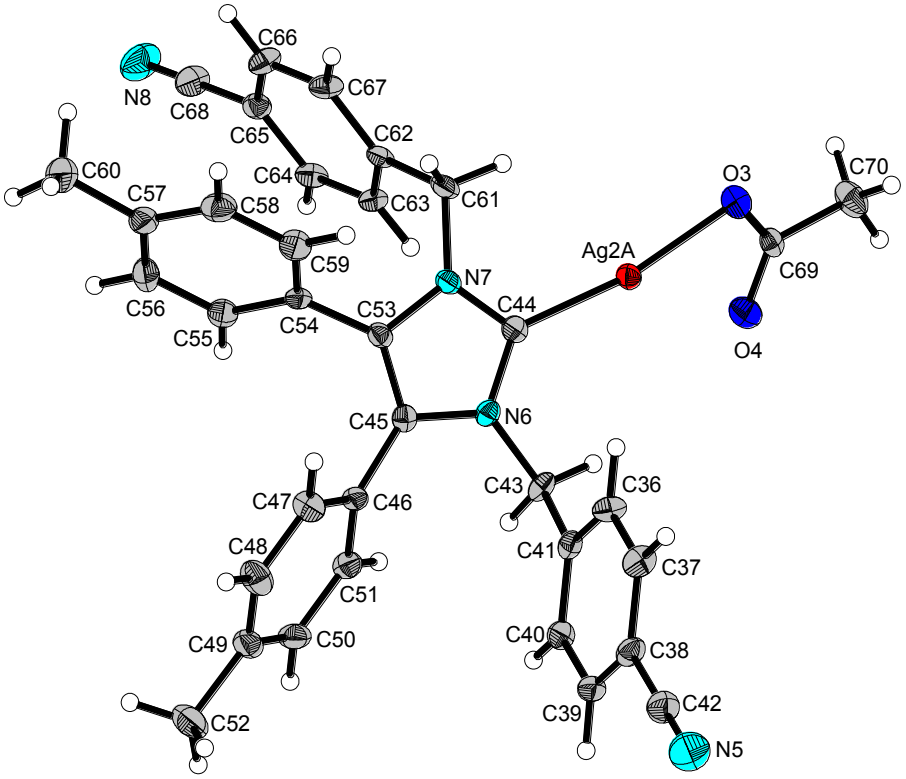

Figure 4.2: X-ray diffraction structure of **2e** showing the major occupied Ag position; thermal ellipsoids are drawn on the 50% probability level.

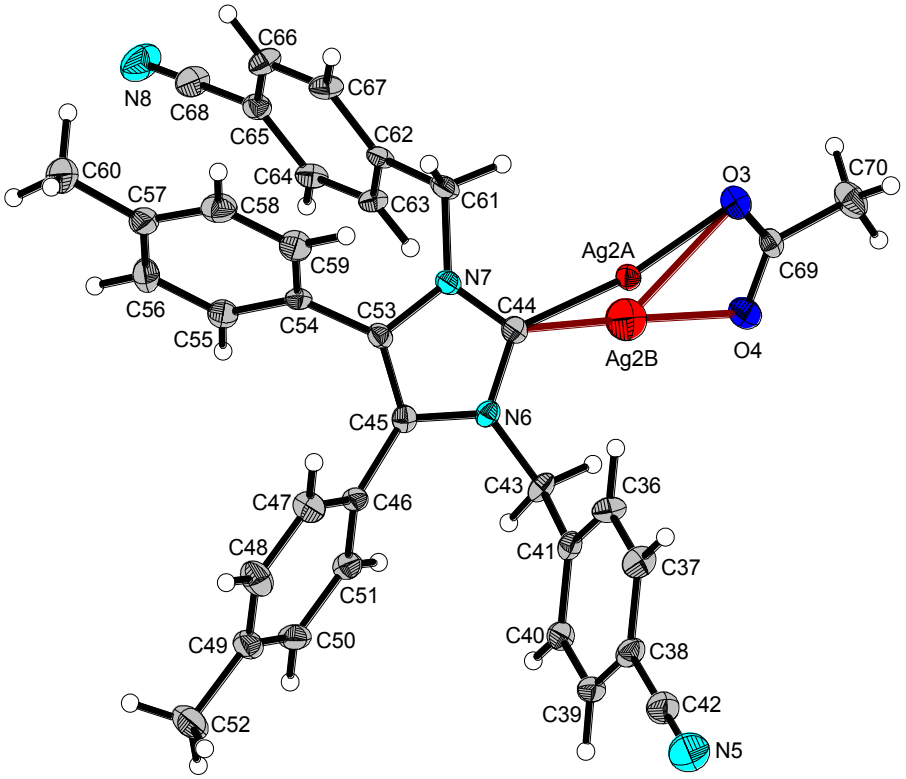

Figure 4.3: X-ray diffraction structure of **2e** showing both Ag positions; thermal ellipsoids are drawn on the 50% probability level, Ag2B with fixed radius.

In **2e** one molecule appears as expected [4, 17, 18, 26], and one is split into a major (95%) and a minor (5%) species. In the major species the Ag-C bond length is 2.049(2) Å, the Ag-O one is 2.110(2) Å and the C-Ag-O angle is 170.37(9)° as seen in Table 4.3. This agrees very well with the first molecule, the geometry in **2a** and previously reported examples of this family of compounds reported by our group [17]. The rather short Ag-O distance together with the monodentate coordination of the acetate to the silver suggests a predominantly covalent character of the Ag(2A)–O(3) bond.

In the minor species of the second molecule (5%, see Figure 4.3) the silver atom binds to both oxygen atoms of the acetate group. The bond lengths to the oxygen atoms are elongated (Ag(2B)–O(4): 2.274(6) Å, and Ag(2B)–O(3): 2.479(6) Å). The bond length to the carbene carbon atom increases as well (Ag(2B)-C(44): 2.202(6) Å; Table 4.3). This bonding pattern is characteristic for a predominantly ionic coordination of the acetate to the silver. Both of these modes have been observed earlier [17, 26] suggesting a rather small energy difference between the major and minor form.

Table 4.1: Crystal data and structure refinement for complexes **2a** and **2e**

		2a	**2e**
Empirical formula		$C_{33}H_{32}N_2O_2Ag$	$C_{35}H_{29}N_4O_2Ag$
Formula weight [g/mol]		595.47	645.49
Crystal system		Monoclinic	Triclinic
Space Group		$P2_1/c$ (#14)	P–1 (#2)
Unit cell dimensions [Å]	a	12.1787(1)	7.8609(1)
	b	8.77455(7)	16.5810(3)
	c	25.4346	23.7243(4)
	α		89.668(2)°
	β	98.4644(8)°	89.978(1)°
	γ		89.995(1)°
Volume [$Å^3$]		2688.40(4)	3092.21(9)
Z		4	4
Density [mg/m^3] (calc.)		1.471	1.387
Absorption coefficient [mm^{-1}]		0.783	0.689
F(000)		1224	1320
Crystal size [mm^3]		0.2205 x 0.1377 x 0.0790	0.2042 x 0.1250 x 0.0356
Theta range for data collection		2.83 to 29.36°	2.99 to 26.41°.
Index ranges		–16<=h<=16	–9<=h<=9
		–11<=k<=12	–20<=k<=20
		–34<=l<=34	–29<=l<=29
Reflections collected		58286	52284
Independent reflections		7058 [R(int) = 0.0314]	12634 [R(int) = 0.0427]
Completeness to θ_{max}		95.6 %	99.6%
Max. and min transmission		0.949 and 0.891	0.976 and 0.905
Data/restraints/parameters		7058 / 0 / 346	12634 / 0 / 769
Goodness-of-fit in F^2		1.094	1.063
Final R indices (I>2σ(I))		R1 = 0.0264	R1 = 0.0254
		wR2 = 0.0645	wR2 = 0.0542
R Indices (all data)		R1 = 0.0318	R1 = 0.0294
		wR2 = 0.0676	wR2 = 0.0561
Largest diff. peak and hole		0.516 and –0.472 $e.Å^{-3}$	0.596 and –0.501 $e.Å^{-3}$

Table 4.2: Selected bond lengths (Å) and bond angles (º) for complexes **2a** and **2e**

2a	**Bond length [Å]**	**2e**	**Bond length [Å]**
Ag–C(8)	2.0548(17)	Ag(1)–C(9)	2.057(2)
Ag–O(1)	2.1100(13)	Ag(1)–O(1)	2.1101(16)
N(1)-C(8)	1.354(2)	N(2)–C(9)	1.356(3)
N(1)–C(9)	1.397(2)	N(2)-C(10)	1.396(3)
C(8)-N(2)	1.355(2)	C(9)-N(3)	1.348(3)
C(10)–N(2)	1.392(2)	C(10)-C(18)	1.365(3)
C(9)–C(10)	1.363(2)	C(18)-N(3)	1.391(3)
		C(9)–Ag(1)–O(1)	176.66(9)
		N(3)–C(9)–N(2)	104.6(2)
		N(2)–C(9)–Ag(1)	127.33(17)
2a	**Bond angle [º]**	**2e**	**Bond angle [º]**
C(8)–Ag–O(1)	178.18(6)	C(9)–Ag(1)–O(1)	176.66(9)
N(1)–C(8)–N(2)	104.76(14)	N(3)–C(9)–N(2)	104.6(2)
N(1)–C(8)–Ag	128.30(12)	N(2)–C(9)–Ag(1)	127.33(17)
N(2)–C(8)–Ag	126.93(12)	N(3)–C(9)–Ag(1)	128.00(18)
C(10)–C(9)–N(1)	106.01(14)	C(18)–C(10)–N(2)	105.8(2)
C(9)–C(10)–N(2)	106.59(14)	C(10)–C(18)–N(3)	106.5(2)
C(8)–N(2)–C(10)	111.24(14)	C(9)–N(2)–C(10)	111.50(19)
C(32)–O(1)–Ag	107.35(11)		
O(2)–C(32)–O(1)	124.14(17)	C(34)–O(1)–Ag(1)	107.87(15)
O(2)–C(32)–C(33)	120.71(17)	O(2)–C(34)–O(1)	124.8(2)
O(1)–C(32)–C(33)	115.12(16)	O(2)–C(34)–C(35)	119.0(2)
		O(1)–C(34)–C(35)	116.2(2)

Table 4.3: Selected bond lengths (Å) and bond angles (º) for both types of species of complex **2e**.

2e (95% species)	**Bond length [Å]**	**2e (5% species)**	**Bond length [Å]**
Ag(2A)-C(44)	2.049(2)	Ag(2B)-C(44)	2.202(6)
Ag(2A)-O(3)	2.1103(17)	Ag(2B)-O(4)	2.274(6)
		Ag(2B)-O(3)	2.479(6)
N(6)-C(44)	1.361(3)	N(6)-C(44)	1.361(3)
N(6)-C(45)	1.402(3)	N(6)-C(45)	1.402(3)
C(44)-N(7)	1.346(3)	C(44)-N(7)	1.346(3)
C(45)-C(53)	1.357(4)	C(45)-C(53)	1.357(4)
C(53)-N(7)	1.397(3)	C(53)-N(7)	1.397(3)
2e (95% species)	**Bond angle [º]**	**2e (5% species)**	**Bond angle [º]**
C(44)-Ag(2A)-O(3)	170.37(9)	C(44)-Ag(2B)-O(4)	177.3(3)
		C(44)-Ag(2B)-O(3)	124.5(3)
		O(4)-Ag(2B)-O(3)	55.66(13)
N(7)-C(44)-N(6)	104.5(2)	N(7)-C(44)-N(6)	104.5(2)
N(6)-C(44)-Ag(2A)	131.33(19)	N(6)-C(44)-Ag(2B)	110.5(2)
N(7)-C(44)-Ag(2A)	124.14(18)	N(7)-C(44)-Ag(2B)	141.3(2)
C(44)-N(6)-C(45)	111.3(2)	C(44)-N(6)-C(45)	111.3(2)
C(53)-C(45)-N(6)	106.0(2)	C(53)-C(45)-N(6)	106.0(2)
C(44)-N(7)-C(53)	111.7(2)	C(44)-N(7)-C(53)	111.7(2)
C(45)-C(53)-N(7)	106.6(2)	C(45)-C(53)-N(7)	106.6(2)
C(69)-O(3)-Ag(2A)	107.00(15)	C(69)-O(3)-Ag(2B)	84.9(2)
		C(69)-O(4)-Ag(2B)	94.8(2)
O(4)-C(69)-O(3)	124.5(2)	O(4)-C(69)-O(3)	124.5(2)
O(4)-C(69)-C(70)	120.0(2)	O(4)-C(69)-C(70)	120.0(2)
O(3)-C(69)-C(70)	115.5(2)	O(3)-C(69)-C(70)	115.5(2)

4.5.2 Biological evaluation

In previous studies, we already synthesised and biologically evaluated symmetrically substituted 1,3-bis-(*p*-substituted-benzyl)-4,5-diarylimidazole silver acetates ([17,21]). From these studies, the earliest reported complex **SBC3** (1,3-bisbenzyl-4,5-bisphenyl-imidazole-2-ylium silver acetate) [21] worked as a lead compound for further substituent optimisation to enhance antibacterial and cytotoxic activity.

4.5.2.1 Cytotoxicity Studies

The log dose response curves for complexes **2a-e** against the human renal cancer cell line Caki-1 and the human breast cancer cell line MCF-7 are shown in Figures 4.4 and 4.5 respectively. All NHC-silver acetate complexes exhibit unique IC_{50} values against both cell lines which indicates that the cytotoxic activity of the compounds is directly influenced by the different *p*-substituents (-H, $-CH_3$, $-OCH_3$, $COOCH_3$, -CN) on the benzyl rings.

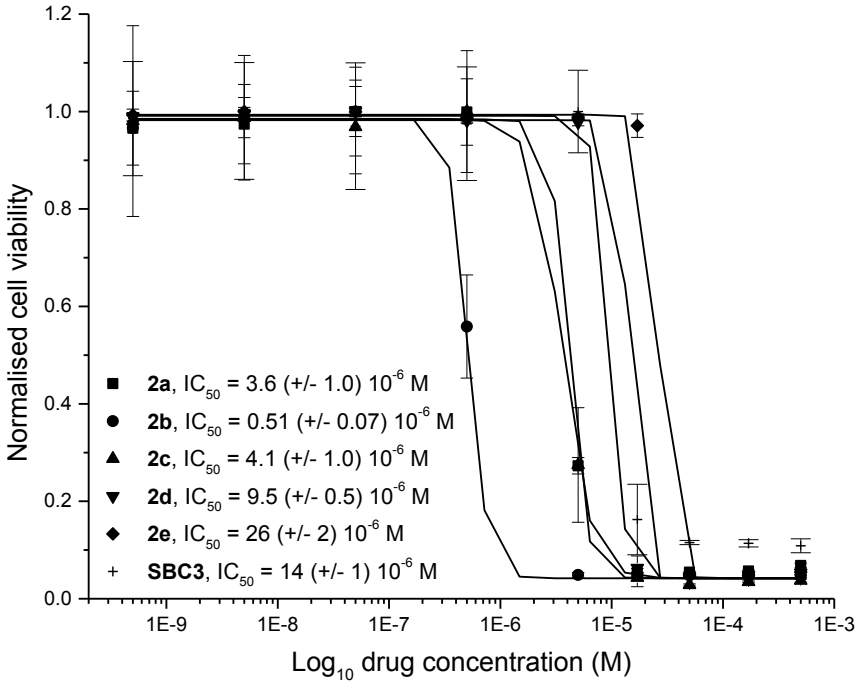

Figure 4.4: Cytotoxicity curves from typical MTT assays showing the effect of compounds **2a-e** on the viability of Caki-1 cells.

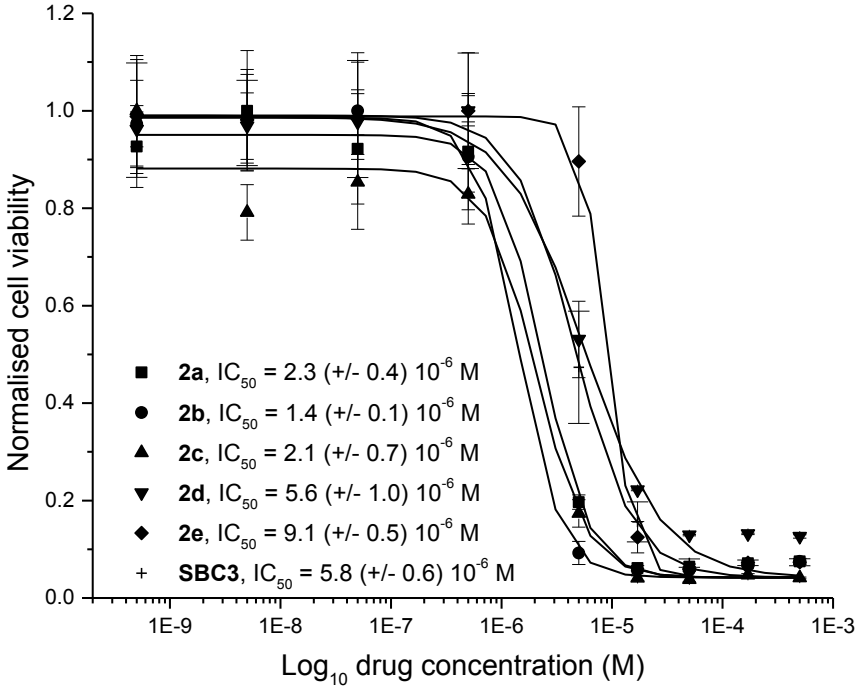

Figure 4.5: Cytotoxicity curves from typical MTT assays showing the effect of compounds **2a-e** on the viability of MCF-7 cells.

The highest activity is observed for compound **2b** with an IC_{50} value of 0.51 (± 0.07) µM against Caki-1 and an IC_{50} = 1.4 (± 0.1) µM against MCF-7. Compared to our previously reported NHC-silver(I) acetate complexes [17] and especially compared to our lead compound **SBC3** (IC_{50} = 14 (± 1) µM against Caki-1 and IC_{50} = 5.8 (± 0.6) µM against MCF-7), complex **2b** exhibits a remarkable increase in cytotoxic activity. By removing the CH_3 groups in the *para* position on the benzyl rings, the cytotoxic activity drops by a factor of 6 (**2a**, IC_{50} = 3.0 (± 0.6) µM) and replacing it with other groups leads to a decrease in activity of up to 50-fold (**2e**, IC_{50} = 26 (± 2) µM). Additionally the IC_{50} value of the NHC precursor **1b** against Caki-1 was determined to evaluate the effect of silver acetate on the activity of the compound. With an IC_{50} = 4.8 (± 0.3) µM **1b** shows a high cytotoxic potential by itself, but in combination with silver acetate, forming the NHC silver(I) complex **2b** the synergistic effect of both parts leads to a superior activity against this particular cell line.

4.5.2.2 Antibacterial testing

Using the Kirby-Bauer disk diffusion method, the antibacterial activity of the NHC-silver acetate complexes was tested and summarised in Figures 4.6 and 4.7.

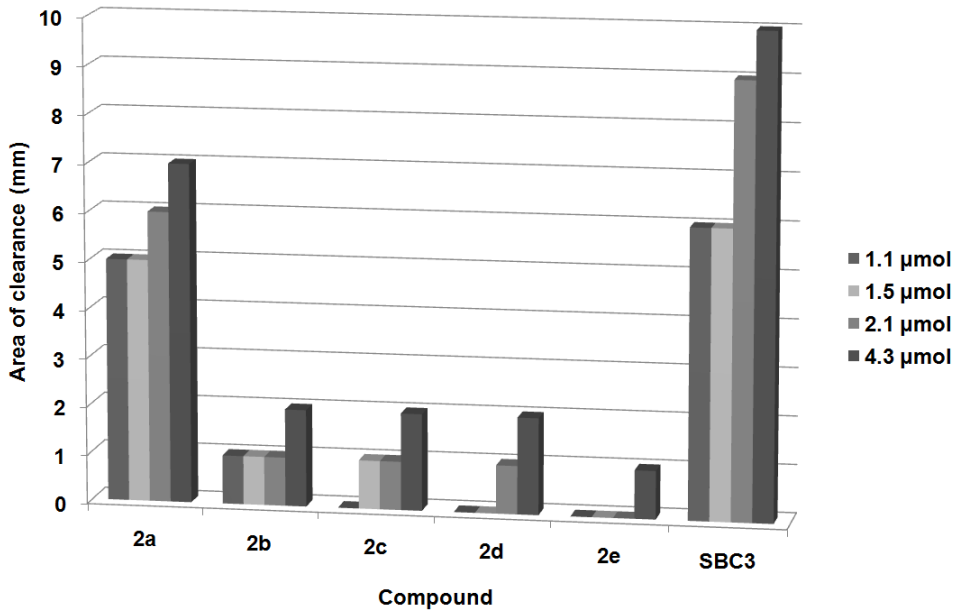

Figure 4.6: Area of clearance on *Escherichia coli* (Gram -ve) by **2a-e**

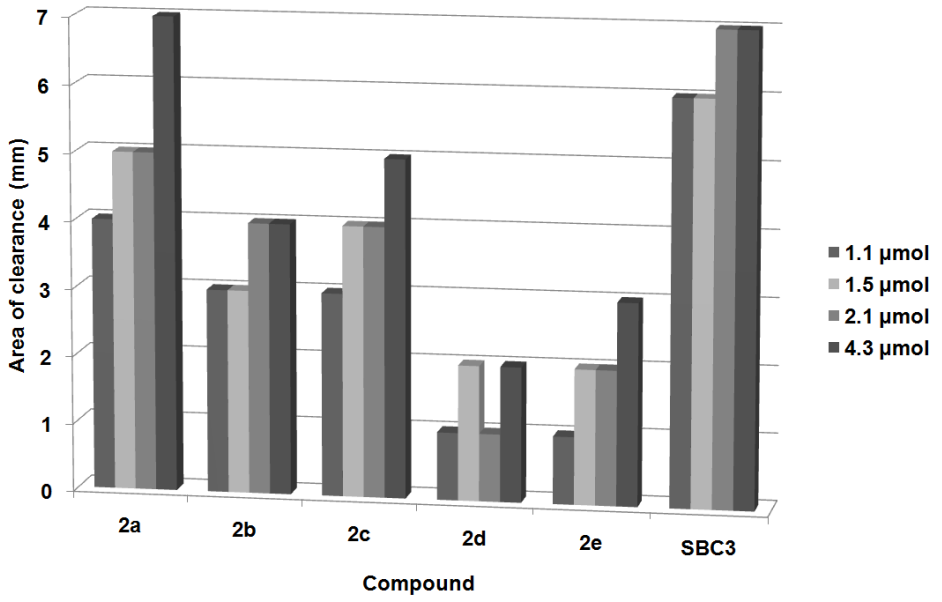

Figure 4.7: Area of clearance on *Staphylococcus aureus* (Gram +ve) by **2a-e**.

The metal salt (silver(I) acetate) used to prepare the complexes and the solvent (DMSO) used to prepare the stock solutions played no role in growth inhibition on the same bacteria as previously reported [23,26].An area of clearance of 0 mm was considered as no activity, areas of 1-3 mm as low, 4-7 mm as medium, and areas of clearance ≥ 8 mm as high activity.

The primary aim was to synthesise a derivative of **SBC3**, that would exhibit better antimicrobial properties than this leading compound against Gram-positive *Staphylococcus aureus* (**SBC3**, Area of clearance = 7 mm) and Gram-negative *Escherichia coli* (**SBC3**, Area of clearance = 10 mm) bacteria strains. Almost no antibacterial activity was observed for compounds **2b**, **2d** and **2e** against both bacteria strains. Medium antibacterial activity was observed for compound **2c** against Gram-positive *Staphylococcus aureus* (Area of clearance = 5 mm) but no antibacterial activity was observed against Gram-negative bacteria *Escherichia coli*. The best antibacterial activity was observed for the compound **2a** against both bacteria strains with an area of clearance of 7 mm (Fig. 4.6 and 4.7). Therefore no improvement in antibacterial activity for the herein presented compounds **2a-e** over **SBC3** was observed.

4.6 Conclusion and Outlook

Five new symmetrically substituted *N*-Heterocyclic carbene–silver (I) acetate complexes (**2a**-**e**) were synthesised by the reaction of symmetrically substituted *N*-Heterocyclic carbenes (**1a**-**e**) with silver(I) acetate. Some of the complexes have shown medium to high antibacterial activity, especially against the Gram-positive bacteria strain *Staphylococcus aureus*, but no improvement in comparison to our lead compound **SBC3** was observed. In contrast to this, the antitumor activity has been greatly enhanced and the NHC-silver complexes **2a**-**e** yielded IC_{50} values of 3.0 (± 0.6), 0.51 (± 0.07), 4.2 (± 1.2), 9.0 (± 0.6), 26 (± 2) μM against the Caki-1 renal cancer cell-line (**SBC3** IC_{50} = 14 (± 1) μM). At the same time these NHC–silver complexes were found to have IC_{50} values against the human breast cancer cell line MCF-7 of 2.3 (± 0.4), 1.4 (± 0.2), 3.0 (± 0.5), 3.4 (± 1.2), 14 (± 2) μM, respectively (**SBC3** IC_{50} = 5.8 (± 0.6) μM).

One of the compounds presented in this paper, 1,3-bis-(4-methylbenzyl)-4,5-bis-(4-methylphenyl)-imidazole-2-ylidene silver(I) acetate (**2b**) shows the highest cytotoxic activity [IC_{50} = 0.51 (± 0.07) μM] compared to all *N*-Heterocyclic carbene–silver complexes synthesised by our research group (see [17-22, 24-26]). Here, the activity of an already cytotoxic imidazolium is strongly enhanced by deprotonation and coordination to silver acetate resulting in a water-soluble and neutral drug molecule. This indicates its high potential as an anticancer drug and gives a good insight into possible further substitution patterns.

Acknowledgement

This project was funded by the UCD School of Chemistry and Chemical Biology.

4.7 References

[1] I. Ott, R. Gust, Anticancer Agents Med Chem 7 (2007) 95–110.
[2] G. Gasser, I. Ott, N. Metzler-Nolte, J. Med. Chem. 54 (2011) 3–25.
[3] K.M. Hindi, M.J. Panzner, C.A. Tessier, C.L. Cannon, W.J. Youngs, Chem. Rev. 109 (2009) 3859–3884.
[4] K.M. Hindi, T.J. Siliciano, S. Dumus, M.J. Panzner, D.A. Medvetz, D.V. Reddy, L.A. Hogue, C.E. Hovis, J.K. Hillard, R.J. Mallet, C.A. Tessier, C.L. Cannon, W.J. Youngs, J. Med. Chem. 51 (2008) 1577–1583.
[5] R. Rubbiani, I. Kitanovic, H. Alborzinia, S. Can, A. Kitanovic, L.A. Onambele, M. Stefanopoulou, Y. Geldmacher, W.S. Sheldrick, G. Wolber, A. Prokop, S. Wölfl, I. Ott, J. Med. Chem. 53 (2010) 8608–8618.
[6] M.-L. Teyssot, A.-S. Jarrousse, M. Manin, A. Chevry, S. Roche, F. Norre, C. Beaudoin, L. Morel, D. Boyer, R. Mahiou, A. Gautier, Dalton Trans. (2009) 6894–6902.
[7] M. Skander, P. Retailleau, B. Bourrié, L. Schio, P. Mailliet, A. Marinetti, J. Med. Chem. 53 (2010) 2146–2154.
[8] J.C.Y. Lin, R.T.W. Huang, C.S. Lee, A. Bhattacharyya, W.S. Hwang, I.J.B. Lin, Chem. Rev. 109 (2009) 3561–3598.
[9] J.C. Garrison, W.J. Youngs, Chem. Rev. 105 (2005) 3978–4008.
[10] D.A. Medvetz, K.M. Hindi, M.J. Panzner, A.J. Ditto, Y.H. Yun, W.J. Youngs, Met Based Drugs (2008) 384010–384016.
[11] A. Melaiye, R.S. Simons, A. Milsted, F. Pingitore, C. Wesdemiotis, C.A. Tessier, W.J. Youngs, J. Med. Chem. 47 (2004) 973–977.
[12] M.-L. Teyssot, A.-S. Jarrousse, A. Chevry, A. De Haze, C. Beaudoin, M. Manin, S.P. Nolan, S. Díez-González, L. Morel, A. Gautier, Chem. Eur. J. 15 (2009) 314–318.
[13] A. Kascatan-Nebioglu, A. Melaiye, K.M. Hindi, S. Durmus, M.J. Panzner, L.A. Hogue, R.J. Mallett, C.E. Hovis, M. Coughenour, S.D. Crosby, A. Milsted, D.L. Ely, C.A. Tessier, C.L. Cannon, W.J. Youngs, J. Med. Chem. 49 (2006) 6811–6818.
[14] L. Kaps, B. Biersack, H. Müller-Bunz, K. Mahal, J. Münzner, M. Tacke, T. Mueller, R. Schobert, J. Inorg. Biochem. 106 (2012) 52–58.
[15] S. Ray, R. Mohan, J.K. Singh, M.K. Samantaray, M.M. Shaikh, D. Panda, P. Ghosh, J. Am. Chem. Soc. 129 (2007) 15042–15053.
[16] W. Liu, K. Bensdorf, A. Hagenbach, U. Abram, B. Niu, A. Mariappan, R. Gust, Eur. J. Med. Chem. 46 (2011) 5927–5934.
[17] F. Hackenberg, G. Lally, H. Müller-Bunz, F. Paradisi, D. Quaglia, W. Streciwilk, M. Tacke, J. Organomet. Chem. (2012).
[18] F. Hackenberg, A. Deally, G. Lally, S. Malenke, H. Müller-Bunz, F. Paradisi, S. Patil, D. Quaglia, M. Tacke, Int. J. Inorg. Chem. 2012 (2012).
[19] S. Patil, M. Tacke, Insights into Coordination, Bioinorganic and Applied Inorganic Chemistry (2011) 555–566.
[20] S. Patil, A. Deally, F. Hackenberg, L. Kaps, H. Müller-Bunz, R. Schobert, M. Tacke, Helv. Chim. Acta 94 (2011) 1551–1562.
[21] S. Patil, A. Deally, B. Gleeson, H. Müller-Bunz, F. Paradisi, M. Tacke, Metallomics 3 (2011) 74–88.
[22] S. Patil, A. Deally, B. Gleeson, F. Hackenberg, H. Müller-Bunz, F. Paradisi, M. Tacke, Z. Allg. Anorg. Chem. 637 (2011) 386–396.

[23] B. Gleeson, J. Claffey, D. Ertler, M. Hogan, H. Müller-Bunz, F. Paradisi, D. Wallis, M. Tacke, Polyhedron 27 (2008) 3619–3624.
[24] S. Patil, K. Dietrich, A. Deally, B. Gleeson, H. Müller-Bunz, F. Paradisi, M. Tacke, Appl. Organomet. Chem. 24 (2010) 781–793.
[25] S. Patil, K. Dietrich, A. Deally, B. Gleeson, H. Müller-Bunz, F. Paradisi, M. Tacke, Helv. Chim. Acta 93 (2010) 2347–2364.
[26] S. Patil, J. Claffey, A. Deally, B. Gleeson, M. Hogan, L.M. Menéndez Méndez, H. Müller-Bunz, F. Paradisi, M. Tacke, Eur. J. Inorg. Chem. 2010 (2010) 1020–1031.
[27] CrysalisPro Version 1.171.34.49, Agilent Technologies, 2011.
[28] G.M. Sheldrick, Acta Crystallogr. A64 (2008) 112–122.
[29] H. Bredereck, R. Gompper, D. Hayer, Chem. Ber. 92 (1959) 338–343.
[30] A. Bondi, H.E. Spaulding, E.D. Smith, C.C. Dietz, Am. J. Med. Sci. 213 (1947) 221–225.
[31] S.E. Luria, Bacteriol. Rev. 11 (1947) 1–40.
[32] W.A. Herrmann, C. Kocher, Angew. Chem. Int. Ed. 36 (1997) 2162–2187.
[33] J.C. Garrison, C.A. Tessier, W.J. Youngs, J. Organomet. Chem. 690 (2005) 6008–6020.
[34] M. Viciano, E. Mas-Marzá, M. Sanaú, E. Peris, Organometallics 25 (2006) 3063–3069.
[35] C.P. Newman, G.J. Clarkson, J.P. Rourke, J. Organomet. Chem. 692 (2007) 4962–4968.
[36] V. Lillo, J. Mata, J. Ramírez, E. Peris, E. Fernandez, Organometallics 25 (2006) 5829–5831.
[37] Y. Han, Y.-T. Hong, H.V. Huynh, J. Organomet. Chem. 693 (2008) 3159–3165.
[38] P. de Frémont, N.M. Scott, E.D. Stevens, T. Ramnial, O.C. Lightbody, C.L.B. Macdonald, J.A.C. Clyburne, C.D. Abernethy, S.P. Nolan, Organometallics 24 (2005) 6301–6309.

Chapter 5 Ru(II)- and Au(I)-NHC complexes

Work published as:

Novel Ruthenium(II) and Gold(I) NHC complexes: Synthesis, characterisation and evaluation of their anticancer properties, Frauke Hackenberg, Helge Müller-Bunz, Raymond Smith, Wojciech Streciwilk, Xiangming Zhu, Matthias Tacke, Organometallics, 2013, DOI: 10.1021/om400819p

Novel Ruthenium(II) and Gold(I) NHC complexes: Synthesis, characterisation and evaluation of their anticancer properties

Frauke Hackenberg, Helge Müller-Bunz, Raymond Smith, Wojciech Streciwilk, Xiangming Zhu, Matthias Tacke

UCD School of Chemistry and Chemical Biology
University College Dublin, Belfield, Dublin 4, Ireland

For Table of Contents only

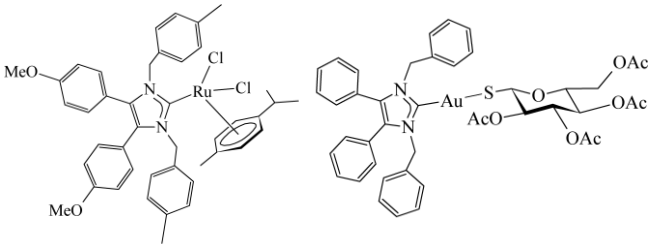

5 **13**

5.1 Abstract

The synthesis, characterisation as well as the biological evaluation of novel Ru(II)-and Au(I)-*N*-heterocyclic carbenes is reported. The NHC-ruthenium(II) complexes (**1-6**) were synthesized by reacting the appropriately substituted imidazolium bromides with Ag_2O, forming the NHC-silver bromide *in situ* followed by transmetallation with dimeric *p*-cymene ruthenium(II) dichloride. In an analogous manner the NHC-gold(I) chloride complexes (NHC-Au(I)Cl) **7-9** were synthesized, utilizing dimethylsulfido gold(I) chloride as the transmetallating agent.

The ligand exchange on the NHC-gold(I) chlorides was achieved by either reacting the complexes with silver acetate to yield the NHC-gold(I) acetates (NHC-Au(I)OAc) **10-12**, or by reacting the NHC-gold(I) chlorides under basic conditions with 2',3',4',6'-tetra-*O*-acetyl-1-thio-β-D-glucopyranose (*SR*) to give the NHC-gold(I)-(2',3',4',6'-tetra-*O*-acetyl-β-D-glucopyranosyl-1-thiolate)-complexes (NHC-Au(I)*SR*) **13-15**. The Ru(II)-NHC complex **1** and the Au(I)-NHC complex **9** were characterized by single X-ray diffraction. Also the IC_{50} values of these 15 complexes were determined by an MTT-based assay against the human cancer cell lines Caki-1 (renal) and MCF-7 (breast). The Ru(II) complexes **1-6** revealed the following IC_{50} values against Caki-1 of >500, 94 (± 5), 93 (± 2), 170 (± 20), 39 (± 5) and 13 (± 2) μM, and against MCF-7 of >500, 80 (± 15), 19 (± 1), 7.1 (± 1.2), 2.4 (± 0.7) and 7.0 (± 1.2) μM, respectively. IC_{50} values of 67 (± 7), 16 (± 2), 41 (± 1), 31 (± 2), 42 (± 5), 18 (± 1), 14 (±2), 17 (±2) and 58 (± 2) μM against Caki-1 and 8.4 (± 0.4), 30 (± 3), 12 (± 1), 23 (± 3), 12 (± 1), 25 (± 3), 6.1 (± 1.5), 9.3 (± 1.6) and 14 (± 2) μM against MCF-7 were found for the Au(I) complexes **7-15**.

5.2 Keywords:

NHC; gold; ruthenium; acetate; thioglucopyranose; anticancer drug.

5.3 Introduction

N-Heterocyclic carbenes (NHCs) are easy to prepare and exhibit versatile ligand properties. NHCs can form stronger bonds to metal centres than phosphines; the resulting complexes are more stable towards moisture, air and heat [1], they play important roles in catalysis [2] and biomedical applications [3] as well as other fields like luminescent and functional materials applications [4]. Their metal-complexes are as versatile as their applications, ranging from zinc over rhodium to platinum; the latter of particular interest since the discovery of Cisplatin as an effective anticancer drug. But also other metal-NHCs have been intensively investigated for their biological applications. Silver, known since antique times for its antibacterial properties, is used widely in the synthesis and evaluation of novel potential anticancer and antibacterial agents [5]. Our group has reported imidazolium based silver halide and silver acetate complexes [6–10], leading to the discovery of the highly antibacterial complex SBC3 (1,3-diphenyl-4,5-diphenyl-imidazol-2-ylidene silver(I) acetate), which shows remarkable activity against *E. coli*, *MRSA* and *Pseudomonas aeruginosa* [11]. Furthermore, SBC1 (1-methyl-3-(*p*-cyanobenzyl)-benzimidazol-2-ylidene silver acetate) was found to exhibit strong cytotoxic activity against the human renal cancer cell line Caki-1, leading to further *in vivo* investigation of its possible usefulness as novel anticancer agent [12]. Unfortunately, it was found that SBC1 does not show tumour growth inhibition, which might be overcome in future by binding the complex to a targeted linker or formulation of the complex.

Ruthenium, a transition metal mostly used in NHC-catalysis chemistry also slowly made its way into anticancer applications. Among the Ru(III)-based drugs, two of them, namely, NAMI-A and KP1019 are currently in phase II clinical trials. Recently the synthesis and preliminary biological evaluation of a new NAMI-A analogue, called AziRu has been reported, where a pyridine ligand replaces the imidazole of NAMI-A. This compound is one of the most promising ruthenium complexes in terms of anticancer activity currently known, being more cytotoxic than NAMI-A and showing high *in vitro* antiproliferative activity [13]. Furthermore Grubbs and Hoveyda-Grubbs catalysts have been investigated for possible anticancer activity, but demonstrated overall weak to medium efficiency as tumour

cell proliferation inhibitors. On the other hand benzimidazol-2-ylidene-Ru(II) complexes have been reported to exhibit strong antiproliferative effects when the cellular uptake was efficient [14].

However, the largest contribution to metal-based anticancer drugs is made on the field of gold(I/III) complexes. One of the best studied Au(I)-complexes is Auranofin, a drug used for over 20 years in the treatment of rheumatoid arthritis, which on its own just exhibits moderate antitumour activity. But since the development of Auranofin many other Au(I) and Au(III) complexes with different ligands (mostly phosphine or NHC) have been investigated. For example, Ott *et al.* reported the synthesis and biological evaluation of a series of benzimidazol-2-ylidene-gold(I) complexes and found strong antiproliferative effects against MCF-7, HT-29 (cancerous) and HEK-293 (non-cancerous) cells as well as TrxR inhibition for the NHC-Au-PPh_3 complexes [15]. Demir *et al.* studied the reproductive toxicity [16] and the oxidative damage of Au(I)-NHC complexes on heart tissue of rats [17], while Gust *et al.* investigated the influence of counter ion exchange and oxidation states of the metal (Au(I) vs. Au(III)) on the *in vitro* behaviour of [1,3-diethyl-4,5-diarylimidazol-2-ylidene] gold(I/III) complexes [18].

In this paper we present a series of 6 new Ru(II)-NHC complexes as well as 9 novel Au(I)-NHC complexes, their synthesis and *in vitro* biological evaluation against the human cancer cell lines Caki-1 (renal) and MCF-7 (breast).

5.4 Results and discussion

In Scheme 5.1 the synthetic route for the unsymmetrically and symmetrically substituted *N*-heterocyclic carbene (*p*-cymene)ruthenium(II) dichloride complexes is given. The initial precursors were synthesized and characterized following procedures published earlier by our group [8–10,19]. (1-Methyl-3-(*p*-cyanobenzyl)-benzimidazol-2-ylidene)(η^6-*p*-cymene) ruthenium(II) dichloride (**1**), an analogue of the well studied NHC-silver acetate SBC1 [8,12] was obtained in 37.5% yield, while the complexes (1,3-Dibenzyl-4,5-diphenyl-imidazol-2-ylidene)(η^6-*p*-cymene)-ruthenium(II) dichloride (**2**), (1,3-Di(*p*-methylbenzyl)-4,5-di(*p*-methylphenyl)-imidazol-2-ylidene)(η^6-*p*-cymene)-ruthenium(II) dichloride (**3**), (1,3-Di(*p*-methylbenzyl)-4,5-di(*p*-isopropylphenyl)-imidazol-2-ylidene)(η^6-*p*-cymene)-ruthenium(II) dichloride (**4**), (1,3-Di(*p*-methylbenzyl)-4,5-di(*p*-methoxyphenyl)-imidazol-2-ylidene](η^6-*p*-cymene)-ruthenium(II) dichloride (**5**) and (1,3-Di(*p*-methoxybenzyl)-4,5-di(*p*-isopropylphenyl)-imidazol-2-ylidene)(η^6-*p*-cymene)-ruthenium(II) dichloride (**6**) gave moderate to good yields of 76.0, 51.5, 40.2, 64.5 and 68.6% respectively. All complexes were synthesized following the carbene transfer route, more precisely transmetallation of the *in situ* generated NHC-silver(I) bromide complexes with dichloro-(*p*-cymene)-ruthenium(II) dimer after initial metallation of the NHC-bromide precursors with Ag_2O at rt in darkness. This procedure is probably one of the most general methods, because it generates an air stable intermediate under mild reaction-conditions, thus allowing an easy access to a wide range of transition metal complexes. It is often used successfully when other methods fail [20]. The use of Ag–NHC complexes as carbene transfer reagents provides in many cases a convenient way to overcome the difficulties arising from using strong bases, inert atmospheres, and complicated workups. This method was used for the preparation of complexes **1-9**.

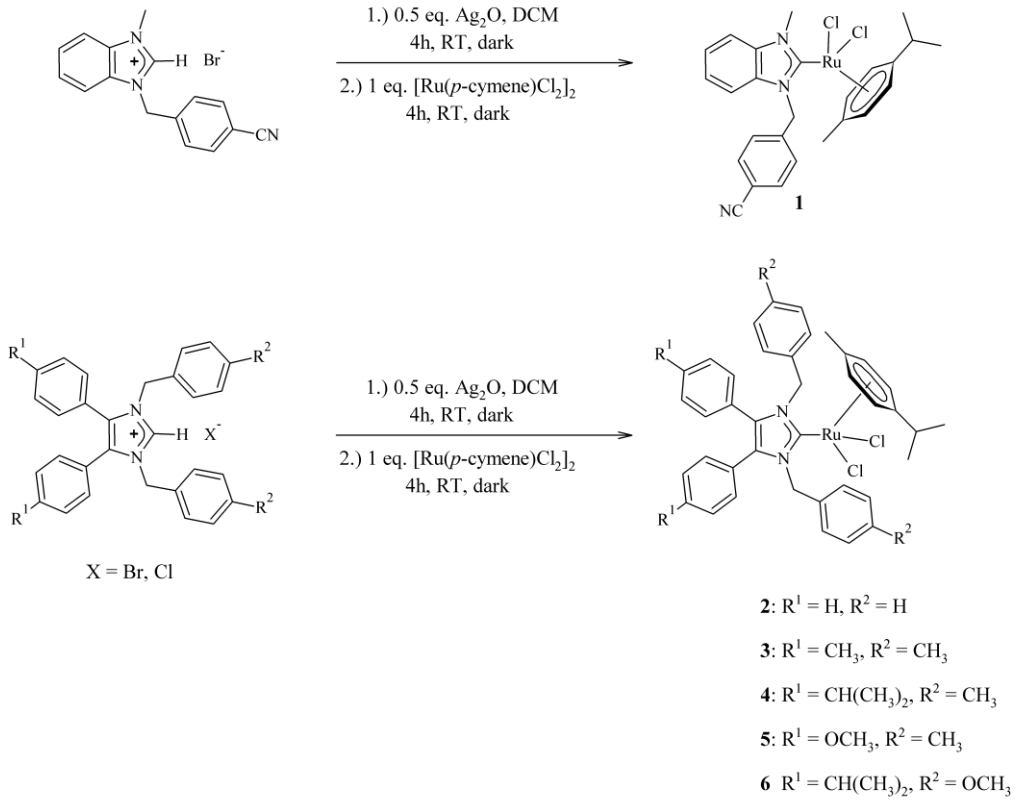

Scheme 5.1: General reaction scheme for the synthesis of unsymmetrically substituted NHC-Ru(II)(*p*-cymene)Cl_2 (**1**) and symmetrically substituted NHC-Ru(*p*-cymene)Cl_2 (**2-6**) complexes.

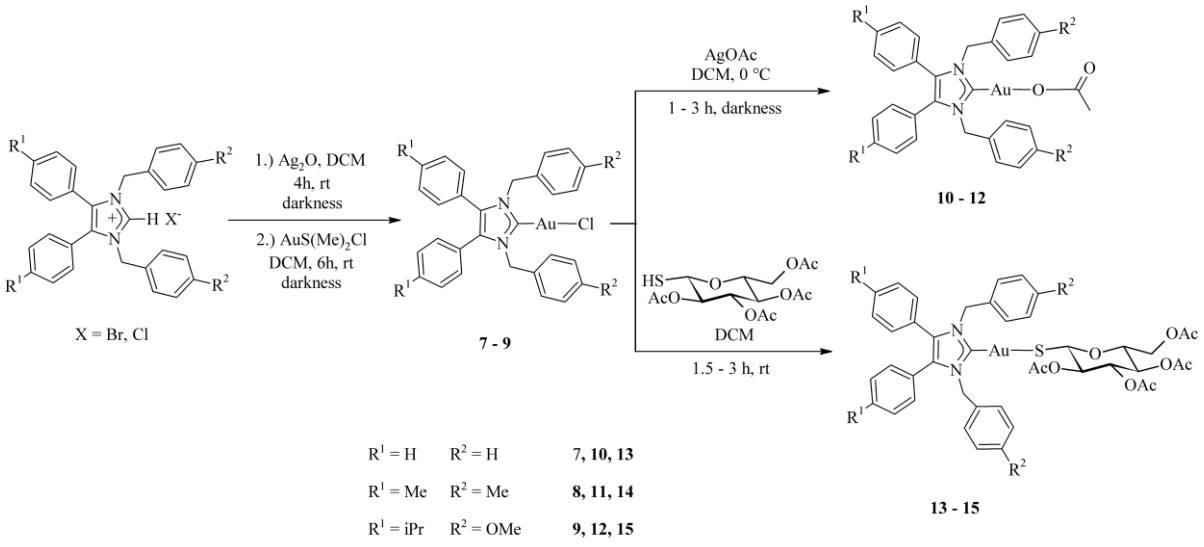

Scheme 5.2: General reaction scheme for the synthesis of symmetrically substituted NHC-Au(I)Cl (**7-9**), NHC-Au(I)OAc (**10-12**) and NHC-Au(I)*SR*(**13-15**) complexes

Scheme 5.2 shows the synthesis of the NHC-Au(I)Cl complexes (**7-9**) as well as the NHC-Au(I)OAc (**10-12**) and NHC-Au(I)*SR* (**13-15**) complexes which were obtained by ligand exchange. Also here the symmetric substituted precursor were synthesized and characterized following our earlier publications [8,10,19]. After generating the NHC-Ag(I) bromide complexes *in situ* under the exclusion of light at rt, addition of chloro(dimethylsulfido)gold(I) in dichloromethane and stirring for further 6 h, the NHC-Au(I) chloride complexes (1,3-Dibenzyl-4,5-diphenyl-imidazol-2-ylidene) gold(I) chloride (**7**), (1,3-Di(*p*-methylbenzyl)-4,5-di(*p*-methylphenyl)-imidazol-2-ylidene) gold(I) chloride (**8**) and (1,3-Di(*p*-methoxybenzyl)-4,5-di(*p*-isopropylphenyl)-imidazol-2-ylidene) gold(I) chloride (**9**) were obtained in 48.7, 73.4 and 83.2% yield, respectively. (1,3-Dibenzyl-4,5-diphenyl-imidazol-2-ylidene) gold(I) acetate (**10**), (1,3-Di(*p*-methylbenzyl)-4,5-di(*p*-methylphenyl)-imidazol-2-ylidene) gold(I) acetate (**11**) and (1,3-Di(*p*-methoxybenzyl)-4,5-di(*p*-isopropylphenyl)-imidazol-2-ylidene) gold(I) acetate (**12**) were obtained in 69.0, 53.3 and 67.9% yield by reacting the appropriately substituted NHC-Au(I) chloride with 1.2 equivalents of silver acetate in CH_2Cl_2 at 0°C for 1-3 h under the exclusion of light. By reacting the appropriately substituted NHC-Au(I)Cl complexes (**7-9**) with 1.05 equivalents of 2',3',4',6'-tetra-*O*-acetyl-1-thio-β-D-glucopyranose (*SR*) (synthesized according to literature[21]) and 1.09 equivalents of triethylamine in CH_2Cl_2 at rt for 2 h the complexes (1,3-Dibenzyl-4,5-diphenyl-imidazol-2-ylidene) gold(I) (*SR*) (**13**), (1,3-Di(*p*-methylbenzyl)-4,5-di(*p*-methylphenyl)-imidazol-2-ylidene) gold(I) (*SR*) (**14**), (1,3-Di(*p*-methoxybenzyl)-4,5-di(*p*-isopropylphenyl)-imidazol-2-ylidene) gold(I) (*SR*) (**15**) were recovered in good yields of 70.8, 66.9 and 75.1%.

All complexes were fully characterized by spectral (^{1}H NMR, ^{13}C NMR, IR, mass), elemental analysis studies and melting point determination. The melting points revealed a similar thermal stability of the Ru(II)-complexes **1-6** (mp: 185-270°C) compared to the Au(I) chlorides **7-9** (mp: 230-252°C), while Au(I) acetates **10-12** (mp: 82-167) and Au(I) *SR* complexes **13-15** (mp: 59-118°C) exhibited much lower melting points. Especially the *SR* substituted complexes show a very low thermal stability which can be attributed to the sugar moiety.

5.4.1 NMR spectra of complexes

In all complexes the formation of the NHC-metal bond was indicated in the ^{1}H NMR by the loss of the C^{2}-proton (9.27 - 11.51 ppm) and a downfield shift of the NCN carbon in the ^{13}C NMR from 137.20-159.83 ppm to 176.08-201.53 ppm. NMR spectra of the Ru(II)-NHC complexes **2-6** clearly indicate that the former symmetric benzyl groups [8–10,19] in position 1 and 3 at the imidazole ring are now found to have an unsymmetrically geometry, due to the newly formed bond to the Ru(*p*-cymene)Cl_2 moiety. The bulky substituents around the ruthenium force one of the benzyl arms out of the symmetrical geometry and therefore, the CH_2 groups are no longer represented by a singlet in the proton NMR, but split up to give two separate doublets at 5.30-5.21 ppm and 5.15-5.08 ppm. The NMR spectra of the chloro complexes **7-9** and the acetate complexes **10-12** showed the number of signals expected for complexes with a symmetrical 1,3-di(*p*-benzyl)-4,5-diaryl-imidazol-2-ylidene unit, For the *SR* substituted complexes **13-15**, the signals for the 1,3-di(*p*-benzyl)-4,5-diaryl-imidazol-2-ylidene unit were also detected, although the CH_2 groups on position 1 and 3, and the methyl as well as methoxy groups in complexes **14** and **15** were magnetically inequivalent on the ^{1}H NMR timescale due to the chirality of the glucopyranosyl moiety.

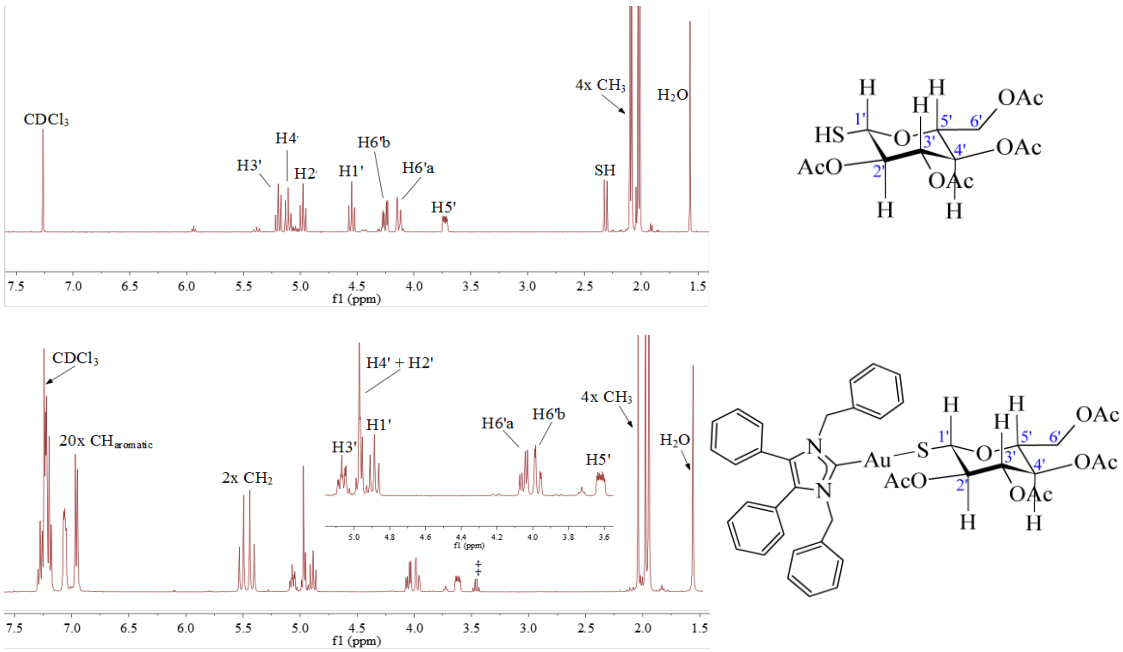

Figure 5.1: ^{1}H NMR spectra (400 MHz, $CDCl_3$) for 2',3',4',6'-tetra-*O*-acetyl-1-thio-β-D-glucopyranose (upper) and complex **13** (lower). (‡ indicates pentane)

5.4.2 Structural discussion

The solid state structure of the NHC-Ru(II)(*p*-cymene)Cl_2 complex (**1**) and the NHC-Au(I)Cl complex (**9**) were determined by single crystal X-ray diffraction. Crystals of **1** and **9** grew from slow infusion of pentane into concentrated chloroform solutions and crystallized in the monoclinic space groups $P2_1/c$(#14) (**1**) and C2/c(#15) (**9**). As already indicated by the 1H NMR measurements, the benzyl arm on the imidazole ring in complex **1** is forced to the back due to the bulkiness of the chlorido- and *p*-cymene-substituents on the ruthenium. The crystal structure of **1** (Figure 5.2) shows a three legged piano stool geometry and the angles involving Ru and the legs of the stool are near 90° (with a range of 86-91°). The Ru-centroid distance of 1.684 Å and the Ru-carbene distance of 2.052 Å are in good agreement with similar reported complexes [22]. Furthermore, the benzimidazole ring shows no deformation and is completely planar.

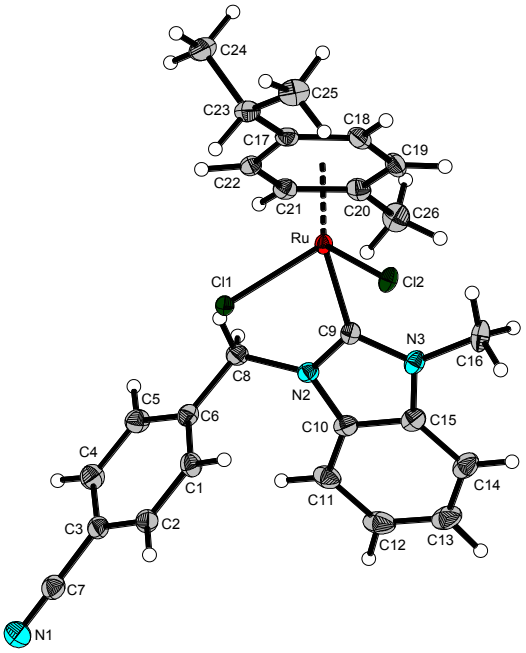

Figure 5.2: X-ray diffraction structure of **1**; thermal ellipsoids are drawn on the 50% probability level

Complex **9** (Figure 5.3) is located on a crystallographic 2-fold axis, which forces the C(9)-Au-Cl angle to be completely linear with 180.0° and the bond

distances Au-Cl of 2.2851(9) Å and Au-C(9) of 1.988(3) Å are in agreement with the literature [23,7]. The thermal ellipsoids are drawn at 30% probability, because the crystal had to be measured at slightly higher temperatures (150 K) since the crystal goes through a destructive phase transition in the region between 140 K and 150 K. Moreover, it is to mention that the isopropyl groups in *para* position on the phenyl rings are disordered over 3 positions.

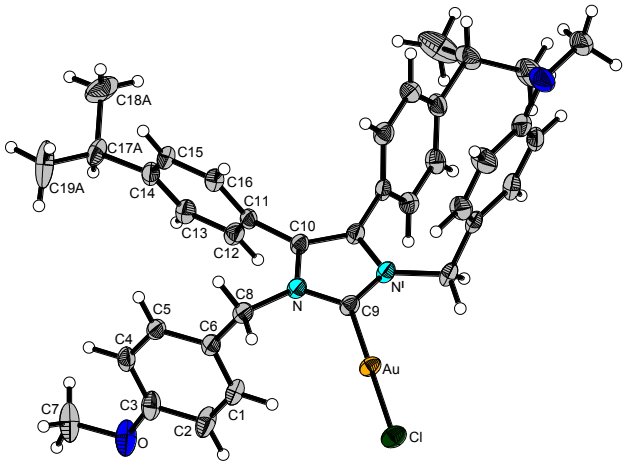

Figure 5.3: X-ray diffraction structure of **9**; thermal ellipsoids are drawn on the 30% probability level, disorder neglected; symmetry operation: [I] 1-x, y, 1.5-z

Table 5.1: Crystal data and structural refinement for **1** and **9**

	1	**9**
Empirical formula	$C_{26}H_{27}N_3Cl_2Ru$	$C_{75}H_{81}N_4O_4Cl_5Au_2$
Formula weight (g/mol)	553.48	1673.62
Crystal system	Monoclinic	Monoclinic
Space group	$P2_1/c$(#14)	C2/c(#15)
Unit cell dimensions		
a (Å)	13.2135(2)	11.1988
b (Å)	17.0126(2)	20.6671
c (Å)	11.9512(2)	17.4530
α (°)	90	90
β (°)	116.291(2)	105.969(2)
γ (°)	90	90
V ($Å^3$)	2408.67	
Z	4	2
Density (mg/m^3)(calc.)	1.526	1.431
Absorption coefficient (mm^{-1})	0.892	3.992
F(000)	1128	1668
Crystal size (mm^3)	0.2525 x 0.1796 x 0.1350	0.2905 x 0.2268 x 0.1242
θ (°)	2.95 to 29.55	3.54 to 29.41
Index ranges	-17≤h≤17	-15≤h≤15
	-23≤k≤23	-26≤k28
	-16≤l≤16	-23≤l≤18
Reflections collected	43619	18716
Independent reflections R_{int}	6318 (0.0310)	4850 (0.0259)
Completeness to θ_{max} (%)	99.2	99.7
Maximum and minimum transmission	0.925 and 0.859	0.723 and 0.490
Data/restraints/parameters	6318/0/293	4850/16/230
Goodness-of-Fit (GOF) on F^2	1.033	1.112
Final R indices [I > 2σ(I)]	R1=0.0283, wR2=0.0708	R1=0.0258, wR2=0.0595
R indices (all data)	R1=0.0335, wR2=0.0746	R1=0.0292, wR2=0.0607
Largest difference in peak and hole (e $Å^{-3}$)	1.036 and -0.818	0.604 and -0.721

Table 5.2: Selected bond lengths [Å] and angles [º] for **1** and **9**

Bond length [Å]				**Bond angle [°]**			
	1		**9**		**1**		**9**
Ru-C(9)	2.052(2)	Au-C(9)	1.988(3)	C(9)-Ru-Centroid	126.98(6)	C(9)-Au-Cl	180.0
Ru-Cl(1)	2.4599(5)	Au-Cl	2.2851(9)	Cl(1)-Ru-Centroid	126.22(1)	N#1-C(9)-N	105.5(3)
Ru-Cl(2)	2.4346(5)	N-C(9)	1.353(3)	Cl(2)-Ru-Centroid	125.58(1)	N-C(9)-Au	127.24(14)
Ru-Centroid	1.684(3)	N-C(10)	1.399(3)	C(9)-Ru-Cl(1)	88.45(6)	C(9)-N-C(10)	110.6(2)
N(2)-C(9)	1.371(3)	C(10)-C(10)#	1.352(5)	C(9)-Ru-Cl(2)	90.90(6)	C(10)#1-C(10)-N	106.66(15)
N(2)-C(10)	1.396(3)			Cl(1)-Ru-Cl(2)	86.260(16)		
N(3)-C(9)	1.359(3)			N(2)-C(9)-N(3)	105.59(17)		
N(3)-C(15)	1.388(3)			N(2)-C(9)-Ru	126.42(14)		
C(10)-C(15)	1.386(3)			N(3)-C(9)-Ru	127.72(15)		
				N(2)-C(10)-C(15)	106.22(18)		
				N(3)-C(15)-C(10)	106.68(18)		

5.4.3 Biological evaluation

The IC_{50} values against the cancer cell lines Caki-1 (renal) and MCF-7 (breast) for complexes **1-15** are shown in Table 5.3. All compounds were well soluble in DMSO and stable in the biological medium over the period of the testing time.

Table 5.3: IC_{50} values [µM] against Caki-1 and MCF-7 of Cisplatin, Ru(II)-NHC complexes **1-6** and Au(I)-NHC complexes **7-15**. Values obtained by typical MTT-based assays after 48 h drug exposure followed by 24 h recovery time.

	Cisplatin	**1**	**2**	**3**	**4**	**5**	**6**	
Caki-1	3.3	> 500	94 (± 5)	93 (± 2)	170 (± 20)	39 (± 5)	13 (± 2)	
MCF-7	14	> 500	80 (± 15)	19 (± 1)	7.1 (± 1.2)	2.4 (± 0.7)	7.0 (± 1.2)	
	7	**8**	**9**	**10**	**11**	**12**	**13**	**14**	**15**
Caki-1	67 (± 7)	16 (± 2)	41 (± 1)	31 (± 2)	42 (± 5)	18 (± 1)	14 (± 2)	17 (± 2)	58 (± 2)
MCF-7	8.4 (± 0.4)	30 (± 3)	12 (± 1)	23 (± 3)	12 (± 1)	25 (± 3)	6.1 (± 1.5)	9.3 (± 1.6)	14 (± 2)

In comparison to Cisplatin, which exhibited an IC_{50} value of 3.3 µM against Caki-1, the ruthenium complexes **1-6** did not show higher activity. In case of the unsymmetrical substituted complex **1**, coordination of the ruthenium-(*p*-cymene)-dichloride moiety to the imidazolium bromide led to a complete loss of activity of the resulting complex, while the other 5 complexes showed little (**4**), moderate (**2**,**3**,**5**) and good activity (**6**). Surprisingly, if their activity is tested against MCF-7, far stronger cytotoxicity was observed. Again, **1** did not show any activity, but medium (**2**), good (**3**) and high activity (**4-6**) were found for the other Ru(II)-NHCs, with the latter 3 showing better activity than Cisplatin against this specific cell line. Most interesting are the results found for complex **4**, where an increase in activity against the breast cancer cell line MCF-7 of a factor of 24 was observed when compared to the value obtained for Caki-1. Furthermore, the exchange of the isopropyl (**4**) for methoxy groups (**5**) in *para* position of the phenyl substituents in

position 4 and 5 on the imidazole led to a further 3-fold increase in activity against MCF-7. Also, **5** is 16-fold more active against MCF-7 than Caki-1 and nearly 6 times more active against MCF-7 than Cisplatin. These findings indicate that a) the substitution pattern on the imidazole has major influences on the activity of these complexes and b) that the mode of action of these complexes, resulting in cell death, has to be different for the two cell lines.

With exception for the NHC-Au(I)Cl complex **8** and the NHC-Au(I)OAc complex **12**, also the Au(I)-NHC complexes show higher activity against MCF-7 than Caki-1. Medium to good activity was found for all 9 complexes against Caki-1 with **14** expressing the best activity, having a value of 14 (± 2) µM. In general, the NHC-Au(I)*SR* complexes (**13-15)** exhibited better or equal activity against both cell lines if compared to their corresponding NHC-Au(I)Cl (**7-9**) and better activity than their NHC-Au(I)OAc analogues (**10-12)**. The only exceptions are found for the [(1,3-di(p-methoxybenzy)-4,5-di(p-isopropylphenyl)-imidazol-2-ylidene) gold(I) X] complexes **9** (X = Cl), **12** (X = OAc) and **15** (X = *SR*), where the complex containing the acetate group shows significant better activity against Caki-1 (18 ± 1 µM) than the chlorido- (41 ± 1 µM) and *SR*-containing (58 ± 2 µM) analogues. Lower IC_{50} values of the NHC-Au(I)*SR* complexes **13-15** are most likely to be attributed to the higher solubility of the complexes as well as possible enhanced cellular uptake due to the thioglucopyranose moiety.

5.5 Conclusion and Outlook

In summary, a series of six novel NHC-Ru(II)(*p*-cymene)Cl_2 complexes **1-6**, three NHC-Au(I)Cl **7-9**, three NHC-Au(I)OAc **10-12** and three NHC-Au(I)*SR* **13-15** complexes have been synthesized by applying the silver carbene transfer route. The IC_{50} values of the complexes **1-15** against the human cancer cell lines Caki-1 (renal) and MCF-7 (breast) have revealed moderate to good results, with complexes **4-6**, **7**, **13** and **14** showing low micromolar activity against MCF-7. Special attention has to be drawn to the Ru(II)-NHC complexes **4** and **5** where the complexes have shown 24-fold and 16-fold higher activity against MCF-7 than Caki-1. Additionally, the thioglucopyranose-substituted Au(I)-NHC complexes **13-15** have shown overall good activity against both cell lines, superior to the results obtained for the NHC-Au(I)Cl and NHC-Au(I)OAc complexes **7-12**. This finding shows, that substitution of previously determined lead structures with biological vectors can improve the activity against certain cancer cell lines. Further work to improve the activity as well as selectivity and investigation of the mode of action of these potential anticancer drugs will be undertaken.

5.6 Materials and Methods

5.6.1 General conditions:

All reactions were carried out under aerobic conditions. All Ag_2O and silver(I) acetate reactions were carried out under exclusion of light. Dimethylsulfido-gold(I) chloride, dichloro-ruthenium(II)(*p*-cymene) dimer, silver oxide, silver acetate and triethylamine were procured commercially from Sigma-Aldrich Chemical Company and were used without further purification. The solvents were of analytical grade and used without further purification or drying. The synthesis of the appropriately substituted imidazolium bromides was reported previously by our group [8–10,19].IR Spectra were recorded on a Perkin-Elmer Paragon 1000 FT-IR spectrometer employing a KBr disc. NMR Spectra were measured either on a Varian 300 MHz or 400 MHz spectrometer. All chemical shifts are reported in ppm and referenced to TMS. ESI MS was performed on a quadrupole tandem mass spectrometer (Quattro Micro, Micromass/Water's Corp., USA), using solutions in 100% MeOH. MS spectra were obtained in the ES+ (electron spray positive ionisation) mode for all compounds. CHN Analysis was carried out in an Exeter Analytical CE-440 elemental analyzer. Crystal Data was collected using an Agilent Technologies (former Oxford Diffraction) SuperNova diffractometer fitted with an Atlas detector. **1** and **9** were measured with Mo-Kα (0.71073 Å), **1** at 100 K, **9** at 150 K. A five times (**1**) and four times (**9**) redundant dataset was collected, assuming that the Friedel pairs are not equivalent. An analytical absorption correction based on the shape of the crystal was performed [24]. The structure was solved by direct methods using SHELXS-97 [25] and refined by full matrix least-squares on F^2 for all data using SHELXL-97 [25]. Hydrogen atoms were added at calculated positions and refined using a riding model. Their isotropic thermal displacement parameters were fixed to 1.2 (1.5 for methyl groups) times the equivalent ones of the parent atom. Anisotropic thermal displacement parameters were used for all non-hydrogen atoms. A suitable crystal of **1** and **9** was grown in a saturated solution of chloroform with slow infusion of pentane. Further details about the data collection are listed in Table 1 and 2.

CCDC 955702 (for **1**) and CCDC 955703 (for **9**) contain the supplementary crystallographic data for this paper. These data can be obtained free of charge from the Cambridge Crystallographic Data Centre via www.ccdc.cam.ac.uk/data_request/cif.

5.6.2 Synthesis:

(1-Methyl-3-(*p*-cyanobenzyl)-benzimidazol-2-ylidene)(η^6-*p*-cymene) ruthenium(II) dichloride (**1**)

1-Methyl-3-(*p*-cyanobenzyl)-benzimidazolium bromide [8] (131 mg, 0.400 mmol) and Ag_2O (46 mg, 0.20 mmol) were stirred in 15 mL dichloromethane in darkness at rt for 4 h. Dichloro-(*p*-cymene)-ruthenium(II) dimer (123 mg, 0.200 mmol) was added and the mixture was stirred for 4 h in darkness at rt. After filtration through a celite plug to remove the AgBr by-product the solvent was reduced to 5 mL and 20 mL pentane were added to precipitate the crude product. Filtration and washing with 2x20mL pentane and 2x20mL diethylether gave the product in 37.5% yield (81 mg, 0.15 mmol).

^{1}H NMR (300 MHz, $CDCl_3$, δ ppm): 7.58 (d, J = 8.3 Hz, 2H, $CH_{cyanobenzyl}$), 7.42 (d, J = 8.1 Hz, 1H, $CH_{cyanobenzyl}$), 7.33-7.24 (m, 3H, $CH_{cyanobenzyl}$ + $CH_{benzimidazol}$), 7.15 (d, J = 8.1 Hz, 1H, $CH_{benzimidazol}$), 6.88 (d, J = 8.1 Hz, 1H, $CH_{benzimidazol}$), 4.29 (s, 2H, CH_2), 2.98 (p, J = 6.9 Hz, 1H, C*H*$(CH_3)_{2cymene}$), 2.05 (s, 3H, CH_3), 1.27 (d, J = 6.9 Hz, 6H, CH(C*H*$_3)_{2cymene}$).

^{13}C NMR (101 MHz, $CDCl_3$, δ ppm): 190.98 (NCN), 142.75 (CN), 136.09, 134.69, 132.46, 132.45, 127.42, 123.56, 123.46 ($C_{cyanobenzyl}$ + $C_{benzimidazol}$), 110.93, 110.27, 110.17, 99.12 (C_{cymene}), 52.82 (CH_2), 36.88 (CH_3), 30.83 (C*H*$(CH_3)_{2cymene}$), 18.82 (CH(C*H*$_3)_{2cymene}$).

IR (KBr): 3042 (m), 2960 (m), 2869 (w), 2229 (s), 1607 (m), 1507 (w), 1375 (s), 1345 (s).

MS (m/z, QMS-MS/MS): 517.3 [M^+-Cl].

Micro Analysis calculated for $C_{26}H_{27}N_3Cl_2Ru$ (553.49): C, 56.42; H, 4.92; N, 7.59%. Found: C, 56.58; H, 4.81; N, 7.50%.
Decomposition Temperature: 270°C.

(1,3-Dibenzyl-4,5-diphenyl-imidazol-2-ylidene)(η^6-*p*-cymene)-ruthenium(II) dichloride (**2**)

1,3-Dibenzyl-4,5-diphenyl-imidazolium bromide [8] (193 mg, 0.400 mmol) and Ag_2O (46 mg, 0.20 mmol) were stirred in 15 mL dichloromethane in darkness at rt for 4 h. Dichloro-(*p*-cymene)-ruthenium(II) dimer (123 mg, 0.200 mmol) was added and the mixture was stirred for 4 h in darkness at rt. After filtration through a celite plug to remove the AgBr by-product the solvent was reduced to 5 mL and 20 mL pentane were added to precipitate the crude product. Filtration and washing with 2x20mL pentane and 2x20mL diethylether gave the product in 76.0% yield (215 mg, 0.304 mmol).

^{1}H NMR (300 MHz, $CDCl_3$, δ ppm): 7.27 (m, 7H, CH_{benzyl} + CH_{phenyl}), 6.99 (m, 13H, CH_{benzyl} + CH_{phenyl}), 6.40 (d, 2H, J = 17.3 Hz, CH_{cymene}), 5.24 (d, 2H, J = 5.7 Hz, CH_2), 5.20 (d, 2H, J = 17.3 Hz, CH_{cymene}), 5.11 (d, 2H, J = 5.7 Hz, CH_2), 2.47 (m, 1H, C*H*$(CH_3)_{2isopropyl}$), 1.82 (s, 3H, CH(C*H*$_3)_{2cymene}$), 1.10 (s, 3H, CH(C*H*$_3)_{2cymene}$), 1.08 (s, 3H, CH(C*H*$_3)_{2cymene}$).

^{13}C NMR (101 MHz, $CDCl_3$, δ ppm): 206.88 (NCN), 139.56, 134.94, 130.62, 128.56, 128.48, 128.29, 127.90, 127.02, 125.52 ($C_{imidazol}$ + C_{benzyl} +C_{phenyl}), 105.79, 94.78, 86.24, 83.37 (C_{cymene}), 53.41 (CH_2), 30.89 (C*H*$(CH_3)_{2cymene}$), 22.53 (CH(C*H*$_3)_{2cymene}$), 17.67 ($CH_{3cymene}$).

IR (KBr): 3059 (m), 2963 (m), 2869 (w), 1605 (s), 1496 (s), 1445 (s), 1372 (m), 1343 (s).

MS (m/z, QMS-MS/MS): 670.5 [M^+-Cl].

Micro Analysis calculated for $C_{39}H_{38}N_2Cl_2Ru$ (706.71): C, 66.28; H, 5.42; N, 3.96%. Found: C, 66.08; H, 5.23; N, 3.69%.

Melting Point: 210-211°C.

(1,3-Di(*p*-methylbenzyl)-4,5-di(*p*-methylphenyl)-imidazol-2-ylidene)(η^6-*p*-cymene)-ruthenium(II) dichloride (**3**)

1,3-Di(*p*-methylbenzyl)-4,5-di(*p*-methylphenyl)-imidazolium bromide [10] (215 mg, 0.400 mmol) and Ag_2O (46 mg, 0.20 mmol) were stirred in 15 mL dichloromethane in darkness at rt for 4 h. Dichloro-(*p*-cymene)-ruthenium(II) dimer (123 mg, 0.200 mmol) was added and the mixture was stirred for 4 h in darkness at rt. After filtration through a celite plug to remove the AgBr by-product the solvent was reduced to 5 mL and 20 mL pentane were added to precipitate the crude product. Filtration and washing with 2x20mL pentane and 2x20mL diethylether gave the product in 51.5% yield (157 mg, 0.206 mmol).

^{1}H NMR (300 MHz, $CDCl_3$, δ ppm): 7.12 (d, 4H, J = 7.7 Hz, $CH_{methylbenzyl}$), 6.83 (m, 12H, $CH_{methylbenzyl}$ + $CH_{methylphenyl}$), 6.35 (d, 2H, J = 17.5 Hz, CH_{cymene}), 5.21 (d, 2H, J = 6.0 Hz, CH_2), 5.11 (d, 2H, J = 17.5 Hz, CH_{cymene}), 5.08 (d, 2H, J = 6.0 Hz, CH_2), 2.34 (s, 6H, $CH_{3methylbenzyl}$), 2.16 (s, 6H, $CH_{3methylphenyl}$), 1.78 (s, 3H, $CH_{3cymene}$), 1.09 (s, 3H, $CH(CH_3)_{isopropyl}$), 1.07 (s, 3H, $CH(CH_3)_{isopropyl}$).

^{13}C NMR (101 MHz, $CDCl_3$, δ ppm): 177.00 (NCN), 138.19, 136.87, 136.46, 134.88, 130.50, 129.18, 128.59, 125.49, 125.29 ($C_{imidazol}$ + $C_{methylbenzyl}$ + $C_{methylphenyl}$), 105.27, 94.35, 86.35, 83.19 (C_{cymene}), 52.88 (CH_2), 30.37 ($CH(CH_3)_{2isopropyl}$), 22.58, 22.30, 21.15, 21.05, 17.56, 15.24, 14.02 ($CH_{3methylbenzyl}$ + $CH_{3methylphenyl}$ + $CH(CH_3)_{cymene}$).

IR (KBr): 3025 (w), 2976 (m), 2921 (s), 2869 (m), 1516 (s), 1442 (s), 1370 (s), 1343 (m).

MS (m/z, QMS-MS/MS): 726.6 [M^+-Cl].

Micro Analysis calculated for $C_{43}H_{46}N_2Cl_2Ru$ (762.82): C, 67.70; H, 6.08; N, 3.67%. Found: C, 67.09; H, 5.82; N, 3.41%.

Melting Point: 207-211°C.

(1,3-Di(*p*-methylbenzyl)-4,5-di(*p*-isopropylphenyl)-imidazol-2-ylidene)(η^6-*p*-cymene)-ruthenium(II) dichloride (**4**)

1,3-Di(*p*-methylbenzyl)-4,5-di(*p*-isopropylphenyl)-imidazolium bromide [19] (297 mg, 0.500 mmol) and Ag_2O (58 mg, 0.25 mmol) were stirred in 15 mL dichloromethane in darkness at rt for 4 h. Dichloro-(*p*-cymene)-ruthenium(II) dimer (153 mg, 0.250 mmol) was added and the mixture was stirred for 4 h in darkness at rt. After filtration through a celite plug to remove the AgBr by-product the solvent was reduced to 5 mL and 20 mL pentane were added to precipitate the crude product. Filtration and washing with 2x20mL pentane and 2x20mL diethylether gave the product in 40.2% yield (165 mg, 0.201 mmol).

^{1}H NMR (400 MHz, $CDCl_3$, δ ppm): 7.07 (d, J = 7.7 Hz, 4H, $CH_{methylbenzyl}$ + $CH_{isopropylphenyl}$), 6.90 - 6.62 (m, 12H, $CH_{methylbenzyl}$ + $CH_{isopropylphenyl}$), 6.27 (d, J = 17.2 Hz, 2H, CH_{cymene}), 5.23 (d, J = 5.9 Hz, 2H, CH_2), 5.12 (m, 6H, CH_2 + CH_{cymene}), 2.71 (p, J = 6.9 Hz, 2H, C*H*$(CH_3)_{2isopropylphenyl}$), 2.49 (m, 1H, C*H*$(CH_3)_{2isopropylcymene}$), 2.32 (s, 6H, CH(C*H*$_3)_{2isopropylcymene}$), 1.82 (s, 3H, $CH_{3cymene}$), 1.09 (s, 18H, $CH_{3methylbenzyl}$ + CH(C*H*$_3)_{2isopropylphenyl}$).

^{13}C NMR (101 MHz, $CDCl_3$, δ ppm): 176.90 (NCN), 148.89, 136.79, 136.35, 134.73, 130.57, 129.09, 125.89, 125.85, 125.53 (C_{phenyl} + C_{benzyl} + $C_{imidazol}$), 105.56, 94.50, 86.22, 83.25 (C_{cymene}) 53.15 (CH2), 33.65, 30.42 (CH_{3cymne}), 23.67 ($CH_{3benzyl}$), 22.58 ($CH_{3benzyl}$), 21.03 ($CH_{3phenyl}$), 17.69 ($CH_{isopropyl}$).

IR (KBr): 2960 (s), 2926 (w), 2870 (m), 1635 (w), 1516 (s), 1440 (w), 1363 (w), 1336 (m).

MS (m/z, QMS-MS/MS): 782.6 [M^+-Cl].

Micro Analysis calculated for $C_{47}H_{54}N_2Cl_2Ru$ (818.92): C, 68.93; H, 6.65; N, 3.42%. Found: C, 68.13; H, 6.53; N, 3.33%.

Melting Point: 208-211°C.

(1,3-Di(*p*-methylbenzyl)-4,5-di(*p*-methoxyphenyl)-imidazol-2-ylidene](η^6-*p*-cymene)-ruthenium(II) dichloride (**5**)

1,3-Di(*p*-methylbenzyl)-4,5-di(*p*-methoxyphenyl)-imidazolium bromide [9] (228 mg, 0.400 mmol) and Ag_2O (46 mg, 0.20 mmol) were stirred in 15 mL dichloromethane in darkness at rt for 4 h. Dichloro-(*p*-cymene)-ruthenium(II) dimer (122 mg, 0.200 mmol) was added and the mixture was stirred for 4 h in darkness at rt. After filtration through a celite plug to remove the AgBr by-product the solvent was reduced to 5 mL and 20 mL pentane were added to precipitate the crude product. Filtration and washing with 2x20mL pentane and 2x20mL diethylether gave the product in 64.5% yield (205 mg, 0.258 mmol).

^{1}H NMR (300 MHz, $CDCl_3$, δ ppm): 7.12 (d, J = 7.6 Hz, 4H, $CH_{methylbenzyl}$ + $CH_{methoxyphenyl}$), 6.92 - 6.68 (m, 8H, $CH_{methylbenzyl}$ + $CH_{methoxyphenyl}$), 6.54 (d, J = 8.7 Hz, 4H, $CH_{methylbenzyl}$ + $CH_{methoxyphenyl}$), 6.33 (d, J = 17.2 Hz, 2H, CH_{cymene}), 5.21 (d, J = 6.0 Hz, 2H, CH_2), 5.09 (m, 4H, CH_2 + CH_{cymene}), 3.64 (s, 6H, $OCH_{3methoxyphenyl}$), 2.43 (m, 1H, C*H*$(CH_3)_{2isopropyl}$), 2.33 (s, 6H, $CH_{3methylbenzyl}$), 1.08 (d, J = 6.8 Hz, 6H, CH(C*H*$_3)_{2isopropyl}$).

^{13}C NMR (101 MHz, $CDCl_3$, δ ppm): 176.73 (NCN), 159.41 (C-O), 136.84, 136.49, 134.65, 131.92, 129.22, 125.28, 120.73, 113.35 ($C_{methoxyphenyl}$ + $C_{methylbenzyl}$), 105.31, 94.31, 86.38, 83.17 (C_{cymene}), 55.04 ($OCH_{3methoxyphenyl}$), 52.91 (CH_2), 30.37 (C*H*$(CH_3)_{2isopropyl}$), 22.57 (CH(C*H*$_3)_{2isopropyl}$), 21.04 ($CH_{3methylbenzyl}$), 17.58 ($CH_{3cymene}$).

IR (KBr): 2963 (m), 2870 (w), 2836 (w), 1603 (s), 1520 (s), 1507 (s), 1290 (m), 1250 (s).

MS (m/z, QMS-MS/MS): 758.7 [M^+-Cl].

Micro Analysis calculated for $C_{43}H_{46}Cl_2N_2O_2Ru$ (794.81): C, 64.98; H, 5.83; N, 3.52%. Found: C, 64.35; H, 5.63; N, 3.56%.

Melting Point: 185-187°C.

(1,3-Di(*p*-methoxybenzyl)-4,5-di(*p*-isopropylphenyl)-imidazol-2-ylidene)(η^6-*p*-cymene)-ruthenium(II) dichloride (**6**)

1,3-Di(*p*-methoxybenzyl)-4,5-di(*p*-isopropylphenyl)-imidazolium chloride [19] (200 mg, 0.344 mmol) and Ag_2O (40 mg, 0.17 mmol) were stirred in 15 mL dichloromethane in darkness at rt for 4 h. Dichloro-(*p*-cymene)-ruthenium(II) dimer (105 mg, 0.172 mmol) was added and the mixture was stirred for 4 h in darkness at rt. After filtration through a celite plug to remove the AgCl by-product the solvent was reduced to 5 mL and 20 mL pentane were added to precipitate the crude product. Filtration and washing with 2x20mL pentane and 2x20mL diethylether gave the product in 68.6% yield (201 mg, 0.236 mmol).

^{1}H NMR (400 MHz, $CDCl_3$, δ ppm): 6.86 (m, 16H, $CH_{methoxybenzyl}$ + $CH_{isopropylphenyl}$), 6.21 (d, 2H, J = 16.7 Hz, CH_{cymene}), 5.30 (d, 2H, J = 6.0 Hz, CH_2), 5.22 (d, 2H, J = 16.7 Hz, CH_{cymene}), 5.15 (d, 2H, J = 6.0 Hz, CH_2), 3.82 (s, 6H, OCH_3), 2.75 (p, 2H, J = 6.9 Hz, C*H*$(CH_3)_{2isopropyl}$), 2.62 (m, 1H, C*H*$(CH_3)_{2isopropylcymene}$), 1.91 (s, 3H, $CH_{3cymene}$), 1.15 (m, 18H, CH(C*H*$_3)_{2isopropylphenyl}$ + CH(C*H*$_3)_{2isopropylcymene}$).

^{13}C NMR (101 MHz, $CDCl_3$, δ ppm): 176.55 (NCN), 158.40 (C-O), 148.89, 134.69, 131.65, 130.50, 126.84, 125.86, 113.79, 105.95 ($C_{imidazol}$ + $C_{methoxybenzyl}$ + $C_{isopropylphenyl}$), 105.95, 94.87, 86.00, 83.40 (C_{cymene}), 55.29 (OCH_3), 52.92 (CH_2), 33.66 (C*H*$(CH_3)_{2cymene}$), 30.50 (C*H*$(CH_3)_{2isopropylphenyl}$), 23.68 (CH(C*H*$_3)_{2cymene}$), 22.57 (CH(C*H*$_3)_{2isopropylphenyl}$), 17.87 ($CH_{3cymene}$).

IR (KBr): 2961 (m), 1614 (m), 1513 (s), 1339 (m), 1245 (s), 1177 (s), 1034 (s).

MS (m/z, QMS-MS/MS): 815.9 [M^+-Cl], 645.7 [M^+-(Cl_2(*p*-cymene)], 545.5 [M^+-(Ru(*p*-cymene)Cl_2)].

Micro Analysis calculated for $C_{47}H_{54}N_2O_2Cl_2Ru$ (850.92): C, 66.34; H, 6.40; N, 3.29%. Found: C, 66.19; H, 6.26; N, 3.50%.

Melting Point: 197-199°C.

(1,3-Dibenzyl-4,5-diphenyl-imidazol-2-ylidene) gold(I) chloride (**7**)

1,3-Dibenzyl-4,5-diphenyl-imidazolium bromide [8] (241 mg, 0.500 mmol) and Ag_2O (65 mg, 0.28 mmol) were dissolved in 10 mL dichloromethane and stirred for 4 h at rt in darkness. Chloro(dimethylsulfido)gold(I) (147 mg, 0.500 mmol) was added and the mixture was stirred for 6 h at rt in darkness before filtering through a short silica plug to remove the AgBr by-product. The solvent was reduced to 5 mL under reduced pressure and 30 mL pentane was added to precipitate the off white crude. After washing with further 50 mL cold pentane the white product was isolated in 48.7% yield (154 mg, 0.243 mmol).

^{1}H NMR (300 MHz, $CDCl_3$, δ ppm): 7.28 (m, 2H, CH_{benzyl}), 7.20 (m, 10H, CH_{benzyl} + CH_{phenyl}), 6.97 (m, 8H, CH_{phenyl}), 5.42 (s, 4H, CH_2).

^{13}C NMR (101 MHz, $CDCl_3$, δ ppm): 171.45 (NCN), 135.57, 132.03, 130.68, 129.34, 128.57, 128.54, 128.06, 127.45, 127.25 ($C_{imidazol}$ + C_{benzyl} + C_{phenyl}), 52.98 (CH_2).

IR (KBr): 3057 (m), 2962 (w), 1497 (s), 1448 (s), 1025 (s).

MS (m/z, QMS-MS/MS): 597.2 [M^+-Cl], 401.1 [M^+-AuCl].

Micro Analysis calculated for $C_{29}H_{24}AuClN_2$ (632.93): C, 55.03; H, 3.82; N, 4.43%. Found: C, 55.02; H, 3.87; N, 4.29%.

Melting Point: 240-242°C.

(1,3-Di(*p*-methylbenzyl)-4,5-di(*p*-methylphenyl)-imidazol-2-ylidene) gold(I) chloride (**8**)

1,3-Di(*p*-methylbenzyl)-4,5-di(*p*-methylphenyl)-imidazolium bromide [10] (204 mg, 0.380 mmol) and Ag_2O (46 mg, 0.20 mmol) were dissolved in 10 mL dichloromethane and stirred for 4 h at rt in darkness. Chloro(dimethylsulfido)gold(I) (112 mg, 0.380 mmol) was added and the mixture was stirred for 6 h at rt in darkness before filtering through a short silica plug to remove the AgBr by-product. The solvent was reduced to 5 mL under reduced pressure and 30 mL pentane

was added to precipitate the off white crude. After washing with further 50 mL cold pentane the white product was isolated in 73.4% yield (192 mg, 0.279 mmol).

^{1}H NMR (300 MHz, $CDCl_3$, δ ppm): 7.02 (dd, J = 8.0 Hz, 8H, $CH_{methylphenyl}$ + $CH_{methylbenzyl}$), 6.93 (d, J = 8.1 Hz, 4H, $CH_{methylphenyl}$ + $CH_{methylbenzyl}$), 6.86 (d, J = 8.1 Hz, 4H, $CH_{methylphenyl}$ + $CH_{methylbenzyl}$), 5.34 (s, 4H, CH_2), 2.30 (s, 6H, $CH_{3methylphenyl}$), 2.29 (s, 6H, $CH_{3methylbenzyl}$).

^{13}C NMR (101 MHz, $CDCl_3$, δ ppm): 180.44 (NCN), 139.22, 137.69, 132.88, 130.59, 129.22, 129.18, 127.50, 127.47, 124.48 ($C_{methylphenyl}$ + $C_{methylbenzyl}$ + $C_{imidazol}$), 52.51 (CH_2), 21.28 ($CH_{3methylphenyl}$), 21.10 ($CH_{3methylbenzyl}$).

IR (KBr): 3025 (w), 2921 (m), 2863 (w), 1516 (s), 1506 (s), 1446 (s), 1413 (s), 1351 (m), 1184 (s).

MS (m/z, QMS-MS/MS): 712.8 [M^++Na], 653.2 [M^+-Cl].

Micro Analysis calculated for $C_{33}H_{32}AuClN_2$ (689.04): C, 57.52; H, 4.68; N, 4.07%. Found: C, 57.32; H, 4.66; N, 3.99%.

Melting Point: 250-252°C.

(1,3-Di(*p*-methoxybenzyl)-4,5-di(*p*-isopropylphenyl)-imidazol-2-ylidene) gold(I) chloride (**9**)

1,3-Di(*p*-methoxybenzyl)-4,5-di(*p*-isopropylphenyl)-imidazolium chloride [19] (291 mg, 0.500 mmol) and Ag_2O (56 mg, 0.28 mmol) were dissolved in 10 mL dichloromethane and stirred for 4 h at rt in darkness. Chloro(dimethylsulfido)gold(I) (148 mg, 0.500 mmol) was added and the mixture was stirred for 6 h at rt in darkness before filtering through a short silica plug to remove the AgCl by-product. The solvent was reduced to 5 mL under reduced pressure and 30 mL pentane was added to precipitate the off white crude. After washing with further 50 mL cold pentane the white product was isolated in 83.2% yield (323 mg, 0.416 mmol).

^{1}H NMR (300 MHz, $CDCl_3$, δ ppm): 7.08 (d, J = 8.1 Hz, 4H, $CH_{isopropylphenyl}$ + $CH_{methoxyphenyl}$), 6.98 (dd, J = 3.5, 8.5 Hz, 8H, $CH_{isopropylphenyl}$ + $CH_{methoxyphenyl}$), 6.69

(d, J = 8.7 Hz, 4H, $CH_{isopropylphenyl}$ + $CH_{methoxyphenyl}$), 5.31 (s, 4H, CH_2), 3.74 (s, 6H, OCH_3), 2.85 (p, J = 6.9 Hz, 2H, $CH_{isopropyl}$), 1.20 (s, 6H, $CH_{3isopropyl}$), 1.18 (s, 6H, $CH_{3isopropyl}$).

^{13}C NMR (101 MHz, $CDCl_3$, δ ppm): 170.25 (NCN), 159.20 (C-O), 150.09, 131.67, 130.74, 129.09, 127.90, 126.57, 124.85, 113.77 ($C_{isopropylphenyl}$ + $C_{methoxyphenyl}$ + $C_{imidazol}$), 55.21 (OCH_3), 52.34 (CH_2), 33.82 ($CH_{isopropyl}$), 23.75 ($CH_{3isopropyl}$).

IR (KBr): 2960 (m), 2835 (w), 2361 (w), 1613 (m), 1512 (s), 1445 (m), 1245 (s), 1177 (s), 1042 (m).

MS (m/z, QMS-MS/MS): 544.2 [M^+-AuCl].

Micro Analysis calculated for $C_{37}H_{40}AuClN_2O_2$ (777.15): C, 57.18; H, 5.19; N, 3.60%. Found: C, 56.90; H, 5.22; N, 3.45%.

Melting Point: 230-231°C.

(1,3-Dibenzyl-4,5-diphenyl-imidazol-2-ylidene) gold(I) acetate (**10**)

(1,3-Dibenzyl-4,5-diphenyl-imidazol-2-ylidene) gold(I) chloride (63 mg, 0.10 mmol) and silver acetate (20 mg, 0.12 mmol) were dissolved in 5 mL dichloromethane and stirred for 3 h at 0°C. 2 mL methanol were added and the mixture was filtered through a short silica plug to remove the AgCl by-product. The solvent was removed under reduced pressure and the yellow oily crude was re-dissolved in 5 mL diethylether, precipitated by addition of 25 mL pentane, filtered and dried under suction. The product was obtained in 69.0% yield (45 mg, 0.069 mmol).

^{1}H NMR (400 MHz, $CDCl_3$, δ ppm): 7.28 (t, 2H, J=7.5 Hz, CH_{benzyl} + CH_{phenyl}), 7.19 (m, 10H, CH_{benzyl} + CH_{phenyl}), 7.03 (dd, 4H, J=7.1, 2.5 Hz, CH_{benzyl} + CH_{phenyl}), 6.94 (d, 4H, J=7.3 Hz, CH_{benzyl} + CH_{phenyl}), 5.43 (s, 4H, CH_2), 2.05 (s, 3H, $CH_{3acetate}$).

^{13}C NMR (101 MHz, $CDCl_3$, δ ppm): 177.27 (NCN), 164.67 (C=O), 135.65, 132.11, 130.70, 129.31, 128.55, 128.53, 127.99, 127.61, 127.32 (C_{phenyl} + C_{benzyl} + $C_{imidazol}$), 53.07 (CH_2), 23.82 ($CH_{3acetate}$).

IR (KBr): 3062 (w), 3031 (w), 1629 (s), 1496 (m), 1359 (m), 1307 (s).

MS (m/z, QMS-MS/MS): 614.4 [M^+-$COCH_3$], 597.2 [M^+-$OCOCH_3$].

Micro Analysis calculated for $C_{31}H_{27}AuN_2O_2$ (656.53): C, 56.71; H, 4.15; N, 4.27%. Found: C, 56.51; H, 4.03; N, 4.16%.

Melting Point: 82-84°C.

(1,3-Di(*p*-methylbenzyl)-4,5-di(*p*-methylphenyl)-imidazol-2-ylidene) gold(I) acetate (**11**)

(1,3-Di(*p*-methylbenzyl)-4,5-di(*p*-methylphenyl)-imidazol-2-ylidene) gold(I) chloride (69 mg, 0.10 mmol) and silver acetate (20 mg, 0.12 mmol) were dissolved in 5 mL dichloromethane and stirred for 1.5 h at 0°C. 2 mL methanol were added and the mixture was filtered through a short silica plug to remove the AgCl by-product. The solvent was removed under reduced pressure and the yellow oily crude was re-dissolved in 5 mL diethylether, precipitated by addition of 25 mL pentane, filtered and dried under suction. The product was obtained in 53.3% yield (38 mg, 0.053 mmol).

^{1}H NMR (400 MHz, $CDCl_3$, δ ppm): 7.15 - 6.90 (m, 12H, $CH_{methylbenzyl}$ + $CH_{methylphenyl}$), 6.85 (d, J= 7.9 Hz, 4H, $CH_{methylbenzyl}$ + $CH_{methylphenyl}$), 5.36 (s, 4H, CH_2), 2.30 (s, 12H, $CH_{3methylbenzyl}$), 2.28 (s, 3H, $CH_{3methylphenyl}$), 2.06 (s, 3H, $CH_{3acetate}$).

^{13}C NMR (101 MHz, $CDCl_3$, δ ppm): 176.08 (NCN), 166.50 (C=O), 139.17, 137.61, 132.96, 131.90, 130.62, 129.21, 129.14, 127.63, 124.55 ($C_{methylbenzyl}$ + $C_{methylphenyl}$ + $C_{imidazol}$), 52.59 (CH_2), 23.85 ($CH_{3acetate}$), 21.28 ($CH_{3methylbenzyl}$), 21.09 ($CH_{3methylphenyl}$).

IR (KBr): 3026 (w), 2921 (m), 2862 (w), 1639 (s), 1517 (s), 1358 (s), 1301 (s).

MS (m/z, QMS-MS/MS): 670.4 [M^+-$COCH_3$], 653.4 [M^+-$OCOCH_3$].

Micro Analysis calculated for $C_{35}H_{35}AuN_2O_2$ (712.63): C, 58.99; H, 4.95; N, 3.93%. Found: C, 58.64; H, 4.81; N, 3.66%.

Melting Point: 166-167°C.

(1,3-Di(*p*-methoxybenzyl)-4,5-di(*p*-isopropylphenyl)-imidazol-2-ylidene) gold(I) acetate (**12**)

(1,3-Di(*p*-methoxybenzyl)-4,5-di(*p*-isopropylphenyl)-imidazol-2-ylidene) gold(I) chloride (50.0 mg, 0.064 mmol) and silver acetate (12.8 mg, 0.077 mmol) were dissolved in 5 mL dichloromethane and stirred for 1.5 h at 0°C. 2 mL methanol and 10 ml diethylether were added and the mixture was filtered through a short silica plug to remove the AgCl by-product. Another 15 mL diethylether were passed through the plug to wash out all of the product. The solvent was removed under reduced pressure at 15°C and by addition of 25 mL cold pentane the product was precipitated, then filtered and dried under suction. The product was obtained in 67.9% yield (35 mg, 0.044 mmol).

^{1}H NMR (400 MHz, $CDCl_3$, δ ppm): 7.08 (d, 4H, J = 7.9 Hz, $CH_{methoxybenzyl}$), 6.94 (d, 4H, J = 8.6 Hz, $CH_{isopropylbenzyl}$), 6.88 (d, 4H, J = 7.9 Hz, $CH_{methoxybenzyl}$), 6.68 (d, 4H, J = 8.6 Hz, $CH_{isopropylbenzyl}$), 5.32 (s, 4H, CH_2), 3.73 (s, 6H, OCH_3), 2.85 (p, 2H, J = 6.9 Hz, $CH_{isopropyl}$), 2.07 (s, 3H, $CH_{3acetate}$).

^{13}C NMR (101 MHz, $CDCl_3$, δ ppm): 177.30 (NCN), 163.35 (C=O), 159.17 (C-O), 150.06, 131.76, 130.76, 129.30, 127.99, 126.57, 124.93, 113.73 ($C_{imidazol}$ + $C_{isopropylbenzyl}$ + $C_{methoxybenzyl}$), 55.20 (OCH_3), 52.42 (CH_2), 33.82 ($CH_{isopropyl}$), 23.87 ($CH_{3acetate}$), 23.75 ($CH_{3isopropyl}$).

IR (KBr): 2960 (m), 1643 (s), 1609 (m), 1513 (s), 1360 (s), 1306 (s), 1250 (s), 1176 (m), 1022 (m).

MS (m/z, QMS-MS/MS): 741.8 [M^+-$O(CO)CH_3$], 545.4 [M^+-$AuO(CO)CH_3$].

Micro Analysis calculated for $C_{39}H_{43}AuN_2O_4$ (800.74): C, 58.50; H, 5.41; N, 3.50%. Found: C, 58.45; H, 5.25; N, 3.55%.

Melting Point: 161-163°C.

(1,3-Dibenzyl-4,5-diphenyl-imidazol-2-ylidene) gold(I) (2',3',4',6'-tetra-*O*-acetyl-β-D-glucopyranosyl-1-thiolate) (**13**)

(1,3-Dibenzyl-4,5-diphenyl-imidazol-2-ylidene) gold(I) chloride (63 mg, 0.10 mmol), 2',3',4',6'-tetra-*O*-acetyl-1-thio-β-D-glucopyranose (38 mg, 0.11 mmol) and triethylamine (15.2 µL, 0.109 mmol) were dissolved in 6 mL dichloromethane and stirred for 3 h at rt. After removal of the solvent under reduced pressure the crude was redissolved in 20 mL THF and passed through a short silica plug. The THF was reduced to 3 mL and pentane was added to precipitate the product. Filtering off the solvent and drying under suction gave the product in 70.8% yield (68 mg, 0.071 mmol).

^{1}H NMR (400 MHz, $CDCl_3$, δ ppm): 7.27 (d, J = 7.4 Hz, 2H, CH_{benzyl} + CH_{phenyl}), 7.22 (m, 10H, CH_{benzyl} + CH_{phenyl}), 7.07 (d, J = 3.48 Hz, 4H, CH_{benzyl} + CH_{phenyl}), 6.96 (d, J = 7.0 Hz, 4H, CH_{benzyl} + CH_{phenyl}), 5.51 (d, J = 15.1 Hz, 2H, CH_2), 5.42 (d, J = 15.1, 2H, CH_2), 5.07 (ddd, J = 2.4, 6.8, 9.3 Hz, 1H, H3'), 4.97 (m, 2H, H4',H2'), 4.89 (t, J = 9.7 Hz, 1H, H1'), 4.05 (dd, J = 5.1, 12.2 Hz, 1H, H6b'), 3.97 (dd, J = 2.5, 12.2 Hz, 1H, H6a'), 3.63 (ddd, J = 2.5, 5.2, 10.2 Hz, 1H, H5'), 2.04 (s, 3H, OCH_3), 1.98 (s, 3H, OCH_3), 1.95 (s, 6H, OCH_3).

^{13}C NMR (101 MHz, $CDCl_3$, δ ppm): 183.32 (NCN), 170.79, 170.28, 169.87, 169.51 (C=O), 136.09, 131.83, 130.70, 129.18, 128.56, 128.50, 127.94, 127.51, 127.42 (C_{phenyl} + C_{benzyl} + $C_{imidazol}$), 83.08 (C1'), 77.60 (C2'), 75.63 (C5'), 74.34 (C3'), 69.17 (C4'), 63.08 (C6'), 52.43 (CH_2), 21.19, 20.79, 20.70, 20.66 (CH_3).

IR (KBr): 3061 (w), 3032 (w), 2944 (w), 2858 (w), 1752 (s), 1449 (m), 1365 (m), 1227 (s), 1034 (s).

MS (m/z, QMS-MS/MS): 983.7 [M^++Na], 961.3 [M^++H].

Micro Analysis calculated for $C_{43}H_{43}AuN_2O_9S$ (959.84): C, 53.75; H, 4.51; N, 2.92%. Found: C, 53.35; H, 4.32; N, 2.78%.

Melting Point: 116-118°C.

(1,3-Di(*p*-methylbenzyl)-4,5-di(*p*-methylphenyl)-imidazol-2-ylidene) gold(I) (2',3',4',6'-tetra-*O*-acetyl-β-D-glucopyranosyl-1-thiolate) (**14**)

(1,3-Di(*p*-methylbenzyl)-4,5-di(*p*-methylphenyl)-imidazol-2-ylidene) gold(I) chloride (69 mg, 0.10 mmol), 2',3',4',6'-tetra-*O*-acetyl-1-thio-β-D-glucopyranose (38 mg, 0.11 mmol) and triethylamine (15.2 µL, 0.109 mmol) were dissolved in 6 mL dichloromethane and stirred for 1.5 h at rt. After removal of the solvent under reduced pressure the crude was redissolved in 20 mL THF and passed through a short silica plug. The THF was reduced to 3 mL and pentane was added to precipitate the product. Filtering off the solvent and drying under suction gave the product in 66.9% yield (68 mg, 0.067 mmol).

^{1}H NMR (400 MHz, $CDCl_3$, δ ppm): 7.00 (dd, J = 13.7, 7.4 Hz, 12H, $CH_{methylbenzyl}$ + $CH_{methylphenyl}$), 6.86 (d, J = 7.8 Hz, 4H, $CH_{methylbenzyl}$ + $CH_{methylphenyl}$), 5.38 (d, J = 7.1 Hz, 4H, CH_2), 5.00 (m, 4H, H3', H4', H2', H1'), 4.02 (dd, J = 11.1, 3.7 Hz, 2H, H6a', H6b'), 3.63 (ddd, J = 10.2, 5.0, 2.6 Hz, 1H, H5'), 2.30 (s, 12H, $CH_{3methylbenzyl}$ + $CH_{3methylphenyl}$), 2.06 (s, 3H, OCH_3), 1.99 (s, 3H, OCH_3), 1.97 (s, 3H, OCH_3), 1.95 (s, 3H, OCH_3).

^{13}C NMR (101 MHz, $CDCl_3$, δ ppm): 182.61 (NCN), 170.79, 170.32, 169.83, 169.42 (C=O), 139.02, 137.53, 133.34, 131.59, 130.61, 129.16, 127.47, 124.74 ($C_{methylbenzyl}$ + $C_{methylphenyl}$ + $C_{imidazol}$), 83.07 (C1'), 77.18 (C2'), 75.62 (C5'), 74.42 (C3'), 69.18 (C4'), 63.05 (C6'), 52.01 (CH_2), 21.28 ($CH_{3methylbenzyl}$), 21.18 (CH_3), 21.08 ($CH_{3methylphenyl}$), 20.75, 20.70, 20.65 (CH_3).

IR (KBr): 3026 (w), 2948 (w), 2865 (w), 1753 (s), 1365 (m), 1227 (s), 1034 (s).

QMS-MS/MS: 957.7 [M+-O(CO)CH_3].

Micro Analysis calculated for $C_{47}H_{51}AuN_2O_9S$ (1016.95): C, 55.51; H, 5.05; N, 2.75%. Found: C, 55.49; H, 5.03; N, 2.79%.

Melting Point: 88-90°C.

(1,3-Di(*p*-methoxybenzyl)-4,5-di(*p*-isopropylphenyl)-imidazol-2-ylidene) gold(I) (2',3',4',6'-tetra-*O*-acetyl-β-D-glucopyranosyl-1-thiolate) (**15**)

(1,3-Di(*p*-methoxybenzyl)-4,5-di(*p*-isopropylphenyl)-imidazol-2-ylidene) gold(I) chloride (78 mg, 0.10 mmol), 2',3',4',6'-tetra-*O*-acetyl-1-thio-β-D-glucopyranose (38 mg, 0.11 mmol) and triethylamine (15.2 µL, 0.109 mmol) were dissolved in 6 mL dichloromethane and stirred for 1.5 h at rt. After removal of the solvent under reduced pressure the crude was redissolved in 20 mL THF and passed through a short silica plug. The THF was reduced to 3 mL and pentane was added to precipitate the product. Filtering off the solvent and drying under suction gave the product in 75.1% yield (83 mg, 0.075 mmol).

^{1}H NMR (400 MHz, $CDCl_3$, δ ppm): 7.08 (d, J = 7.9 Hz, 4H, $CH_{isopropylphenyl}$ + $CH_{methoxyphenyl}$), 6.92 (dd, J = 8.2, 19.6 Hz, 8H, $CH_{isopropylphenyl}$ + $CH_{methoxyphenyl}$), 6.71 (d, J = 8.6 Hz, 4H, $CH_{isopropylphenyl}$ + $CH_{methoxyphenyl}$), 5.34 (s, 4H, CH_2), 5.02 (m, 4H, H3', H4', H2', H1'), 4.08 (dd, J = 4.9, 12.2 Hz, 1H, H6b'), 3.99 (dd, J = 2.3, 12.2 Hz, 1H, H6a'), 3.75 (s, 6H, OCH_3), 3.65 (ddd, J = 2.3, 4.7, 9.8 Hz, 1H, H5'), 2.85 (p, J = 6.9 Hz, 2H, $CH_{isopropyl}$), 2.05 (s, 3H, OCH_3), 1.97 (s, 3H, OCH_3), 1.94 (s, 3H, OCH_3), 1.92 (s, 3H, OCH_3), 1.20 (s, 6H, $CH_{3isopropyl}$), 1.19 (s, 6H, $CH_{3isopropyl}$).

^{13}C NMR (101 MHz, $CDCl_3$, δ ppm): 201.52 (NCN), 170.82, 170.35, 169.84, 169.47 (C=O), 159.13 (C-$O_{methoxybenzyl}$), 149.92, 131.47, 130.75, 129.11, 128.32, 126.52, 113.75, 109.98 ($C_{isopropylphenyl}$ + $C_{methoxyphenyl}$ + $C_{imidazol}$), 83.08 (C1'), 77.18 (C2'), 75.62 (C5'), 74.37 (C3'), 69.16 (C4'), 63.01 (C6'), 55.19 ($OCH_{3methoxybenzyl}$), 51.85 (CH_2), 33.81 ($CH_{isopropyl}$), 23.76 ($CH_{3isopropyl}$), 21.18, 20.71, 20.67, 20.64 (CH_3).

IR (KBr): 2961 (m), 2871 (w), 2839 (w), 1750 (s), 1613 (m), 1514 (s), 1248 (s), 1034 (s).

QMS-MS/MS: 1127.9 [M^++Na], 1106.1 [M^++H].

Micro Analysis calculated for $C_{51}H_{59}AuN_2O_{11}S$ (1105.05): C, 55.43; H, 5.38; N, 2.54%. Found: C, 55.41; H, 5.38; N, 2.44%.

Melting Point: 59-62°C.

5.6.3 Cytotoxicity studies:

Preliminary *in vitro* cell tests were performed on the human cancerous renal cell line Caki-1 and the human cancerous breast cell line MCF-7 in order to compare the cytotoxicity of the compounds presented in this paper. These cell lines were chosen based on their regular and long-lasting growth behaviour. The cells were obtained from the ATCC (American Tissue Cell Culture Collection) and maintained in Dulbecco's Modified Eagle Medium containing 10% (v/v) FCS (fetal calf serum), 1% (v/v) penicillin streptomycin and 1% (v/v) L-glutamine. Cells were seeded in 96-well plates containing 200 µL microtitre wells at a density of 5,000-cells/200 µL of medium and were incubated at 37°C for 24 h to allow for exponential growth. Then the compounds used for the testing were dissolved in the minimal amount of DMSO (dimethylsulfoxide) possible and diluted with medium to obtain stock solutions of 5×10^{-4} M in concentration and less than 0.7% of DMSO. The cells were then treated with varying concentrations of the compounds and incubated for 48 h at 37°C. Then, the solutions were removed from the wells and the cells were washed with PBS (phosphate buffer solution) and fresh medium was added to the wells. Following a recovery period of 24 h incubation at 37°C, individual wells were treated with 200 µL of a solution of MTT (3-(4,5-Dimethylthiazol-2-yl)-2,5-diphenyltetrazolium bromide) in medium. The solution consisted of 22 mg of MTT in 40 mL of medium. The cells were incubated for 3 h at 37°C. The medium was then removed and the purple formazan crystals were dissolved in 200 µL DMSO per well. For all tests cells with low passage numbers were used. A Wallac Victor (Multilabel HTS Counter) Plate Reader was used to measure absorbance at 540 nm. Cell viability was expressed as a percentage of the absorbance recorded for control wells. The values used for the dose response curves represent the values obtained from four consistent MTT-based assays for each compound tested.

Corresponding Author:

matthias.tacke@ucd.ie

Acknowledgement:

This project was funded by the UCD School of Chemistry and Chemical Biology.

5.7 References

(1) a) Herrmann, W. A.; Elison, M.; Fischer, J.; Köcher, C.; Artus, G. R. J. *Angew. Chem. Int. Ed. Engl.* **1995,** *34* (21), 2371–2374. b) Peris, E.; Mata, J.; Loch, J. A.; Crabtree, R. H. *Chem. Commun.* **2001** (2), 201–202.

(2) a) Izquierdo, J.; Hutson, G. E.; Cohen, D. T.; Scheidt, K. A. *Angew. Chem. Int. Ed.* **2012,** *51* (47), 11686–11698. b) Cohen, D. T.; Scheidt, K. A. *Chem. Sci.* **2011,** *3* (1), 53–57. c) Velazquez, H. D.; Verpoort, F. *Chem. Soc. Rev.* **2012,** *41* (21), 7032–7060.

(3) a) Oehninger, L.; Rubbiani, R.; Ott, I. *Dalton Trans.* **2013,** *42* (10), 3269–3284. b) Liu, W.; Gust, R. *Chem. Soc. Rev.* **2013,** *42* (2), 755–773. c) Gautier, A.; Cisnetti, F. *Metallomics*. **2012,** *4* (1), 23–32. d) Lin, J. C. Y.; Huang, R. T. W.; Lee, C. S.; Bhattacharyya, A.; Hwang, W. S.; Lin, I. J. B. *Chem. Rev.* **2009,** *109* (8), 3561–3598.

(4) Mercs, L.; Albrecht, M. *Chem. Soc. Rev.* **2010,** *39* (6), 1903–1912.

(5) a) Banti, C. N.; Hadjikakou, S. K. *Metallomics*. **2013,** *5* (6), 569–596. b) Patil, S.; Tacke, M. *Insights into Coordination, Bioinorganic and Applied Inorganic Chemistry*. **2011,** 555–566. c) Garrison, J. C.; Youngs, W. J. *Chem. Rev.* **2005,** *105* (11), 3978–4008.

(6) a) Patil, S.; Dietrich, K.; Deally, A.; Gleeson, B.; Müller-Bunz, H.; Paradisi, F.; Tacke, M. *Appl. Organomet. Chem.* **2010,** *24* (11), 781–793. b) Patil, S.; Claffey, J.; Deally, A.; Gleeson, B.; Hogan, M.; Menéndez Méndez, L. M.; Müller-Bunz, H.; Paradisi, F.; Tacke, M. *Eur. J. Inorg. Chem.* **2010,** *2010* (7), 1020–1031. c) Patil, S.; Dietrich, K.; Deally, A.; Gleeson, B.; Müller-Bunz, H.; Paradisi, F.; Tacke, M. *Helv. Chim. Acta*. **2010,** *93* (12), 2347–2364. d) Patil, S.; Deally, A.; Gleeson, B.; Hackenberg, F.; Müller-Bunz, H.; Paradisi, F.; Tacke, M. *Z. Allg. Anorg. Chem.* **2011,** *637* (3-4), 386–396. e) Hackenberg, F.; Deally, A.; Lally, G.; Malenke, S.; Müller-Bunz, H.; Paradisi, F.; Patil, S.; Quaglia, D.; Tacke, M. *Int. J. Inorg. Chem.* **2012,** *2012,* 13 pages.

(7) Patil, S.; Deally, A.; Hackenberg, F.; Kaps, L.; Müller-Bunz, H.; Schobert, R.; Tacke, M. *Helv. Chim. Acta*. **2011,** *94* (9), 1551–1562.

(8) Patil, S.; Deally, A.; Gleeson, B.; Müller-Bunz, H.; Paradisi, F.; Tacke, M. *Metallomics*. **2011,** *3* (1), 74–88.

(9) Hackenberg, F.; Lally, G.; Müller-Bunz, H.; Paradisi, F.; Quaglia, D.; Streciwilk, W.; Tacke, M. *J. Organomet. Chem.* **2012,** *717,* 123–134.

(10) Hackenberg, F.; Lally, G.; Müller-Bunz, H.; Paradisi, F.; Quaglia, D.; Streciwilk, W.; Tacke, M. *Inorganica Chim Acta*. **2013,** *395,* 135–144.

(11) Sharkey, M. A.; O'Gara, J. P.; Gordon, S. V.; Hackenberg, F.; Healy, C. P. F.; Patil, S.; Schaible, B.; Tacke, M. *Antibiotics*. **2012** (1), 25–28.

(12) Fichtner, I.; Cinatl, J.; Michaelis, M.; C. Sanders, L.; Hilger, R.; N. Kennedy, B.; L. Reynolds, A.; Hackenberg, F.; Lally, G.; J. Quinn, S.; McRae, I.; Tacke, M. *LDDD*. **2012,** *9* (9), 815–822.

(13) a) Mangiapia, G.; D'Errico, G.; Simeone, L.; Irace, C.; Radulescu, A.; Di Pascale, A.; Colonna, A.; Montesarchio, D.; Paduano, L. *Biomaterials*. **2012,** *33* (14), 3770–3782. b) Simeone, L.; Mangiapia, G.; Vitiello, G.; Irace, C.; Colonna, A.; Ortona, O.; Montesarchio, D.; Paduano, L. *Bioconjugate Chem.* **2012,** *23* (4), 758–770.

(14) a) Oehninger, L.; Stefanopoulou, M.; Alborzinia, H.; Schur, J.; Ludewig, S.; Namikawa, K.; Muñoz-Castro, A.; Köster, R. W.; Baumann, K.; Wölfl, S.; Sheldrick, W. S.; Ott, I. *Dalton Trans.* **2013,** *42* (5), 1657–1666. b) Oehninger, L.; Alborzinia, H.; Ludewig, S.; Baumann, K.; Wölfl, S.; Ott, I. *ChemMedChem*. **2011,** *6* (12), 2142–2145.

(15) a) Rubbiani, R.; Kitanovic, I.; Alborzinia, H.; Can, S.; Kitanovic, A.; Onambele, L. A.; Stefanopoulou, M.; Geldmacher, Y.; Sheldrick, W. S.; Wolber, G.; Prokop, A.; Wölfl, S.; Ott, I. *J. Med. Chem.* **2010,** *53* (24), 8608–8618. b) Rubbiani, R.; Can, S.; Kitanovic, I.; Alborzinia, H.; Stefanopoulou, M.; Kokoschka, M.; Mönchgesang, S.; Sheldrick, W. S.; Wölfl, S.; Ott, I. *J. Med. Chem.* **2011,** *54* (24), 8646–8657.

(16) Ciftci, O.; Beytur, A.; Vardi, N.; Ozdemir, I. *Drug Development and Industrial Pharmacy*. **2012,** *38* (1), 40–46.

(17) Ciftci, O.; Ozdemir, I.; Cakir, O.; Demir, S. *Toxicol Ind Health*. **2011,** *27* (8), 735–741.

(18) Liu, W.; Bensdorf, K.; Proetto, M.; Hagenbach, A.; Abram, U.; Gust, R. *J. Med. Chem.* **2012,** *55* (8), 3713–3724.

(19) Streciwilk, W.; Cassidy, J.; Hackenberg, F.; Müller-Bunz, H.; Paradisi, F.; Tacke, M. *J. Organomet. Chem.* **2013,** submitted.

(20) Magill, A. M.; McGuinness, D. S.; Cavell, K. J.; Britovsek, G. J.; Gibson, V. C.; White, A. J.; Williams, D. J.; White, A. H.; Skelton, B. W. *Journal of Organometallic Chemistry*. **2001,** *617-618,* 546–560.

(21) a) Fulton, D. A.; Stoddart, J. F. *J. Org. Chem.* **2001,** *66* (25), 8309–8319. b) Orth, R.; Pitscheider, M.; Sieber, S. *Synthesis*. **2010,** *2010* (13), 2201–2206.

(22) a) Prades, A.; Viciano, M.; Sanaú, M.; Peris, E. *Organometallics*. **2008,** *27* (16), 4254–4259. b) DePasquale, J.; White, N. J.; Ennis, E. J.; Zeller, M.; Foley, J. P.; Papish, E. T. *Polyhedron*. **2012,** *58,* 162–170. c) DePasquale, J.; Kumar, M.; Zeller, M.; Papish, E. T. *Organometallics*. **2013,** *32* (4), 966–979.

(23) a) Baker, M. V.; Barnard, P. J.; Berners-Price, S. J.; Brayshaw, S. K.; Hickey, J. L.; Skelton, B. W.; White, A. H. *J. Organomet. Chem.* **2005,** *690* (24-25), 5625–5635. b) Frémont, P. de; Scott, N. M.; Stevens, E. D.; Nolan, S. P. *Organometallics*. **2005,** *24* (10), 2411–2418.

(24) *CrysalisPro;* Agilent Technologies, **2011**.

(25) Sheldrick, G. M. *Acta Crystallogr.* **2008,** *A64* (1), 112–122.

Chapter 6 Discussion, Conclusion and Outlook

In 2010, two silver(I)-NHC lead structures (Figure 6.1) with remarkable cytotoxicity (SBC1) and antibacterial activity (SBC3) were discovered in our group by Dr. S. Patil, which have been further evaluated *in vitro* and *in vivo* in the following years in cooperation with our group [1, 2]. Since these two complexes were taken as a starting point for this thesis, it is necessary to summarise the experimental results on these:

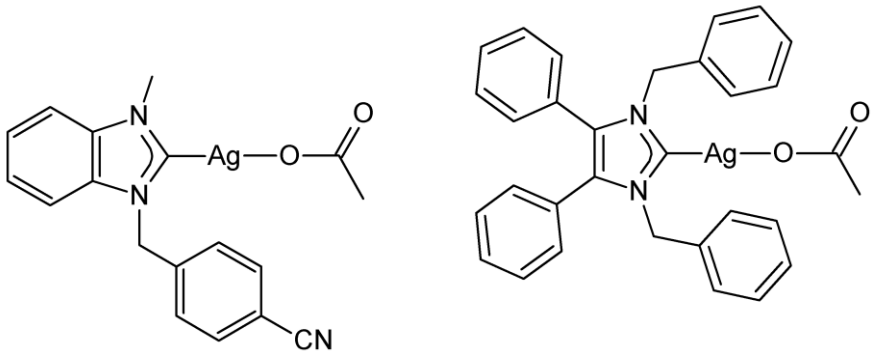

Figure 6.1: NHC-Ag(I)OAc lead structures SBC1 (left) and SBC3 (right) [3]

SBC1 has shown activity against several cancer cell lines (MCF-7 (breast), Caki-1 (renal), PC-3 (prostate), UKF-NB-3 and UKF-NB-6 (neuroblastoma)) in the low micromolar range and exhibited HSA and DNA binding. Unfortunately, *in vivo* tests in zebrafish resulted in high mortality at concentrations of 10 µM and above. Also, the *in vivo* experiment using non-tumour bearing mice showed that the toxicity of SBC1 was under- and the MTD overestimated. This led to the situation that three out of eight tumour bearing mice in the xenograft experiment died when they were exposed to daily dosages of 50 mg/kg. Even in the group which received the lower dosage, two out of eight mice died during the treatment. The relatively high T/C values of 78% and 75% combined with the significant toxicity of SBC1 demonstrated that the compound is toxic and does not have a useable therapeutic index in its given formulation.

Generally, one can conclude that SBC1 is a potent cytotoxic and resistance-breaking anticancer agent, which shows very little selectivity *in vivo*.

But SBC1 might become a useful compound when bonded to a targeted delivery vector like a protein or formulated in a suitable micelle for selective uptake into cancer cells.

SBC3 shows significant activity against the *M. bovis BCG Pasteur* and *M. smegmatis* as well as against *Salmonella typhimurium*, MSSA and MRSA. The best activities are found for *E. coli* and *P. aeruginosa*, which makes SBC3 already as active as conventional β-lactam antibiotics against these two bacterial strains. Especially breaking the resistance in MRSA is a good argument for the further development of silver-based antibiotic drug candidates like SBC3.

The research undertaken, which is described in this thesis, is based on these findings and it has been shown that through appropriate substitution patterns and exchange of the transition metal promising new anticancer drug candidates have been found.

6.1 An overview about the synthesis and characterisation of the various NHC transition metal complexes of this thesis

The synthesis of all compounds resulted in medium to high yields and high purity, which was confirmed by NMR (^{1}H and ^{13}C), microanalysis, mass spectrometry and IR. Especially NMR characterisation of the compounds has proven to be a quick and easy tool to determine the formation of the desired NHC-metal complexes. Upon formation of the carbene-metal bond the ^{1}H NMR signal for the C^{2} proton of the respective imidazolium halide vanishes, and a highfield shift is observed in the ^{13}C NMR for the C^{2} in all complexes. Additionally, besides in the case of the NHC-Au(I)Cl complexes, the ^{1}H and ^{13}C signals for the bonded ligands (acetate, *p*-cymene and thioglucopyranose) are observed, exhibiting signal shifts in both NMR spectra which could only be attributed to bound and not free ligand. Microanalysis gave indication that the complexes are all monomeric and also mass spectrometry confirmed the formation of the desired complexes.

Furthermore, 6 crystal structures of differently substituted NHC-Ag(I)OAc complexes, 1 crystal structure of a NHC-Ru(II)(*p*-cymene)Cl_2 complex and 1

crystal structure of a NHC-Au(I)Cl complex were obtained. Of special interest was the structure of the Ru-NHC complex, since it is visible in the solid state structure that the benzyl ring in position 3 on the imidazole bends towards the back of the molecule due to the bulkiness of the *p*-cymene and Cl_2 ligands, giving an indication why two magnetically different CH_2 groups are observed in the ^1H NMR of the NHC-Ru(II)(*p*-cymene)Cl_2 spectra.

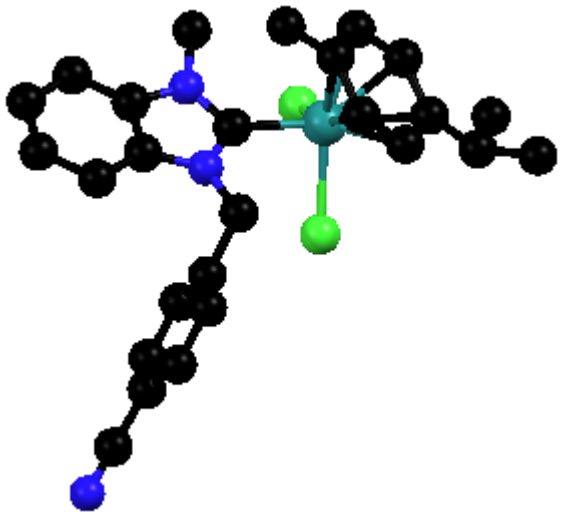

Figure 6.2: Crystal structure of (1-methyl-3(*p*-cyanobenzyl)-benzimidazol-2-ylidene)ruthenium(II)(*p*-cymene)dichloride

Summarising, it can be said that the presented NHC-silver(I)/-ruthenium(II)/ and -gold(I) complexes are easily accessible from cheap starting materials, give moderate to high yields and the synthesis does not require any harsh conditions and is not excessively sensitive towards moisture and air.

6.2 A summary about the biological activity of the various NHC transition metal complexes of this thesis

Presented in this section are the various substituted NHC transition metal complexes and their corresponding *in vitro* cytotoxicity (IC_{50}) as well as antibacterial (if applicable) values at highest drug concentration, based on the previously described MTT- and Kirby Bauer disc diffusion assays.

Table 6.1: Chapter 2: Non-symmetrically *p*-benzyl-substituted (benz)imidazole NHC-silver(I) acetate complexes and their respective IC_{50} values (μM) against Caki-1, and areas of clearance (mm) against *E. coli* and *S. aureus.*

Compound	**1**	**2**	**3**
	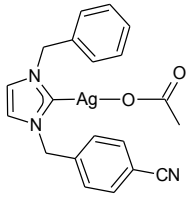	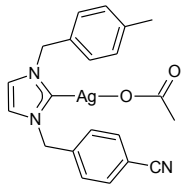	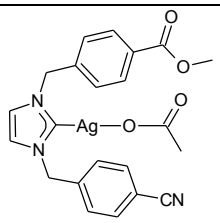
Caki-1	25 (± 1)	13 (± 2)	5.4 (± 0.8)
E. coli	6	7	3
S. aureus	7	3	3

Compound	**4**	**5**	**6**	**7**
	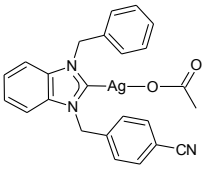	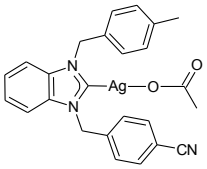	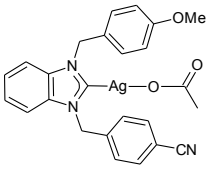	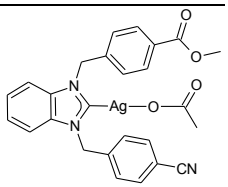
Caki-1	16 (± 2)	7.1 (± 1.0)	20 (± 4)	14 (± 1)
E. coli	6	3	6	5
S. aureus	6	6	7	8

Table 6.2: Chapter 3 and Chapter 4: 4,5-Diaryl-imidazole NHC-silver(I) acetate complexes and their respective IC_{50} values (μM) against Caki-1 and MCF-7, and areas of clearance (mm) against *E. coli* and *S. aureus*.

Compound	**8**	**9**	**10**	**11**	**12**
	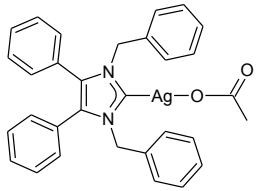	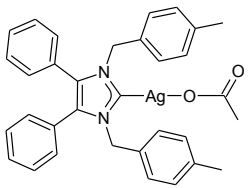	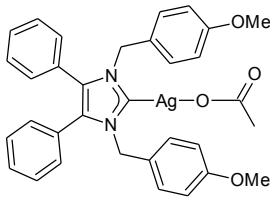	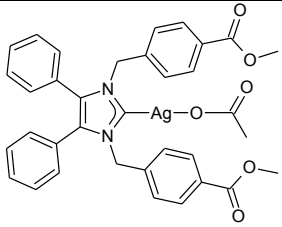	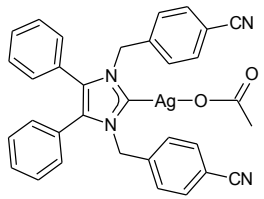
Caki-1	14 (± 1)	3.6 (± 1.0)	4.2 (± 0.5)	33 (± 2)	59 (± 4)
MCF-7	5.8 (± 0.6)	3.5 (± 0.4)	5.4 (± 0.3)	28 (± 1)	25 (± 2)
E. coli	10	8	8	6	5
S. aureus	7	5	8	4	2

Compound	**13**	**14**	**15**	**16**	**17**
	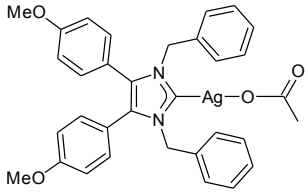	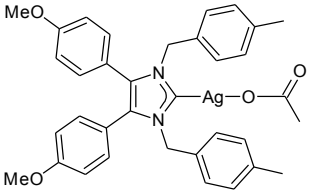	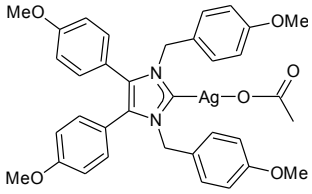	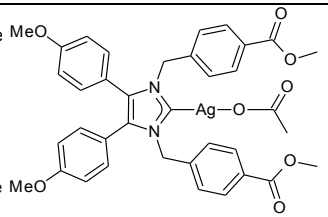	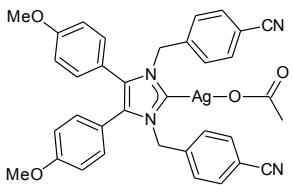
Caki-1	21 (± 1)	21 (± 2)	21 (± 1)	34 (± 2)	46 (± 2)
MCF-7	11 (± 2)	5.0 (± 0.3)	6.5 (± 0.4)	17 (± 1)	13 (± 1)
E. coli	8	3	2	1	2
S. aureus	8	2	5	2	3

Compound	18	19	20	21	22
	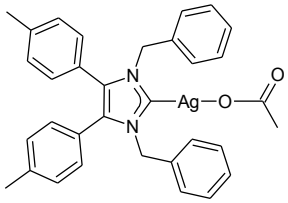	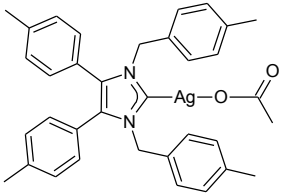	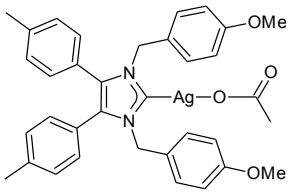	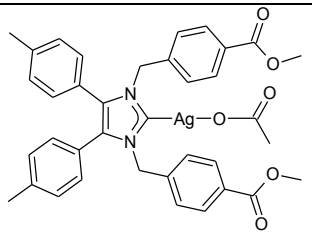	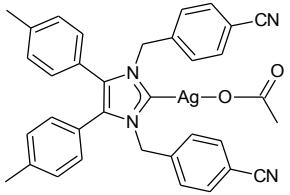
Caki-1	3.6 (± 1.0)	0.51 (± 0.07)	4.1 (± 1.0)	9.5 (± 0.5)	26 (± 2)
MCF-7	2.3 (± 0.4)	1.4 (± 0.1)	2.1 (± 0.7)	5.6 (± 1.0)	9.1 (± 0.5)
E. coli	7	2	2	2	1
S. aureus	7	4	5	2	3

Table 6.3: Chapter 5: Benzimidazole- and 4,5-diaryl-substituted imidazole NHC-ruthenium(II) (*p*-cymene) dichloride complexes their respective IC_{50} values (μM) against Caki-1 and MCF-7

Compound	23	24	25	26	27	28
	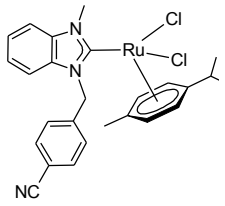	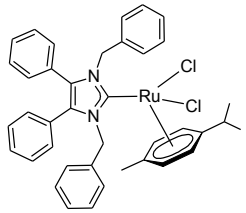	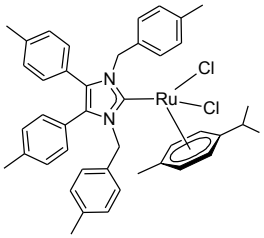	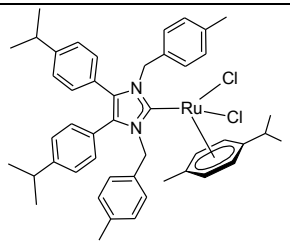	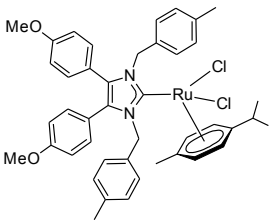	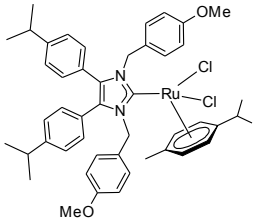
Caki-1	> 500	94 (± 5)	93 (± 2)	170 (± 20)	39 (± 5)	13 (2)
MCF-7	> 500	80 (± 15)	19 (± 1)	7.1 (± 1.2)	2.4 (± 0.7)	7.0 (± 1.2)

Table 6.4: 4,5-diaryl-substituted imidazole NHC-gold(I)X complexes (X = Cl, OAc, *SR*) and their respective IC_{50} values (μM) against Caki-1 and MCF-7.

Compound	**29**	**30**	**31**
	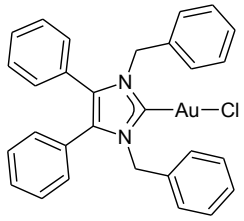	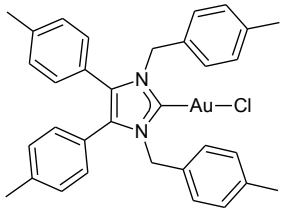	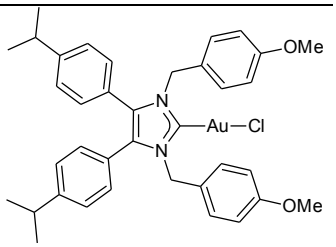
Caki-1	67 (± 7)	16 (± 2)	41 (± 1)
MCF-7	8.4 (± 0.4)	30 (± 3)	12 (± 1)

Compound	**32**	**33**	**34**
	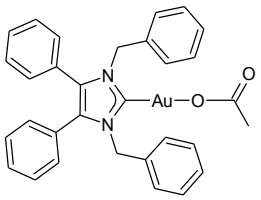	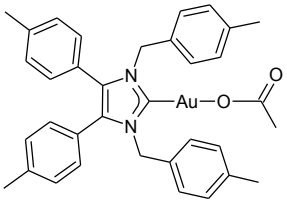	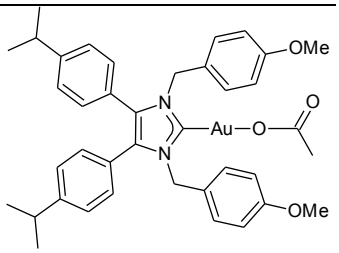
Caki-1	31 (± 2)	42 (± 5)	18 (± 1)
MCF-7	23 (± 3)	12 (± 1)	25 (± 3)

Compound	**35**	**36**	**37**
	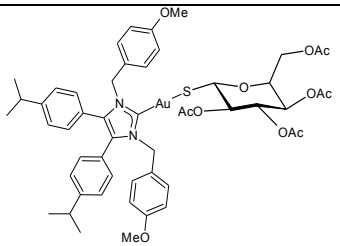	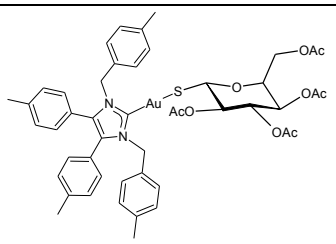	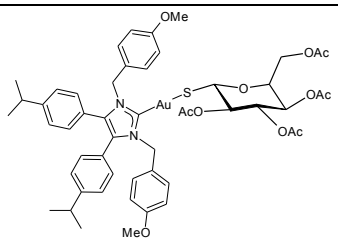
Caki-1	14 (± 2)	17 (± 2)	58 (± 2)
MCF-7	6.1 (± 1.5)	9.3 (± 1.6)	14 (± 2)

Initially, all complexes were solely tested against the human renal cancer cell line Caki-1 (Complex **1-7**), but after the first year a second cancerous cell line, namely MCF-7 (human breast carcinoma) was introduced to get a direct comparison of activity against different cancer types by the newly synthesised complexes (**8-37**). In the compounds that were tested on both cell lines, the IC_{50} values were found to be, in nearly all cases, better against the MCF-7 cell line. All *in vitro* cell tests were based on the MTT assay, where the tetrazolium salt is

reduced to formazan in the presence of living cells, which can then be dissolved in DMSO and the absorbance measured at 540 nm. The preliminary *in vitro* antibacterial results for the NHC-silver(I) acetates **1-22** were all obtained by applying the Kirby-Bauer disc diffusion method where the area of clearance (radius from disc border to visible bacteria growth) was measured after 24 h of incubation with different complex concentrations. Only the results for the highest concentrations (0.44 µM) are presented.

Table 6.1 and Table 6.2 show the IC_{50} values as well as areas of clearance of the 22 tested NHC-Ag(I)OAc complexes. It was found that the unsymmetrically substituted complexes **1-7** do not show improved cytotoxic (lowest value found for **3**: 5.4 (± 0.8) µM) as well as antibacterial activity (widest area of clearance found for **2** against *E. coli*: 7 mm; and for **7** against *S. aureus*: 8 mm) if compared to SBC1 (IC_{50} against Caki-1: 1.2 (± 0.6) µM) and SBC3 (area of clearance against *E. coli*: 10 mm; *S. aureus*: 7 mm). These findings were the first indication that this specific substitution pattern might not lead towards potential new antibiotics or anticancer drug candidates. It was later discovered that the complexes had a relative short bench lifetime (2-8 weeks), which was indicated by the observation of a grey or brown to black discoloration of the initial white complexes. Therefore, further investigations into the biological activity of symmetrically substituted SBC3 derivatives were pursued, which led to the discovery of the highly active 1,3-di(*p*-methylbenzyl)-4,5-di(*p*-methylphenyl)imidazol-2-ylidene silver(I) acetate complex **19**. With high stability as well as good solubility and IC_{50} values of 0.51 (± 0.07) µM (Caki-1) and 1.2 (± 0.1) µM (MCF-7) it has shown to be a promising new anticancer drug candidate and is currently under further investigation.

Furthermore, two interesting trends in antibacterial as well as cytotoxic activity have been observed. Firstly, upon changing the substituents in *para* position on the 1,3-dibenzyl-arms from H, CH_3 an OCH_3 towards $COOCH_3$ or CN, in every compound family (complexes **8-12**, **13-17** and **18-22**) the cytotoxic activity is reduced up to 7-fold against Caki-1 and up to 5-fold against MCF-7. This may be attributed to the lower lipophilicity of these complexes. Secondly, high antibacterial activity has only been found for structurally similar complexes to SBC3 (see complexes **8**, **9**, **10**, **13** and **18**). This trend suggests that an unsubstituted benzyl and/or phenyl ring has to be present in the complexes in order to exhibit high antibacterial activity against both bacterial strains.

Summarizing, it can be said that several highly cytotoxic complexes have been found, identifying **19** as a new lead structure for further investigations, but unfortunately none of the complexes **8-22** can be considered as an improved antibacterial drug candidate since all highly antibacterial acting complexes are also found to be highly cytotoxic.

For further studies the most promising NHC-silver(I) acetates have been used as templates to investigate the influence of other transition metals (namely ruthenium and gold) on the cytotoxic activity against Caki-1 and MCF-7. Exchanging the silver acetate moiety against ruthenium (*p*-cymene) dichloride (**23-28**) or gold chloride (**29-31**), gold acetate (**32-34**) and gold thioglucopyranose (**35-37**) resulted in an overall weaker cytotoxic profile (IC_{50} values (µM) for silver acetate analogues of **23**: 1.2 (± 0.6) (Caki-1) [3] and 23 (± 1) (MCF-7) (unpublished results); **26**: 4.6 (± 0.6) (Caki-1) and 2.1 (± 0.8) (MCF-7); **28**/**31**/**34**/**37**: 5.5 (± 0.6) (Caki-1) and 3.4 (± 0.6) (MCF-7) [4]). Interestingly, upon transmetallation of SBC1 to its ruthenium containing analogue **22**, the cytotoxic activity is completely lost. Nevertheless, some interesting results have been obtained which might lead to further investigation of the mode of action and cellular targets of these complexes. Especially the Ru(II)-NHC complexes **26** and **27** which show 24-fold and 16-fold better activity against MCF-7 than Caki-1 indicate that there might be different mechanisms of cellular uptake and/or of cell death induction present in the two different cell lines. Furthermore, the SBC3 gold chloride (**29**) and gold thioglucopyranose (**35**) analogues exhibited good IC_{50} values against MCF-7 with 8-fold and 2-fold better activity than against Caki-1, respectively.

In conclusion, several NHC-silver(I) acetates with IC_{50} values in the micromolar region have been synthesised and the identified lead structures were successfully transmetallated to their ruthenium and gold analogues. Evaluation of the obtained derivatives for their *in vitro* cytotoxic activity revealed two promising Ru(II)-NHC (**26**, **27**) and two Au(I)-NHC (**29**, **35**) complexes which hopefully will show good results in further studies.

6.3 An Outlook towards the future of biologically active NHC-transition metal complexes

While promising results have been obtained in this study, it is obvious that further work has to be carried out before undergoing advanced *in vivo* tests as well as clinical trials. Some steps which might be undertaken to investigate and optimise these already highly antibacterial and cytotoxic complexes are outlined in the following paragraph:

- Human serum albumin binding studies to determine if this is a possible mechanism of uptake into cells.
- Carrying out DNA binding assays, CD spectroscopy and DNA denaturation experiments might reveal if DNA is a target.
- Investigation of the possible inhibition of disulfide reductases (TrxR and GR) and proteases (trypsin and catB) as well as the interaction with non-enzymatic thiol and selenol containing biomolecules
- NCI60 cell line panel test to get an overview about which cancer cells are specifically targeted by the potential new drug candidates.
- *In vivo* tests with zebrafish larvae and / or non-tumour bearing mice to determine the MTD of the optimised complexes.
- Transmetallation to further known bioactive metals, such as palladium, iridium, rhodium and platinum.
- Synthesis of other NHC-Au(I) complexes with different thioglucopyranose derivatives to enhance the solubility in aqueous medium and to take a step further into the direction of a targeted uptake of the drugs.

6.4 References

[1] M. A. Sharkey, J. P. O'Gara, S. V. Gordon, F. Hackenberg, C. P. F. Healy, S. Patil, B. Schaible, M. Tacke; *Antibiotics*, **2012**, 25–28.

[2] I. Fichtner, J. Cinatl, M. Michaelis, L. C. Sanders, R. Hilger, B. N. Kennedy, A. L. Reynolds, F. Hackenberg, G. Lally, S. J. Quinn, I. McRae, M. Tacke; *LDDD*, 9, **2012**, 815–822.

[3] S. Patil, A. Deally, B. Gleeson, H. Müller-Bunz, F. Paradisi, M. Tacke; *Metallomics*, 3, **2011**, 74–88.

[4] W. Streciwilk, J. Cassidy, F. Hackenberg, H. Müller-Bunz, F. Paradisi, M. Tacke; *J. Organomet. Chem,* **2013**, doi:10.1016/j.jorganchem.2013.09.033.

Appendix

Celltest protocol

Day 1: Seed the plates in 96-well plates containing 200 µl microtitre wells

- Split cells:
  - Remove old medium
  - Add trypsin/EDTA (3 ml) to cells in flask and place in the incubator for no longer than 5 min. Add 7 ml medium to the flask to deactivate Trypsin and pipette into a 50 ml tube. Centrifuge for 3 min at 1500 rpm.
  - Remove supernatant.
  - Add 2 ml phosphate buffer solution and remove immediately.
  - Re-suspend the cells in 20 ml of medium and place 10 ml in new flask.
  - Take note of generation number, cell line, user name and date on new flask
- Seed the plates
  - Take remaining 10 ml and add 30 ml medium.
  - Pipette 200 µl in a 9x3 and 6x3 pattern into 4 x 96-well-plates

Day 2: Add drugs. Incubate for 48 hours at 37°C

- Remove old medium
- Add drugs/control
  - Med = medium
  - DMSO = 9.93 ml medium + 70 µl DMSO
  - Dissolve drug in DMSO first, then add medium

Drug concentrations:

A: $5x10^{-4}$ M (9.93 ml medium + 70 µl DMSO)
B: $(5/3)x10^{-4}$ M (2 ml of **A** + 4 ml medium)
C: $5x10^{-5}$ M (1 ml of **A** + 9 ml medium)
D: $(5/3)x10^{-5}$ M (2 ml of **C** + 4 ml medium)
E: $5x10^{-6}$ M (0.2 ml of **C** + 1.8 ml medium)
F: $5x10^{-7}$ M (0.2 ml of **E** + 1.8 ml medium)
G: $5x10^{-8}$ M (0.2 ml of **F** + 1.8 ml medium)
H: $5x10^{-9}$ M (0.2 ml of **G** + 1.8 ml medium)
I: $5x10^{-10}$ M (0.2 ml of **H** + 1.8 ml medium)

	A	A	A	G	G	G	DMSO	DMSO	DMSO		
	B	B	B	H	H	H	DMSO	DMSO	DMSO		
	C	C	C	I	I	I	DMSO	DMSO	DMSO		
	D	D	D	Med	Med	Med					
	E	E	E	Med	Med	Med					
	F	F	F	Med	Med	Med					

Day 3: Day off

Day 4: Wash with PBS. Recovery period of 24 hours at 37°C

- Remove medium/drugs
- Wash with 200 µl phosphate buffer solution
- Add 200 µl fresh medium

Day 5: Measure ABS

- Remove old medium
- Add 200 µl MTT solution (22mg MTT/40ml medium)
- Wait for exactly 3 hours and remove MTT
- Add DMSO (200 µl) and measure absorption at 540 nm
- Plot data in Origin on a logarithmic scale and apply sigmoidal fit to determine the IC_{50} value

Preparation of medium

- Place FBS, penicillin and glutamine in water bath until they become liquid
- Add into medium:
  - 25 ml FBS
  - 3 ml penicillin
  - 3 ml glutamine
- Place medium back into fridge

Change medium in cell flask on day 5

- Remove old medium
- Wash with approximately 3 ml PBS
- Remove PBS
- Add 10 ml fresh medium

Kirby-Bauer disk diffusion test protocol

Preparing LB medium:

5g N-Z-amine

2.5g bacto yeast

2.5g NaCl

Fill up to 500 ml with H_2O. Close lid, shake and open lid a bit. Cover with 1 stripe of autoclave film and autoclave for 15 min. Let cool down to 60-70°C and close completely. Let cool down to RT.

Preparing agar medium:

5g N-Z-amine

25g bacto yeast

2.5g NaCl

7.5g Agar

Fill up to 500 ml with H_2O. Close lid, shake and open lid a bit. Cover with 1 stripe of autoclave film and autoclave for 15 min. Let cool down to 60-70°C and close completely. Apply thin film of agar medium to petri dishes and let cool down in fume hood. Once cooled down, label dishes and cover with para film. Store in fridge.

All bacteria were individually cultured from a single colony in sterile LB medium overnight at 37°C in an orbital shaker incubator. All the work carried out was performed under sterile conditions.

For each strain, 70 µL of culture were spread evenly on agar-LB medium. Four 5 mm diameter Whatman paper discs were placed evenly separated on each plate. Two stock solutions (9:1 DMSO:H_2O) of every compound were prepared at 2.2 µM and 4.4 µM to be able to test the effect of different concentrations. Each plate was then tested with 5 µL and 7 µL of 2.2 µM solution and 5 µL and 10 µL for the 4.4 µM solution. The plates were covered and placed in an incubator at 37°C for 24 h. The plates were then removed and the area of clearance, which is defined as the distance between the edge of the filter paper disc and the beginning of the bacterial growth, was measured for each sample in mm.